

**A Thesis Submitted for the Degree of PhD at the University of Warwick**

**Permanent WRAP URL:**

<http://wrap.warwick.ac.uk/163821>

**Copyright and reuse:**

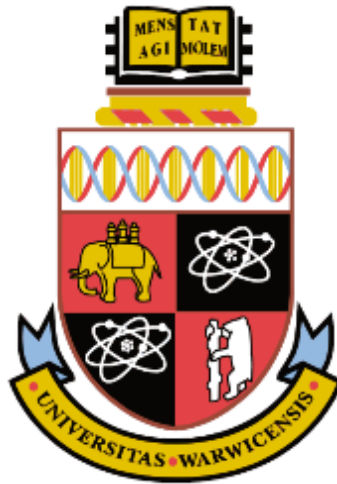
This thesis is made available online and is protected by original copyright.

Please scroll down to view the document itself.

Please refer to the repository record for this item for information to help you to cite it.

Our policy information is available from the repository home page.

For more information, please contact the WRAP Team at: [wrap@warwick.ac.uk](mailto:wrap@warwick.ac.uk)



# **Glyoxalase 1 inducer therapy for the treatment of experimental diabetic kidney disease**

By Ohoud Al-ghamdi

A thesis submitted in fulfilment of the requirements for the degree of

**Doctor of Philosophy in Systems Biology**

Warwick Medical School, University of Warwick

# Table of contents

<b>Table of contents</b> .....	<b>2</b>
<b>Table of Figures</b> .....	<b>8</b>
<b>List of tables</b> .....	<b>11</b>
<b>Acknowledgment</b> .....	<b>12</b>
<b>Declaration</b> .....	<b>13</b>
<b>Abstract</b> .....	<b>14</b>
<b>Abbreviations</b> .....	<b>16</b>
<b>1 Introduction</b> .....	<b>20</b>
1.1 Diabetes .....	20
1.1.1 Definition and historical background .....	20
1.1.2 Diabetes classification .....	22
1.1.3 Prevalence of diabetes .....	23
1.1.4 Diagnosis of diabetes mellitus.....	24
1.1.5 Type 1 diabetes mellitus.....	25
1.1.5.1 Genetic factors.....	26
1.1.5.2 Environmental factors .....	26
1.1.5.3 Pathogenesis of type 1 diabetes millitus.....	27
1.1.6 Type 2 diabetes mellitus.....	28
1.1.6.1 Genetic factors.....	28
1.1.6.2 Environmental factors .....	29
1.1.6.3 Pathogenesis of type 2 diabetes mellitus .....	30
1.2 Complications of diabetes .....	32
1.2.1 Acute complications .....	32
1.2.2 Chronic complications.....	33
1.3 Diabetic macrovascular complications.....	33
1.3.1 Peripheral vascular disease.....	33
1.3.2 Diabetic cardiovascular disease.....	34
1.3.3 Cerebrovascular disorders .....	37
1.4 Diabetic microvascular complications .....	38
1.4.1 Diabetic neuropathy .....	38
1.4.2 Diabetic retinopathy .....	39
1.4.3 Diabetic kidney disease .....	40

1.4.3.1	Diagnosis of DKD .....	43
1.4.3.2	Nephrons structure .....	45
1.4.3.3	Pathology of DKD.....	48
1.4.3.4	Treatment of DKD.....	49
1.4.3.5	Cellular models of DKD.....	51
1.5	Glycation .....	52
1.5.1	Glycation definition.....	52
1.5.2	Molecular structures of advanced glycation end-products.....	55
1.5.3	Historical background of glycation research.....	56
1.5.4	Glycation in diabetes and diabetic complications research.....	58
1.5.5	Glycation and diabetic kidney disease .....	59
1.6	Dicarbonyls .....	61
1.6.1	Dicarbonyl stress .....	61
1.6.2	Measurment of glycation adducts.....	62
1.6.3	Repair of glycated protein .....	63
1.7	The glyoxalase system, definition and function .....	63
1.7.1	Glyoxalase 1 .....	65
1.7.2	Glyoxalase 2 .....	68
1.7.3	S-D-Lactoylglutathione .....	70
1.7.4	D-Lactate .....	71
1.7.5	Non-glyoxalase detoxification of methylglyoxal .....	72
1.7.6	Glyoxalase 1 - a critical role in enzymatic defence against glycation .....	74
1.7.7	Development of Glo1 inducer therapeutics.....	75
1.7.8	Glyoxalase inhibitors.....	76
1.8	Introduction to mass spectrometry .....	77
1.8.1	Mass spectrometry.....	77
1.8.2	Ionisation methods .....	78
1.9	Project- specific background .....	80
1.9.1	Therapeutic approaches to counter dicarbonyl stress.....	80
1.9.2	Resveratrol.....	80
1.9.2.1	Effect of tRSV on diabetes .....	85
1.9.2.1.1	Effects of tRSV on blood glucose levels.....	85
1.9.2.1.2	Effects of tRSV on blood insulin levels .....	86

1.9.2.1.3	Effect of tRSV on protection of $\beta$ -cells.....	88
1.9.3	Hesperetin.....	89
1.9.3.1	Effect of hesperetin on diabetes and its complications .....	90
1.9.3.2	Antioxidant effects of hesperetin .....	91
1.9.3.3	Role of hesperetin in glycation.....	91
1.9.3.4	Anti-inflammatory effects of hesperetin .....	92
1.9.4	Proteomics.....	94
1.9.4.1	Label-free quantification .....	95
1.9.4.2	Sample preparation for label-free quantification.....	96
1.10	Aims and objectives of this project .....	97
<b>2</b>	<b>Materials and methods.....</b>	<b>98</b>
2.1	Materials.....	98
2.1.1	Cells and tissues .....	98
2.1.2	Cell culture reagents.....	98
2.1.3	Substrates, cofactors, enzymes and consumables .....	99
2.1.4	Other consumables .....	99
2.1.5	Sample quantification assay kits .....	100
2.1.6	Instrumentation and software .....	100
2.2	Cell culture methods.....	101
2.2.1	Cell culture experimentation .....	103
2.2.1.1	Effect of high glucose on growth of renal cells.....	103
2.2.1.2	The effect of Glo1 inducer on renal cell growth .....	103
2.2.1.3	Characterisation of glyoxalase system in renal cells in model hyperglycaemia .....	103
2.2.1.4	Effect of Glo1 inducers on the glyoxalase system in renal cells <i>in vitro</i>	103
2.3	Analytical methods.....	104
2.3.1	Total protein assay Bicinchoninic acid assay (BCA).....	104
2.3.2	Enzymatic activity assay .....	105
2.3.2.1	Activity of glyoxalase 1 .....	105
2.3.2.2	Activity of glyoxalase 2 .....	105
2.3.2.3	Methylglyoxal reductase activity .....	106
2.3.2.4	Methylglyoxal dehydrogenase activity .....	107
2.4	Immunoblotting for Glo1 .....	107

2.4.1	Sample preparations .....	107
2.4.2	Western blotting .....	108
2.5	D-Glucose assay .....	108
2.6	D-lactate assay .....	110
2.7	L-lactate assay .....	111
2.8	Proteomics of cytosolic protein methodology .....	112
2.8.1	Filter Aided Sample Preparation (FASP Protocol) .....	112
2.8.2	Protocol of Lys-C-Trypsin protease digestion of cytosolic protein .....	113
2.8.3	C <sub>18</sub> Stage tip.....	113
2.8.4	Peptide separation, protein quantitation and identifications .....	114
2.8.5	Proteomic Data analysis .....	115
2.8.6	Statistical analysis .....	115
<b>3</b>	<b>Results.....</b>	<b>116</b>
3.1	Characterisation of the effects of high glucose concentration on primary human renal cells <i>in vitro</i> .....	116
3.1.1	Effects of high glucose concentration on growth and viability of hRPTE cells <i>in vitro</i> .....	118
3.1.2	Effect of high glucose concentration on growth and viability of MCs <i>in vitro</i> .....	119
3.1.3	Characterisation of the glyoxalase system of hRPTE cells incubated in low and high glucose conditions <i>in vitro</i> .....	120
3.1.4	Glyoxalase 1 protein content of hRPTE cells incubated in low and high glucose concentration <i>in vitro</i> .....	121
3.2	Metabolism of methylglyoxal by renal cells in high glucose <i>in vitro</i> .....	122
3.2.1	Effect of high glucose concentration on D-glucose consumption, D-lactate and L-lactate formation in hRPTE cells <i>in vitro</i> .....	122
3.2.1.1	Consumption of D-glucose by hRPTE cells incubated in low and high glucose <i>in vitro</i> .....	122
3.2.1.2	Flux of formation of D-lactate and L-lactate in hRPTE cells cultured in low and high glucose conditions <i>in vitro</i> .....	123
<b>4</b>	<b>Results.....</b>	<b>125</b>
4.1	Characterisation of the effects of the Glo1 inducer tRSV-HSP on the human renal cells incubated in high glucose concentration <i>in vitro</i> .....	125

4.1.1	Growth and viability of hRPTE cells incubated in 7.2 mM and 25.0 mM glucose concentration with and without Glo1 inducer <i>in vitro</i> .....	127
4.1.2	Growth and viability of MCs incubated in 5.5 mM glucose with and without HSP and tRSV <i>in vitro</i> .....	129
4.1.3	Effect of Glo1 inducer on enzymatic activity related to dicarbonyl metabolism in hRPTE cells <i>in vitro</i> .....	130
4.1.4	Effect of Glo1 inducer on enzymatic activity related to dicarbonyl metabolism in MCs <i>in vitro</i> .....	132
4.2	Characterisation of the effect of Glo1 inducer on the D-glucose consumption, D-lactate and L-lactate formation by hRPTE cells in hyperglycaemia <i>in vitro</i> .....	134
4.2.1	Effect of Glo1 inducers on the consumption of D-Glucose by hRPTE cells <i>in vitro</i> .....	134
4.2.2	Effect of Glo1 inducers on flux of formation of D-lactate and L-lactate by hRPTE cells in hyperglycaemia <i>in vitro</i> .....	135
4.3	Characterisation of the effect of Glo1 inducer on the D-glucose consumption, D-lactate and L-lactate formation by MCs in hyperglycaemia <i>in vitro</i> .....	137
4.3.1	Effect of Glo1 inducers on the consumption of D-Glucose by MCs <i>in vitro</i> .....	137
4.3.2	Effect of Glo1 inducers on flux of formation of D-lactate and L-lactate by MCs in hyperglycaemia <i>in vitro</i> .....	138
<b>5</b>	<b>Results</b> .....	<b>140</b>
5.1	Studying the modification of cytosolic proteins in renal cells: high mass resolution proteomics analysis .....	140
5.1.1	Studying the modification of cytosolic proteins in hRPTE: high mass resolution proteomics analysis .....	142
5.1.2	Studying the modification of cytosolic proteins in MCs: high mass resolution proteomics analysis .....	144
5.1.2.1	Differentially expressed proteins between low and high glucose cultures of MCs .....	146
5.1.2.2	Differentially expressed proteins between Glo1 inducer treatment and controls in low glucose cultures of MCs .....	147

<b>6</b>	<b>Discussion.....</b>	<b>174</b>
6.1	Effect of glucose concentration on growth and viability of primary human renal cells <i>in vitro</i> .....	175
6.2	The effect of high glucose and dicarbonyl stress on the glyoxalase system in primary human renal cells <i>in vitro</i> . .....	176
6.3	The effect of high glucose on dicarbonyl metabolism in primary human renal cells <i>in vitro</i> . .....	177
6.4	Effect of Glo1 inducers on growth and viability of primary human renal cells <i>in vitro</i> .....	178
6.5	Effect of Glo1 inducers on the glyoxalase system in primary human renal cells <i>in vitro</i> . .....	178
6.6	Effect of Glo1 inducers on dicarbonyl metabolism in primary human renal cells <i>in vitro</i> . .....	180
6.7	The effect of high glucose concentration on the cytosolic proteome of renal cells <i>in vitro</i> .....	181
6.8	The effect of Glo 1 inducer on the cytosolic proteome of MCs <i>in vitro</i> . .....	183
<b>7</b>	<b>Conclusion and further work .....</b>	<b>186</b>
7.1	Conclusion.....	186
7.2	Limitations.....	187
7.3	Further work .....	188
<b>8</b>	<b>References .....</b>	<b>189</b>



## Table of Figures

Figure 1.1: Mechanism of action of insulin.....	31
Figure 1.2: Explanation of metabolic dysfunction participated in hyperglycaemia inducing diabetic complications. ....	36
Figure 1.3: Pathological lesions of DKD. ....	42
Figure 1.4: Anatomical outline of renal filtration.....	47
Figure 1.5: Main advanced glycation end products in chronic kidney disease. ....	53
Figure 1.6: The major pathways of modification of lysine and arginine protein residues by glucose and MG in diabetes.....	54
Figure 1.7: Protein glycation, oxidation and nitration adduct residues in physiological system. ....	55
Figure 1.8: Timeline of historical discoveries in research on the glycation to 2010.....	58
Figure 1.9: Physiological dicarbonyl metabolites. ....	62
Figure 1.10: The glyoxalase system and its metabolites. ....	64
Figure 1.11: Human Glo1 gene. ....	65
Figure 1.12: Crystal structure of human Glo1.....	67
Figure 1.13: Non glyoxalase detoxification of dicarbonyl metabolites.....	73
Figure 1.14: Basic components of a mass spectrometer.....	78
Figure 1.15: Electrospray ionisation.....	79
Figure 1.16: Resveratrol chemical structure.....	80
Figure 1.17: Hesperetin chemical structure.....	89
Figure 2.1: Morphology of human renal proximal tubular epithelial cells (hRPTECs).....	102
Figure 2.2: Morphology of human mesangial cells (MCs) ....	102
Figure 2.3: Calibration curve for BCA assay. ....	104
Figure 2.4: The catalytic reactions of the glyoxalase system. ....	106
Figure 2.5: Reaction scheme for detection of glucose via hexokinase and glucose 6 phosphate dehydrogenase. ....	109
Figure 2.6: Calibration curve for D-glucose.....	109
Figure 2.7: Calibration curve for D-lactate assay.....	111
Figure 2.8: Calibration curve for L-lactate.....	112
Figure 3.1: Growth curve of hRPTE cells in media containing 7.2 mM and 25.0 mM glucose in vitro. ....	118

Figure 3.2: Growth curve of MCs cells in media containing 5.5 mM and 25.0 mM glucose <i>in vitro</i> .....	119
Figure 3.3: Enzymatic activities of the glyoxalase system in hRPTE cells <i>in vitro</i> .....	120
Figure 3.4: Glyoxalase 1 protein content of hRPTE cells incubated in high glucose (25 mM) <i>in vitro</i> .....	121
Figure 3.5: Consumption of D-glucose by hRPTE cells incubated in high glucose <i>in vitro</i> .....	122
Figure 3.6: Flux of formation of D-lactate and L-lactate in hRPTE cells cultured in low and high glucose conditions <i>in vitro</i> .....	124
Figure 4.1: Growth curve of hRPTE cells with and without tRSV-HSP (5 and 10 $\mu$ M) combination and individually <i>in vitro</i> .....	128
Figure 4.2: Growth curve of MCs in media containing 5.5 mM glucose with and without 5 $\mu$ M and 10 $\mu$ M HSP and tRSV.....	129
Figure 4.3 : Enzymatic activities of glyoxalase system in hRPTE cells <i>in vitro</i> .....	131
Figure 4.4: Enzymatic activities of the glyoxalase system in MCs cells <i>in vitro</i> .....	133
Figure 4.5: Effect of Glo1 inducers on consumption of D-glucose by hRPTE cells <i>in vitro</i> .....	134
Figure 4.6: Flux of formation of D-lactate and L-lactate in hRPTE cells cultured in low and high glucose conditions with and without Glo1 inducer <i>in vitro</i> .....	136
Figure 4.7: Effect of Glo1 inducers on consumption of D-glucose by MCs <i>in vitro</i> .....	137
Figure 4.8: Flux of formation of D-lactate and L-lactate in MCs cultured in low and high glucose conditions with and without Glo1 inducer <i>in vitro</i> .....	138
Figure 5.1: Principal component analysis (PCA) for all hRPTE cell samples.....	142
Figure 5.2: Comparison of protein profile of hRPTE cells cultured in low and high glucose conditions with and without Glo1 inducer <i>in vitro</i> .....	143
Figure 5.3: Histograms of normalised protein abundance for all samples.....	145
Figure 5.4: Principal component analysis (PCA) for all MCs samples.....	145
Figure 5.5: Comparison of protein profiles from MCs cultured in low versus high glucose conditions <i>in vitro</i> .....	146
Figure 5.6: Comparison of protein profile of MCs cultured in low glucose condition with and without Glo1 inducer <i>in vitro</i> .....	147
Figure 5.7: Manhattan plot of Functional Enrichment Analysis of differently expressed cytosolic proteins from MCs.....	148
Figure 5.8: Manhattan plot of Functional enrichment analysis of downregulated proteins of MCs in hyperglycaemia.....	153

Figure 5.9: Manhattan plot of Functional enrichment analysis of differently expressed proteins of MCs treated by Glo1 inducer..... 154

Figure 5.10: GO enrich terms in MCs treated by Glo1 inducer summarised by REVIGO... 159

## List of tables

Table 1.1: Timeline of the study of diabetes mellitus.....	21
Table 1.2: Diagnostic criteria for diabetes mellitus .....	25
Table 1.3: Prognosis of DKD by GFR and albuminuria category .....	44
Table 1.4: eGFR equations .....	44
Table 1.5: Some dietary sources of resveratrol.....	82
Table 1.6: Preclinical effects for resveratrol.....	83
Table 1.7: Summary on the anti-inflammatory properties of hesperidin, HSP and related compounds .....	93
Table 3.1: Values of Glo1 and Glo2 activity in hRPTE cells incubated in media containing low and high glucose <i>in vitro</i> .....	120
Table 3.2: Values of different analytical assays performed on hRPTE cells medium contains high and low glucose <i>in vitro</i> .....	124
Table 4.1: Effect of Glo1 inducers on Glo1 and Glo2 activity in hRPTE cells <i>in vitro</i> .....	130
Table 4.2: Effect of Glo1 inducers on Glo1 and Glo2 activity in MCs <i>in vitro</i> .....	133
Table 4.3: Effect of Glo1 inducers on formation of D-lactate and L-lactate in hRPTE cells <i>in vitro</i> .....	135
Table 4.4: Effect of Glo1 inducers on formation of D-lactate and L-lactate in MCs <i>in vitro</i>	139
Table 5.1: Functional enrichment analysis of differentially expressed proteins in MCs.....	149
Table 5.2: Functional enrichment analysis of differentially expressed proteins in MCs treated by Glo1 inducer.....	155
Table 5.3: Proteins in the cytoplasmic extract increased significantly in abundance in MCs by treatment with high glucose concentration. ....	160
Table 5.4: Proteins in the cytoplasmic extract decreased significantly in abundance in MCs by treatment with high glucose concentration. ....	160
Table 5.5: Cytosolic proteins upregulated significantly in MCs treated by Glo1 inducer in normal glucose condition.....	161
Table 5.6: Cytosolic proteins downregulated significantly in MCs treated by Glo1 inducer in normal glucose condition.....	165

بِسْمِ اللَّهِ الرَّحْمَنِ الرَّحِيمِ

## Acknowledgment

In the name of Allah, the most beneficial and the most merciful Alhamdulillah, all praises to Allah for the strengths, knowledge and his blessing in completing this thesis. I would like to express my appreciation to the people named below, without whom this research would not have been completed.

Special appreciation goes to my supervisor, Dr Daniel Mitchell, for his supervision and consistent help and guidance during my study at the University of Warwick. His invaluable support of constructive feedback and advice all through the experimental and thesis works have contributed to complete this project. Not forgotten, my appreciation to my previous supervisors, Professor Paul J Thornalley and Dr Naila Rabbani, for their support and knowledge regarding this project. I would like to thank Dr Mingzhan Xue for all his advice in the molecular biology and cell culture work. I am also thankful to Dr Andrew Bottrill and Dr Cleidi Zampronio for their help in the proteomics and mass spectrometry works and technical advice and help in the Mass spectrometry experiment. Sincere thanks to all my colleagues in Protein Damage and Systems Biology Research Group members for their help, smiles and support.

My deepest gratitude goes to my family, to the beloved parents; Mr. Ali Alghamdi and Mrs. Faizah Busaeed for all their support, prayers advice and their patient during my absence from home. They always give me the hidden strength in my life. To all my brothers, especially Fahad for accompanying me in my overseas journey, thank you for your support and encouragement. Last but not least, I am grateful to the Saudi Embassy in London for their support in their administrative work.

## **Declaration**

I am aware of the University of Warwick regulations governing plagiarism and I declare that this thesis has not been previously accepted for any degree. I state that this thesis is all my own independent investigation except where I have stated, the research presented was performed by myself under the supervision of Dr Daniel Mitchell, Dr Naila Rabbani and Prof Paul Thornalley.

Ohoud Al-ghamdi

## Abstract

Diabetic kidney disease (DKD), one of the most common diabetic complications, is identified as a progressive kidney disease in patients with diabetes resulting from angiopathy of the capillaries in renal glomeruli. DKD affects nearly 40% of patients with diabetes and is characterised by increased albuminuria and decreased glomerular filtration rate (GFR). Hyperglycaemia and inflammation enhance DKD through increased glycation formation. Current treatments address only ca. 15% of the risk of DKD development. Development of DKD and other microvascular complications of diabetes is linked to glycemic control. In hyperglycaemia, dysregulation of glucose metabolism drives the activation of multiple metabolic pathways potentially damaging to the kidney, for example mitochondrial dysfunction with NADPH oxidase-driven increased formation of reactive oxygen species, the polyol pathway, the hexosamine pathway, and increased formation advanced glycation endproducts (AGEs). Driving the latter process leads to increased formation and decreased metabolism of the reactive dicarbonyl metabolite, methylglyoxal (MG), leading to increased concentrations of MG – an abnormal metabolic state called dicarbonyl stress. MG is the precursor of the major quantitative and damaging AGE in physiological systems, arginine residue derived hydroimidazolone, MG-H1. Most MG, ca. 99%, formed in the body is metabolised by glyoxalase 1 (Glo1) of the glyoxalase system. Glo1 activity decreased in the kidney in diabetes. The host research team have recently developed a new strategy for treatment of DKD: induction of Glo1 expression by small molecule activators of transcription factor Nrf2; Nrf2 binds a functional antioxidant response element in the GLO1 gene and increase expression. The optimised Glo1 inducer is a combination of *trans*-resveratrol and hesperetin (tRSV-HESP) this coformulation increases Glo1 expression and might drive improvements in microvascular complications of diabetes linked to hyperglycemia. The aim of this project is to evaluate the effect of Glo1 inducer treatment on human renal cell dysfunction in high glucose concentration primary cultures *in vitro*. Thesis work set out to characterise the glyoxalase system in primary human renal cells (Tubular epithelial cells and Mesangial cells) in models of hyperglycaemia *in vitro* and investigate the effects of the Glo1 inducer treatment, tRSV-HESP, on human renal cell function and protein expression in high glucose cultures *in vitro*. Data indicated that Glo1 inducer treatment had a significant impact on MG metabolism, as determined by measuring D-lactate flux, in both primary proximal tubular epithelial cells and primary mesangial cells, with evidence of treatment-induced increases in Glo1 levels shown via Western blot. Also, data showed significant, quantitative changes in proteomic

profiles between treatment groups in mesangial cells, but much less so in proximal tubular epithelial cells. Where detected, tRSV-HESP affected expression of key functional clusters involved in energy metabolism. Paradoxically, changes in Glo1 levels did not reach statistical significance between experimental groups. A striking discovery was that the impact of tRSV-HESP on proteomic profile for both sets of cells was greatly diminished by the presence of high glucose (25 mM) in the cultures. Taken together, these findings suggest that tRSV-HESP has potential to modulate therapeutically the Glo1 system and reduce dicarbonyl stress, but that any potential pharmacological effects would require greater glucose control prior to starting treatment.



## Abbreviations

<b>Abbreviations</b>	<b>Full name</b>
2-h PG	2-hour plasma glucose
3,4-DGE	3,4-dideoxyglucosone-3-ene
3-DG	3-Deoxyglucosone
3DG-H	3-DG-derived hydroimidazolones
HBA1 <sub>c</sub>	Glycated haemoglobin
ACEIs	Angiotensin converting enzyme inhibitors
ACN	Acetonitrile
ADA	American diabetes association
AGEs	Advanced glycation endproducts
AKR	Aldoketo reductase
ALDH	Aldehyde dehydrogenase
AMPK	Activated protein kinase
ARBs	Angiotensin II receptor blockers
ARE	Antioxidant response element
ATP	Adenosine triphosphate
BCA	Bicinchoninic acid assay
BSA	Bovine serum albumin
BMI	Body mass index
CAA	2-chloroacetamide
CEL	N <sub>ε</sub> -1-carboxyethyl-lysine
CHD	Coronary heart disease
CKD-EPI	Chronic kidney disease epidemiology collaboration group
CML	N <sub>ε</sub> -Carboxymethyl-lysine
Cr	Creatinine
CRM	Charge residue model
CVD	Cardiovascular disease
cysC	Cystatin C
DCCT	Diabetes control and complications trial
DETAPAC	Diethylenetriaminepenta-acetic acid
DHAP	Dihydroxyacetone phosphate
DKA	Diabetic ketoacidosis

DKD	Diabetic kidney disease
DMSO	Dimethylsulphoxide
DPNs	Diabetic peripheral neuropathy
ECM	Extracellular matrix
EC <sub>50</sub>	Half maximal effective concentration
EDTA	Ethylenediaminetetra-acetic acid
eGFR	Estimated GFR
EI	Electron ionization
ESI	Electrospray ionisation
ESRD	Endstage renal disease
FBS	Foetal bovine serum
FDR	False discovery rate
FL	N-ε-fructosyl-lysine
FPG	Fasting plasma glucose
GA3P	Glyceraldehyde-3-phosphate
GBM	Glomerular basement membrane
GDM	Gestational diabetes mellitus
GFR	Glomerular filtration rate
Glo1	Glyoxalase 1
Glo2	Glyoxalase 2
GLUT	Glucose transporter
GLUT1	Glucose transporter type 1
GLUT4	Glucose transporter type 4
GSH	Reduced glutathione
GWAS	Genome wide association studies
HAGH	Hydroxyacylglutathione hydrolase
HDL	High-density lipoprotein
HESP	Hesperetin
HK	Hexokinase
HLA	Human leukocyte antigen
HPLC	High phase liquid chromatography
IDF	International diabetes federation
IEM	Ion evaporation method

IFG	Impaired fasting glucose
IGT	Impaired glucose tolerance
IR	Insulin receptor
IRE	insulin response element
IRS-1	Insulin receptor substrates IRS-1
IRS-2	Insulin receptor substrates IRS-2
LC-MS/MS	Liquid chromatography with tandem mass spectrometric detection
LDL	Low-density lipoprotein
MALDI	Matrix-assisted laser desorption /ionisation
MC	Mesangial cells
MeOH	Methanol
MG	Methylglyoxal
MG-H1	MG-derived hydroimidazolone
MG-LDL	MG-modified LDL
MHC	Major histocompatibility complex
MODY	Maturity onset diabetes of the young
MRE	Metal responsive element
MS	Mass spectrometry
NAD <sup>+</sup>	Nicotinamide adenine dinucleotide
NADH	Nicotinamide adenine dinucleotide (reduced form)
NFK	N-formylkynurenine
NGSP	National glycohaemoglobin standardization program
NIDDM	Non-insulin dependent diabetes
NO	Nitric oxide
NOD	Non-obese diabetic
NPDR	Non-proliferative diabetic retinopathy
Nrf2	Nuclear factor erythroid 2-related factor 2
OGTT	Oral glucose tolerance test
Ox-LDL	Oxidized-low density lipoprotein
PBS	Phosphate buffer saline
PCA	Perchloric acid
PDR	Proliferative diabetic retinopathy

PGC	Plasma glucose criteria
PGC-1 $\alpha$	Peroxisome proliferator-activated receptor- $\gamma$ coactivator
pI	Isoelectric point
PI3	Phosphoinositide-3
PKC	Protein kinase C
PPAR $\gamma$	Peroxisome proliferator-activated receptor $\gamma$
PVD	Peripheral vascular disease
RAGE	Receptor for advanced glycation endproducts
RAS	Renin-angiotensin-system
ROS	Reactive oxygen species
hRPTEC	Human Renal proximal tubular epithelial cells
SIRT1	Sirtuin1
STZ	Streptozotocin
T1DM	Type 1 diabetes mellitus
T2DM	Type 2 diabetes mellitus
TCEP	Tris-(2-carboxyethyl) phosphine hydrochloride
TGF- $\beta$ 1	Transforming growth factor- $\beta$ 1
TNF- $\alpha$	Tumor necrosis factor
TNS	Trypsin neutralizing solution
tRSV	<i>trans</i> -Resveratrol
UACR	Urinary albumin to creatinine ratio
UKPDS	United Kingdom Prospective Diabetes Study
WHO	World health organisation

# 1 Introduction

## 1.1 Diabetes

### 1.1.1 Definition and historical background

Diabetes mellitus is a complex metabolic disorder and one of the most common, non-communicable chronic diseases globally, characterised by hyperglycemia and caused by deficiency or resistance to the action of insulin. Chronic hyperglycemia is associated with long-term complications arising from dysfunctions of different organs, especially the eyes, kidneys, peripheral nerves, heart, and blood vessels. There are many pathologies involved in the progression of diabetes. These range from autoimmune damage of the pancreatic beta-cells, causing insulin deficiency, to metabolic and inflammatory abnormalities that give rise to insulin resistance. In the case of insulin resistance, abnormalities in the metabolism of carbohydrates, lipids, and proteins arise due to deficiencies in the action of insulin on the target cells.

The first description of diabetes was in Egypt in about 1500 BC. It was known in the ancient literature as a condition associated with excessive urination. In the same period, Indian physicians recognised that the urine from people with diabetes attracted insects. The term “Diabetes” (meaning “to pass through”) was coined by the ancient Greek physician Apollonius of Memphis in 230 BC (Laios et al., 2012). Throughout the history of diabetes, most physicians believed that diabetes was a disorder of the kidneys. In the late 17th Mathew Dobson identified sugar in the urine of patients with diabetes. At about the same time, another English physician Thomas Cowley revealed the link of diabetes to pancreas. The main treatment for the disease during the middle ages was to reduce calorie & carbohydrate and increase protein in diet, and also use agents like digitalis and opium to suppress appetite (Poretsky, 2010). Progress in research led to the discovery of insulin by Frederick Banting and Charles Best in 1921. They successfully ran the first clinical trial to treat a 14-year-old boy with Type 1 diabetes. **Error! Reference source not found.** reviews the main events in the history of diabetes.

**Table 1.1: Timeline of the study of diabetes mellitus**

<b>Time</b>	<b>Event</b>
Circa 1500 BC	First written reference by ancient Egyptians described diabetes in literature
230 BC	The term “diabetes” from Greek “passing through”
First century AD	First clinical description of diabetes
First century AD	First distinction between the two main types of diabetes mellitus
1776	Mathew Dobson found sugar in the urine of diabetic subjects
1788	Thomas Cowley found a link of diabetes to pancreas
1869	Discovery of islets of Langerhans in pancreas by Paul Langerhans
1889	Removal of the pancreas in dogs discovered the immediate development of diabetes by Oscar Minkowski and Joseph von Mehring
1893	Edouard Laguesse suggested that islets of Langerhans might be the source of substance involved in the control of blood glucose
1907	Georg Zuelzer succeeded in using pancreatic extracts “acomatol” on diabetic dogs
1921-1922	Frederick Banting, Charles Best, James Collip, and John J.R. Macleod discovered insulin
1928	Synthalin introduced as an oral treatment for diabetes
1936	Discovery of a long-acting insulin (Protamine Zinc Insulin)
1938	Neutral Protamine Hagedorn insulin was created
1939	C. Ruiz and L.L. Silva noticed the hypoglycaemic effects of sulphonamide antibiotics
1952	Lente insulin was discovered
1956	Oral sulphonylurea developed as a treatment of type 2 diabetes
1958	Frederic Sanger got the Nobel prize for his discover of the structural formula of bovine insulin
1961	American company called Becton-Dickinson introduced insulin in a single-use syringe
1966	The first transplant of the pancreas performed by University of Minnesota
1969	Dorothy Hodgkin used X-ray crystallography to determine the three-dimensional structure of porcine insulin
1978	Recombinant human insulin developed by Robert Crea and David Goeddel
1979	Demonstrating of HbA <sub>1c</sub> test for measurement of glycaemic control

1988	Endocrinologist Dr Gerald Reaven introduced the concept of the metabolic syndrome of which diabetes forms a part
1993	Diabetes Control and Complications Trial (DCCT) found that the intensive glycaemic control slowed the development of diabetic complications
1995	Precose and Metformin produced as treatments for type 2 diabetes
1998	United Kingdom Prospective Diabetes Study (UKPDS) suggested the relationship of metabolic control with progression of diabetic complications in type 2 diabetes
2001	Association of diet and exercise with development of type 2 diabetes suggested by Diabetes Prevention Programme
2007	Genome-Wide Association Studies for Diabetes identified Novel loci in association with type 2 diabetes
2007	Using of stem cells from bone marrow for treatment of Type 1 diabetes
2008	Suzanna M. de la Monte coined the term “type 3 diabetes” to define insulin resistance in the brain.
2013	The University of Cambridge trials an artificial pancreas that combines a continuous glucose monitoring and insulin pump Edward Damiano introduces the iLet device, which he calls “a bridge to a cure”
2015	a bionic pancreas that delivers both insulin and glucagon every 5 minutes.

---

Modified from (Zajac et al., 2010).

### 1.1.2 Diabetes classification

Several pathogenic mechanisms contribute to the development of diabetes, ranging from autoimmune damage of the pancreatic cells with resulting in insulin insufficiency, to cellular defects that cause insulin resistance. According to the American Diabetes Association (ADA), the recent diabetes classification is established into these common types:

- (i) Type 1 diabetes mellitus (T1DM) - produced by T cell-mediated autoimmune damage of pancreatic  $\beta$  cells and causes total insulin deficiency.
- (ii) Type 2 diabetes mellitus (T2DM) - caused predominantly by insulin resistance with gradual, progressive loss of insulin secretion by  $\beta$  cells.
- (iii) Gestational diabetes mellitus (GDM), occurring during pregnancy and usually resolving at term.

- (iv) Other types of diabetes, for example: monogenic diabetes syndromes, such as neonatal diabetes and maturity onset diabetes of the young (MODY), disorders of the pancreas (e.g. cystic fibrosis), and some drugs or chemicals that induce diabetes/hyperglycaemia such as glucocorticoids, drugs used to treat HIV/AIDS and medications used post-organ transplantation (ADA, 2020a).

### **1.1.3 Prevalence of diabetes**

The prevalence of diabetes is increasing in many countries worldwide at an alarming rate and despite improvements in medical treatment, diabetes remains the seventh leading cause of mortality globally (WHO, 2016). According to the International Diabetes Federation (IDF), in 2019 there was an estimated 463 million people with diabetes worldwide, particularly in low- and middle-income countries. Almost 50% of all deaths are attributed to hyperglycaemia and happen before the age of 70 (WHO, 2016). According to IDF, in 2019 the regions with the highest number of diabetic cases of adults (20–79 years) are the Western Pacific Island nations and countries of the Middle East, with 163 and 88 million cases, respectively. While the top 3 countries with the highest prevalence of diabetes (20–79 years) in 2019 are China (116 million), India (77 million), and the United States of America (31 million). These countries are projected to remain in the top 3 by 2030, with 140, 101 and 34 million people with diabetes, respectively (IDF, 2019). While Africa is the region with the highest level of undiagnosed diabetes – estimated at 60% of people with diabetes (IDF, 2019). According to regional type 1 diabetes data, Europe has the highest number of children and adolescents (0–19 years) with type 1 diabetes mellitus (T1DM) at 297,000, and 1 in 6 live births are affected by hyperglycaemia in pregnancy (IDF, 2019).

Most premature deaths and losses in productive life in diabetes are related to co-morbidities, for example metabolic and vascular complications. Diabetes causes the development of many complications such as (a) microvascular complications: neuropathy, retinopathy, diabetic kidney disease (DKD), and (b) macrovascular complications: cardiovascular disease (CVD) – coronary heart disease (CHD) and peripheral vascular disease such as limb claudication. Both types of vascular disease can decrease life expectancy in patients with diabetes. For instance, CVD is the major cause of mortality in T2DM individuals accounting for approximately 60-70% of deaths in diabetics within industrialised countries (Devereux, 2010). While DKD increases further the risk of death by 3 - 6 fold in advanced DKD, as demonstrated by measuring the decrease in GFR and development of end stage renal disease (ESRD) (Go et al., 2004). As this number continues to increase, there is an urgent need



to improve novel therapies for DKD and other diabetic complications. It has been around 20 years since the latest trials led to new drugs licensed for diabetic nephropathy and at present the average survival rate of patients with DKD is similar to that of the average survival rate of patients diagnosed with cancer (de Zeeuw and Heerspink, 2016).

#### **1.1.4 Diagnosis of diabetes mellitus**

As research advances, the traditional paradigms of type 2 diabetes mellitus (T2DM) prevalence being only in adults and T1DM arising only in children are no longer accurate, as both types can happen in both age groups (ADA, 2020a). Hence, it is important to distinguish between diabetes types due to the heterogeneous properties of T1DM and T2DM, where the clinical presentations and disease progression may vary considerably. Classification is essential to determine the right treatment. While with some patients, symptoms cannot clearly confirm a diagnosis of type 1 or type 2 diabetes. For instance, in patients with type 1 diabetes, the classic symptoms are polyuria (urinary frequency), polydipsia (excessive thirst), and about 30 % of patients present with diabetic ketoacidosis (DKA), which is caused by insulin deficiency, decreased glycolysis, and increased gluconeogenesis, leading to uncontrolled production of ketone bodies (Dabelea et al., 2014).

While in adults this is variable, they may not show the symptoms seen in children and may have temporary remission from the need for insulin (Humphreys et al., 2019, Hope et al., 2016). Sometimes, patients with T2DM may present with DKA (Zhong et al., 2018), especially patients from ethnic minorities (Newton and Raskin, 2004). Although it is difficult to differentiate diabetes type, the diagnostic criteria become more recognisable over time.

Diabetes is diagnosed depending on plasma glucose criteria (PGC), based on the fasting plasma glucose (FPG) or the 2-hour plasma glucose (2-h PG) value following a 75 g oral glucose tolerance test (OGTT) or the glycated haemoglobin (HbA<sub>1c</sub>) test (ADA, 2020a) (Table 1.2). Diagnostic criteria for diabetes depending on glucose values involve a FPG  $\geq$ 126 mg/dL (7.0 mM) or 2-h PG  $\geq$  200 mg/dL (11.1 mM) during the OGTT (ADA, 2020a). These tests are used as well to diagnose either diabetes or prediabetes, along with some of the clinical case scenarios to classify the disease. Diagnosis of pre-diabetes is important to evaluate risk factors for potential diabetes by checking the impaired glucose tolerance (IGT) and impaired fasting glucose (IFG) functions. Criteria for identification of IGT and IFG are: IFG defined as FPG levels 100 mg/dL (5.6 mM) to 125 mg/dL (6.9 mM) and IGT as 2-h PG in the 75g OGTT 140 mg/dL (7.8 mM) to 199 mg/dL (11.0 mM) (ADA, 2020a). The risk of having T2DM depends on some factors such as: genetic, lifestyle and therapeutic intervention factors.

**Table 1.2: Diagnostic criteria for diabetes mellitus**

FPG $\geq$ 126 mg/dL (7.0 mM). Fasting is defined as no caloric consumed for at least 8 h. OR
2-h Plasma glucose $\geq$ 200 mg/dL (11.1 mM) during an OGTT. The test should be done as described by the World Health Organization (WHO), using a glucose load containing the equivalent of 75 g anhydrous glucose dissolved in water. OR
HBA <sub>1c</sub> $\geq$ 6.5% (48 mmol/mol). The test should be done in a laboratory using a method that is NGSP certified and standardized to the Diabetes Control and Complications Trial (DCCT) assay. OR
In a patient with classic symptoms of hyperglycaemia or hyperglycaemic crisis, a random plasma glucose $\geq$ 200 mg/dL (11.1 mM).

From (ADA, 2020a). \*In the absence of unequivocal hyperglycaemia, results should be confirmed by repeat testing.

### 1.1.5 Type 1 diabetes mellitus

T1DM – known also as insulin-dependent diabetes, is a chronic metabolic disorder caused by autoimmune destruction of pancreatic  $\beta$  cells which results in a deficiency of insulin secretion leading to hyperglycaemia. The onset of T1DM was previously considered to occur just in childhood, but this opinion has changed over the last decade, because it has been shown to occur at any age (Atkinson et al., 2014), although most frequently in young people. According to the IDF in 2019, globally there are 1,110,100 cases aged 0 - 19 years estimated to have T1DM. The European region has the highest prevalence of children and adolescents (0 - 19 years) with T1DM, with approximately 296,500 cases reported in 2019. The number of newly diagnosed children with T1DM is 31,100 each year in Europe (IDF, 2019). While the top 3 countries having the highest number of T1DM cases aged 0-14 years are India, the United States of America and Brazil, including both existing and newly diagnosed patients. In terms of incidence per 100 thousand population annually, Finland, Sweden and Kuwait have the highest incidence percentage of T1DM in the 0–14 years group every year (IDF, 2019). The clinical symptoms of T1DM are polyuria, increased thirst and weight loss, with most cases also presenting with DKA – production of high levels of ketone bodies (acetoacetate,  $\beta$ -

hydroxybutyrate) in the blood. In the UK nearly a quarter of first diagnoses of T1DM present with ketoacidosis (Lansdown et al., 2012), and this was similar in France (Choleau et al., 2015), Poland (Szypowska et al., 2016), the United States of America (Dabelea et al., 2014) and many other countries.

#### **1.1.5.1 Genetic factors**

Type 1 diabetes presents in some patients without any family history of the disease. Nearly 10 to 15% of cases have a relative with the disease. However, relatives of patients are at high risk of developing the disease, nearly 6% patients' children, 5% of their siblings and 50% of monozygotic twins develop the disease, compared to 0.4 percent prevalence in the general population (Beyan et al., 2012, Redondo et al., 2008). These values indicate a complex-trait pattern of disease inheritance, consisting of multiple genetic factors and environmental triggers. More than 50 genes that are associated with the development and pathology of T1DM have been identified by genome-wide association studies (GWAS) (Størling and Pociot, 2017). The major genes associated with predisposition to T1DM are the major histocompatibility complex (MHC), also called the human leukocyte antigen (HLA) complex which located on chromosome 6 (Noble and Valdes, 2011). HLA complex genes are responsible for nearly 40–50% of the genetic risk of the disorder and its progression. There are addition key susceptibility genes such as the insulin gene itself, the protein tyrosine phosphatase non-receptor type 22 (*PTPN22*), interleukin 2 receptor alpha (*IL2Ra*), the cytotoxic T-lymphocyte antigen 4 gene (*CTLA4*), and the vitamin D 1 alpha hydroxylase gene, (*CYP27B1*). Further genetic loci have been discovered that contribute to disease risk but with a lower prevalence level, whether alone or combined by other autoimmune disorders (Størling and Pociot, 2017, Aly et al., 2006).

#### **1.1.5.2 Environmental factors**

Separate from genetic factors, considerable research supports the role of exogenous risk factors in the onset of T1DM, for instance viral disease and toxic factors. Some types of viruses have been found to be environmental agents that cause T1DM by direct damage of  $\beta$ -cells or stimulating the release of islet antigens – examples include rubella, mumps, cytomegalovirus, rotavirus and enteroviruses (Bodansky et al., 1986, Helmke et al., 1986, Pak et al., 1988, Honeyman et al., 2000, Yeung et al., 2011, Hyöty and Taylor, 2002). Amongst chemicals factors, streptozotocin (STZ) and alloxan have been used in diabetes studies within animal species as inducers of T1DM (Szkudelski, 2001). Furthermore, dietary agents have been

identified and data indicate that gliadin (a protein present in gluten), bovine omega-3 fatty acids and some vitamins may associated with the risk of developing of T1DM (Serena et al., 2015, Ali, 2010). To date, no intervention has been discovered to avoid or delay the onset of T1DM disease (Skyler, 2015), and treatment is achieved by glucose control and insulin therapy. Individuals with T1DM are exposed to the risk of developing hyperglycaemia, ketosis and diabetic ketoacidosis and require regular exogenous insulin administration via injection (ADA, 2017).

### **1.1.5.3 Pathogenesis of type 1 diabetes mellitus**

T1DM develops mainly through autoimmune damage of pancreatic  $\beta$ -cells and insulin replacement treatment is vital for survival. Pathogenesis is a consequence of humoral and cellular autoimmune reactions that produce destructive antibodies and autoreactive T cell clones directed against key antigens from  $\beta$ -cells (Holt et al., 2011, Mallone and van Endert, 2008). Histological studies show that in patient with T1DM onset, pancreas biopsies demonstrate criteria for insulinitis (inflammation of pancreatic islet cells) along with infiltration of the islets of Langerhans by immune cells including T- and B lymphocytes, monocytes, and macrophages (Campbell-Thompson et al., 2013, Gepts and Lecompte, 1981, Hänninen et al., 1992). Autoantibodies and cytotoxic T cell responses trigger  $\beta$ -cell destruction. This initial pancreatic inflammation with increases in the mononuclear cell levels in the islets accompanied with decrease in beta-cells mass, subsequently leads to insulin production decrease. Consequently, several metabolic signs start to appear such as the steady decrease in the insulin response to glucose in the blood, impaired oral glucose tolerance also fasting hyperglycaemia (Holt et al., 2011, Eisenbarth, 1986).

This is known as ‘autoimmune’ T1DM. However, diagnosis of insulin-dependent disorders in some individuals can be confirmed without the presence of autoantibodies. This is characterized as ‘idiopathic’ T1DM (Seino et al., 2010). It commonly occurs in African-Caribbean individuals and is described by insulinopenia and/or ketoacidosis. In these cases, remission can occur, where the function of  $\beta$ -cells may resume and glycaemia may return to normal levels (Leu and Zonszein, 2010). In general, the progression and development of T1DM is affected by the titre and intensity of the autoantibodies, genetic susceptibility, and environmental triggers (Ali, 2010).

### **1.1.6 Type 2 diabetes mellitus**

T2DM is a chronic metabolic disease characterized by increased in glucose level caused by insulin resistance and progressively causes a loss of insulin secretion by pancreatic  $\beta$ -cells (ADA, 2020a). Type 2 diabetes is also known as non-insulin dependent diabetes (NIDDM) because individuals with T2DM do not require exogenous insulin for survival at onset but may require this later when metabolic control by diet and other medications are not sufficient without therapeutic insulin injections. This type of diabetes accounts for approximately 90% of all diabetes cases worldwide and its occurrence mainly in people over 40 years. Individuals with high IGT have a high risk of developing T2DM (Shaw et al., 1999). In 2019, 373.9 million people aged 20–79 years worldwide, 7.5% of the adult population, are expected to have IGT (IDF, 2019). This number is estimated to increase to 453.8 million (or 8.0% of the adult population) by 2030 and to 548.4 million (or 8.6% of the adult population) by 2045. People with T2DM usually remain undiagnosed over a period of years because hyperglycaemia develops gradually. As a result, at the time of diagnosis some patients have already developed early-stage vascular complications. Typical symptoms of T2DM are similar to those of T1DM but less dramatic and the cases may be totally symptomless. The common symptoms may include increased thirst, blurred vision, feeling tired and slow healing of cuts or wounds, while ketoacidosis is not common in T2DM.

#### **1.1.6.1 Genetic factors**

Type 2 diabetes is heterogeneous, complex trait disorder caused by genetic and environmental risk factors. Studies of concordance suggest that heritability for T1DM was greater than that for T2DM, where the contribution of both genetic and environmental effects have the same significant risk of developing the disease (Kaprio et al., 1992). A positive family history of type 2 diabetes increases the risk of developing the disease in offspring (Stumvoll et al., 2005). For example, 15 - 25% of first degree relatives of individuals with T2DM develop IGT or diabetes (Pierce et al., 1995), and when both parents are affected by T2DM, the risk of developing T2D is the disease increases to 70% (Fonseca and John-Kalarickal, 2010). GWAS have systematically revealed more than 400 genetic loci linked to T2DM, mainly in populations of Europeans (Scott et al., 2017, Mahajan et al., 2018), Asians (Imamura et al., 2016), while more limited studies have been carried out in Hispanics/Latinos (Qi et al., 2017, Parra et al., 2011) and African-Americans (Palmer et al., 2012, Ng et al., 2014).

In particular, some of the genetic mutations with strong association with type 2 diabetes include: glucose transporter isoform-2 (GLUT-2) which is responsible for transport of glucose into pancreatic beta cells and consequently prompting the insulin secretion cascade (Dupuis et al., 2010), peroxisome proliferator-activated receptor  $\gamma$  (PPAR  $\gamma$ ) – a transcription factor which regulates fatty acid storage and glucose metabolism, insulin receptor substrate 1 (IRS1) which is part of the insulin signalling cluster and decreases insulin sensitivity (Voight et al., 2010), transcription factor 7-like 2 (TCF7L2) which affects insulin secretion and glucose production (Cauchi et al., 2007), and calpain-10 (CAPN10) which is associated with type 2 diabetes risk in Mexican-Americans (Tursinawati et al., 2020).

### **1.1.6.2 Environmental factors**

Environmental risk factors react strongly with susceptibility genes and have been studied and very clearly demonstrated. There are many environmental risk factors linked to the aetiology of T2DM such as obesity, sedentary lifestyle, unhealthy diet and mothers with history of GDM. Many studies reported that obesity with body mass index (BMI)  $\geq 30$  kg/m<sup>2</sup>, is a major independent risk factor for T2DM regardless of genetic predisposition (Schnurr et al., 2020). The main cause of fat obesity, and consequently glucose tolerance, is the dietary energy supply whereby increasing fat and simple sugar consumption and lowering starch and fibre intake reduces glucose tolerance (Ozougwu et al., 2013). Large number of studies showed that lack of physical activity increases the risk of developing T2DM, while physical activity has been found to enhance insulin sensitivity, improve abnormal glucose tolerance and insulin resistance, enhance glucose uptake by muscle cells and reduce intra-abdominal fat deposition (Garcia-Hermoso et al., 2014, Shakil-ur-Rehman et al., 2017). Recent studies have reported that intensive lifestyle modifications have been effective in preventing T2DM on subjects aged 23 to 67 years who were at high risk of developing the disease - the study used 6 month mobile-based intervention techniques in trying to change behaviour to promote dietary and physical activity, this study group reported a significant decrease in energy, fat, and carbohydrate intake compared with the control group (Xu et al., 2020b).

In relation to the diet, nutrition of pregnant mothers and/or lactation may affect disease susceptibility of the offspring early in their lives and during adulthood (Poher et al., 2016, Wang, 2013). For instance, poor maternal nutrition and shorter length of breastfeeding increase the infant risk for obesity and diabetes (Bider-Canfield et al., 2017, Gunderson et al., 2018). In addition, consuming a high-fat diet during pregnancy plays a role as a factor that increases the

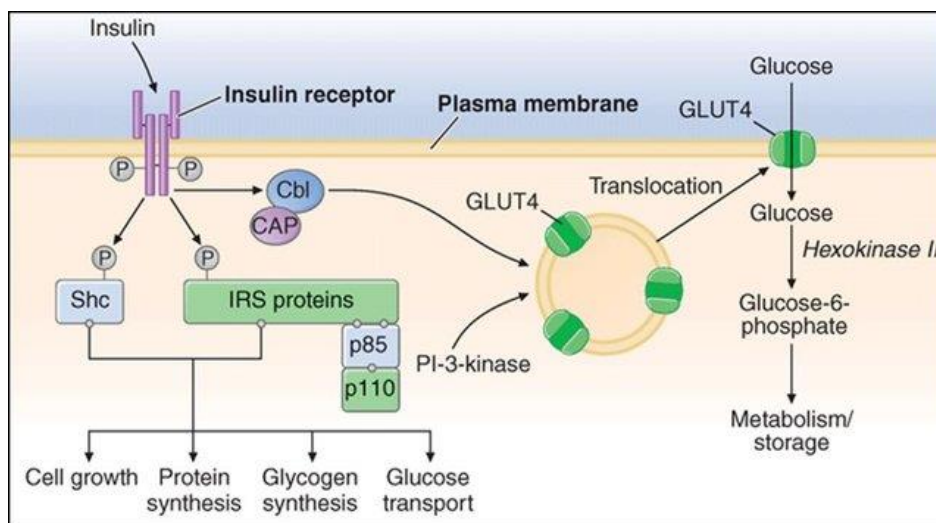
risk of metabolic syndrome occurring in offspring, including adiposity, impaired insulin and glucose tolerance in studies conducted in mice (Vuguin et al., 2013). Insufficient consumption of specific micronutrients, like vitamin B12 which is essential for both pregnant and lactating women, increases the risk of T2DM in offspring later in their lives (Yajnik et al., 2008, Stewart et al., 2011). Another study found that lower serum B12 and folic acid levels are associated with higher obesity and insulin resistance during pregnancy in a non-diabetic subjects (Knight et al., 2015). Moreover, in pregnant mothers who were diagnosed with gestational diabetes during the second half of pregnancy, their infants were subsequently found to be at higher risk of developing obesity and T2DM (Nehring et al., 2013).

### **1.1.6.3 Pathogenesis of type 2 diabetes mellitus**

T2DM develops more slowly than T1DM, and in T2DM the clinical symptoms develop gradually. In T2DM, the pathological sequence is complex and includes many different elements that accumulate and act in concert to give rise to the full disorder. In T2DM, abnormalities in insulin action and later insulin secretion are associated with the pathogenesis of the disease. However, it is clear from the clinical studies that type 2 diabetes initially presents with insulin resistance. Before the onset of the disease in the stage of pre-diabetes, individuals have normoglycaemia but hyperinsulinemia where the pancreas is trying to compensate for insulin resistance by secreting more of the insulin hormone itself. Therefore, individuals progress to IGT later with mild postprandial hyperglycaemia. Over time, pancreatic  $\beta$ -cell function fails and insulin secretion declines, causing persistent hyperglycaemia. Contributing to this there are some pathophysiologic abnormalities associated with the development of T2DM, such as: elevated free fatty acid levels, increased inflammatory cytokine levels, raised adipokines, mitochondrial dysfunction in relation to insulin resistance, and glucotoxicity & lipotoxicity.

To understand the mechanisms of insulin resistance, many studies have been carried out. The insulin receptor (IR) is a plasma membrane glycoprotein consisting of two extracellular  $\alpha$ -subunits and two transmembrane  $\beta$ -subunits which are linked by disulphide bridges. Along the insulin signalling pathway, insulin interacts with the target cells by binding to the  $\alpha$ -subunit of the IR which triggers the activation of tyrosine kinase activity in the  $\beta$ -subunit, which in turn results in the autophosphorylation of the  $\beta$ -subunit (Figure 1.1). Accordingly, the activation of  $\beta$ -subunit leads to phosphorylation of the insulin receptor substrates IRS-1 and IRS-2. IRS phosphorylation is found to be impaired in the adipocytes and

skeletal muscle cells of patients with T2DM (Danielsson et al., 2005). Phosphoinositide-3(PI3)-kinase, which plays a key role in the insulin-stimulated translocation of the glucose transporter type 4 (GLUT4) and glycogen synthase activation, is activated by binding to tyrosine-phosphorylated IRS-1 and IRS-2 molecules. The activity of PI3-kinase was found to be inhibited in muscle of T2DM subjects (Thies et al., 1990, Cusi et al., 2000). In addition, the initial mechanism of insulin action involves stimulating glucose transport into muscle and fat cells by translocation of the GLUT4, from intracellular vesicles to the cell surface (Zisman et al., 2000). In patients with T2DM, while the expression of GLUT4 was normal, there was found to be impaired translocation of this transporter to the plasma membrane. This is probably caused by impaired cell signalling or dysfunctional proteins involved in the translocation process, because gene polymorphism & expression, and muscle protein levels of GLUT4 were normal (Kelley et al., 1996, Kruszynska and Olefsky, 1996).



**Figure 1.1: Mechanism of action of insulin**

Adapted from (Ingle et al., 2018).



## **1.2 Complications of diabetes**

### **1.2.1 Acute complications**

Acute diabetic complications occur abruptly in the short term and can happen at any point during the patient's lifetime, therefore prompt medical attention and medical surveillance is often required. Acute complications, which can be life-threatening include DKA, hyperosmolar non-ketotic coma, lactic acidosis and hypoglycaemia.

DKA is a serious metabolic complication of diabetes characterised by low insulin levels with significant hyperglycaemia. With the lack of insulin-mediated glucose delivery, the adipose tissues mobilise stored energy and release free fatty acids (lipolysis), which the liver transforms into ketone bodies as an energy source, therefore these bodies reduce blood pH, causing hyperketonaemia and acidosis. This condition is much more common in T1DM than T2DM. Proper and fast treatment of DKA usually leads to a full recovery, while poor glycemic control and delayed treatment may progress to cerebral oedema or death.

Hyperosmolar non-ketotic coma is an acute complication with similar symptoms to DKA but is an entirely different condition that needs a different treatment regime. It more commonly occurs in individuals with T2DM and is characterised by severe hyperglycaemia resulting in dehydration, increased blood osmolarity, stupor and coma but without ketosis or acidosis. As with DKA, fast medical treatment is important, starting with fluid volume replacement. Correction of hyperglycaemia needs to be handled carefully, as it may progress to cerebral oedema if it occurs too rapidly.

Lactic acidosis is a condition associated with the excessive lactic acid accumulation in blood, leading to acidosis without any significant ketoacidosis. It is caused by the imbalance between increased formation and impaired metabolism/decreased clearance of circulating lactate and hydrogen ions (DeFronzo et al., 2016). Some risk factors increase the incidence of lactic acidosis by increased lactate production (for instance, cardiac failure and pulmonary disease), reduced lactate metabolism (for instance, hepatic failure) and reduced metformin and lactate excretion (e.g. in renal failure) (Seetho and Wilding, 2014). Cerebral oedema can occur if treatment of acidosis and electrolyte imbalance is too rapid, and so careful treatment is required.

Hypoglycaemia is the condition that develops when blood glucose is lower than the normal level (less than 4 mmol/L or 72 mg/dL). Hypoglycaemia is more common in people with T1DM that regularly inject insulin, followed by people with T2DM using insulin, and T2DM patient treated with sulfonylurea drugs such as gliclazide (Diana Sherifali and Robyn,

2018). Some risk factors are associated with hypoglycaemia such as increased age, erratic diet, and use of beta blocker drugs such as atenolol.

### **1.2.2 Chronic complications**

Chronic complications of diabetes increase the incidence of secondary comorbidities and increase the mortality rate of diabetic patients (they are also known as long-term complications). Hyperglycaemia can either damage large blood vessels causing macrovascular complications or damage small blood vessels causing microvascular complications.

### **1.3 Diabetic macrovascular complications**

The main pathological mechanism underpinning macrovascular diabetic complications is characterised by atherosclerosis, which leads to narrowing of arterial walls. Atherosclerosis is caused by chronic inflammation, plaque formation and damage to the arterial walls in the peripheral and/or coronary vascular systems (Fowler, 2011). Depending on the location of the atherosclerotic damage, different types of macrovascular diseases arise such as: peripheral vasculopathy (e.g., limb claudication), cerebrovascular and CVD.

#### **1.3.1 Peripheral vascular disease**

Peripheral vascular disease (PVD), also known as the peripheral arterial disease, is a common circulatory disease characterised by occlusion of the peripheral arteries and caused by atherosclerosis, or vasospastic disorders (frequent vascular smooth muscle spasms that cause vasoconstriction in the small blood vessels). PVD is caused by the development of the atheroma (fatty deposits) inside the arterial walls, narrowing the lumen of the arteriolar vessel and consequently obstructing blood flow to the affected tissues. This mainly affects the distal limb vessels such as the tibial and peroneal arteries. Typical symptoms of PVD is intermittent claudication, which involves pain in limb muscles when walking that resolves during rest (Lane et al., 2017). Complications may progress to critical limb ischemia or infection which may lead to tissue necrosis, requiring amputation.

Epidemiological studies confirmed the correlation between PVD and diabetes. The risk of PVD is increased in diabetic patients even in the absence of coronary heart disease (Wilcox et al., 2018). In addition, patients with peripheral arterial disease and diabetes are 5 times more likely to develop critical limb ischemia, while about twice as likely to develop intermittent claudication (leg pain when walking and caused by narrowed blood vessels in the lower limbs and poor blood circulation to the muscles) compared with non-diabetic patients (Norgren et al.,

2007). Moreover, a study found that for every 1% increase in glycosylated haemoglobin there was a related 26% increased risk of peripheral arterial disease (Selvin et al., 2004).

The need for an amputation in relation to diabetes is increased in the UK, where diabetic patients are 20 times more likely to require an amputation than non-diabetic patients. Blood circulation is poor in diabetic patients, causing ulcers that do not heal and infections, leading to gangrene, which would then necessitate amputation. According to a study by Vadiveloo *et al.*, the risk of having foot ulceration increased by 15% and 34% in patients with diabetes, with more than 50% of those developing an infection that may cause a lower extremity amputation and premature death (Vadiveloo et al., 2018). Lower extremity amputation greatly affects the psychology and quality of life of diabetic patients (Garcia-Morales et al., 2011, Laiteerapong et al., 2011), causing premature mortality in some cases (Hambleton et al., 2009, Armstrong et al., 2007, Laiteerapong et al., 2011).

### **1.3.2 Diabetic cardiovascular disease**

Cardiovascular complications of diabetes, driven by the increased development of atherosclerosis, are the main cause of morbidity and mortality annually around the world. At a younger age, patients with diabetes are two to three times more likely to have CVD than non-diabetic individuals (IDF, 2020). Moreover, a systematic review by the IDF concluded that around 9–41% of middle-aged diabetic patients (49–69 years) of middle and high income countries are estimated to have CVD (IDF, 2020). Mechanisms of cardiovascular disorder in diabetes have been investigated and there are many interacting processes that are implicated in the development of this complication. Among these pathophysiological mechanisms, endothelial and smooth muscle cell dysfunction, platelet hyperactivity, and fibrinolysis are implicated, in addition exposure to thrombosis and susceptibility to inflammation. The major mechanism of CVD is vascular endothelial dysfunction. Endothelium is a single layer of endothelial cells that located in the inner surface of the blood vessel lumen, this layer forms an interface between the blood and the vessel wall. These cells operate specific functions that include:

- (1) regulating the tone of the underlying vascular smooth muscle cells including fluid filtration, haemostasis, neutrophil recruitment to damaged tissues, and hormone trafficking.
- (2) providing a link between blood and tissue that controls blood pressure, nutrient delivery and immune response during inflammation.

(3) secretion of humoral factors, such as Von Willebrand factor, that act as cofactors for activating antithrombin in the coagulation cascade.

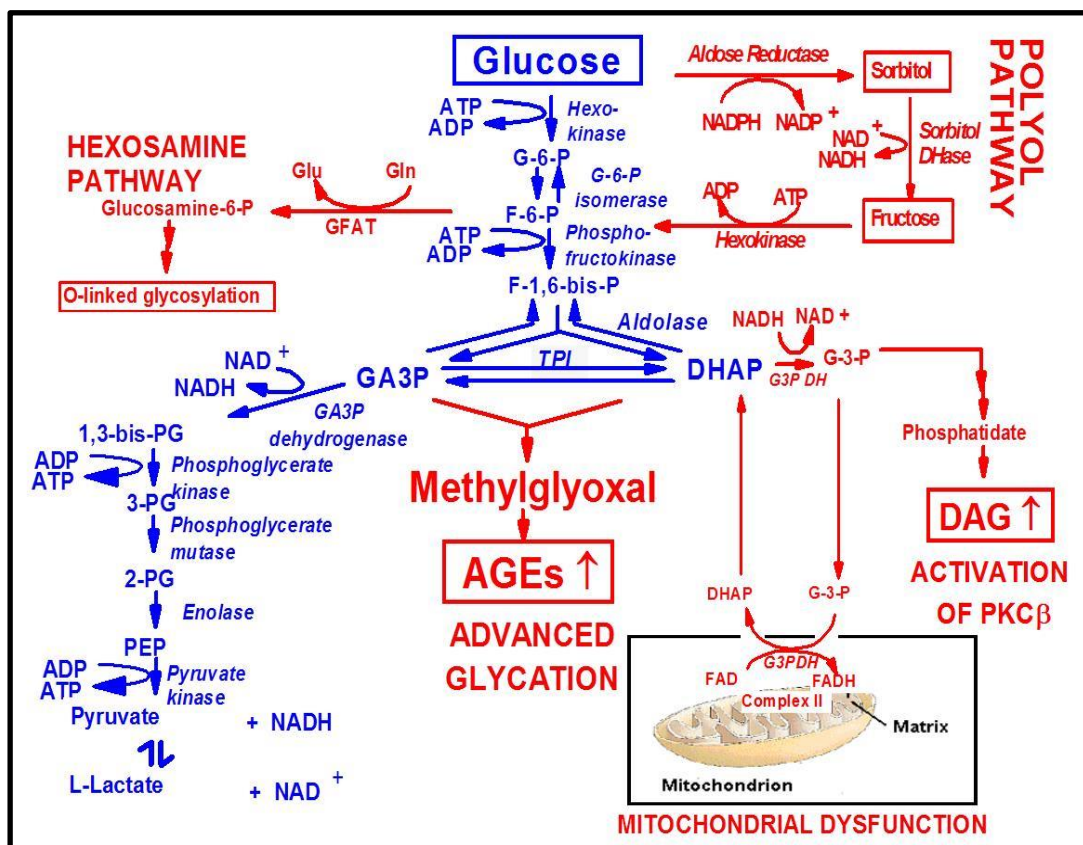
(4) performing a vital role in the structure and function of blood vessels through production of crucial bioactive elements such as endothelium-derived relaxing factors, including nitric oxide (NO), prostaglandins, vasoactive factors such as endothelin, angiotensin II and reactive oxygen species (ROS).

Due to these crucial roles, any dysfunction in these cells can lead to serious health problems in the body.

Endothelial dysfunction is the condition where maintaining vascular permeability, blood rheology and homeostasis has failed. Endothelial damage can be characterized by deficiency in NO levels and results in increased superoxide anion ( $O_2^-$ ) release (Roe and Ren, 2012). This step is considered to be an early stage in atherosclerosis. In diabetes, high glucose concentration causes a deficiency in NO production and increases in superoxide release (De Vriese et al., 2000). Excess glucose also causes increases in fatty acid uptake and oxidation (Finck et al., 2003), with increased oxidation of free fatty acids there is increased formation of ROS as demonstrated by activation of protein kinase C (PKC) and the appearance of advanced glycation endproducts (AGEs). Hyperglycaemia also induces the production of endothelin-1 through the activation of the endothelin-A receptor; angiotensin II and endothelin-1 cause vasoconstriction (Böhm and Pernow, 2007, Li et al., 2013a). The effect of endothelin-1 also includes the progression of myocardium – the muscular middle layer of the wall of the heart - hypertrophy by activating the renin-angiotensin system which increases water and renal sodium retention (Colafella et al., 2019). Hyperglycaemia escalates the development of atherosclerosis via promotion of ROS and AGEs production, decreased endothelial NO synthase activity, activation of NF- $\kappa$ B and increased polyol pathway flux, where the excessive intracellular glucose is reduced via the action of aldose reductase to generate alcohol (sorbitol) which is subsequently oxidized to fructose. Sorbitol is hydrophilic and does not diffuse easily through cell membranes and accumulates intracellularly, therefore cellular osmolarity increases, causing cell damage. Meanwhile, fructose formed by this pathway can become phosphorylated to produce glyating agents that participate in the formation of AGEs. Ultimately hyperglycaemia induces overexpression of intercellular adhesion molecules (ICAMs) and inflammatory cytokine expression (Yuan et al., 2019). An

overall mechanism underpinning hyperglycaemia and metabolic dysfunction is illustrated in Figure 1.2.

Hyperglycaemia is usually associated with dyslipidaemia, proinflammatory mediators like tumour necrosis factor- $\alpha$  (TNF- $\alpha$ ) and this increases the adhesion & accumulation of macrophages in the sub-endothelial space that internalize oxidized-low density lipoprotein (ox-LDL). Subsequently, macrophages engulf ox-LDL to produce foam cells and the accumulation of these cells forms fatty streaks as an early atherosclerotic lesion. In addition, secretion of matrix metalloproteinases, collagen degradation, increased migration of vascular smooth muscle cells & endothelial cells, all cause atherosclerotic plaque formation (Forbes and Cooper, 2013, Tuttolomondo et al., 2012).



**Figure 1.2: Explanation of metabolic dysfunction participated in hyperglycaemia inducing diabetic complications. Adapted from (Babaei-Jadidi, 2003).**

— The Embden–Meyerhof pathway (Glycolysis), the conversion of glucose to intermediate (glucose-6-phosphate) followed by conversion of the intermediate into pyruvate. — Biochemical disfunction in hyperglycaemia, increased polyol pathway activity, increased hexosamine pathway activity, activation of PKC, increased oxidative stress and increased formation of advanced glycation end products.

### **1.3.3 Cerebrovascular disorders**

Cerebrovascular conditions are one of the main causes of morbidity and mortality in diabetic patients. These are a group of brain dysfunctions linked to reduced or blocked circulation to the brain. It is caused by pathologic alterations in blood vessels at different locations and can lead to stroke when cerebral vessels are directly affected. Earliest linking of diabetes as a potent risk factor for stroke was seen in 1968 in the Honolulu Heart Study (Burchfiel et al., 1994). Since then, many studies have demonstrated that stroke is considered as a significant complication of diabetes in different populations (Kissela et al., 2005, Zabala et al., 2020). In addition the association between duration of diabetes and risk of stroke has recently been investigated, where longer duration increases the risk of stroke in diabetic patients (Ashburner et al., 2016, Kim, 2020). Even prediabetes cases have a higher future risk of developing stroke (Lee et al., 2012). Stroke is the most common form of cerebrovascular event. Despite findings that mortality rates caused by stroke decreased worldwide, its incidence has substantially increased throughout the past three decades (Benjamin et al., 2019). Type 2 diabetic patients usually have co-morbidities that increase the risk of stroke such as obesity, hypertension and dyslipidaemia (Dutton and Lewis, 2015).

The key pathological basis of cerebrovascular disorders is atherosclerosis through narrowing of the arterial walls within the body and the brain. As described in the previous section, this starts with endothelial inflammation and damage, oxidised lipids from LDL which then accumulate in the endothelial part of the vessel wall (Cohen, 2006). Macrophages then moves to the arterial wall, which accumulate oxidised lipids to produce foam cells which can activate T-lymphocytes. Subsequently, these T-lymphocytes encourage the spread of smooth muscle inside the arterial walls and collagen accumulation. Ultimately this causes the formation of a lipid dense atherosclerotic plaque accompanied with fibrosis. In patients with diabetes, in addition to the atheroma development, other lesions can form through platelet adhesion, coagulation, increases in local NO and ROS formation (Demarin et al., 2006, Spiess et al., 2018). Damage to blood vessels in this way can cause ischaemic stroke through thrombus formation that can occlude cerebral arteries, or haemorrhagic stroke through rupture of damaged cerebral blood vessels.

## **1.4 Diabetic microvascular complications**

Diabetic microvascular complications develop through persistent hyperglycaemia-driven damage of the smaller blood vessels in the body, especially capillaries. Microvascular complications target a particular subtype of cells including retinal cells (capillary endothelial cells, pericytes and neuroglial cells) consequently leading to retinopathy; renal cells (mesangial cells, podocytes, tubular epithelial cells and glomerular endothelial cells) causing diabetic kidney disease; neuronal cells (Schwann cells and peripheral neurones) causing neuropathic disease which can lead to severe infections, lower limb amputation, and impotence.

Indeed, microvascular endothelial cells are thought to be major targets of hyperglycemic damage because these cells cannot downregulate glucose transport rates when blood glucose concentration is elevated, resulting in intracellular hyperglycemia. Furthermore, these cells are thought to be major targets of hyperglycemic damage due to major dependence on facilitated diffusion uptake of glucose by the glucose transporter 1 (GLUT1). Therefore, high blood glucose in diabetes causes high cytosolic glucose concentrations which in turn lead to dysregulation of glucose metabolism (Brownlee, 2005).

### **1.4.1 Diabetic neuropathy**

Diabetic neuropathy is a common complication of diabetes that affects more than 50% of the estimated 460 million people worldwide with diabetes (Saeedi et al., 2019). Diabetic neuropathy involves a wide spectrum of clinical syndromes that influence various regions of the nervous system, including proximal and distal peripheral sensory, motor nerves, and the autonomic nerves. Depending on the symptoms, anatomical region and distribution, it is divided into categories. Different diabetic neuropathies include diabetic peripheral neuropathy (DPNs) affecting the hands and lower limbs, autonomic neuropathies affecting the internal organs to cause cardiac autonomic neuropathy, gastrointestinal dysmotility, diabetic cystopathy and impotence. Focal neuropathies can occur, despite not being a common form of diabetic neuropathy, and involve dysfunction of single peripheral nerves causing isolated mononeuropathies, or less commonly to nerve roots leading to radiculopathy or polyradiculopathy (Feldman et al., 2019).

Typical DPN, also known as symmetrical polyneuropathy, is the most frequently occurring type of DPN. It is linked to persistent hyperglycaemia, metabolic dysfunctions and cardiovascular risk factors. Clinical symptoms are varied depending on the class of sensory fibres affected. The common symptoms of small fibre involvement include neurogenic pain,

dysesthesias and vibration commonly experienced in the feet. While the involvement of large fibres might cause numbness and tingling. Many pathways for the pathological mechanisms have been found in the aetiology of diabetic neuropathy such as: oxidative-nitrosative stress, dicarbonyl stress, polyol pathway dysfunction, AGEs, and activation of the PKC and hexosamine pathways (Bierhaus et al., 2012, Yagihashi et al., 2011). Further factors considered to be important in the pathogenesis of diabetic neuropathy are: alterations in endoneural metabolism, defective neurotrophic factors, inadequate blood supply to the nerves, and also immune dysfunction (Siemionow and Demir, 2004). Such as with other microvascular complications, risk factors for developing diabetic neuropathy is linked to the duration of diabetes and also, some patients are genetically susceptible (Fowler, 2011). Studies have found that the best way to avert diabetic peripheral neuropathy is to achieve stable glycaemic control (Farvid et al., 2011). This is was demonstrated by the DCCT, in that intensive glycaemic control in patients with T1DM reduced the occurrence and progression of diabetic neuropathy by 60% (DCCT, 1993).

#### **1.4.2 Diabetic retinopathy**

Diabetic retinopathy is a common complication of diabetes and characterised by a spectrum of retinal microvascular lesions. These involve increases in vascular permeability, capillary degeneration, micro-aneurysm formation and excessive neovascularisation. It remains the primary cause of blindness among working age diabetic patients and has many visual or ophthalmic symptoms before development of full visual loss (Fong et al., 2004, Zhang et al., 2010). The disease affects nearly 80% of patients with diabetes for 20 years or more (Kertes and Johnson, 2007). While at least 90% of the new incidents can be decreased by treatment and regular monitoring of the eyes (Tapp et al., 2003), in patients with T2DM, nearly 20% have already developed diabetic retinopathy at the time of diagnosis. In patients with T1DM it is rare to develop severe blindness in the first five years after diagnosis. However, most people with T1DM and T2DM develop retinopathy after 15 years of diagnosis.

Symptoms progress from mild, non-proliferative diabetic retinopathy (NPDR), moderate NPDR, severe NPDR, proliferative diabetic retinopathy (PDR), advanced diabetic eye disease and diabetic maculopathy (Donnelly et al., 2000). The first three stages of NPDR, the mild, moderate and severe usually show no symptoms. The first stage is mild NPDR described by haemorrhages, microaneurysms along with minor intraretinal microvascular abnormalities but without affecting on the macula. This progresses to the moderate NPDR



accompanied by extensive microaneurysms, intraretinal microvascular abnormalities and hard exudates. Then there is the severe NPDR in which many more blood vessels are blocked, developing cotton wool spots, large blot haemorrhages and hard exudates. (Fong et al., 2004, Zhang et al., 2010). Advanced stage, proliferative diabetic retinopathy, where symptoms first appear, is characterised by angiogenesis - the formation of new blood vessels on the retina and posterior surface of the vitreous layer (Fong et al., 2004), patients experience in this stage floaters and sudden vision loss. Severe loss of vision happens in the stage of advanced diabetic eye disease, where fibrovascular proliferation occurs, with tractional retinal detachment, vitreous haemorrhage and thrombotic glaucoma. The last grade is known as diabetic maculopathy and is characterised by leakage in macular area of the eye (macular edema), thickening of the retina, microaneurysms, capillary occlusion along with hard exudates and blurred vision. Patients experience difficulty in performing things like reading & driving and in severe cases it leads to total, irreversible vision loss (Tariq et al., 2013).

Much research has identified factors linked to the development of diabetic retinopathy including duration of diabetes, along with glycaemic control, dyslipidaemia, hypertension, obesity and positive family history of diabetes (Alhowaish, 2013, Raman et al., 2014). To avoid diabetic retinopathy, control and treatment of these linked factors is as essential as good glycaemic control (Xu et al., 2012, Hu et al., 2015, Raman et al., 2014). Pregnancy might be a risk factor developing diabetic retinopathy because of the change in hormones, the systemic vasculature and retinal autoregulatory mechanisms (Mallika et al., 2010). Early diagnosis of diabetic retinopathy and treatment by use of laser photocoagulation is effective in slowing the progression of the disease and reducing visual loss but does not fully restore vision impairment (Fong et al., 2004).

### **1.4.3 Diabetic kidney disease**

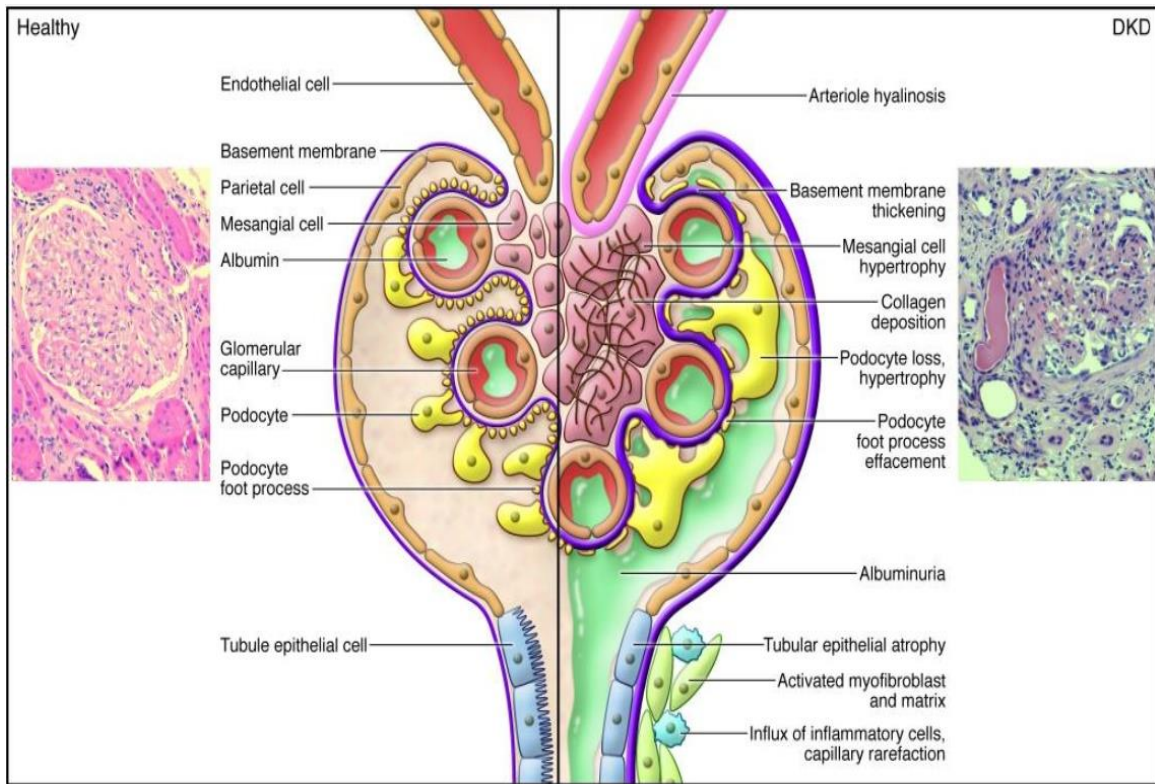
Diabetic kidney disease (DKD), also known as diabetic nephropathy, is a progressive kidney disorder in people with diabetes caused by angiopathy of the capillaries in renal glomeruli. It is associated with poor glycaemic control and is the main reason for dialysis worldwide. DKD is characterized by a sequence of structural and functional changes in the kidneys of patients with diabetes. The structural abnormalities involve renal hypertrophy, mesangial expansion, thickening of glomerular basement membrane, tubular atrophy, interstitial fibrosis, diffuse and nodular glomerulosclerosis and arteriosclerosis

(Pourghasem et al., 2015). Figure 1.3 illustrates healthy compared with diseased kidney in DKD.

People with T2DM should have urinary measurements every year after they are diagnosed, while those with T1DM are recommended to start 5 years after diagnosis (Lewis and Maxwell, 2014). DKD is the most common cause of end stage renal disease (ESRD), cardiovascular disease and mortality worldwide, resulting in a huge economic burden. Epidemiological studies have shown that a high incidence of cardiovascular disease is associated with the combination of ESRD and diabetes (WANG, 2011, Chang et al., 2014). An estimate by the Global Burden of Disease study indicated that nearly 1.2 million patients were known to have died of chronic DKD in the year of 2015 (Wang et al., 2016). While more than 2 million people died prematurely in 2010 because they could not access dialysis or renal transplantation – and this was mostly in low- and middle-income countries in Asia, Africa, Latin America and the Caribbean (Liyanage et al., 2015).

However, data of recent studies have linked the progression of DKD to a host of risk factors such as: duration of diabetes, hypertension, gender, environmental factors, regional differences, genetic susceptibility and glycaemic control. The risk of DKD increases with the duration of diabetes, as the patients live longer with diabetes. Hypertension plays an important role in the development of DKD (Eknoyan et al., 2013). To slow DKD development it is important to control hypertension, as this will reduce death risk among patients with the disease. Hypertension is present in nearly 90% of patients with advanced kidney disease (Eknoyan et al., 2013). The population burden of DKD is correlated with socially defined considerations in many societies around the world. For instance, racial/ethnic minority groups and low-income populations with DKD who are living in high-income countries suffer with poorer hypertension control than their more socially advantaged counterparts (Plantinga et al., 2009).

Recent studies have found an association between apolipoprotein L1 (APOL1) risk variants and development of kidney disease between populations of African ancestry (Peralta et al., 2016, Parsa et al., 2013). Furthermore, the role of genetic background in susceptibility to developing the disease was proven by high concordance in the severity of nephropathy and patterns of glomerular lesions observed in T1DM siblings, even when there was a lack of concordance of glycaemia (Fioretto et al., 1999). In relation to gender, males show a greater risk of developing DKD.



**Figure 1.3: Pathological lesions of DKD.**

Adapted from (Reidy et al., 2014).

#### **1.4.3.1 Diagnosis of DKD**

The progression of DKD involves increased albumin in the urine. Therefore, it is diagnosed easily, depending on the measurement of urinary excretion of albumin which passes through different phases. Urinary excretion of albumin starts at normoalbuminuria (<30 mg per 24 hour), then microalbuminuria (>30 – 300 mg per 24 hour) where it is an early stage of diabetic nephropathy called incipient diabetic nephropathy. This typically progresses after 10 – 15 years of diabetes, when microalbuminuria then progresses further to albuminuria (>300mg of albumin in urine per 23 hour) characteristic of overt nephropathy, occurring in 20 - 40% of diabetic patient during the subsequent 10 years. In the following 10 years, the patient is likely to show declining glomerular filtration rate (GFR) to a level <15 ml/min, and this outlines ESRD at which point the patient requires dialysis therapy and/or kidney transplantation. On average half of patients with diabetic nephropathy progress to ESRD (Fineberg et al., 2013, Parchwani and Upadhyah, 2012).

The GFR is considered the most robust marker of overall renal function (Levey and Inker, 2017) where the decline in GFR value is identified as a clinical endpoint of decline in kidney function, as well as albuminuria category. Table 1.3 classifies DKD based on the GFR rate and albuminuria category (Eknoyan et al., 2013). Estimated GFR (eGFR) is measured using different equations based on various markers, the most accurate equation based of the study of (White et al., 2019) was creatinine/cystatin C ratio (Cr/cysC). Table 1.4 outlines the eGFR equations developed by the chronic kidney disease & epidemiology collaboration group (CKD-EPI).

**Table 1.3: Prognosis of DKD by GFR and albuminuria category.**

				Persistent albuminuria measurement			
				Description and value range			
				A1	A2	A3	
				Normal to mildly increased	Moderately increased	Severely increased	
				<30 mg/g <3 mg/mmol	30 – 300 mg/g 3-30 mg/mmol	>300mg/g >30 mg/mmol	
GFR categories (ml/min/1.73 m <sup>2</sup> )	Description and range	<b>G1</b>	Normal to high	≥90			
		<b>G2</b>	Mildly decreased	60-89			
		<b>G3a</b>	Mildly to moderately decreased	45-59			
		<b>G3b</b>	Moderately to severely decreased	30-44			
		<b>G4</b>	Severely decreased	15-29			
		<b>G5</b>	Kidney failure	<15			

Green: low risk (if no other markers of kidney disease, no DKD); Yellow: moderately increased risk; Orange: high risk; Red: very high risk) From (Eknoyan et al., 2013).

**Table 1.4: eGFR equations**

eGFR-EPI	Equation Year	Equation
<b>Cr</b>	2009	$eGFR = 141 \times \min(Cr/\kappa, 1)^\alpha \times \max(Scr/\kappa, 1)^{-1.209} \times 0.993^{Age} \times 1.018 \text{ (for female)} \times 1.159 \text{ (for black)}$ Where $\kappa = 0.7$ for female or $0.9$ for male Where $\alpha = -0.329$ for female or $-0.411$ for male
<b>cysC</b>	2012	$eGFR = 133 \times \min(cysC/0.8, 1)^{-0.499} \times \max(cysC/0.8, 1)^{-1.328} \times 0.996^{Age} \times 0.932$ (if female)
<b>Cr/cysC</b>	2012	$eGFR = 135 \times \min(Cr/\kappa, 1)^\alpha \times \max(Cr/\kappa, 1)^{-0.601} \times \min(cysC/0.8, 1)^{-0.375} \times \max(cysC/0.8, 1)^{-0.711} \times 0.995^{Age} \times 0.969 \text{ (for female)} \times 1.08 \text{ (for black)}$ Where $\kappa = 0.7$ for female or $0.9$ for male

Key: Cr is the plasma creatinine (in mg/dL), cysC is the serum cystatin C (in mg/l) modified from (White et al., 2019).

### 1.4.3.2 Nephrons structure

For better understanding of DKD pathology, the structure of nephrons should be highlighted. The kidney is a highly vascularized organ, consisting of nearly one million nephrons in adult humans. The nephron is the principal structural and functional unit of the kidney involved in a remarkable diversity of physiological activities through various cell types. Each type of cells has a specific set of structural and functional characteristics. The glomerulus (plural: glomeruli), is a network of small blood vessels (capillaries), located at the beginning of each nephron unit in the kidney. Glomerular structure (illustrated in Figure 1.4) consists of:

**(i) Epithelial podocyte** (facing the urinary collection side)

Podocytes are very specialized epithelial cells because of their unique structure, surrounding the capillaries of the glomerulus leaving slits between them, and blood is filtered through these slits. This structure is vital in creating the selective permeability of the filtration barrier. Abnormality in this type of cells causes proteinuria - a feature of most glomerular diseases (Pavenstädt et al., 2003).

**(ii) Glomerular endothelial cells** (facing the blood circulatory side)

These cells occupy a large percentage of the capillary surface and play a vital role in driving the filtration process through the glomerular capillary wall due to their unique structure which includes many pores known as fenestrae. The important feature of this structure is to prevent the passage of protein out of the blood circulation as it passes through the glomerulus (Satchell and Braet, 2009). Reduction or loss of these fenestrations reduces the GFR and subsequently contributes to renal failure.

**(iii) Mesangial cells** (between the capillaries)

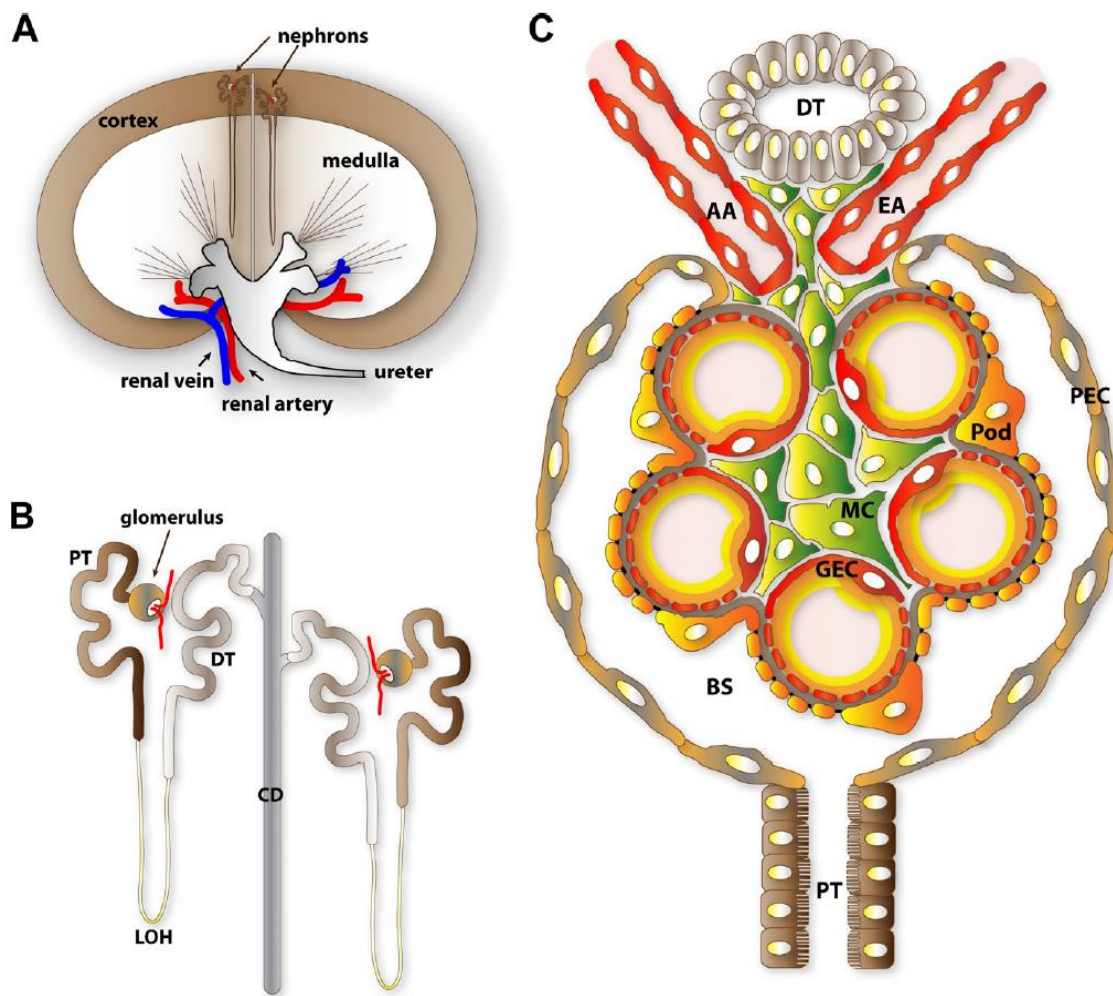
The other main feature of the glomerulus is the population of mesangial cells. Mesangial cells located inside the glomerulus and between the capillaries known as intraglomerular mesangial cells. While the extraglomerular mesangial cells are found outside of the glomerulus, in the space between the afferent and efferent arterioles and near to the vascular pole of the glomerulus (Barajas, 1997). Mesangial cells are quite irregular in shape and this gives them a contractile feature which is important to make them capable of sensing and altering the filtration pressure of the glomerulus.

#### **(iv) Glomerular basement membrane (GBM)**

The glomerular basement membrane (GBM) of the kidney is the basal lamina of the glomeruli. This layer consists of a three-layered extracellular matrix (ECM) which lies between the podocytes and the glomerular endothelial cells, and is responsible for plasma ultrafiltration.

The GBM is a very dynamic, highly charged structure that provides structural and biochemical support to the cells (Bosman and Stamenkovic, 2003), with differentiation in the molecular composition depending on the cell type and cell function in the kidney, and mainly acting in cell adhesion and cell-to-cell communication events (Abedin and King, 2010). ECM forms this layer of the GBM and lies between the podocytes and the glomerular endothelial cells. The ECM component is the selectively permeable glomerular filtration barrier that separates the vascular space from the urinary space (Miner, 2012). Thickening in the GBM is considered as one of the earliest detectable features of DKD. The ECM is present in:

- (i) The glomeruli within the GBM, Bowman's capsule and the mesangium.
- (ii) The tubulointerstitium tubular basement membrane, peritubular capillary basement membrane and interstitial ECM.
- (iii) In larger vessels, within and around the vessels (Genovese et al., 2014). These layers of the glomerular enable the flow of plasma water and small solutes while preventing the passage of large plasma proteins like albumin. The presence of high levels of albumin in the urine is an indicator of a failure in at least one of these layers.



**Figure 1.4: Anatomical outline of renal filtration**

A) This graphic illustrates kidney structure. Glomeruli, the filtration parts of nephrons, within the kidney cortex. (B) Structure of the nephrons. The vascularized glomerulus is found at the proximal end and is linked through renal tubules where urinary filtrate composition is refined through resorption and secretion. (C) glomeruli cells. GEC, glomerular endothelial cells; AA, afferent arteriole; EA, efferent arteriole; Pod, podocyte; MC, mesangial cells; PEC, parietal epithelial cells; PT, proximal tubule; DT, distal tubule; LOH, loop of Henle; CD, collecting duct; BS, Bowman's space. Adapted from (Scott and Quaggin, 2015).



### 1.4.3.3 Pathology of DKD

The pathogenesis of DKD is very complex. Progression of DKD in patients with diabetes depends on different factors between metabolic, hemodynamic and intracellular stress, which are usually affected by hyperglycaemia. Hyperglycaemia mediates dysfunction in intracellular metabolism at several checkpoints, including glycolysis, mitochondrial function, NADPH, increase in the accumulation of ROS, increased glucose flux by both polyol and hexosamine pathways, and accumulation of AGEs. Changes in intracellular homeostasis includes hypoxia, oxidative stress, also endoplasmic reticulum stress, and these are considered to be the main pathological features of DKD (Brownlee, 2005, Forbes and Cooper, 2013). This leads to the final process of dicarbonyl stress, an abnormal metabolic condition of perturbations in the balance of the reactive dicarbonyl metabolite methylglyoxal (MG), caused by increased formation and reduced metabolism/breakdown of reactive dicarbonyl metabolites. MG is known as the precursor of the main quantitative and damaging AGE in physiological systems, which is the arginine residue-derived adduct hydroimidazolone, MG-H1 (Thornalley et al., 2003). These stress pathways result in the up-regulation of transforming growth factor- $\beta$ 1 (TGF- $\beta$ 1) and this consequently mediates ECM synthesis. Moreover, hemodynamic alterations such as systemic and glomerular hypertension are linked with a hyperactive renin-angiotensin system and these have been extensively involved in the development of DKD (Brenner et al., 2001, Har et al., 2013). Angiotensin II is an essential regulator of kidney functions that sustain renal vascular resistance and arterial pressure. Increased in angiotensin II is implicated in the permeability induction of glomerular capillaries, preferential efferent arteriole constriction, along with stimulation of cell proliferation and ECM synthesis of mesangial cells (Dronavalli et al., 2008).

Until recently, DKD was known as a progressive microvascular complication that affects mainly the glomerulus. This commonly accepted view has now altered to include changes in all four renal subcomponents, involving glomeruli, tubules, interstitium and blood vessels. The main clinical pathologic features of DKD include constant albuminuria (proteinuria), reduction in the GFR, consequent damage in tubular cells, and tubulointerstitial lesions, ultimately causing renal failure (Parving et al., 1981, Nath, 1992, Burton and Harris, 1996, Abbate et al., 2006). Because of this, DKD is detected mainly based on the measurement of albuminuria. Another early histopathological hallmark of DKD is the progressive accumulation of ECM proteins initiating in the mesangium, then in the tubulointerstitium as the disease progresses (Najafian and Mauer, 2009). The major ECM proteins are: fibronectin,

laminin, collagens type I, III, IV and VI (Mason and Wahab, 2003). Accumulation of ECM leads to prominent alterations in the nephron structure, including mesangial expansion, accompanied with increased thickness of the GBM, followed by glomerular hyperfiltration, and increase in glomerular hydrostatic pressure, which drives microalbuminuria (Mason and Wahab, 2003). In diabetic conditions, high glucose concentration increases ROS production, which plays a vital role in the ECM generation and accumulation in the glomeruli and tubulointerstitium. This consequently drives the progression of renal fibrosis (Ha and Lee, 2005). Podocyte loss is also considered an early feature of DKD. Nakamura *et al.*, detected podocytes in the urinary sediment of diabetic individuals compared with healthy volunteers, where these cells were absent (Nakamura *et al.*, 2000). Another study conducted in rodents established that podocyte apoptosis increased dramatically in response to high glucose concentration in mice with either type 1 and type 2 diabetes (Susztak *et al.*, 2006). Damage to the GBM affects the flow and filtration of proteins in the bloodstream, by increasing permeability of different proteins, and this causes accumulation in Bowman's space in the distinct regions known as Kimmelstiel–Wilson nodules. In advanced stages of DKD, both diabetic glomerulosclerosis and interstitial fibrosis is present. Hyaline arteriosclerosis might be prominent within the glomerular tuft below the endothelial cells or the parietal epithelial cells (capsular drop) (Najafian *et al.*, 2015). Progression to ESRD, DKD stage 5 is indicated when  $GFR < 15 \text{ ml/min/1.73 m}^2$ .

#### **1.4.3.4 Treatment of DKD**

The level of failure in kidney function following the progression of nephropathy varies among diabetic patients and is affected by some factors such as blood glucose, blood pressure, lipid and albuminuria control. The efficacy of optimizing hyperglycemia in delaying the onset of microalbuminuria or macroalbuminuria is well-proven in many studies (Bilous, 2008, Holman *et al.*, 2008). In contrast, intensive glycaemia control in T2DM patients with DKD is associated with the risk of cardiovascular mortality, compared with standard glycaemia control. This is due to the risk of developing hypoglycemia which can increase the risk of death events (Papademetriou *et al.*, 2015). However, tight control of blood pressure in diabetes delays the development of DKD and cardiac diseases. Several studies advise the level of blood pressure to be 140/90 mmHg for diabetic individuals regardless of DKD (Pilmore *et al.*, 2014, James *et al.*, 2014). While patients who develop micro or macroalbuminuria are suggested a target of 130/80 mmHg (Ruzicka *et al.*, 2014). Studies showed that diabetic individuals with blood

pressure lower than 130/80 mmHg have the same decrease in GFR due to age as healthy subjects (Schrier et al., 2002, Giunti et al., 2006). This can be reached through dietary restriction, by reducing the consumption of salt – as many studies have demonstrated that high salt intake is associated with increased risk of DKD progression (Sugiura et al., 2018, Kang et al., 2021). The ADA recommends that nutritional sodium restriction to less than 2300 mg/day could be useful to control blood pressure (ADA, 2020b). In addition, blood pressure was significantly reduced in both T1DM and T2DM patients after following dietary salt restriction, and this was equivalent to that of single-drug treatment (Suckling et al., 2010).

Lipid management is also crucial in management of DKD, with many experimental investigations finding that circulating lipoproteins are linked to the progression of glomerulosclerosis and tubulointerstitial damage. The Study of Heart and Renal Protection (SHARP) trial evaluated the efficiency and safety of LDL-cholesterol lowering agents, simvastatin plus ezetimibe, in treatment of patients with moderate-to-severe kidney disease along with reducing the incidence of atherosclerotic events (Baigent et al., 2011). In addition, dietary protein restriction as being beneficial in delaying the progression of DKD is still controversial. Some studies suggest that a low dietary protein intake is linked with the improvement of GFR in patients with diabetic nephropathy (Nezu et al., 2013). In contrast, another trial study found no significant difference between low-protein diet (0.89 g/kg/day) and a normal-protein diet (1.02 g/kg/day) in 82 patient with T1DM with nephropathy (Hansen et al., 2002). Nevertheless, the majority of experts believe that a high-protein diet might exacerbate DKD disease. Therefore, according to ADA, the allowance for daily intake of protein is roughly 0.8 g/kg body weight per day (ADA, 2020b).

When diabetic patients develop microalbuminuria, the combination of antidiabetic with nephroprotective medication is required. Throughout the last two decades until recently, only medications that block the renin-angiotensin- system (RAS) have proven their nephroprotective effect on DKD, while many other trials failed to be effective (De Zeeuw et al., 2010, Parving et al., 2012). RAS medications were effective in reducing proteinuria, managing hypertension and reducing cardiovascular risk (White et al., 2005, Giovanna et al., 2012). Unless the patient with DKD suffer intolerance to this medication, angiotensin converting enzyme inhibitors (ACEIs) or angiotensin II receptor blockers (ARBs) are given, despite these medications being considered as secondary prevention of DKD development by ADA guidelines (ADA, 2020b). However, patients with DKD must also have at least annual measurements of renal function and urinary albumin to creatinine ratio (UACR).

Once ESRD has developed, patients need renal replacement treatment including hemodialysis, peritoneal dialysis, or kidney transplantation. Although constant dialysis is an option for patients to delay death, the survival of patients with diabetes by either haemodialysis or peritoneal dialysis is less than non-diabetic patients with ESRD in developed and developing nations (Mousavi et al., 2011, Schroijen et al., 2013). Treatment by dialysis is affected by some factors such as availability and convenience, socioeconomic and dialysis center factors, patient motivation, danger of infection, status of the peripheral vasculature to create adequate vascular access for hemodialysis, and status of the abdomen for peritoneal dialysis (Wauters and Uehlinger, 2004, McDonald et al., 2009, Mousavi et al., 2010, Tamadon and Beladi-Mousavi, 2013). Kidney transplantation is the preferred solution for diabetic patients with ESRD and is linked with a much better survival and quality of life compared with dialysis. Despite the fact that this therapy has been enhanced in recent years, strong rejection risks and complications linked with post-transplant steroid therapy have persisted. The use of ACE-Is and ARBs, however, is thought to address only 15% of the risk of progression of DKD. Consequently, DKD progresses in 50% of diabetic patients with diabetic nephropathy. The on-treatment mortality is high at 10 deaths per 100 patient treatment years, which is higher than on average for treatment of cancer. **Effective treatment of DKD therefore remains a major unmet need.**

#### **1.4.3.5 Cellular models of DKD**

Cell culture systems have been employed in many studies to evaluate the effect of hyperglycemia on cellular proliferation and protein function to avoid the implications of performing these studies on animals (Park et al., 2001, Peres et al., 2017). Within the last few years, there has been commercial availability of human primary renal cells for studying cell function and response, which is favored over immortalised cells lines. For instance, Larkin *et al.*, has indicated that human tubular epithelial cells in primary culture respond to hyperglycemia noticeably differently over the HK-2 human tubular epithelial cell line in thiamine transporter expression: whereby in primary cell cultures, thiamine transporters were down regulated by 70 – 80%, while the cell line showed no change in expression (Larkin et al., 2012). Hence, the literature evidence supports using primary human cells in research. Other mammalian renal cell primary cultures are also of value, and cell lines can be used, but data from these should be treated with caution.

The effect of high glucose concentration has been examined on cellular respiration and energy production of human primary mesangial cells and the proximal tubular cell line, HK-2.

Comparisons were made to determine the bioenergetic profiles of these cells and to evaluate if diabetes mediates mitochondrial oxidative damage and ATP deficiency (Czajka and Malik, 2016). Hyperglycaemia was more likely to lead mitochondrial oxidative damage and ATP deficiency which play major roles in the progression of the diabetic nephropathy in both cell types. Another recent study performed using biopsies taken from diabetic nephropathy patients and controls who undergone nephrectomy due to renal carcinoma. This study focussed on the main elements of kidney inflammation (interleukin release) and the expression of ECM proteins in diabetic kidney, and was conducted along with the HK-2 cell line (Salti et al., 2020). Another study used primary proximal tubule cells and was conducted to study the role of kallikrein in tubular pro-inflammatory responses and the effect of protease-activated receptor 4 activation in kallikrein-mediated signaling in the progression of DKD (Yiu et al., 2014).

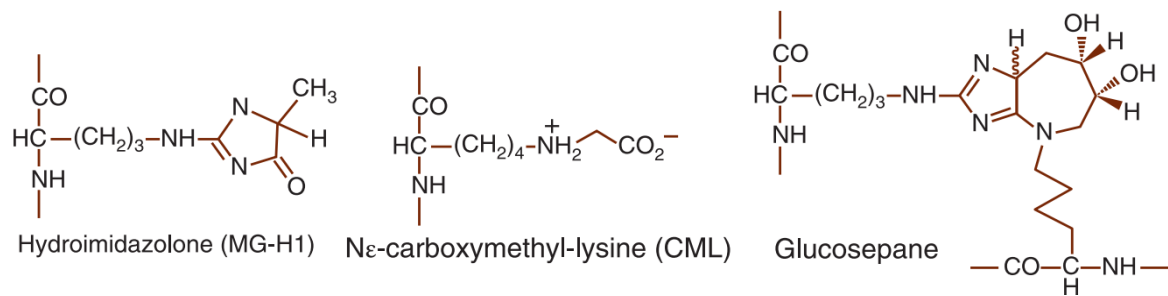
Primary culture of animal cells is also used extensively in diabetes research. Proximal tubular cells of rabbit were studied under hyperglycemic conditions (25mM) to examine the effect of aminoguanidine, rotenone and apocynin on the reversal of changes detected in these cells, such as the increase level of AGEs, mitochondrial metabolism, and also in NADPH oxidase activity (Han et al., 2005). Primary rat cells including tubular epithelial cells and podocytes have been widely used in T2DM research to study the role of ER stress in the pathogenesis of diabetic nephropathy (Ju et al., 2019, Cybulsky et al., 2005). Primary cultures of glomerular epithelial cells derived from dissected rat glomeruli, incubated in normal and high glucose concentrations have been used to highlight the pathogenic processes of epithelial injury caused in early DKD including hypertrophy, glomerular hyperfiltration and microalbuminuria (Hwang et al., 2013).

## **1.5 Glycation**

### **1.5.1 Glycation definition**

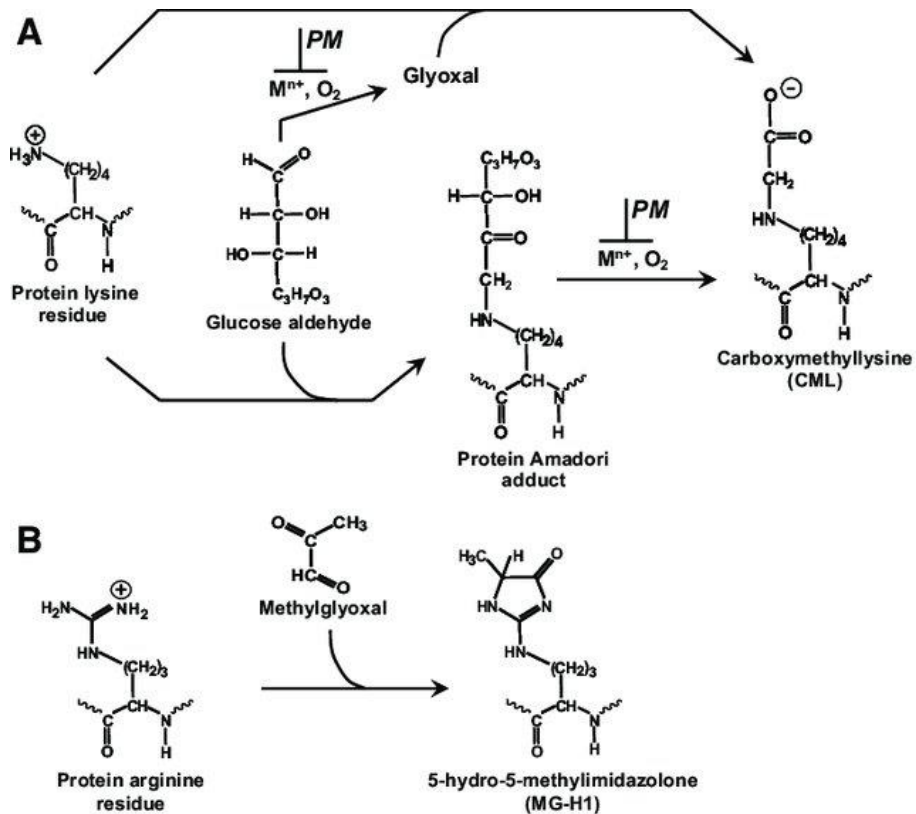
In diabetes, hyperglycaemia is linked to the development of diabetic macro and macrovascular complications. Studies implicate the critical role of glycation as a contributing cause of these complications. Glycation refers to the non-enzymatic, spontaneous reaction between sugars or related derivatives and proteins, nucleic acids and basic phospholipids to form AGEs (Thornalley et al., 2010, Thornalley and Rabbani, 2014). This process is known as glycation or the Maillard reaction. In this project, I have investigated protein glycation in physiological systems as a result of the condensation reactions of Maillard type. There are two categories of glycation adducts: (i) early glycation adducts called the Schiff's base and Amadori

products, or fructosamine residues made at the early stages of glycation – also known as the Maillard reaction; and (ii) AGE adducts which are thought to be created in late stages of the Maillard reaction but rather produced in both early and advanced stages (Rabbani and Thornalley, 2012b). In physiological systems, examples of the main precursors of AGEs, the early-stage glycation adducts are: N-ε-fructosyl-lysine (FL) and the dicarbonyl metabolites MG, glyoxal, and 3-deoxyglucosone (3-DG) (Thornalley and Rabbani, 2014). The main AGEs quantitatively are MG-derived hydroimidazolone (MG-H1), FL-derived N-ε-carboxymethyl-lysine (CML) and the crosslinked adduct glucosepane (Figure 1.5) (Rabbani and Thornalley, 2018). The reaction of glucose or its derivatives with polypeptides form glycated amino acid residues, which are known as AGE residues of proteins also known as protein-bound AGEs in renal research (Figure 1.6). AGE-glycated proteins are degraded in cells by proteolysis to form glycated amino acids, known as AGE free adducts, which are excreted later by the kidneys. AGEs might also appear in the body via by intake of glycated proteins present in diet, mainly as AGE free adducts.



**Figure 1.5: Main advanced glycation end products in chronic kidney disease.**

(Rabbani and Thornalley, 2018).



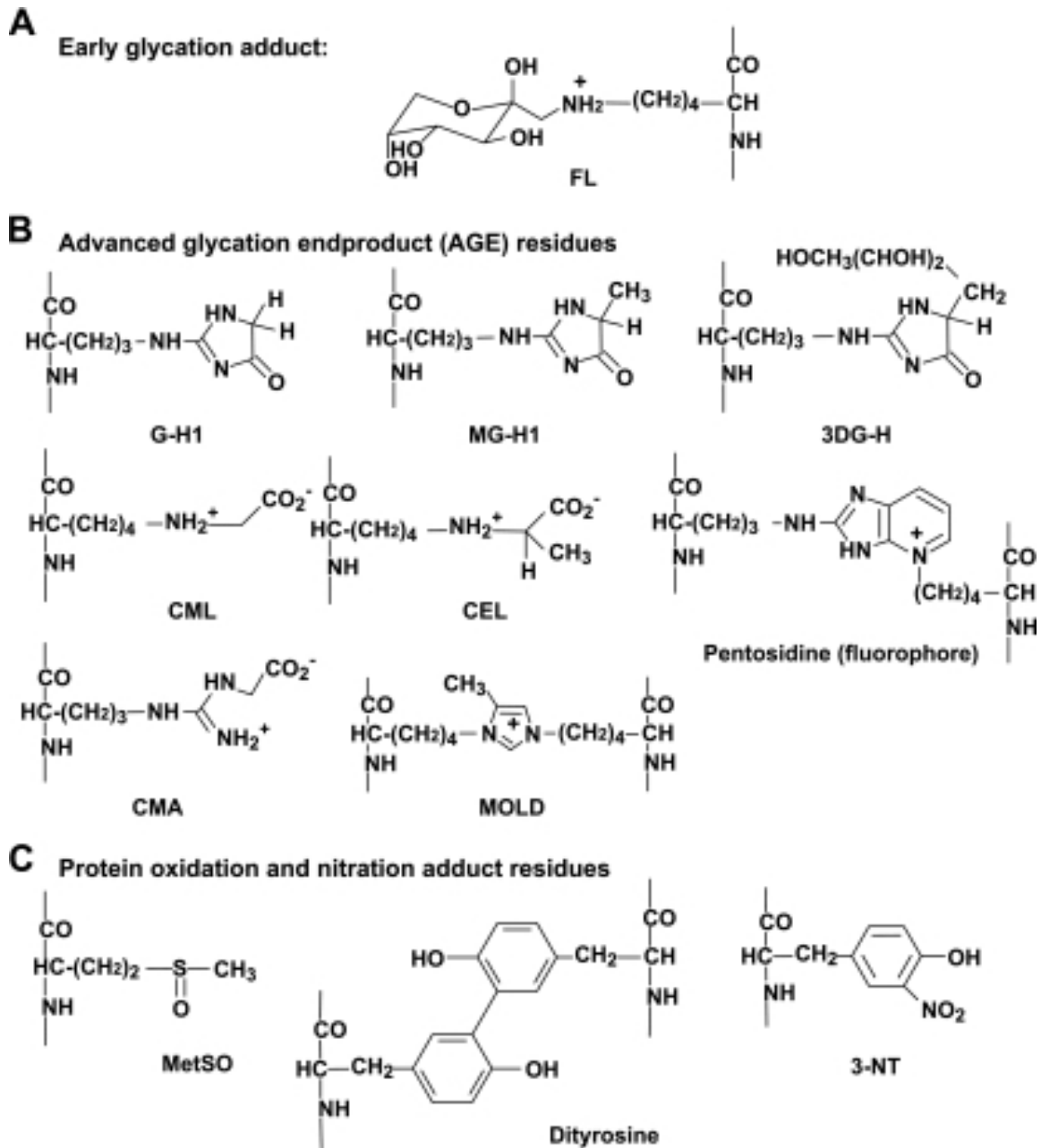
**Figure 1.6: The major pathways of modification of lysine and arginine protein residues by glucose and MG in diabetes.**

(A) Modification of lysine to CML by glucose under oxidative conditions. Blocking of oxidative pathways (e.g., with PM), inhibits CML formation. (B) Modification of arginine residue to MG-H1 by MG. Adapted from (Pozzi, 2009).

### 1.5.2 Molecular structures of advanced glycation end-products

AGEs are a heterogeneous and complex group of compounds (Thornalley et al., 2003).

Figure 1.7 illustrates key examples.



**Figure 1.7: Protein glycation, oxidation and nitration adduct residues in physiological system.**

(A) Early glycation adducts (B) Advanced glycation endproducts. (C) Oxidation and nitration adduct. Adapted from (Thornalley and Rabbani, 2014).



### 1.5.3 Historical background of glycation research

The historical progress of studies on the glyoxalase system is shown in Figure 1.8. In the early 1990s, the glyoxalase system was discovered and described as an enzymatic system that stimulates the conversion of MG to D-lactate in physiological systems (Dakin and Dudley, 1913, Neuberg, 1913). In 1929, a link between MG and glyoxalase in glycolysis was found by Neuberg (Neuberg and Kobel, 1929). Furthermore, Embden discovered that fructose 1,6-bisphosphate was transformed into 3-phosphoglycerate as a result of the oxidation of glyceraldehyde 3-phosphate, in addition to the hypothesis that 3-phosphoglycerate was a precursor of pyruvate and L-lactate (Embden, 1932). Subsequently, Otto Meyerhof presented the Embden—Meyerhof pathway which comprises the metabolism of glucose to L-lactic acid (Meyerhof, 1933). In 1932, GSH was discovered by Karl Lohmann (Lohmann, 1932), while the reaction involving GSH and MG to produce hemithioacetal was described by (Jowett and Quastel, 1933). In 1936 Yamazoye found that the hemithioacetal is converted to S-D-lactoylglutathione (Yamazoye, 1936).

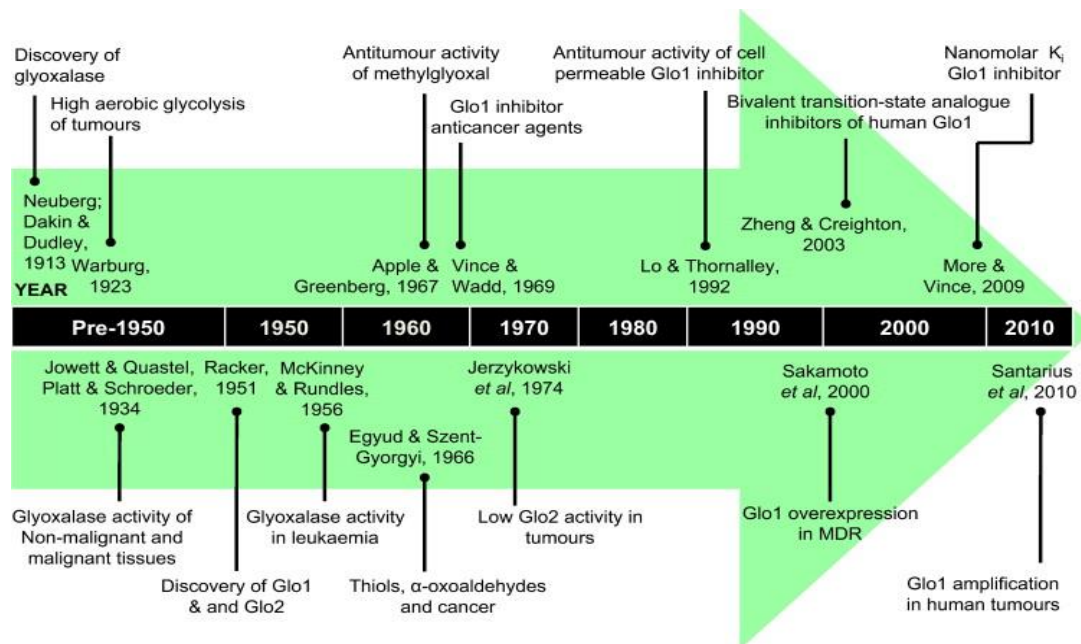
The existence of the glyoxalase system in living organisms was found to have wide distribution by Morgan and Gowland-Hopkins, who proposed that this enzymatic system has a crucial role in cell function (Hopkins and Morgan, 1945). In 1951, Racker found that the metabolism of MG occurred via two successive metabolic steps of the glyoxalase system including the Glo1 and Glo2 enzymes, and in the latter step, the resulting product was D-lactate (Racker, 1951, Thornalley, 1990).

In the last century, many studies investigated the links between cancer and the glyoxalase system. In the 1960s, Szent-Gyorgyi and his colleagues revealed the conflict of glyoxalase enzymes and MG in the regulation of cellular growth and how it could be used for cancer therapy (Szent-Gyorgyi et al., 1963, Szent-Gyorgyi et al., 1967). There was a hypothesis that MG retards cellular growth, while Glo1 activity shows the opposite effect to this growth inhibition. This was followed by the discovery of other growth factors which weakened this hypothesis. Vince and Wadd suggested that Glo1 inhibitors could be exploited as anticancer substances. Glo1 inhibitors increased the concentration of the endogenous MG, which is toxic to tumour cells (Vince and Wadd, 1969).

The glyoxalase system was also linked to diabetes, after Thornalley discovered an increase in MG levels in red blood cells after culturing under hyperglycaemic conditions *in vitro* (Thornalley, 1988). In 1989, it was found that the formation of MG, S-D-lactoylglutathione and D-lactate was higher in patients with diabetes compared with healthy subjects (Thornalley et al., 1989).

Further studies have determined that glycation by MG is one of the main pathways producing diabetic vascular complications (Ahmed et al., 2005b, Thornalley et al., 2003). In 1993, further studies showed that the major source of MG in mammalian metabolism system is the spontaneous trace level degradation of triosephosphates, with around 0.1% of glucotriose flux degrading to form MG (Phillips and Thornalley, 1993). In 1994, it was discovered that MG is one of the key glycating agents that generates AGEs (Lo et al., 1994). In 1998, Glo1 overexpression in endothelial cells cultured in hyperglycaemic conditions inhibited the increase of MG accumulation and formation of AGEs (Shinohara et al., 1998), while the accumulation of MG was noticed in cultured cells in under oxidative stress (Abordo et al., 1999). Studies by Brouwers and co-workers on diabetic rodents showed that Glo1 overexpression has a key role in inhibiting vascular intracellular glycation, endothelium damage and attenuation of early renal impairment in diabetic rats. The findings linked diabetes and the increased formation of AGEs to the initiation of vascular endothelium dysfunction and oxidative stress (Brouwers et al., 2010).

Glycation research has been very intensive recently, especially with proteomics approaches, cell signalling research, therapeutics development, and food processing. Recently, it has been discovered that the increased formation and accumulation of glycated proteins have contributed to many diseases, including diabetic complications (Ahmed et al., 2005b, McCance et al., 1993), kidney failure (Agalou et al., 2005), cardiovascular disorders, and Alzheimer's disease (Chen et al., 2004, Ahmed et al., 2005a). Many studies are also evaluating the links to glycation in arthritis and cirrhosis (Ahmed et al., 2004, Ahmed et al., 2006), anxiety disorders, schizophrenia (Arai et al., 2010, Hamsch et al., 2010), and Parkinson's disease (Kurz et al., 2011). Lately the stimulation of glyoxalase 1 expression or "Glo1 inducers" has gained new importance in anti-glycation agents where Phase 1/Phase2A clinical trials of Glo1 inducer compounds have shown reduced MG, MG-derived AGEs and enhanced metabolic and vascular health in obesity studies (Xue et al., 2016).



**Figure 1.8: Timeline of historical discoveries in research on the glycation to 2010.**

(Rabbani and Thornalley, 2012b).

#### 1.5.4 Glycation in diabetes and diabetic complications research

There is increasing evidence that hyperglycaemia plays a key role in the pathological processes observed in T2DM onset and its complications leading to different pathways of biochemical dysfunctional, including increased polyol pathway activity, hexosamine pathway activity, activation of PKC, oxidative stress and increased formation AGEs (Ahmed and Thornalley, 2007, Gerstein *et al.*, 2008). Evidence indicates that prediabetes is linked to oxidative stress (overproduction of ROS) that induces  $\beta$  cell dysfunction and insulin resistance, the main hallmarks of type 2 diabetes, and this occurs long before hyperglycaemia emerges (Leahy, 2005, Henriksen *et al.*, 2011). As the diabetic process continues, multiple sources produce ROS and one of these sources is AGEs. Hyperglycaemia increases the formation of AGEs which then stimulates a cascade of toxic pathways in cells, invoked by binding to the receptor of AGEs known as (RAGE). Moreover, it was recently found that an alternative source of AGEs is in the diet and this is implicated in the progression of T2DM and its complications (Di Pino *et al.*, 2017, Vlassara and Uribarri, 2014). Taken together, AGEs play a key role in insulin resistance,  $\beta$  cell dysfunction and diabetic complications.

One of the earliest studies that linked glycated proteins to diabetes was in 1968 with the discovery of a glycated form of haemoglobin, now identified as HbA1c, found in red blood cells of diabetic patients (Rahbar, 1968). Recent studies indicated that plasma of patients with

T2DM showed an acceleration in the concentration of glyoxal, MG and 3-deoxyglucosone due to increased levels of circulating glucose (Scheijen and Schalkwijk, 2014). More evidence revealed that serum and tissues of diabetic patients with T1DM and T2DM showed an increase in AGEs concentration, such as: CML (Schalkwijk et al., 2004, Shanija et al., 2018), MG-hydroimidazolone (Bora et al., 2020), pentosidine (Machowska et al., 2016), and glucosepane (Fan et al., 2010). Moreover, many studies indicated that there is a correlation between increased AGEs in diabetic tissues and diabetes duration and complications (Heidari et al., 2020, Koska et al., 2018, Guerin-Dubourg et al., 2017). There are also events where pathological changes arise when an AGE-modified protein has a different function, for instance MG-modified LDL (MG-LDL) in the bloodstream, which binds more readily to arterial walls, facilitating the atherosclerotic process (Rabbani et al., 2011c).

### **1.5.5 Glycation and diabetic kidney disease**

In DKD research, most of the previous studies have focused mainly on direct glycation of proteins, while glycated nucleotides and phospholipids by MG and glyoxal have been comparatively less studied and reviewed. In diabetes, glycation of proteins induces changes in structure/conformation, function and ionic state of proteins (for example loss of enzymatic activity) and this consequently leads to cell and tissue dysfunction. Protein glycation occurs predominantly at steady rate of  $\leq 1\text{-}5\%$  of protein substrate and thus might effect slightly on protein function (Rabbani and Thornalley, 2016).

In DKD studies, dicarbonyl stress has been shown to play an important role in progression of the disease. In animal models, nephropathy developed in Glo1-deficient mice (Giacco et al., 2014). Dicarbonyl stress could be a result of renal failure, as it was demonstrated that dicarbonyl stress arises with loss of glycation product clearance in bilateral nephrectomised experimental rats (Rabbani et al., 2007). Dicarbonyl stress appears also in patients with DKD (Rabbani and Thornalley, 2012a) with increases in the levels of MG, but without increase in D-lactate formation in subjects without diabetes (Ficek et al., 2017). D-Lactate is used as an indicator of MG metabolic flux (Rabbani et al., 2016). ***This indicates that the main factor of dicarbonyl stress in DKD is down-regulation of Glo1 enzyme expression or function rather than increased levels of MG production in nondiabetic conditions.*** Decreased excretion of urinary MG is not counted as a main association factor, since little MG is already excreted, while this could be a more significant factor for 3-DG accumulation (Rabbani et al., 2016).

Normally, glycated proteins are eliminated from the body as AGE “free adducts”. In chronic renal failure patients experience decline in GFR, such that the clearance of these adducts decreases - and consequently AGE free adduct levels increase in the plasma (Rabbani et al., 2007, Agalou et al., 2005). Many studies have demonstrated that, for instance, in patients requiring hemodialysis or peritoneal dialysis treatment there was a 4- to 40-fold increase in AGE free adducts, in addition to AGE residues of plasma protein showing 2- to 5-fold increases (Agalou et al., 2005). Accumulation of AGEs is influenced by the flux of AGE formation and efficiency of AGE excretion by the kidneys. To detect the flux of AGE formation, AGE free adducts are measured in dialysate and urine. In patients who were receiving peritoneal dialysis, flux of AGE formation showed significant increases compared with healthy controls - with 9-fold increase for MG-H1, 2-fold increase for CML, pentosidine, and 3-DG-derived hydroimidazolones (3DG-H). MG-H1 was 4- to 713-fold higher compared with other AGEs in peritoneal dialysis patients, suggesting that MG-H1 is a major AGE that accumulates in renal failure.

Analysis of AGE residue contents in plasma have been identified as indicators of death risk linked to renal diseases (Schwedler et al., 2002, Agalou et al., 2005). The level of AGE residue content in the plasma is affected by reduced presence of albumin in the vascular compartment in due to the complication of albuminuria (Rabbani et al., 2011a). There is also an increased transcapillary filtration level of albumin that is induced by the co-morbidities of hypertension and atherosclerosis (Masania et al., 2016). In addition, reduced albumin synthesis and catabolism occurs in renal disease (Ahmed et al., 2004). To counter this, other indicators should be used in order to measure AGE formation in the kidney such as determining total body flux of the formation of AGEs or alternative measurements such as: i) urinary or dialysate flux formation of AGE free adducts, ii) plasma AGE free adducts levels, when it is important to take into consideration the correction for decline in GFR in DKD within its first to fourth stages, and iii) plasma AGE free adduct levels immediately before the dialysis. Correction factors may also be used to account for the influences of AGEs derived from diet (Rabbani and Thornalley, 2018).

The metabolism of AGEs is catalysed by enzymatic systems of the precursor glycation agents or glycation adduct. MG and glyoxal are metabolized primarily by the glyoxalase system. The 3-DG AGE and 3,4-dideoxyglucosone-3-ene (3,4-DGE; a cytotoxic glucose degradation detected in fluids of peritoneal dialysis with glucose osmolyte), are metabolised by aldoketo reductase pathways and aldehyde dehydrogenase pathways, respectively. Each

healthy human kidney contains a high level of aldose reductase, nearly 2% of entire protein content. The enzyme was detected in the inner medulla which mainly reduces glucose to sorbitol under high extracellular osmotic pressure (Nishimura et al., 1993). Stable-state concentrations of FL residues are controlled by the fructosamine-3-phosphokinase enzyme, leading to degradation of precursor lysine residues (Thornalley and Rabbani, 2014). In animal models, it has been reported that AGE accumulate in the glomeruli and at other sites of microvascular complications (Karachalias et al., 2010, Karachalias et al., 2003). AGEs are known to affect renal cultured cells, in diabetic models. For instance, in podocytes and mesangial cells, histone-modifying proteins have been linked to AGE-induced complications (Liu et al., 2015).

## **1.6 Dicarbonyls**

### **1.6.1 Dicarbonyl stress**

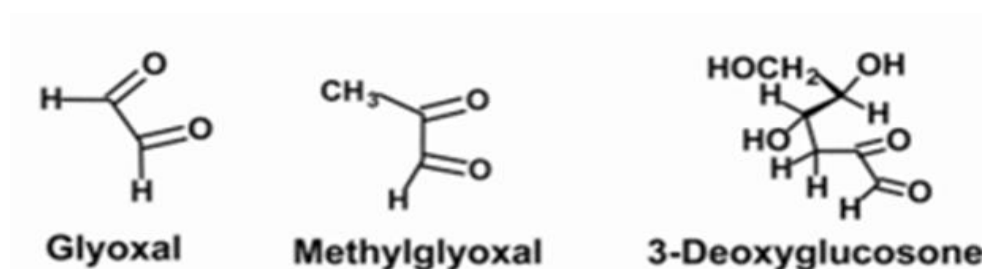
Dicarbonyl stress is characterised by the abnormal accumulation of dicarbonyl metabolites ( $\alpha$ -oxoaldehydes) – for example: MG, glyoxal, 3-Deoxyglucosone (3-DG) – leading to protein and DNA modification that causes cell and tissue dysfunction in ageing and various diseases (Rabbani and Thornalley, 2018). The reaction of each of MG, glyoxal and 3-DG with proteins occurs predominantly with the arginine side-chain guanidino groups to produce a particular group of AGEs. Imbalance between the synthesis and degradation of dicarbonyl metabolites, and also the high exposure to exogenous dicarbonyls, causes a state of dicarbonyl stress (Rabbani and Thornalley, 2015). Dicarbonyl metabolites are produced endogenously and found in all tissues, body fluids and also dialysis fluids (Rabbani and Thornalley, 2012a). Several studies have shown the increased concentration of MG in ageing plants, increased plasma and tissue levels of MG in diabetes, and increased MG, glyoxal, 3-DG levels and other dicarbonyls in renal failure (Rabbani and Thornalley, 2015). Typical levels of glyoxal, MG and 3-DG in human plasma are in the range of 50 - 150 nM, where it found to be at levels of 1 - 4  $\mu$ M in plant and mammalian cells. If dicarbonyl levels increase beyond this, dicarbonyl stress can develop and cause impaired health and disease (Rabbani and Thornalley, 2015).

Glyoxal is produced physiologically by the slow, non-enzymatic oxidative degradation of glucose and by glycation of proteins mediated by glucose. It is additionally generated by the autoxidation of glycolaldehyde, which in turn is produced by oxidative degradation of serine residues by hypochlorite in the phagocyte respiratory burst by myeloperoxidase. Glyoxal is

also generated by lipid peroxidation and the degradation of nucleotides (Thornalley, 1985, Loidl-Stahlhofen and Spitelier, 1994, Anderson et al., 1997, Thornalley et al., 1999, Rabbani and Thornalley, 2012a).

MG is an alpha-dicarbonyl compound and dominant glycating element in physiological systems. In most organisms, MG is generated mostly from the degradation of triose phosphates glyceraldehyde-3-phosphate (GA3P) and dihydroxyacetone-phosphate (DHAP). It is also formed by the metabolism of ketone bodies and through the oxidation of aminoacetone during the catabolism of threonine. Degradation of glycated proteins and monosaccharides increases the flux of MG formation (Reichard et al., 1986, Lyles and Chalmers, 1992, Rabbani and Thornalley, 2015).

3-DG is created in the enzymatic repair of glycated proteins through the degradation of frutosamine-3-phosphate, degradation of fructose-3-phosphate, also through the slow non-enzymatic oxidative degradation of glucose and proteins glycated by glucose (Lal et al., 1997, Thornalley et al., 1999, Delpierre et al., 2000, Rabbani and Thornalley, 2012a).



**Figure 1.9: Physiological dicarbonyl metabolites.**

### 1.6.2 Measurement of glycation adducts

To measure glycation adduct concentration in human samples, immunoassay and fluorescence techniques have been commonly used. Immunoassay has been widely used to detect AGEs (Ahmed and Thornalley, 2007, Jung et al., 2011), although these methods have some limitations, including: (i) inadequate antibody specificity, for example the binding of N $\epsilon$ -carboxymethyl-lysine (CML) by monoclonal antibody 6D12 was thought to be specific for this AGE, while it binds to N $\epsilon$ -(1-carboxyethyl) lysine (CEL), (ii) using of proteins blocking to reduce non-specific binding of the antibody (e.g. bovine serum albumin) might contain glycation adduct. Rabbani *et al.* avoided this by applying of synthetic polythreonine which does not contain amino acid substrates of glycation where the microplate-blocking polypeptide (Rabbani et al., 2011b).

Fluorescence had been used as well widely, but as the previous method it had some disadvantages. For instance, this method is limited to measure few numbers of fluorescent AGEs only. In addition, for robust quantitation a chromatographic resolution phase is essential, also this technique may not represent the actual sample concentration of AGEs due to the non-AGE fluorophores, for instance, N-formylkynurenine (NFK) interfere with AGE excitation-emission spectra (Šebeková et al., 2001).

The most reliable analytical method for identifying and quantifying AGEs is liquid chromatography-tandem mass spectrometry (LC-MS/MS), this technique characterised by high sensitivity and specificity (Thornalley et al., 2003, Thornalley and Rabbani, 2014). It is the best method to identify protein oxidation and nitration markers, with more newly advance of measuring free adducts in the fluids, the complete amino acid metabolite might be measured simultaneously. One disadvantage of LC-MS/MS is that it is costly and unavailable for clinical use.

### **1.6.3 Repair of glycated protein**

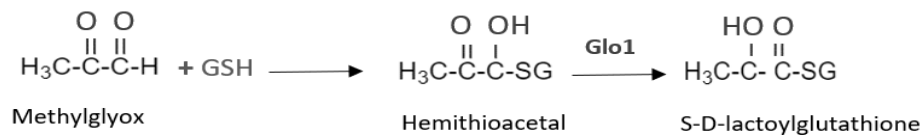
It was initially believed that protein adducts that were formed by reaction of oxidation and glycation simply accumulate in cells and tissues during life and remain in the body. This is believed to be the case for oxidation and glycation adducts which are chemically stable and cannot be repaired enzymatically *in situ*. For example, dityrosine and CML residues have been found on articular cartilage in human healthy skeletal tissues (Verzijl et al., 2000). While in most protein adducts formed by oxidation and glycation, this is not the same. For many protein adducts formed by oxidation and glycation that are accessible, there are a number of repair systems in nature that can reverse adduct formation. For instance, fructosamine 3-kinase is an enzyme that readily phosphorylates fructoselysine (FL), leading to de-glycation and repair of early glycated proteins (Delpierre et al., 2000).

### **1.7 The glyoxalase system, definition and function**

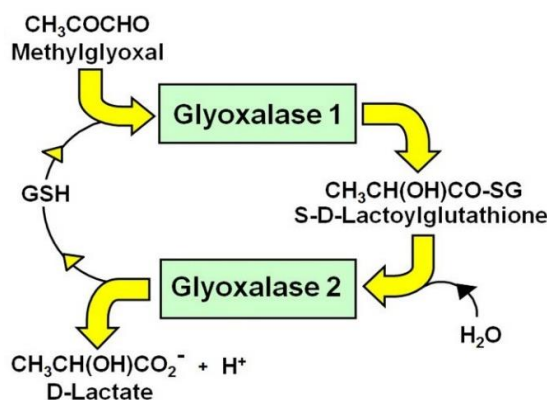
The glyoxalase system is an enzymatic pathway present in the cytosol of all mammalian cells, plants, bacteria, fungi and protocista (Xue et al., 2011). This system consists of 2 enzymes, Glo1, Glo2, and a catalytic amount of glutathione-Figure 1.10. The main function of this system is reducing the toxicity of MG and the other reactive aldehydes that are found normally in cellular metabolism (Rabbani and Thornalley, 2015). The metabolism of MG progresses by 2 sequential reactions of these enzymes. Glo1 converts the isomerisation of the



hemithioacetal developed non-enzymatically from reduced glutathione (GSH) and MG  $\text{CH}_3\text{COCHO}$  to S-D-lactoylglutathione  $\text{CH}_3\text{CH}(\text{OH})\text{CO-SG}$ . Then Glo2 converts S-D-lactoylglutathione to D-lactate, with reformation of the GSH used in the Glo1-catalysed reaction in the following cycle (Thornalley et al., 1989) (**Error! Reference source not found.**). The first action by Glo1 reduces the toxic risk of MG, and other reactive dicarbonyls, to tolerable concentrations. MG is the main element of highest metabolic flux in physiological systems. Other known elements are glyoxal, hydroxypyruvaldehyde and 4,5-dioxoalderate (Thornalley, 1993).



MG is the major physiological substrate for the Glo1 enzyme. MG markedly accumulates if Glo1 is suppressed *in situ* by depletion of GSH and by the presence of cell permeable Glo1 inhibitors (Thornalley, 1993, Thornalley et al., 1996, Abordo et al., 1999). Glyoxal, hydroxypyruvaldehyde ( $\text{HOCH}_2\text{COCHO}$ ) and 4,5-doxoalderate ( $\text{H-COCOCH}_2\text{CH}_2\text{CO}_2\text{H}$ ) are also other substrates that are metabolized by Glo1 (Thornalley, 1993, Thornalley et al., 1996, Abordo et al., 1999, Thornalley, 1998b). The glyoxalase system, and mainly the activity of Glo1, suppresses the increase of the reactive  $\alpha$ -oxoaldehydes and therefore inhibits  $\alpha$ -oxoaldehyde-mediated glycation reactions (Shinohara et al., 1998). Hence, Glo1 is a major anti-glycation defence enzyme (Thornalley, 2003b, Thornalley, 2003a).

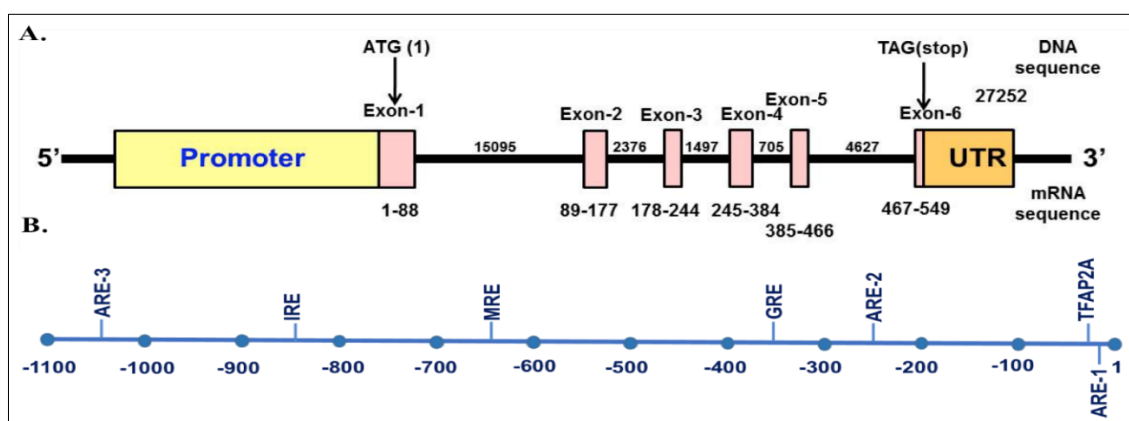


**Figure 1.10: The glyoxalase system and its metabolites.**  
Adapted from (Rabbani et al., 2021).

### 1.7.1 Glyoxalase 1

Glo1 is part of the glyoxalase system present in the cytosol of human cells. Expression and activity of Glo1 is found around 3 times higher in foetal tissues than in adult tissues (Thornalley, 1991). In human tissues and blood cells there is roughly 0.2 µg of Glo1 per gram of total protein (Larsen et al., 1985).

The human Glo1 gene is found on chromosome 6 at band number 21.2. Gene cloning showed that the Glo1 gene is 12.0 kb in length and comprises of 5 introns separated by 6 exons (Ranganathan et al., 1999) (Figure 1.11). Human Glo1 is a dimeric Zn<sup>2+</sup> metalloenzyme, expressed at a diallelic genomic locus. These alleles encode 2 similar subunits in heterozygotes making three allozymes in heterozygotes: Glo1-1, Glo1-2 and Glo2-2. The molecular mass of all these allozymes, based on primary sequence is found to be 42 kDa. The apparent Glo1 molecular mass is 46 kDa, determined by gel filtration, due to a non-spherical shape (Thornalley, 1993). Each allozyme includes one Zn<sup>2+</sup> ion per subunit and isoelectric point (pI) values range from 4.8-5.1. The allozymes carry different charge densities and can be resolved by ion exchange chromatography and non-denaturing gel electrophoresis (McLellan and Thornalley, 1991, Schimandle and Vander Jagt, 1979). Glo1 alleles are inherited in a simple co-dominant manner, with the existence of specific expression of the phenotype (Thornalley, 2003b). In humans the Glo1 translational product consists of 184 amino acids. The expression products of the two Glo1 alleles differ in amino acid sequence only at position 111. Where alanine residue is present in the subunit Glo1-A, in subunit Glo1-E there is a glutamic acid residue present (Kim et al., 1995).



**Figure 1.11: Human Glo1 gene.**

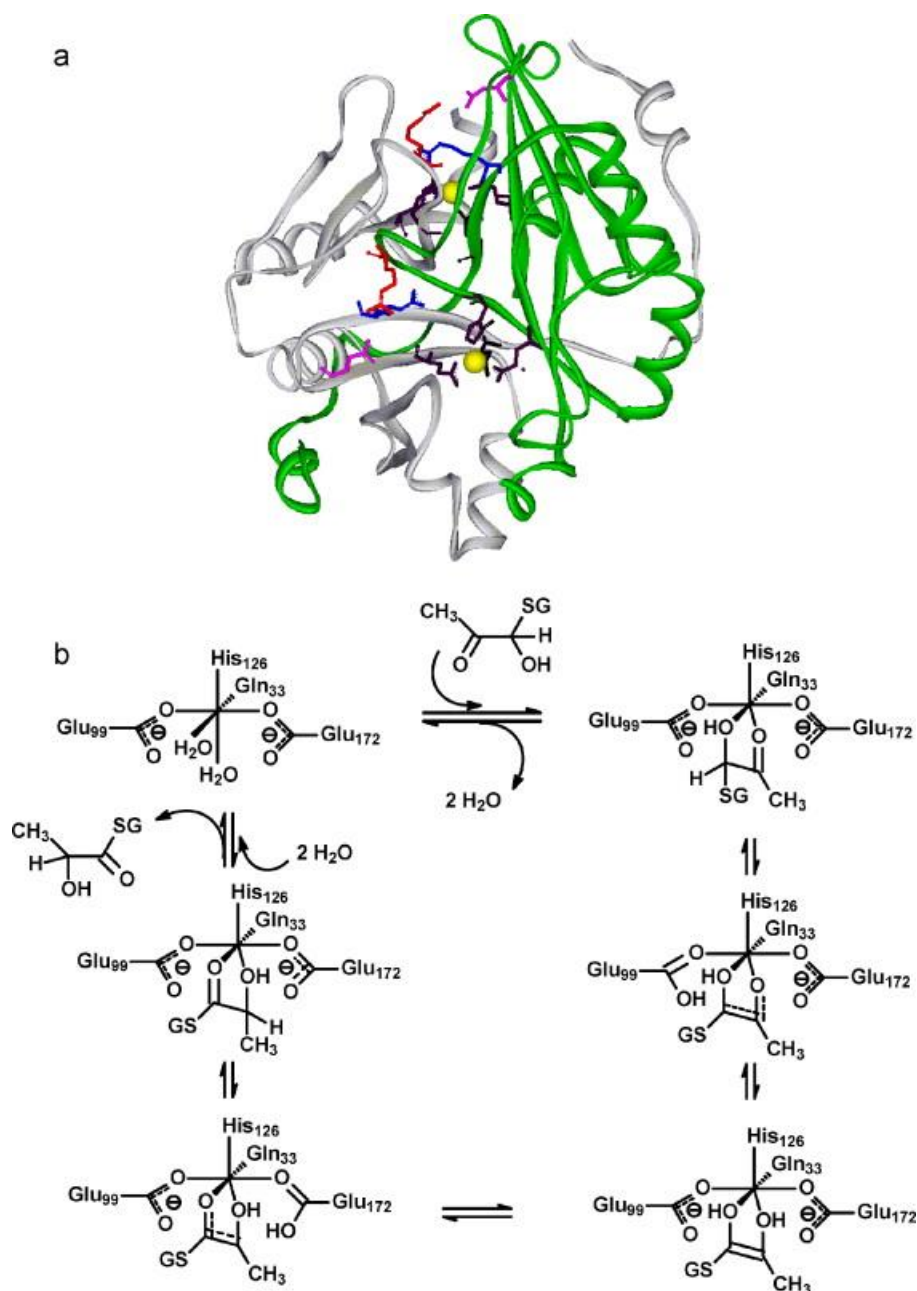
A. Representation of the human GLO1 gene (Yellow: promoter region, Pink: exon, Orange: untranslated region (UTR), Blue: regulatory elements). B. Promoter sequence of human GLO1 with positions of regulatory elements (Ranganathan et al., 1999).

In post-translational processing, the N-terminal methionine residue of Glo1 is removed, while the remaining N-terminal alanine is blocked by acetylation. Further phosphorylation and acetylation creates different forms of the protein with varying pI values (Xue et al., 2011). There is a vicinal disulphide bridge connecting cysteine residues 19 and 20. In addition, cysteine-139 and cysteine-61 may also form of an intra-molecular disulphide. Cysteine-139 includes a mixed disulfide with glutathione. Glo1 activity was found not to be affected by N-terminal acetylation and C19/C20 disulphide formation, but glutathionylation on cysteine-139 clearly was seen to be an inhibitor of Glo1 activity *in vitro* (Birkenmeier et al., 2010). Modification of Glo1 by S-nitrosylation, via exposure to nitric oxide (NO), occurs on cysteine-139. The presence of cysteine-19 and cysteine-20 is essential cysteine-139 S-nitrosylation which occurs on the acidic,  $\alpha$ -form of Glo1 (De Hemptinne et al., 2007). The basic, reduced form of Glo1 is the NO-responsive form, with no intramolecular disulfide bonding (De Hemptinne et al., 2007). Glo1 is a substrate for calcium-calmodulin-dependent protein kinase II (CaMKII). Primarily but not exclusively, phosphorylation of Glo1 occurs at Thr-107 on the basic, reduced and NO-responsive form (Santarius et al., 2010, de Hemptinne et al., 2009, Xue et al., 2011, Birkenmeier et al., 2010).

The GLO1 promoter region includes binding sites for the following control elements: insulin response element (IRE), metal responsive element (MRE) and glucocorticoid responsive element (GRE), located from -842 to -848bp, -647 to -654bp and -363 to -368bp respectively (Ranganathan et al., 1999), in addition to activating enhancer binding protein 2 alpha (AP-2 alpha) located from -24 to -32 (Orso et al., 2010), E2F – binding to transcription factor E2F4 (Conboy et al., 2007) and ARE-1 located from -10 to -19, ARE-2 from -252 to -261 and ARE-3 from -1051 to -1060 (Xue et al., 2012) – See Figure 1.11. Oxidative stress induces Glo1 in the nematode organism *Onchocerca volvulus*, but the mechanism is not fully understood (SOMMER et al., 2001), although it might occur through the nematode orthologue of the stress response transcription factor Nrf2.

The crystal structure of human Glo1 enzyme in a complex with S-benzyl-glutathione, has been determined to 1.7 Å resolution by Cameron *et al.* (Cameron et al., 1997). Each monomer comprises of two structurally equivalent domains linked by a stretch of 20 residues and anteceded by a long arm of the N-terminal region (Figure 1.12a). The active site is located at the interface of the dimer, with the inhibitor and crucial Zn<sup>2+</sup> ion interacting with side chains from both subunits. The binding site of the zinc ions involves two structurally equivalent

residues from each domain: Gln-33A, Glu-99A, His-126B, Glu-172B plus two water molecules (Thornalley, 2003b).



**Figure 1.12: Crystal structure of human Glo1.**

(a) Solid ribbon image of the crystal structures of human glyoxalase 1. Subunits, A (grey ribbon) and B (green ribbon),  $Zn^{2+}$  ions (yellow balls) and coordinating amino acid residues Gln33A, Glu 99A, His126B and Glu172B (black sticks) and GSH moiety binding site (Arg37, Asn103 and Arg122—blue, pink and red sticks) are shown. (b) Catalytic mechanism of human glyoxalase I for the isomerisation of the R-hemithioacetal—adapted from (Xue et al., 2011, Cameron et al., 1997).

The catalytic mechanism proposed for the Glo1 reaction involves a base-catalysed shielded proton move from C1 to C2 of the active site-bound hemithioacetal (Figure 1.12b). This allows the formation of an ene-diol intermediate with rapid ketonisation and thioester product formation. Both the hemithioacetal R- and S-forms are attached in the active site of Glo1 and are then deprotonated; the following reprotonation of the putative ene-diol intermediate occurs stereo-specifically to create only the R-2-hydroxyacylglutathione enantiomer derivative. It has been suggested that both Glu-172 and Glu-99 provide the catalytic base for the S-substrate enantiomer and the R-substrate enantiomer respectively. These reaction mechanisms create a cis-ene-diol intermediate coordinated directly to the  $Zn^{2+}$  ion. This later is deprotonated to a cis-ene-diolate by Glu-172 which then reprotonates C2 stereospecifically to produce R-2-hydroxyacylglutathione (Himo and Siegbahn, 2001). The formation of S-Glycolylglutathione, S-D-lactoylglutathione and S-L-glyceroylglutathione derive from glyoxal, methylglyoxal and hydroxypyruvaldehyde via Glo1, respectively. Subsequently, they pass on to hydrolysis by the associated Glo2 enzyme to form glycolate, D-lactate and L-glycerate (Clelland and Thornalley, 1991).

Glo1 is found in other mammalian species with similar characteristics to the human enzyme. The enzyme is normally dimeric in mammals, plants and bacteria. Glo1 in yeast is a monomer of 32 and 37 kDa for *Saccharomyces cerevisiae* and *Schizosaccharomyces pombe*, respectively, with two copies of a segment corresponding to the monomer of the human Glo1 enzyme. The sequence identity of the human Glo1 enzyme with the bacterial orthologue in *Pseudomonas putida* is 55%, while with Glo1 orthologue of *Saccharomyces cerevisiae* between residues 1-182 and 183-326 is 47% (Thornalley, 2003b). This might suggest that Glo1 of various species may have developed via divergent evolution from a common ancestral enzyme (Xue *et al.*, 2011).

### 1.7.2 Glyoxalase 2

Glyoxalase 2 (Glo2) activity is found in the cells of both eukaryotic and prokaryotic organisms (Thornalley, 1993). It has been discovered in yeast such as *Saccharomyces cerevisiae* and *Hansenula mrakii* (Inoue and Kimura, 1992, Murata *et al.*, 1986), protozoa such as the malaria parasite *Plasmodium falciparum* (Vander Jagt, 1993) and species of *Leishmania* (Darling and Blum, 1988), helminths including cestodes, digeneans and nematodes (Brophy *et al.*, 1990, Pemberton and Barrett, 1989) and also fungal species such as *Candida albicans* (Talesa *et al.*, 1990).

Human Glo2 has two major isoforms: mitochondrial and cytosolic. The mitochondrial form has a molecular weight of 33.8 kDa (determined from primary sequence) and a predicted isoelectric point of 8.3, while the cytosolic Glo2 has a slightly lower molecular weight of 29.2 kDa (SDS-PAGE estimate; primary sequence determination is 28,860 Da) and predicted isoelectric point also of 8.3 (Allen et al., 1993, Ridderström et al., 1996, Cordell et al., 2004). Human Glo2 is a thiolesterase and has an extensive range of substrate specificity for glutathione thiol esters, primarily S-2-hydroxyacylglutathione derivatives (Xue et al., 2011).

The human cytosolic Glo2 consists of two domains, the first, N-terminal domain contains 1-173 amino acids and the second C-terminal domain contains of 174-260 residues. The first domain is folded into a four-layered  $\beta$ -sandwich, while the second domain is mostly  $\alpha$ -helical in character. The active site includes a binuclear metal ion-binding site involving zinc (II) and iron (II) ions, and a substrate-binding site covers the domain interface (Limphong et al., 2009, Xue et al., 2011). Furthermore, there is a hydroxide ion connected to both metal ions. This ion is found at 2.9 Å from the carbonyl carbon of the substrate in a location that might act as the nucleophile during catalysis (Cameron et al., 1999). The metal ion binding in Glo2 is essential for its activity (Dragani et al., 1999, Limphong et al., 2009). The ratio of hydrolysis of S-D-lactoylglutathione to GSH and D-lactate passing catalysis by Glo2 followed Michaelis-Menten kinetics where the  $k_{cat}$  and  $K_M$  values had been determined as  $727\text{ s}^{-1}$  and  $146\text{ }\mu\text{M}$  respectively (Allen et al., 1993). Glo2 has also found to be acetylated at lysine-229 (Choudhary et al., 2009).

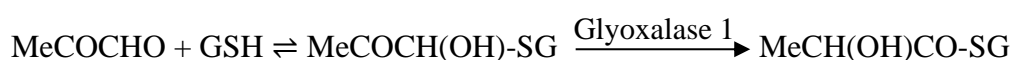
The human Glo2 gene is also known as hydroxyacylglutathione hydrolase (HAGH). It is located on chromosome 16 in region 16p13.3. Glo2 genetic polymorphism is very rare. Typically, just one phenotype - HAGH1 is expressed. Additionally, a rare second type known as HAGH2 has been detected (Thornalley, 1993). The Glo2 gene consist of 10 exons that are transcribed into two different mRNA species from 9 and 10 exons. The 9-exon-derived transcript encodes the mitochondrial and cytosolic forms of the protein. The Glo2 that targets mitochondria is originated from an AUG codon in the mRNA sequence and is trafficked to the mitochondrial matrix (Cordell et al., 2004), while the cytosolic form is produced by internal ribosome entry at a downstream AUG codon. However, the 10-exon-derived transcript comprises of a termination codon amidst two initiating AUG codons, and just encodes the cytosolic form of Glo2 (Cordell et al., 2004).

The role of Glo2 in mitochondria is undetermined as there is no mitochondrial targeting of Glo1. Glo2 hydrolyses additional acyl-GSH derivatives like S-acetyl-GSH and S-succinyl-

GSH. Recent investigations suggest that there is significant non-enzymatic acetyl and succinyl transfer from acetyl-CoA and succinyl-CoA in mitochondria and an expected acceptor is mitochondrial GSH. Glo2 may consequently maintain GSH levels by repairing endogenous acylations where high levels of acetyl-CoA and succinyl-CoA in mitochondria may require the recruitment of Glo2 to these organelles (Rabbani et al., 2014).

### 1.7.3 S-D-Lactoylglutathione

S-D-lactoylglutathione is a physiological intermediate generated within the glyoxalase system. It is produced by Glo1 catalysis from the reaction of the hemithioacetal adduct of MG and GSH (McLellan et al., 1993).



S-D-Lactoylglutathione is subsequently hydrolysed to GSH and D-lactate by Glo2. It is produced in the cell cytosol and has poor membrane permeability. However, when there is a leakage from cells via the GSH conjugate transporter, then  $\gamma$ -glutamyltransferase - located on the external surface of cell membrane - cleaves S-D-lactoylglutathione to S-D-lactoylcysteinylglycine. Subsequently, S-D-lactoylcysteinylglycine rearranges spontaneously to form N-D-lactoylcysteinylglycine (Tate, 1975) and this can subsequently be cleaved by dipeptidase to form N-D-lactoylcysteine. In the 1980s, Thornalley and co-workers discovered interesting biological effects of S-D-lactoylglutathione when it was added to cultured cells (extracellular compartment). They found that S-D-lactoylglutathione induced growth arrest and toxicity in human leukaemia cells *in vitro* (Thornalley and Tisdale, 1988). Furthermore, in human neutrophils, S-D-Lactoylglutathione affects the rate of stimulus-activated granule secretion. At low concentrations (2 - 5 $\mu$ M) it induced secretion, whereas at higher concentrations (100  $\mu$ M - 5mM) it inhibited secretion (Thornalley et al., 1990).

Concentrations of S-D-lactoylglutathione in the cell are determined by Glo1 and Glo2 enzyme activity also by the level of MG formation, which can be modified in many disorders - mainly diabetes which is associated with changes in the concentrations of S-D-lactoylglutathione (McLellan et al., 1993). Thornalley found that the concentration of S-D-lactoylglutathione in human blood plasma of diabetic patients was significantly higher (54.1 nmol/ml red blood cells) while in non-diabetic subjects (41.1 nmol/ml red blood cells) (Thornalley, 1993). In addition, cytosolic levels of S-D-lactoylglutathione increase in rapidly proliferating tumour cells *in vitro* accompanied by decreases in Glo2 activity, while chemically-induced differentiation of human promyelocytic leukaemia HL60 cells was linked

to decreased S-D-lactoylglutathione concentrations and a significant rise in Glo2 activity (Hooper et al., 1987, Hooper et al., 1988).

#### **1.7.4 D-Lactate**

L-Lactate is the major stereoisomer of lactate formed in the human intermediary metabolism (Drury and Wick, 1965). The other stereoisomer is D-lactate which is usually around 1-5% of the L-lactate concentration in plasma. D-Lactate is found in exogenous sources at high-level in fermented food (e.g. yogurt, pickles and sauerkraut). Additionally, in the gut, D-lactate is also absorbed from microbial fermentation (Mortensen et al., 1991, Hove, 1998, Ewaschuk et al., 2005, De Vrese and Barth, 1991).

D-Lactate is produced endogenously as a result of the intermediary metabolism by the glyoxalase pathway and then it is metabolised by 2-hydroxyacid dehydrogenase to form pyruvate in some human tissues like kidney (Thornalley, 1993). In humans, D-lactate is well metabolised, while it has higher fractional renal excretion rate than L-lactate (Connor et al., 1983). In humans, infusion of D-lactate, as 1.0-1.3 mmol sodium D-lactate/(kg/hr) caused around 90% of the D-lactate to be metabolised while 10% was excreted in urine (Oh et al., 1985). D-lactate metabolism is decreased to approximately 75% of the total clearance with higher infusion levels of 3.0-4.6 mmol/kg/hr (Oh et al., 1985). After meal and exercise, D-lactate concentration increases in the plasma by nearly 2-3 fold (Ohmori and Iwamoto, 1988, Kondoh et al., 1992b).

It was found that D-lactate can traverse cell membranes via special transporters, the inorganic anion exchange system, the special lactate transporter, and additionally via ionic diffusion. Excretion of D-lactate occurs mostly in urine, with minimal excretions in stool and sweat (Oh et al., 1985, Kondoh et al., 1992b, Kondoh et al., 1992a). Increased formation of D-lactate can be used as a marker of the elevated flux of formation of MG in cells wherein D-lactate is not metabolised, e.g. red blood cells and optical lens fibre cells (Thornalley, 1993). Furthermore, D-lactate concentration rises in media of endothelial cells and red blood cells after culturing under hyperglycaemic conditions, and in the plasma and urine of STZ-induced diabetic rodents, plus diabetic patients (Thornalley, 1988, Phillips and Thornalley, 1993, Karachalias et al., 2005, McLellan et al., 1994). The D-lactate concentration in the plasma of healthy adults is around 2 – 20 nM (Thornalley, 1998a, Phillips and Thornalley, 1993, Karachalias et al., 2005, McLellan et al., 1994). Higher concentrations might be reached while the analytical process does not avoid limited racemisation of L-lactate which usually exists at

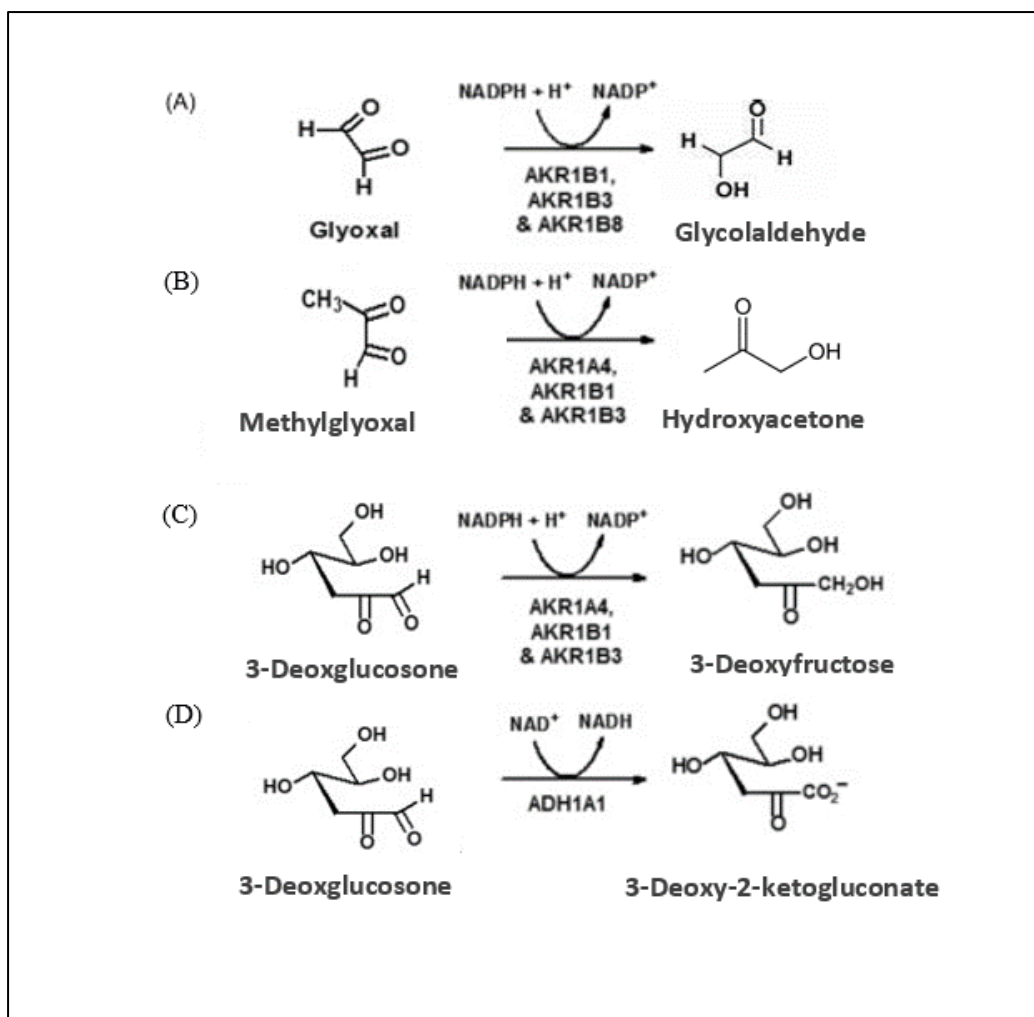


plasma levels >100 fold those of D-lactate (De Vrese and Barth, 1991, McLellan et al., 1992, Ohmori and Iwamoto, 1988, Brandt et al., 1980).

To measure D-lactate, an endpoint enzymatic assay is used with either one absorbance or fluorescence detection of NADH formation in the presence of D-lactic dehydrogenase. The total amount of D-lactate in the sample is equal to the total NADH produced from NAD<sup>+</sup> at endpoint, happening concomitantly with oxidation of D-lactate to pyruvate (McLellan et al., 1992). Furthermore, D-lactate may be detected by reverse phase high phase liquid chromatography (HPLC) by measuring the amount of pyruvate formed after derivatisation with 1,2-diaminobenzene to 2-hydroxy-3-methylquinoxaline (Ohmori and Iwamoto, 1988, Ohmori et al., 1991). However, the endpoint enzymatic assay is easier, and used for the high sensitivity detection with fluorometric detection of NADH achieving a 100% increase in sensitivity (McLellan et al., 1992). Using a microplate method reduces the required sample volume and sensitivity can be increased by 10-20 fold (Thornalley, 1993) compared with traditional spectrophotometric techniques.

#### **1.7.5 Non-glyoxalase detoxification of methylglyoxal**

When there is impairment or inhibition in the glyoxalase system, aldoketo reductase (AKR) isozymes 1B1 (aldose reductase), 1B3 and 1B8 can initiate the metabolism of glyoxal to glycolaldehyde, and AKR isozymes 1A4, 1B1 and 1B3 can metabolise MG primarily to hydroxyacetone (Figure 1.13) (Baba et al., 2009). Metabolism of glyoxal and MG by AKR 1B1 may be the main pathway in the renal medulla where elevated expression of AKR 1B1 outcompetes Glo1 (Larsen et al., 1985, Nishimura et al., 1993). However, levels of both glyoxal and MG may rise in renal failure because of the impairment in Glo1 activity. Glo1 activity in renal and vascular cells could be decreased in renal failure by causes such as reduced levels of GSH resulting from oxidative stress, reduced Glo1 expression and glutathionylation of Glo1.



**Figure 1.13: Non glyoxalase detoxification of dicarbonyl metabolites.**

(A) Metabolism of glyoxal and methylglyoxal by aldoketo reductases. (B) Metabolism of 3-deoxyglucosone by 3-DG reductase (AKRs 1A4, 1B1 and 1B3). (C) Metabolism of 3-deoxyglucosone by 3-DG dehydrogenase reductase (ADH 1A1).

Glo1 expression can be reduced by stimulation of the receptor for advanced glycation endproducts (RAGE), also by suppression of signalling by the transcription factor known as Nuclear factor erythroid 2-related factor 2 (Nrf2). Glo1 and the AKRs 1A4, 1B1, 1B3 and 1B8 are all antioxidant response element (ARE)-linked genes with expression controlled by Nrf2 (Xue et al., 2012, Kwak et al., 2003, MacLeod et al., 2009, Nishinaka and Yabe-Nishimura, 2005, Thimmulappa et al., 2002). Aldose reductase contributes in the reduction of MG to lactaldehyde when GSH is present and to acetol in the case of GSH absence (Vander Jagt et al., 2001, Nemet et al., 2006). Moreover, acetol is re-oxidised to MG slowly and spontaneously (Nemet et al., 2006). Aldehyde dehydrogenase might also participate in MG degradation when there is impairment or absence of the glyoxalase system.

MG can be oxidized to pyruvate by betaine aldehyde dehydrogenase in an NAD-dependent reaction (Nemet et al., 2006). There are more than 17 functional aldehyde dehydrogenase genes that have been identified (Vander Jagt and Hunsaker, 2003). The most vital genes are aldehyde dehydrogenase 1 (ALDH1), aldehyde dehydrogenase 2 (ALDH2) and aldehyde dehydrogenase 3 (ALDH3). These exhibit wide-ranging specificity and detoxify numerous aldehydes in humans (Vander Jagt et al., 2001). These genes have a preferred substrates known as unhydrated aldehydes (Vander Jagt et al., 2001, Nemet et al., 2006). Hence, MG which is a fully hydrated  $\alpha$ -oxoaldehyde is not easily metabolised by ALDH1 and ALDH2 (Vander Jagt et al., 2001, Nemet et al., 2006). However, it is a good substrate for betaine aldehyde dehydrogenase (Izaguirre et al., 1998).

### **1.7.6 Glyoxalase 1 - a critical role in enzymatic defence against glycation**

As mentioned previously, in physiological systems glycation of proteins leads to protein modification which ultimately results in structural and function impairment and also loss of side chain charge. Accumulation of glycation adducts have been linked to many disorders. Glycation of proteins is inhibited and can repaired by enzymatic systems in order to counter this damaging process. The concept of the enzymatic defence against glycation was developed by Thornalley in 2003 and consists of the activities of enzymes that suppress the creation of glycation adducts, in addition to other enzymes that repair sites of early glycation (Thornalley, 2003b). These involve Glo1, aldehyde reductase, aldehyde dehydrogenase, amadoriase and fructosamine 3-kinase. Glo1, aldehyde reductases and aldehyde dehydrogenase enzymes catalyse the breakdown of reactive  $\alpha$ -oxoaldehydes - including MG, glyoxal and 3-DG. In contrast, fructosamine 3-kinase is involved in the detoxification of fructosamine glycation adducts which are created by glucose-driven protein glycation. The enzymatic defences against glycation play a role in reducing defects to the functional proteome. Glycation of proteins, nucleotides and basic phospholipids is not completely prevented and can be occur, although in lower and tolerable levels in normal conditions (Thornalley, 2003b, Thornalley, 2003a). In disease conditions such as diabetes and its complications, the enzymatic systems against glycation are overwhelmed and therefore glycation adducts increase. Glo1 has been found to be the dominant defence enzyme against glycation caused by MG and glyoxal and decreases in Glo1 expression with age could cause development of accelerated ageing and the development of age-linked diseases (Morcos et al., 2005).

### 1.7.7 Development of Glo1 inducer therapeutics

Different experimental mediators have been used to reduce levels of reactive dicarbonyls, and one of the effective current therapeutic mediators proposed for diabetic complications are Glo1 inducers, for several reasons: (i) Glo1 metabolizes more than 97% of MG produced in human metabolism (Rabbani et al., 2016), (ii) this therapy restores reduced activity of Glo1, which is a common characteristic of experimental DKD in animals (Bierhaus et al., 2012, Barati et al., 2007, Palsamy and Subramanian, 2011), and (iii) a number of preclinical examinations found that Glo1 overexpression prevents the progression of diabetic nephropathy, in contrast, decreased expression increases risk the disease (Giacco et al., 2014, Brouwers et al., 2014, Geoffrion et al., 2014). Therapy consisting of small-molecule inducers of Glo1 expression, known as “Glo1 inducers” could be established as Nrf2 activators, stimulating the regulatory antioxidant response element (ARE) in the Glo1 gene to drive transcription (Rabbani and Thornalley, 2019).

Glo1 inducers can reduce cellular and extracellular levels of MG, MG-derived adducts, mutagenesis and endothelial attachment to collagen-4 (Xue et al., 2012). The Thornalley group analysed Glo1 inducers by using a functional reporter test depending on GLO1-ARE linked expression of luciferase (Xue et al., 2012). The best inducer for increasing Glo1 expression was found to be a combination of trans-resveratrol (tRES) and hesperetin (HESP), **termed as “tRES-HESP”** (Xue et al., 2016). Evaluation of tRES-HESP was conducted in a phase I clinical study design in overweight and obese individuals to determine safety pharmacology. Functional evaluations of metabolic health were additionally involved in a phase 2A clinical trial to establish metabolic health benefits in obese subjects (Xue et al., 2016). A randomized, double-blind, placebo-controlled crossover study was conducted in 29 overweight and obese subjects, who were giving oral capsule of tRES-HESP or placebo, every day for 8 weeks and a washout period of 6 weeks. Total tRES and HESP urinary metabolites were significantly increased >2000-fold and >100-fold, respectively, compared with placebo control. Safety assessments were normal at baseline and did not change throughout the study period for both the tRES-HESP and placebo groups. The tRES-HESP coformulation showed an increase in Glo1 enzyme activity by 22% in peripheral blood mononuclear cells of all participants when compared with placebo. Simultaneously, the concentration of MG showed a 37% decrease in the plasma of the tRES-HESP group, while there was no decrease with placebo. In addition, the flux of formation of MG-H1 adducts was nearly 13 nmol/mg

creatinine before treatment start and decreased by 14% after tRES-HESP supplementation, but again, this did not occur with the placebo group (Xue et al., 2016).

While experimental studies using *in vivo* models of DKD have found that overexpression of Glo1 reduced tissue AGEs, albuminuria, and mesangial expansion in diabetic mice, Brouwers with his colleagues showed that Glo1 overexpression in all tissues prevented dicarbonyl stress, AGEs, and oxidative stress which were related to diabetic vascular complications in diabetic rats (Brouwers et al., 2011). Importantly, further studies proved that Glo1 overexpression prevented oxidative stress and impairment of endothelium-dependent vasodilation in STZ-induced diabetic rats. The histological changes associated with DKD progression, for instance increased glomerular volume, decreased podocyte number and increased albuminuria, were attenuated by Glo1 overexpression in diabetic models *in vivo* (Brouwers et al., 2014). Furthermore, studies on Glo1 silencing conducted *in vitro* using vascular endothelial cells and tubular epithelial cells showed that silencing of Glo1 mimicked the effects of diabetes, while Glo1 overexpression in these cells prevented the development of DKD pathology (Giacco et al., 2014). These findings suggests that dicarbonyl stress is a driver of DKD and that overexpression of Glo1 can prevent it.

Human aortal endothelial cells (HAECs) provide an excellent model system that mimics dysfunctional metabolism of endothelial cells in diabetes. Glomerular endothelial cells provide a similar response. Cultured under hyperglycaemic conditions, these cells show an increase in cellular and extracellular concentrations of MG, increased AGEs in cellular protein and ECM protein extracts (Dobler et al., 2006, Stratmann et al., 2016). Studies by Yao et al., showed that culturing HAEC in high glucose medium decreased the activity of Glo1 by 50% (Yao and Brownlee, 2010). Therefore, overexpression of Glo1 can be an important new tool to prevent these diabetic effects (Ahmed et al., 2008, Dobler et al., 2006, Stratmann et al., 2016, Yao and Brownlee, 2010).

### **1.7.8 Glyoxalase inhibitors**

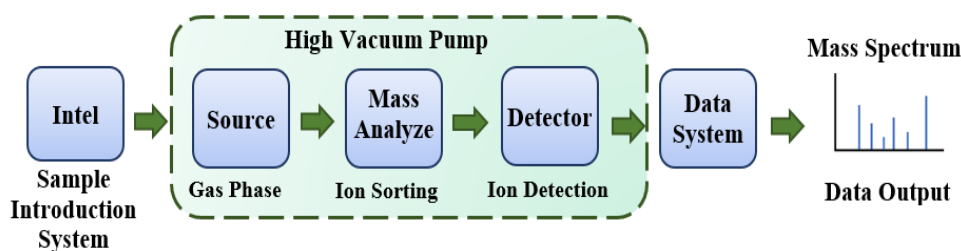
Chemical inhibitors of both Glo1 and Glo2 have been used in some studies to examine the effects of endogenous increases in dicarbonyl metabolites. Previous research found that glutathione thioether S-conjugates are substrate analogues which inhibit the Glo1 enzyme and may find uses as tumour suppressor drugs (Vince et al., 1971, Vince and Daluge, 1971). Later studies were unsuccessful in establishing anti-cancer activity of glutathione thioether S-conjugates because of the need of prodrug modifications to enable cell permeability, and the

need to stabilise them from degradation in the extracellular matrix. Inhibitors of both Glo1 and Glo2 activities were established by Lo and Thornalley (Lo and Thornalley, 1992). Substrate analogue inhibitors of Glo1 enzyme leave some residual inhibitory activity in Glo1 (Bush and Norton, 1985). The issue about cell permeability and extracellular stability of glutathione thioether S-conjugates had been resolved by Lo and Thornalley when they made diester derivatives. Glutathione thioether S-conjugate diesters, for instance the prototype Glo1 cell permeable inhibitor S-p-bromobenzylglutathione cyclohexyl diester (BrBzGSHCp2), tend to be permeable to cells because they have a main solution types that are nonionised and showed stability in the extracellular matrix as esterified glutathione derivatives that do not act as substrates for  $\gamma$ -glutamyl transferase. Within cells, the prodrug glutathione thioether S-conjugates are de-esterified through cellular non-specific esterases, and the active Glo1 inhibitors are formed and trapped in the cytosolic part where they can access the Glo1 enzyme itself (Thornalley, 2003b). The effects of several S-conjugates of glutathione on proliferation and viability of cells were studied (Lo and Thornalley, 1992). The studies indicated that unesterified inhibitors did not cross into cells and were degraded, and no toxicity was observed. Ester derivatives were not cleaved by the enzyme  $\gamma$ -glutamyl transferase and they were more able to access cells, wherein the ester groups would be cleaved to form the active structure of the inhibitor. Consequently, the study of Thornalley found that BrBzGSHCp2 was a cell permeable inhibitor of Glo1 suitable to use in cell-based experiments and also suggested its use as tumour inhibitor and apoptosis inducer (Thornalley et al., 1996)

## **1.8 Introduction to mass spectrometry**

### **1.8.1 Mass spectrometry**

Mass spectrometry is a powerful analytical technique that determines the mass-to-charge ratio ( $m/z$ ) of ions in the gas phase to provide the identification and quantification of unknown molecules in a sample, and to help determine their composition. A mass spectrometer consists of 3 essential parts: a source of ionisation to produce ions from the sample, a mass analyser which measures  $m/z$  parameters, and a detector to determine the ions and measure the relative abundance at a specific  $m/z$  value-Figure 1.14.

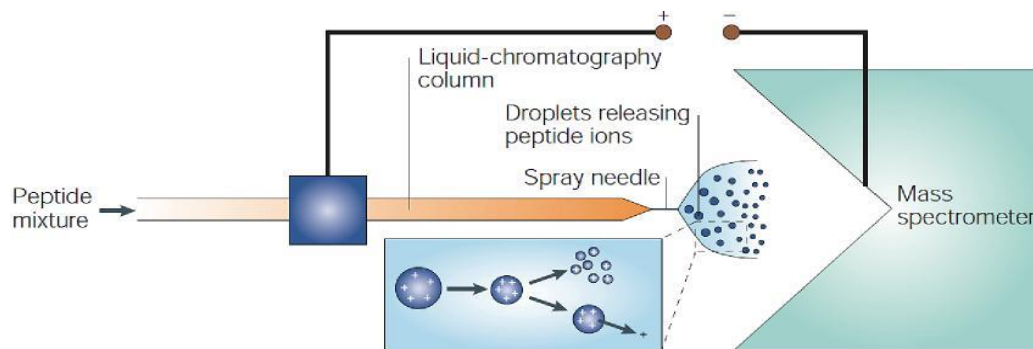


**Figure 1.14: Basic components of a mass spectrometer.**

## 1.8.2 Ionisation methods

Ionization refers to the procedure wherein sample is treated to produce a gas phase ion prior to resolution and introduction to the mass spectrometer. There are different techniques that can be used for particular applications. For example, there are the hard ionization techniques which require the use of high quantities of residual energy to impart a high degree of sample fragmentation, yielding an extremely detailed mass spectrum. An example of this method is electron ionization (EI). The second technique is soft ionisation leaving the parent ion intact (de Hoffmann and Stroobant, 2007). Chemical ionization mass spectroscopy was used in the past to detect small quantities of certain molecules, however the main disadvantage of this technique is that the analyte must be in the gas phase before analysis, and because of that it was not suitable to apply to biological samples, thus it was used for thermally stable analytes only (Feng et al., 2008). The latest advances in ionisation methods have the ability to raise an analyte, whether solid or liquid, into the gas phase as part of the ionisation process, for instance the development of electrospray ionisation ESI (Wong et al., 1988, Fenn et al., 1989), in addition to matrix-assisted laser desorption/ionisation (MALDI) (Karas et al., 1987, Karas and Hillenkamp, 1988, Tanaka et al., 1988).

The electrospray ionization method was first reported by Masamichi Yamashita and John Fenn in 1984 (Yamashita and Fenn, 1984) and has contributed greatly to the study of biological molecules by MS. Electrospray ionisation is a soft ionisation technique - it requires sample introduction in liquid solution of a typical organic solvent such as methanol (MeOH) or acetonitrile (ACN). In the case of positive ions analysis, oxidation reactions are conducted by adding small amounts of acid to the mixture to support the ionisation process. The mixture is then sprayed through the capillary needle (spinneret) while a high electric field is operated. The most common principle of ion formation by electrospray ionization is illustrated in Figure 1.15.



**Figure 1.15: Electro spray ionisation**

Adapted from (Steen and Mann, 2004).

The charged mixture within the capillary creates a conical form called a Taylor cone at the tip of the needle which then releases small, highly charged droplets. Nitrogen gas is usually used as nebulising assisting gas to form these droplets. Two mechanisms were proposed in ion formation by electro spray ionization - the charge residue model (CRM), and the ion evaporation method (IEM). In both methods charge repulsion in the droplet surpasses the surface electrostatic repulsion and subsequently the molecules of solvent evaporate. The repulsion charge generates Coulombic explosion, causing the droplets to divide. In CRM, this process is constantly happening until a multiply charged ion is created. In cases of the high mass-to-charge ratio ions, CRM is the main method to apply. IEM is used to generate ions with low mass-to-charge ratio. The starting procedure is similar however, once the Coulombic explosion occurs, the ions formed as droplets are desorbed in the gas phase and move into the mass spectrometer. High performance liquid chromatography (HPLC) system coupling to ESI, allows for fractional separation the biomolecules within a biological mixture upstream of to MS analysis, often in an online format.

The term MALDI by Kiochi Tanaka refers to a commonly used soft ionisation method (Tanaka et al., 1988). This method is conducted when the sample is adsorbed in a matrix containing organic acid that absorbs UV radiation. Under vacuum conditions, a UV laser is focused on the sample that heats the matrix molecules. Consequently, the laser desorbs the sample and charges it to neutral the analyte and matrix molecule then ejected. MALDI technique is performed with minimal fragmentation and mainly the ions produced are singly charged.

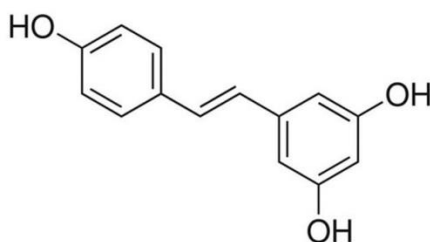


## 1.9 Project- specific background

### 1.9.1 Therapeutic approaches to counter dicarbonyl stress

### 1.9.2 Resveratrol

Resveratrol (3,5,4'-trihydroxylstilbene; RSV) is a natural polyphenol compound consisting of two aromatic rings connected by a methylene bridge (Figure 1.16) (Baur and Sinclair, 2006). It is formed naturally in different plants in response to stress, injury, fungal infection, and ultraviolet (UV) radiation (Soleas et al., 1997). It is found in grapes, red wine, berries, peanuts, and pines, Japanese knotweed, roots of rhubarb and different plants as trace mg/g portions of the plant, and some examples are shown in **Error! Reference source not found.** (Harikumar and Aggarwal, 2008, Shishodia and Aggarwal, 2006). RSV occurs naturally in 2 geometric isomer structures - trans (tRSV) and cis (cis-RSV) isomers; also when exposed to UV radiation the trans-RSV converts to cis-RSV (Constant, 1997). The levels of RSV found in food varies considerably, even in the same foodstuff from season to season and batch to batch. For instance, when grapes are exposed to UV light, the RSV level rises 2 to 10 fold (Shakibaei et al., 2009) -**Error! Reference source not found.** Studies by Francioso and colleagues found for the first time the conversion of trans- to cis- isomer, which can further cyclize to form 2,4,6-trihydroxyphenanthrene (THP), and this is promoted by exposure of red wine to UV light for around 10 minutes (Francioso et al., 2019).



**Figure 1.16: Resveratrol chemical structure**

RSV was first discovered in 1940 after it was isolated from the roots of white hellebore (Takaoka, 1940) then soon after, in 1963, the roots of *Polygonum cuspidatum*, referred to as Japanese knotweed. The latter plant has been used for many years in traditional Chinese treatment and is a rich source of resveratrol. Then in 1992, Siemann and Creasy reported that RSV is present in red wine and suggested that it might have a role in the cardioprotective effects of this drink (Siemann and Creasy, 1992). RSV is suggested as the major wine component which is responsible for the “French paradox”. The French paradox is the phenomenon that has puzzled scientists around the world and refers to the low mortality rate from coronary heart disease while having a lifestyle rich in a high-fat diet and smoking (Yu et

al., 2012, Lippi et al., 2010). Thus RSV attracted huge attention because of its wide range of biological activities and preventive effects on different diseases, as it has roles in cancer chemopreventive activity (Singh et al., 2019), cardioprotective (Kazemirad and Kazerani, 2020), is protective against neurodegenerative diseases, anti-inflammatory stress (Koushki et al., 2018), and has antioxidant properties (Koushki et al., 2018).

The potential mechanisms linked to the health effects of RSV can be summarised as scavenging intracellular ROS (Albani et al., 2009), inhibition of platelet activation and aggregation (Pace-Asciak et al., 1995, Shen et al., 2007, Yang et al., 2008), suppression of cell proliferation by actions of tumourigenic the signal transduction pathways (Woo et al., 2004), prevention of LDL oxidation (Tomé-Carneiro et al., 2012), reduction of cell proliferation and induction of apoptosis by stimulation of mitochondria-dependent pathways (Lucas and Kolodziej, 2015), induction of anti-inflammatory responses through downregulation of proinflammatory cytokines (Capiralla et al., 2012), enhancement of cellular differentiation (Jahan et al., 2018, Liu et al., 2016), and anti-oestrogenic activity via inhibition of CYP1 enzymes (Chang et al., 2001) Table 1.6.

**Table 1.5: Some dietary sources of resveratrol**

<b>Food sources</b>	<b>Average per standard units</b>	<b>Reference</b>
<b>Red wines</b>	0.1–14.3 mg l <sup>-1</sup>	(Burns et al., 2002, Goldberg et al., 1995)
<b>White wines</b>	<0.1 to 1.2 mg l <sup>-1</sup>	
<b>Red grape juice</b>	0.5 mg 100 ml <sup>-1</sup>	
<b>White grape juice</b>	0.05 mg 100 ml <sup>-1</sup>	(Wang et al., 2002, Rimando et al., 2004)
<b>Cranberry juice</b>	0.2 mg 100 ml <sup>-1</sup>	
<b>Fresh grape skin</b>	5–10 mg 100 g <sup>-1</sup>	
<b>Grapes (dry sample)</b>	0.64 mg 100 g <sup>-1</sup>	
<b>Blueberry (dry sample)</b>	0.4 mg 100 g <sup>-1</sup>	
<b>Strawberries (frozen)</b>	0.375 mg 100 g <sup>-1</sup>	(Lyons et al., 2003, Wang et al., 2007, Wang et al., 2008)
<b>Red currant (frozen)</b>	1.5 mg 100 g <sup>-1</sup>	
<b>Cranberry (frozen)</b>	1.9 mg 100 g <sup>-1</sup>	
<b>Bilberry (frozen)</b>	0.678 mg 100 g <sup>-1</sup>	
<b>Raw peanuts</b>	0.15 mg 100 g <sup>-1</sup>	(Burns et al., 2002, Sanders et al., 2000)
<b>Roasted peanuts</b>	0.006 mg 100 g <sup>-1</sup>	
<b>Boiled peanuts</b>	0.52 mg 100 g <sup>-1</sup>	
<b>100% peanut butter</b>	0.047 mg 100 g <sup>-1</sup>	(Hurst et al., 2008, Counet et al., 2006)
<b>Cocoa powder</b>	0.185 mg 100 g <sup>-1</sup>	
<b>Dark chocolate</b>	0.124 mg 100 g <sup>-1</sup>	
<b>Milk chocolate</b>	0.001 mg 100 g <sup>-1</sup>	
<b>Polygonum cuspidatum</b>	181–350 mg 100 g <sup>-1</sup>	(Burns et al., 2002)
<b>Itadori tea</b>	0.97 mg 100 ml <sup>-1</sup>	(Counet et al., 2006)
<b>Darakchasava (Ayur-vedic formula)</b>	0.36 mg/100 ml <sup>-1</sup>	(Paul et al., 1999)

Adapted from (Chachay et al., 2011).

**Table 1.6: Preclinical effects for resveratrol**

<b>Target</b>	<b>Effect</b>
<b>ANTI-CANCER</b>	
<b>Apoptosis induction</b>	↑ Caspase-3,-7,-8,-9; ↑ Cytochrome C (Cyt c); ↑ Bcl-2-associated X protein (Bax); ↑ Bcl-2-like 11 apoptosis facilitator (Bim); ↑ TNF-related apoptosis inducing ligand (TRAIL); ↓ Bcl-2-related protein A1(Bcl-2); B-cell lymphoma-extra large (Bcl-xL); ↓ Bcl-2-related protein A1( BFL-1/A1); ↓ Bcl-2-antagonist killer (Bak); ↓ Bcl-2-associated death promoter (Bad); ↓ BH3 interacting-domain death agonist (Bid); ↓ inhibitor of apoptosis proteins (cIAPs); ↓ X-linked inhibitor of apoptosis protein (XIAP); ↓survivin; ↓ mammalian target of rapamycin (mTOR); ↓ p70S6 kinase (p70S6K); ↓ TNF receptor associated factor (TRAF2); ↓procaspase-8; ↑ apoptotic protease activating factor (APAF-1).
<b>Invasion and Metastasis</b>	↑ Tissue inhibitors of MMP (TIMP-1, -2); ↓ Matrix metalloproteinase (MMP-9, -2); ↓ Vascular endothelial growth factor (VEGF); ↓ Endothelial growth factor receptor (EGFR2); ↓ Fibroblast growth factor (FGF-2); ↓ Metastasis-associated protein (MTA1); ↓ Vascular cell adhesion protein 1 (VCAM-1).
<b>ANTI-CVD/DIABETES /OBESITY</b>	
<b>Vascular inflammation-response inhibition</b>	↓ Tumor necrosis factor alfa (TNF); ↓ Inducible nitric oxide synthase (iNOS); ↓ Cyclooxygenase (COX-2); ↓ Interleukin (IL-6); ↓(IL-8); ↓MMP-9; ↓ Monocyte chemotactic protein (MCP-1); ↓ Prostaglandin E2 (PGE2); ↓ C-reactive protein (CRP); ↓ transforming growth factor (TGFβ); ↓ intercellular adhesion molecule 1(ICAM-1); ↓VCAM-1; ↓Leukocyte recruitment and infiltration; ↓ Platelet aggregation.
<b>Metabolic modulation</b>	↑Metabolic rate; ↑ Insulin sensitivity; ↓Blood glucose; ↓ total cholesterol (Total-c); ↓ Triglycerides (TG); ↓ Free fatty acids (FFA); ↓ low-density lipoprotein cholesterol (LDL-c); ↑ High density lipoprotein cholesterol (HDL-c); ↓Steatosis; ↓ apolipoprotein (ApoB/ApoA1); ↑Adiponectin; ↓ 3-hydroxy-3-methylglutaryl-coenzyme A (HMGCoA reductase); ↓ Preadipocyte proliferation; ↓ Adipogenic differentiation; ↓De novo lipogenesis; ↓Lipogenic gene expression.

<b>Target</b>	<b>Effect</b>
<b>ANTI-AGING</b>	
<b>Inflammation inhibition</b>	↓TNF; ↓iNOS; ↓ soluble CD40 ligand (sCD40L); ↓IL-6; ↓IL-8; ↓MCP-1; ↓ICAM-1; ↓ macrophage inflammatory protein (MIP-); ↓ Chemokine (GRO-); Interferon-gamma (IFN-γ).
<b>Oxidative stress reduction</b>	↑ Nitric oxide (NO); ↑ Superoxide dismutase (SOD); ↑ Glutathione peroxidase (GPx1); ↑ Catalase (CAT); ↓ Reactive oxygen species (ROS); ↓ Vascular endothelial growth factor (VEGF); ↓, Tumor protein p55; ↓ nicotinamide adenine dinucleotide phosphate oxidase (NOX); ↓ malondialdehyde (MDA); ↑mitochondrial biogenesis.

Modified from (Tomé-Carneiro et al., 2013).

### **1.9.2.1 Effect of tRSV on diabetes**

Control of T2DM focuses on three major aspects of metabolic regulation: 1) glycaemic control, 2) enhancement of insulin action and 3) protection of pancreatic  $\beta$ -cells.

#### **1.9.2.1.1 Effects of tRSV on blood glucose levels**

To date, only limited clinical trials had been conducted to examine the health benefits of RSV in humans. In a study of 62 T2DM patients receiving 250 mg/day RSV in the presence of their oral hypoglycaemic treatment for 3 months, there was a significant improvement in disease parameters including glycosylated haemoglobin (HbA<sub>1c</sub>), systolic blood pressure, total cholesterol, urea nitrogen, and total protein, while there was no significant change in body weight, HDL or LDL (Bhatt et al., 2012). A similar study has been conducted by using a dose of 1 g/day in T2DM patients along with their standard antidiabetic medication for 45 days. In this study RSV showed significant decreases in fasting blood glucose, HbA<sub>1c</sub>, insulin, and insulin resistance when compared to patient baseline levels, in contrast to the placebo group that showed a slightly increase in their fasting glucose and LDL levels (Movahed et al., 2013).

Due to the limited studies on human, most broader analyses have been conducted in rodents and demonstrate the potential effects of RSV in improving various metabolic health parameters. Studies of Simas *et al.*, found that diabetic rats treated orally with 150 mg/day RSV showed a significant decrease in blood glucose compared with the streptozotocin (STZ)-diabetic rats after 75 postpartum days (Simas et al., 2017). Moreover, in ob/ob obese mice, oral gavage doses of tRSV at 5 and 15 mg/kg/day did not show a significant decline in blood glucose, while 50 mg/kg/day dose was effective in decreasing blood glucose compared with the control ob/ob mice after 28 days (Sharma et al., 2011). In the study by Yonamine *et al.*, where obese monosodium glutamate-T2DM mice developed hyperglycaemia, insulin resistance, and decreased GLUT4 translocation, treatment with RSV improved glycaemic control and restored all alterations in both muscle and liver (Yonamine et al., 2017). Major enzymes of carbohydrate metabolism such as glucose-6-phosphatase, glucose-6-phosphate dehydrogenase, fructose-1,6-bisphosphatase, hexokinase, glycogen synthase and glycogen phosphorylase, pyruvate kinase and lactate dehydrogenase were found to be significantly increased in liver and kidney of STZ-nicotinamide diabetic rats after treatment with oral 2.5 mg/kg/day tRSV (Palsamy and Subramanian, 2009).

On the other hand, the study of Schmatz *et al.* reported no decrease in blood glucose by administration of tRSV at 10 and 20 mg/kg/day to diabetic rats. It seems that in obesity and chemically induced diabetes, tRSV was less effective when administered intraperitoneally rather than orally (Schmatz *et al.*, 2009a, Schmatz *et al.*, 2009b). Also, the study of Do *et al.*, reported an increase in GLUT4 in db/db mice treated with RSV, despite the effect of RSV on glycaemic control not being clearly evidenced (Do *et al.*, 2012). Some studies have demonstrated that RSV is capable of reducing blood glucose levels in the absence of insulin in animals with moderate diabetes induced by STZ-nicotinamide, wherein glucose uptake increased in insulin-responsive tissues such as hepatocytes, adipocytes, and skeletal muscle cells isolated from STZ induced diabetic rats. This suggests that the effect of tRSV on reducing blood glucose levels might be insulin-independent (Su *et al.*, 2006).

#### **1.9.2.1.2 Effects of tRSV on blood insulin levels**

Human studies focusing on the anti-hyperglycaemic action of RSV are still limited, however, some data suggest that RSV may be capable of decreasing insulin resistance. In overweight T2DM patients, treatment with RSV for 4 weeks showed for the first time a decrease in insulin resistance (Brasnyó *et al.*, 2011). Related findings of Timmers *et al.*, on obese subjects treated with tRSV 150 mg/day for 30 days, showed that RSV induced effects on energy metabolism and metabolic profile in human obesity similar to caloric restriction, also plasma glucose and insulin levels were reduced compared to placebo, suggesting improved insulin sensitivity (Timmers *et al.*, 2011). The more recent study of Zare *et al.*, suggested that RSV supplementation of 480 mg/day for 4 weeks might be effective as adjuvant therapy treatment in insulin resistance among diabetic patients with periodontal disease (Zare Javid *et al.*, 2017).

A number of studies have been performed in humans and animals to discover the role of tRSV as a beneficial compound for enhancing insulin action in diabetes and to elucidate the mechanism of its action. In animals, treatment with tRSV has been claimed to improve insulin sensitivity. A tRSV daily dose of 22 mg/kg/day showed improvements in insulin sensitivity in mice maintained on a high calorie diet (Baur *et al.*, 2006), as well as decreases in blood glucose. The mechanism of action of RSV suggested a strong tendency to induce the stimulation of phosphorylated AMP-activated protein kinase (AMPK), a metabolic regulator that enhances insulin sensitivity and fatty acid oxidation, along with two downstream indicators of activity: the phosphorylation of acetyl-CoA carboxylase at Ser 79 and the reduced expression of fatty

acid synthase (Baur et al., 2006). Similarly, Lagouge *et al.* showed that oral administration of genetically obese, hyperphagic, diabetic KKAy mice with 2 and 4 mg/kg/day tRSV improved insulin resistance and lowered blood glucose (Lagouge et al., 2006). The peroxisome proliferator-activated receptor- $\gamma$  coactivator PGC-1 $\alpha$  and sirtuin 1 gene (SIRT1) activation have been connected to tRSV-induced enhancement of insulin action. In addition, numerous studies on animals show that activation of AMPK and SIRT1 is increased by tRSV (Lagouge et al., 2006, Baur et al., 2006, Lee et al., 2009, Shang et al., 2008, Hausenblas et al., 2015).

In the same context, a study has been carried out on 10 randomized patients with T2DM to examine the effect of RSV on skeletal muscle SIRT1 expression and energy expenditure. Thus, ten patients were given 3 g of RSV or placebo every day for 12 weeks. Results showed that skeletal muscle SIRT1 expression and AMPK expression in the RSV group were significantly increased compared with the placebo group (Goh et al., 2014). A double-blind, randomized, placebo-controlled clinical trial aimed to determine whether RSV supplementation of 500 mg 3 times daily for 90 days could have a measurable effect on metabolic syndrome, insulin sensitivity, and insulin secretion. The study was performed on 24 patients with the diagnosis of metabolic syndrome and divided into the placebo and tRSV treatment groups. Results showed significant decrease in body weight, fat mass, the area under the curve of insulin, and insulin secretion after treatment with tRSV (Méndez-del Villar et al., 2014). In contrast, RSV did not have a significant effect on insulin sensitivity in a study carried out for 6 months on 41 overweight subjects that received a dose of 150 mg/day - although there was a significant change in the HbA<sub>1c</sub> level compared with the placebo group (de Ligt et al., 2020). Further studies conducted on rodents showed that RSV induced a reduction in body fat content within a hypercaloric diet. In Sprague-Dawley rats treated with 30 and 60 mg/kg/day tRSV there were decreases in body fat by 24% and 19%, respectively (Macarulla et al., 2009). Also, mice supplied orally with tRSV 400 mg/kg/day showed increased metabolic rate and reduced fat mass (Um et al., 2010). In addition, Wistar rats given 100 mg/kg/day doses of oral tRSV had reduced body weight (Rocha et al., 2009).

Furthermore, RSV intake was found to cause effects that are similar to those produced by calorie restriction, including decreased age-related cardiac dysfunction, decreased hyperglycaemia and inhibition of gene expression associated with cardiac and skeletal muscle ageing. In laboratory animals, RSV mimics the effects of dietary restriction by inducing gene expression patterns in several tissues that are the equivalent of those invoked by dietary restriction, including decreased albuminuria, reduced inflammation/apoptosis in the vascular



endothelium, increased aortic elasticity, decreased cataract formation, greater motor coordination, and preserved bone mineral density. This was achieved by doses of 100 – 400 mg/kg/day tRSV (Pearson et al., 2008). A lower supplement of tRSV at 4.9 mg/kg/day in mice from middle age caused a change in gene expression similar to caloric restriction with no reduction in body weight, although body weight reduction was observed with actual calorie restriction (Barger et al., 2008).

*In vitro* experiments have shown similar effects of RSV but the high supraphysiological concentrations of *in vivo* studies might impact the results and make conclusions less clear. When rat adipocytes were treated with tRSV (6 – 50  $\mu$ M), there was a decrease in ATP content, triglycerides, lipogenesis and lipolytic response to epinephrine (Szkudelska et al., 2011). The same cells were treated with tRSV (62.5 – 250  $\mu$ M) and showed reduced lipid accumulation as a result of reduced glucose conversion to lipids, as well as increased epinephrine-induced lipolysis (Szkudelska et al., 2009). Effects of tRSV (10, 25 and 50  $\mu$ M) were studied with conjugated linoleic acid in the control of insulin resistance on human adipocytes and the results showed increases in insulin-stimulated glucose transport and decreased inflammation compared with the cells treated by linoleic acid only (Kennedy et al., 2009). This was proposed to be caused by decreases in cellular stress, prevention of activation of extracellular signal-related kinases, inhibition of inflammatory gene expression, and increases in peroxisome proliferator-activated receptor  $\gamma$  (PPAR $\gamma$ ) activity (Szkudelska *et al.*, 2011, Szkudelska *et al.*, 2009). Another study using  $\alpha$ TC9 cells (a mouse pancreatic  $\alpha$ -cell line) showed that RSV induced insulin-related gene expression in pancreatic cells, such as pancreatic and duodenal homeobox 1 (Pdx1) and insulin 2 (Ins2) after being treated with 25  $\mu$ M RSV for 24 hr (Xie et al., 2013).

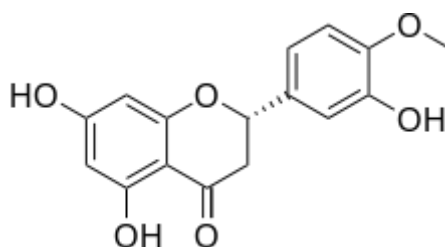
#### **1.9.2.1.3 Effect of tRSV on protection of $\beta$ -cells**

Pancreatic  $\beta$ -cells are considered to be the only source of insulin in the body, and recent studies indicate that RSV is able to attenuate autoimmune destruction of these cells. One of the recent studies on rodents have established that RSV is capable of protecting  $\beta$ -cells, this action is accompanied by the antioxidant property of RSV through enhancing of antioxidant enzymes such as: superoxide dismutase, catalase, glutathione peroxidase and glutathione-S-transferase as well as protecting these cells from free radical damage, moreover, RSV reserved the degenerative cell changes of diabetic rat (Palsamy and Subramanian, 2010). Another study by Lee *et al.*, on Non-obese diabetic (NOD) mice found that RSV delays the development of

diabetes and reduce its severity. RSV increased both total islet number and insulinitis-free islets, through reduction of lymph nodes in the spleen and pancreas of NOD mice. The study demonstrated that RSV downregulated the expression of some inflammatory cell types and prevent its migration to the pancreas (Lee et al., 2011). It should be also emphasized that protective action of RSV in pancreatic cells includes inhibition of cytokine action. Lee *et al.* found that isolated rat pancreatic cells incubated with cytokines showed many negative effects, such as increased DNA binding by NF- $\kappa$ B, increased production of NO, and increased expression of iNOS. All of these deleterious effects appeared to be suppressed by RSV (Lee et al., 2009).

### 1.9.3 Hesperetin

Hesperetin (HSP) is one of the natural phenolic compounds found in plants known as flavanones – derivatives of a core  $\alpha$ -2,3-dihydro-2-phenylchromen-4-one structure (Figure 1.17). It is the main flavonoid occurring in citrus fruits such as lemons and oranges (Khan, 2014). HSP is the aglycone form of Hesperidin (hesperetin 7-rutinoside, hesperetin 6-O- $\alpha$ -L-rhamnosyl-D-glucose). Extraction of Hesperidin for the first time was achieved in 1828, by the French chemist Lebreton when he isolated Hesperidin from citrus peels (Manthey and Grohmann, 1998). Absorption of Hesperidin occurs at low rate following the de-glycosylation process by gut bacteria in the small intestine and colon, while HSP has high variability when supplemented from diet, and is absorbed readily without enteral metabolism (Kanaze et al., 2007). The levels of Hesperidin can vary between fruit types, with the highest concentration in citrus fruits such as oranges, lemons and limes. Previous studies found that the concentration of Hesperidin in orange was 0.0256–0.393 g/kg of the fruit (Peterson et al., 2006b), in lime it was 0.052–0.430 g/kg and in lemon it was 0.019–1.422 g/kg of the net weight (Peterson et al., 2006a).



**Figure 1.17: Hesperetin chemical structure**

HSP is well known to be extremely safe (Li and Schluesener, 2017). Kanaze *et al.*, found that there were no side effects when healthy subjects had a dose as high as 135 mg HSP daily (Kanaze *et al.*, 2007). In animal studies, Hesperidin showed a median LD<sub>50</sub> of 4837.5 mg/kg, and low adverse effects at 1000 mg/kg in rats (Li *et al.*, 2019b). HSP is absorbed effectively, metabolised to the circulating forms of glucuronide and sulphoglucuronide, and excreted in urine (Manach *et al.*, 2003). A clinical study showed that consumption of Hesperidin by healthy volunteers in 0.5 or 1l of a commercial orange juice (444 mg/l hesperidin), led to peak plasma concentrations of HSP of 0.46 µM and 1.28 µM after the 0.5 and 1l intake, respectively (Manach *et al.*, 2003).

### **1.9.3.1 Effect of hesperidin on diabetes and its complications**

Several studies have proved that HSP possesses strong pharmacological effects in many diseases, including antioxidant (Aswar *et al.*, 2014, Shagirtha and Pari, 2011), anti-cancer (Roohbakhsh *et al.*, 2015), anti-inflammatory effects (Ding *et al.*, 2017) and positive effects in diabetes (Iskender *et al.*, 2017). Growing evidence shows that HSP has the ability to modulate several metabolic disorders including diabetes and its complications in both experimental models and human subjects. One clinical trial has shown that oral supplementation of HSP (500 mg daily for 3 weeks) significantly improved lipid profile and insulin resistance in patients with metabolic syndrome. The study also showed a significant reduction in total circulating cholesterol and LDL cholesterol, while glucose concentration did not differ significantly compared to the controls (Rizza *et al.*, 2011).

In studies of diabetes, Hesperidin was shown to regulate blood glucose levels. The study of Jung *et al.* conducted on diabetic mice proved the protective role of Hesperidin on glucose homeostasis through its capacity to stabilise glucose metabolism and lipid profiles. The study also found that Hesperidin significantly enhanced the level of glucokinase mRNA in the treated mice (Jung *et al.*, 2004). Another study by Rekha *et al.* found that STZ-induced diabetic rats treated with Hesperidin (100 mg/kg diet) showed a significant reduction in glucose levels through altering the activity of glucose-regulating enzymes and this also lowered the total blood lipid profiles (Rekha *et al.*, 2019). Noteworthy, Hesperidin not only mitigated diabetes but also reversed its complications, for instance the *in vivo* study of Kouhpayeh *et al.* found that Hesperidin (500 mg/kg) restored endothelium-dependent vasodilation in T1DM rats and reduced urea plasma concentrations near to control animals. In addition, Hesperidin preserved NO levels in aortic endothelial cells in diabetic studies. These results suggested that Hesperidin

exhibited a protective effect as an antioxidant and anti-inflammatory agent. Moreover, administration of Hesperidin to STZ-induced diabetic rats reduced glucose levels and liver & kidney damage markers significantly. It also alleviated oxidative stress and activation of nuclear transcription factor kappa B (NF- $\kappa$ B) and levels of SIRT1 (Iskender et al., 2017).

### **1.9.3.2 Antioxidant effects of hesperetin**

The overall results indicate that hesperetin is a potent antioxidant compound, which might reduce high oxidative stress and increase antioxidant cellular defences. To highlight the antioxidant effects of hesperetin, several studies have been performed so far. The antioxidant mechanism of action of HSP is believed to be exerted through its scavenging activity of ROS and the enhancement of antioxidant cellular defences via increasing the expression of transcription factor nuclear factor-2 erythroid-2 (Nrf2) and its downstream target heme oxygenase-1 (HO-1). Studies by Choi showed that HSP has antioxidant activity when it was tested in STZ-induced-T1DM, and the results showed that HSP increased lipid peroxidation, upregulated GSH, and antioxidant gene expression (Nrf2 and HO-1) (Choi, 2008).

However, most *in vitro* research has applied high concentrations of HSP (50  $\mu$ M) to study the effective role of this compound. Recent studies by Zhu *et al.*, found that HSP provided tremendous antioxidant activity against oxidative stress induced by H<sub>2</sub>O<sub>2</sub> in retinal pigment epithelial cells, their results showing that HSP treatment effectively protected these cells against elevated oxidative stress through inhibiting apoptotic cell death, ROS formation and upregulating the expression of both SOD and GSH, which might underpin the mechanism of activation of the Nrf2/HO-1 signalling pathway (Zhu et al., 2017).

### **1.9.3.3 Role of hesperetin in glycation**

Very few studies have assessed the role Hesperidin and HSP on glycation. The recent *in vitro* study of Dhanya & Jayamurthy examined the potential protective effect of Hesperidin and HSP at 10 $\mu$ M against glycation induction in the skeletal muscle L6 myotubes cell line. The study found that Hesperidin and HSP inhibited protein glycation by 58% and 35%, respectively (Dhanya and Jayamurthy, 2020). Chen *et al.*, administrated HSP orally at 50 and 150 mg/kg for 10 weeks to STZ-induced diabetic rats to evaluate its renoprotective effects and the results showed that HSP improved renal function and reduced proinflammatory cytokine production by reducing the AGEs/RAGE axis and inflammation in the treated rats (Chen et al., 2019).

However, greater understanding of the role of HSP in protecting against the impact of glycation is needed.

#### **1.9.3.4 Anti-inflammatory effects of hesperetin**

The citrus flavonoids including HSP have shown anti-inflammatory effects in many studies. Table 1.7 summarises the anti-inflammatory properties of Hesperidin, HSP and related compounds. To underline the anti-inflammatory properties of HSP, different studies have been conducted recently. In one *in vivo* study that used an animal inflammatory model to study the anti-inflammatory and antioxidative role of naringin and Hesperidin at 30 and 50 mg/kg, the results showed that Hesperidin led to better pharmacological action in alleviating the inflammation without inducing toxicity (Jain and Parmar, 2011). Based the on clinical study of Perche *et al.*, conducted on healthy subjects after consuming orange juice 500 ml daily and Hesperidin at 292 mg in a capsule, Hesperidin showed no immunomodulation effects, and this suggests that even if Hesperidin did not induce immunomodulation in the body, it would not produce inappropriate immune reaction (Perche et al., 2014).

**Table 1.7: Summary on the anti-inflammatory properties of hesperidin, HSP and related compounds**

<b>Study model</b>	<b>Compound (s)</b>	<b>Major findings</b>	<b>References</b>
<b>Rat air pouch model of inflammation</b>	Hesperidin at 50 mg/kg and naringin 30 mg/kg	↓ LPO, ↓ SOD, ↓ catalase, ↓ GSH and ↓ NO in tissue.	(Jain and Parmar, 2011)
<b>Healthy human subjects</b>	Orange juice 500 ml daily and Hesperidin at 292 mg in a capsule	No variations found on leukocyte subset distributions, ROS and cytokine production.	(Perche et al., 2014)
<b>Cyclophosphamide-induced rat model of hepatotoxicity</b>	Hesperidin at 25 or 50 mg/kg	↓ Serum GSH, ↓ catalase, ↓ SOD and ↓ glutathione peroxidase. Furthermore, improved the cyclophosphamide-induced downregulation of PPAR $\gamma$ and upregulation of NF- $\kappa$ B and iNOS mRNA expression in a dose-dependent manner.	(Mahmoud, 2014)
<b>Mouse model of acute prolonged inflammation</b>	Hesperidin methyl chalcone (HMC) at 30 mg/kg	Inhibited TRPV1 agonist-induced inflammation, inhibited carrageenan-induced cytokine (IL-6, IL-10 IL-1 $\beta$ , and TNF- $\alpha$ ) production and NF- $\kappa$ B activation.	(Pinho-Ribeiro et al., 2015)
<b>STZ-induced diabetes rat</b>	HSP at 30mg/kg	↓ Inflammatory markers (IL-1 $\beta$ , TNF- $\alpha$ and ICAM-1), inhibited NF-Kb pathway.	(Yin et al., 2017)
<b>Chronic constriction injury as model of neuropathic pain in rat</b>	Hesperidin at 100mg/kg	Hesperidin can ameliorate neuropathic pain	(Carballo-Villalobos et al., 2017)
<b>Adjuvant-induced arthritis rat</b>	Hesperidin derivative-11 (HDND-11) at 50,100 and 200 mg/kg	Supressed the proliferation and invasion of fibroblast-like synoviocytes (FLS). ↑ SFRP2, ↓ DNMT1, ↓ $\beta$ -catenin.	(Liu et al., 2017)

Adapted and modified from (Yatao et al., 2018).

#### 1.9.4 Proteomics

The term proteomics refers to the science of post-genomics when the entire set of proteins in a particular system (called the “proteome”) or a selected fraction of a proteome are detected, identified and quantified. Further characterisation of protein structure and function such as post-translational modifications and protein turnover can also be investigated. Proteomics studies can also investigate the interaction and the distribution of proteins at the subcellular level (Ong and Mann, 2005).

The first use of the term “proteomics” in mainstream research referred to the use of two-dimensional gel electrophoreses (2-DE) of proteins with excision of separated protein spots from gels for identification by peptide mass spectrometry (following proteolysis by trypsin). In 2-DE experiments, staining patterns of a protein mixture can visually reveal changes (upregulation or downregulation) of specific protein species or subsets. However, use of 2-DE methods has many limitations including limited range of protein detection and that cannot accommodate 7 - 12 orders of magnitude within a sample. In addition, not all individual protein species of interest can be resolved totally into discrete spots, plus extraction protocols to recover peptides and proteins from polyacrylamide gels leads to loss of excised protein samples, especially low abundance species. Therefore, 2-DE gel studies have now largely been replaced by nanoflow liquid chromatography-high resolution mass spectrometry (MS) for proteomics research, especially in complex samples such as cell extracts (Anderson and Anderson, 1998, Aebersold and Mann, 2003). The basic procedure in MS proteomics study involves limited proteolysis by Lys-C and/or trypsin in order to digest proteins to peptides (Fang et al., 2002), partial resolution of peptides applying nanoflow liquid chromatography and ion fragmentation followed by detection of peptide ions by positive ion electrospray ionisation mass spectrometry (ESI-MS). Fragment ion series mass spectra and MS<sup>n</sup> spectra are employed to sequence peptides and identifying specific proteins.

Using of bioinformatics analysis tools is essential for data processing and interpretation, where threshold standards for protein identification have been developed by international consensus. At least two unique peptides are essential to identify a protein. Clear detection and identification of protein-specific peptides demonstrates their presence in the sample. However, when a peptide is not identified or detected this does not necessarily indicate that the protein is absent from the starting sample, as the peptides generated during sample preparation may be under the threshold for identification with any confidence or may be post-translationally modified. Consequently, the Boolean nature of MS protein identification

schemes (existence or absent by setting threshold criteria) provides an insufficient image of protein abundance in the sample. Modern high sensitivity and high mass resolution MS is now able to recognise 1000s proteins per sample, although robust quantitation can be challenging (Aebersold and Mann, 2003). Proteins can be quantitated by two routes - either the measurement of the absolute amount of the protein in a sample, or by comparing the relative change in the amount of protein between two conditions treated. Absolute quantification of protein is determined by measuring the amount of the substance under examination; for example, ng ml<sup>-1</sup> of a protein or the copy number of a protein/cell. In relative quantification, the ratio of specific proteins between two different treatments is measured. This can be used effectively, for instance, in the study of protein abundance changes produced by drug treatment (Ong and Mann, 2005, Sadygov et al., 2004).

#### **1.9.4.1 Label-free quantification**

Label-free quantitation of proteins can be divided into two distinct approaches of quantification: i) spectral counting and ii) peptide ion intensities. Spectral counting includes counting the number of fragment ion spectra (MS/MS) detected for a certain protein. The number of fragment ion spectra rises when protein abundance rises (Liu et al., 2004). However, another approach employed is measuring the chromatographic peak areas of peptide precursor signal intensity (molecular ions). Based on the chromatographic method (for instance, reverse-phase liquid chromatography), the peptides are separated depending on their particular physical properties (e.g. hydrophobicity, charge) followed by ionisation and identification by mass spectrometric analysis. The acquired peptides of a specific mass/charge ratio are then mapped using their coordinates on the mass/charge ratio and retention-time histogram, producing a single mono-isotopic mass peak. The peak intensity is linked to protein abundance which makes the measurement achievable for quantitative experiments (Bondarenko et al., 2002, Chelius and Bondarenko, 2002).

This kind of approach is convenient and straightforward. To have reliable estimations, many experimental and technical aspects should be taken into account and raw LC-MS histograms generated from the experiments have to undergo post-processing procedures such as retention time alignment, detection of features, MS intensities normalisation, peak picking, and noise reduction. Interbatch coefficients of variation obtained by this approach are usually  $\geq 30\%$  (Megger et al., 2013).



#### **1.9.4.2 Sample preparation for label-free quantification**

Proteomics includes the analysis of proteins for many different types of sample such as body fluids (e.g. serum, plasma, urine and bile) and cell extracts or isolated tissues (Megger et al., 2013). This is conducted after cell lysis, where applicable, followed by protein isolation and digestion. The buffers used in lysate preparations and conditions are selected based on the whole or fractional proteome of interest. For instance, membrane proteins, nuclear proteins, cytosolic protein and other compartments based on cellular or plasma fraction (Shevchenko et al., 2012).

Digestion of proteins into smaller and more manageable fragments is performed by using trypsin and/or lys-C, or other proteases such as glutamate-selective Glu-C (Wiśniewski et al., 2009). The most widely applied protease in mass spectrometry is trypsin because it has high proteolytic activity and increased peptide-coverage. There is one disadvantage of using trypsin, which is incomplete digestion. Moreover, trypsin activity is less active against some tightly folded proteins, plus it can be inhibited by some reagents applied in sample preparation (Saveliev et al., 2013). Lys-C is able to overcome the proteolytic resistance of many tightly folded proteins by very efficiently cleaving at solvent-exposed lysine residues, and this improves overall digestion efficiency and specificity. Therefore, supplementing trypsin with Lys-C overcomes trypsin drawbacks (Saveliev et al., 2013). Additionally, one of the commonly employed methods for purifying samples is spin columns and filter digestion (Antharavally et al., 2011). Another technique, used for small protein amounts, is the solution digestion method established by Vekey and colleagues (Turiák et al., 2011).

It is vital to determine the total protein concentration in a sample, particularly if label-free quantification is the method to be performed. Protein measurement after extraction from a sample is required to evaluate whether the protein isolation has been conducted successfully and to determine the volume of protease required for digestion (Megger et al., 2013). Protein measurement is conducted by colorimetric techniques such as Bradford (Bradford, 1976), bicinchoninic acid (BCA) (Smith et al., 1985), biuret, Lowry (Lowry et al., 1951) or Popov assay (Popov et al., 1975). Alternatively, amino acid analysis can be used to determine protein concentration in the sample (Tyler and Wilkins, 2000).

The resulting peptides from a tryptic digestion are partly resolved by reversed phase liquid chromatography (RP-LC) prior analysis by mass-spectrometric analysis. It is essential to use internal standards including stable-isotope coded peptides in order to have high reproducibility within a label free study (Megger et al., 2013). Retention times of these isotopic

standard peptides can be used to detect the performance of LC–MS over a period of time, also serve as markers for the chromatographic alignment processes during data analysis. Currently, there are many mass analysers with high resolution capabilities suitable for free label quantification. Advanced examples include the orbitrap analyser (Panchaud et al., 2008, Aebersold and Mann, 2003). It has very high mass resolution, is simple to handle with regard to the output data, and it is relevant for use on different peptide fragmentation procedures such as electron-transfer dissociation (ETD) and higher energy-collisional dissociation (HCD).

### **1.10 Aims and objectives of this project**

In this project we hypothesised that the Glo1 inducer can prevent or reduce markers of DKD progression in models of renal cell hyperglycaemia *in vitro*. Therefore, the aims of this study set to test this hypothesis by characterising intrinsic protein expression in primary human renal cells and studying the effects of high glucose concentration and Glo1 inducers on cellular Glo1 expression and activity.

The objectives of this thesis are as follows:

- 1) To characterise the metabolic function of the glyoxalase system and dicarbonyl metabolism in primary human renal cell cultures – specifically proximal tubular epithelial and mesangial cells. Models of hyperglycaemia will be established with these cells *in vitro*.
- 2) To study the impact of the Glo1 inducer, tRES-HESP, on human renal cell dysfunction in high glucose cultures *in vitro*, and whether this treatment can reverse cell dysfunction and dicarbonyl stress.
- 3) To characterise quantitatively the intrinsic protein expression profiles of primary human proximal tubular epithelial and mesangial cells via label-free proteomics, also to examine the impact of hyperglycaemic conditions on protein expression.
- 4) To characterise quantitatively the impact of the Glo1 inducer, tRES-HESP, on the protein expression profiles of the primary proximal tubular epithelial and mesangial cells, both in the context of normoglycaemia and hyperglycaemia.

## **2 Materials and methods**

### **2.1 Materials**

#### **2.1.1 Cells and tissues**

Human renal proximal tubular epithelial cells (hRPTECs) were purchased from Lonza, (Slough, UK; catalogue number CC-2553). hRPTECs were originally isolated from the proximal tubule of healthy kidney. Human Mesangial cells (MCs) were purchased from Sciencell Research Laboratories (Buckingham, UK; catalogue number 4200), these cells were isolated from human kidney of healthy individuals, MCs are perivascular cells located within the central portion of the glomerular tuft between capillary loops. All samples were tested for proper morphology, surface adhesion and spread in two-dimensional tissue culture on T75 flasks, and proliferation in custom renal cell culture media. Cells were confirmed as negative for HIV, Hepatitis B, Hepatitis C, mycoplasma, bacteria, and fungi. Primary cells were guaranteed for further expansion through 15 population doublings at the conditions specified by the company.

#### **2.1.2 Cell culture reagents**

The hRPTECs were maintained in renal epithelial cell basal medium (Lonza, catalogue number CC-3190) supplemented with the Lonza growth factor kit including foetal bovine serum (FBS) 0.5 % and 0.1 % of each of the following supplements: Hydrocortisone, human epidermal growth factor (hEGF), epinephrine, insulin, triiodothyronine, transferrin and gentamicin/amphotericin-B (Lonza, catalogue number CC-4127). MCs were cultured in mesangial cell medium (Sciencell Research Laboratories, Buckingham, UK, catalogue number 4201) containing essential and non-essential amino acids, vitamins, organic and inorganic supplements, hormones, growth factors, trace minerals, penicillin/streptomycin and a low concentration of FBS (2%). Trypsin neutralizing solution (TNS) was used to harvest cells (Lonza, catalogue number CC-5002; and Sciencell, catalogue number 0113). Trypan blue dye (catalogue number 302643) and dimethylsulphoxide (DMSO) were purchased from Sigma-Aldrich (Dorset, UK). Trypsin/ethylenediaminetetra-acetic acid (EDTA) solution (porcine pancreas-derived trypsin 0.25% w/v, EDTA 0.02% w/v) was obtained from Invitrogen Life Technologies (Paisley, UK).

### 2.1.3 Substrates, cofactors, enzymes and consumables

RIPA cell lysis buffer 10x strength (0.5 M Tris-HCl, pH 7.4, 1.5 M NaCl, 2.5% deoxycholic acid, 10% NP-40, 10 mM EDTA) was purchased from Millipore, UK (catalogue number 20-188). Methanol, potassium bicarbonate (KHCO<sub>3</sub>) was purchased from Fisher Scientific (Loughborough, UK). Argon compressed gas N5.0 (catalogue number 270050) was purchased from BOC, Coventry, UK. D-(+)-glucose  $\geq 99.5\%$ , *trans*-resveratrol (tRSV, catalogue number R5010), hesperetin  $\geq 95\%$ , (HSP catalogue number W431300), bovine serum albumin (BSA), sodium phosphate monobasic (catalogue number 71505), reduced glutathione (GSH), hydrochloric acid (analytical grade, 1 N; HCl) (catalogue number H1758), S-D-lactoylglutathione, nicotinamide adenine dinucleotide- oxidised form (NAD<sup>+</sup>), nicotinamide adenine dinucleotide phosphate, reduced form (NADPH), perchloric acid (PCA) 60%, glycine, diethylenetriaminepenta-acetic acid (DETAPAC) (catalogue number D6518), sodium D-lactate (catalogue number 71716), sodium L-lactate  $\geq 99\%$  (catalogue number 71718),  $\beta$  nicotinamide adenine dinucleotide ( $\beta$ -NAD<sup>+</sup>), D-lactate dehydrogenase, L-lactic dehydrogenase, tween-20, optima water LC/MS grade, hydrazine H<sub>2</sub>O, urea (catalogue number U5378), ammonium bicarbonate (ABC, catalogue number A6141), tris (2-carboxyethyl) phosphine (TCEP, catalogue number C4706) and 2-chloroacetamide (catalogue number CAA C0267) were purchased from Sigma-Aldrich (Dorset, UK).

High purity MG was prepared in-house from the Warwick Medical School Protein Damage Group research team. MG was prepared by the hydrolysis of MG dimethylacetal in dilute sulphuric acid and purified by fractional distillation under reduced pressure, as described (McLellan and Thornalley, 1992). Phosphatase inhibitors 100x (catalogue number 78420), protease inhibitor cocktail 100x (catalogue number 78430), trypsin/Lys-C (catalogue number A40007) were obtained from Thermo scientific, UK.

### 2.1.4 Other consumables

For immunoblotting assays, the following consumables were purchased: 10 x premixed electrophoresis Tris-glycine running buffer (catalogue number 1610732; 1 x dilution includes 25 mM Tris, 192 mM glycine, pH 8.3), 10 x Tris-buffered-saline TBS (catalogue number 1706435 ; 1 x dilution contains 20 mM Tris, 500 mM NaCl, pH 7.4), 4 x Laemmli buffer (catalogue number 1610747), Criterion TGX stain-free precast gel 4–20% polyacrylamide (catalogue number 3450412), Trans-Blot® Turbo™ PVDF pre-cut blotting transfer pack (catalogue number 1704157), containing filter paper, buffer, polyvinyl difluoride (PVDF)

membrane used with Trans-Blot Turbo transfer system (catalogue number 1704155) from Bio-Rad (Hertfordshire, UK). Protein detection was achieved via chemiluminescence using photographic film purchased from GE Healthcare (Little Chalfont, UK). Spectro™ multicolor broad range protein ladder (10-260 kDa, for 4 – 20% Tris-glycine SDS-PAGE), enhanced chemiluminescence (ECL) reagent kit (cat. no. 32106) and sodium dodecyl sulphate (SDS) (catalogue number 28312B) were purchased from Fisher Scientific. Antibodies including: monoclonal anti-Glo1 produced in rat (cat. no. SAB4200193) and anti-rat IgG antibody (cat. no. A9037) were purchased from Sigma-Aldrich. Anti- $\beta$ -actin mouse monoclonal antibody (cat. no. ab6276) was purchased from Abcam (U.K).

### **2.1.5 Sample quantification assay kits**

Glucose assay kits - hexokinase (cat. no. GAHK20) - was obtained from Sigma-Aldrich. For high sensitivity protein quantification, the Bicinchoninic acid assay (BCA) kit was purchased from Fisher Scientific (Loughborough, UK).

### **2.1.6 Instrumentation and software**

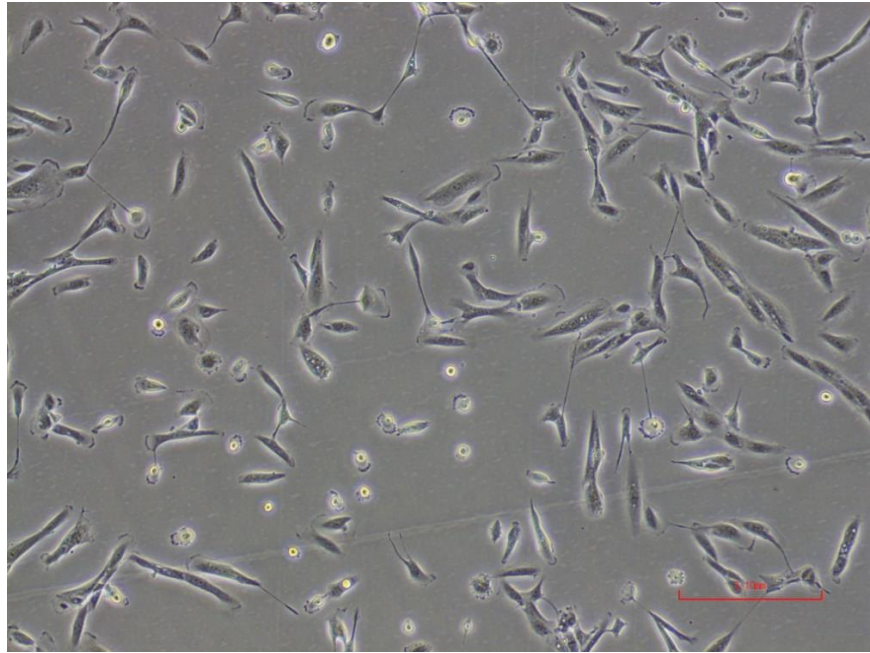
The Bright-Line (™) Haemocytometer for cell counting was purchased from Sigma-Aldrich (UK). The Nikon Eclipse TE2000-S inverted microscope (Nikon UK Limited, Kingston Upon Thames, Surrey, UK) was used for cell counting. The AccuSpin 3R centrifuge and Heraeus Pico 17 centrifuge were used from Fisher Scientific (Loughborough, UK). The sonicator was from Jencons Scientific (UK). A UVIKON XS Spectrophotometer (Northstar Scientific Limited, Sandy, UK) was used to determine activities of Glo1, Glo2, MG reductase and MG dehydrogenase. A FLUOstar OPTIMA microplate reader from BMG Labtech (Aylesbury, U.K) was used for microplate spectrophotometry and fluorimetry. The Trans-Blot Turbo transfer system (catalogue number 1704155) was from Bio-Rad (Hertfordshire, UK). Tissue culture T75 cm<sup>2</sup> T-flasks, 12-well plates, cryotube vials, glass pipettes, falcon tube, Eppendorf tube were purchased from Sigma-Aldrich (Dorset, UK). Microplate U bottom polystyrene 96-well sterile plates were used for protein assay. Hellma™ Far UV Quartz cuvettes with lead were purchased from Fisher Scientific (Loughborough, UK).

Optima software version 2.10 R2 (BMG Labtech) was used for processing data from the microplate assays such as total protein, D-lactate, L-lactate and D-glucose concentration analysis. Western blot protein levels were analysed semi-quantitatively by using of ImageQuant densitometry software (GE Healthcare Life Sciences, Amersham, U.K.). For the

proteomics analysis, raw data was processed using Scaffold™ version 4.8.9 (Proteome Software, Portland, Oregon, USA). Molecular ion fragmentation mass spectra, MS<sup>2</sup>, were searched using SEQUEST and MASCOT engines against a human protein database, Uniprot (<http://www.uniprot.org> June-July 2015). Perseus software version 1.6.12.0, was used for the statistical analysis of large-scale quantitative proteomics data. G:Profiler (<https://biit.cs.ut.ee/gprofiler>) online software system (Raudvere et al., 2019), was used for functional enrichment analyses of differentially expressed proteins, then data were summarised using REVIGO software (Supek et al., 2011).

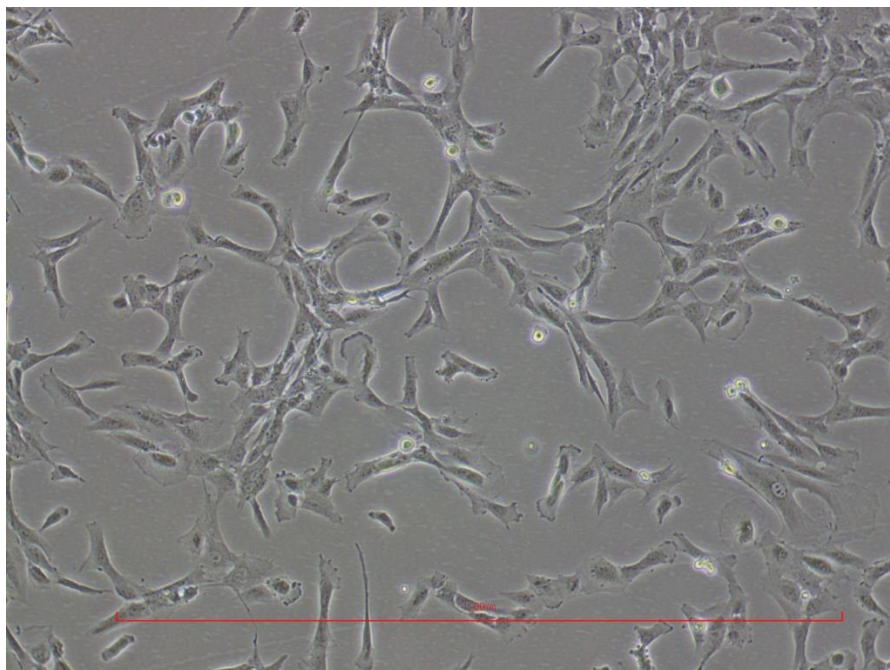
## **2.2 Cell culture methods**

Primary human renal cells (Tubular Epithelial and Mesangial cells) from Lonza and ScienCell Research Laboratories were cultured in pre-warmed culture medium. Medium was supplemented with FBS and the growth factors, as described previously. Cells were incubated at 37 °C, under aseptic conditions and in an atmosphere of 5% carbon dioxide and 100% humidity. Primary cultures received new medium the day after seeding. Subculture was performed every 4 days, and medium was changed on the second day. When confluence reached 80 % at a seeding density of 3,500 cells/cm<sup>2</sup>, cells were rinsed with PBS, harvested using 0.25% trypsin-EDTA and neutralised using TNS. Harvested cells were collected by sedimentation via centrifugation and media samples were centrifuged before storage to remove any detached cells. Overall, all experiments were performed between passages 3 and 5. Passaged cells were cultured in 25 mM high glucose medium by addition of a sterile aqueous stock solution of β-D-glucose and compared with that of low glucose control cells, cultured in 5 mM glucose. Cell and media samples were frozen and stored at –80°C until further analysis. Cell viability ≥ 98% was determined by trypan blue exclusion assay using (0.25 % trypan blue in PBS) (Strober, 2001). Representative images of the tubular epithelial cells and mesangial cells are shown in Figures 2.1 and 2.2.



**Figure 2.1: Morphology of human renal proximal tubular epithelial cells (hRPTECs)**

Cells were seeded at a density of 5000 cells/cm<sup>2</sup> in renal epithelial cell basal medium. Cells were visualized using phase contrast microscopy.



**Figure 2.2: Morphology of human mesangial cells (MCs)**

Cells were seeded at a density of 5000 cells/cm<sup>2</sup> in MCM medium. Cells were visualized using phase contrast microscopy.

## **2.2.1 Cell culture experimentation**

### **2.2.1.1 Effect of high glucose on growth of renal cells**

Primary renal cells hRPTECs and MCs were cultured in 6 well plates at a density of (20000 cells/cm<sup>2</sup>) in triplicate in medium contain two different glucose concentrations (5.0 mM and 25.0 mM). Total cell number including viable and non-viable cells was calculated daily for 6 days, exclusion method was performed using Trypan blue dye to assess viability. Growth curves were then constructed.

### **2.2.1.2 The effect of Glo1 inducer on renal cell growth**

To assess the effect of Glo1 inducer (tRSV-HSP) on renal cells, human renal cells were incubated in 6 well plates (20000 cells/cm<sup>2</sup>) in triplicate and on the second day of culturing, the medium was supplemented with HSP and tRSV separately (5 and 10 µM, respectively) for 6 days, during which time cells were counted daily and cell growth curves constructed.

### **2.2.1.3 Characterisation of glyoxalase system in renal cells in model hyperglycaemia**

Primary renal cells were incubated at a density of (5000 cells/cm<sup>2</sup>) in medium with low and high glucose concentration, 5 mM and 25 mM respectively, for 4 days in triplicate, with changing of medium on the second day of culturing. Cell extracts were used for subsequent total protein content, Glo1, Glo2, MG dehydrogenase and MG reductase activity. Medium was analysed for concentrations of glucose, D-lactate and L- lactate flux formation.

### **2.2.1.4 Effect of Glo1 inducers on the glyoxalase system in renal cells *in vitro***

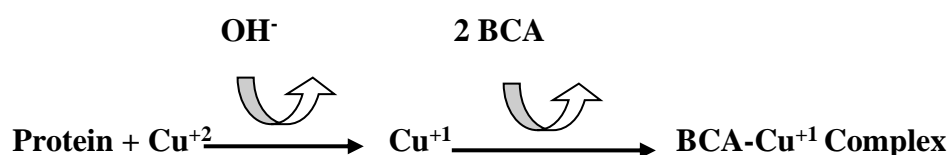
Primary renal cells were cultured at a density of (5000 cells/cm<sup>2</sup>) in medium with low and high glucose concentration, 5 mM and 25 mM respectively, with and without tRSV+HSP (10 µM) for 4 days in triplicate, 5% DMSO negative control had been used, as this solvent was used to solubilise the Glo1 inducer reagent, with changing of medium on the second day of culturing. Cells were analysed for total protein, Glo1, Glo2, MG dehydrogenase and MG reductase activity. Medium was analysed for concentrations of glucose, D-lactate and L- lactate flux formation.



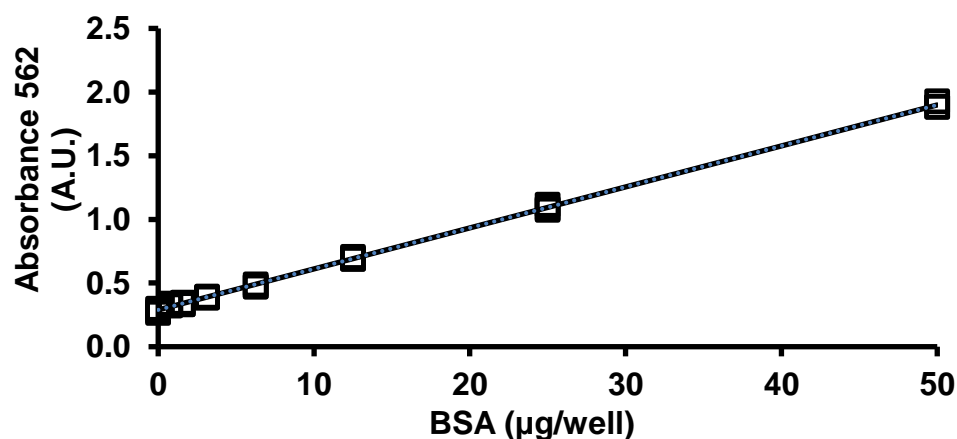
## 2.3 Analytical methods

### 2.3.1 Total protein assay Bicinchoninic acid assay (BCA)

The concentration of protein in cell lysates was quantified by BCA assay - this assay depends on the conversion of  $\text{Cu}^{2+}$  to  $\text{Cu}^{+}$  by proteins in an alkaline solution (Biuret reaction) and the reaction results in the formation of intense purple-colour produced by the chelation of two molecules of BCA with one cuprous ion (Smith et al., 1985). This color strongly absorbs light at a wavelength of 562 nm, the mixture is stable and increases with increasing amount of protein in the sample. The assay was calibrated (1.25 – 50  $\mu\text{g}$  protein/well) using BSA as standard. Stock solutions of BSA were calibrated by UV absorption spectrophotometry using the extinction coefficient  $0.667 (\text{mg/ml})^{-1}\text{cm}^{-1}$  at 279 nm (Peters, 1962).



Each sample was diluted in the range between 125-500  $\mu\text{g}$  protein/ml. Test samples in triplicate, BSA standards and blanks in quadruplicate (25  $\mu\text{l}$  per well) were mixed with 200  $\mu\text{l}$  of the working solution from supplied reagents in a 96-well microplate and shaken for 30 seconds, then the microplate was covered with aluminium foil and incubated at 37  $^{\circ}\text{C}$  for 30 min. Absorbance was read at 562 nm. The amount of protein present in the samples was determined by interpolation of the calibration curve, each experiment was carried out conducting a new titration curve (Figure 2.3).



**Figure 2.3: Calibration curve for BCA assay.**

Linear regression equation: Absorbance at 562 nm (A.U.) =  $(0.289 \pm 0.032) \times \text{BSA} (\mu\text{g}/\text{well})$ ;  $R^2 = 0.99$  ( $n=32$ ).

## 2.3.2 Enzymatic activity assay

### Sample preparation

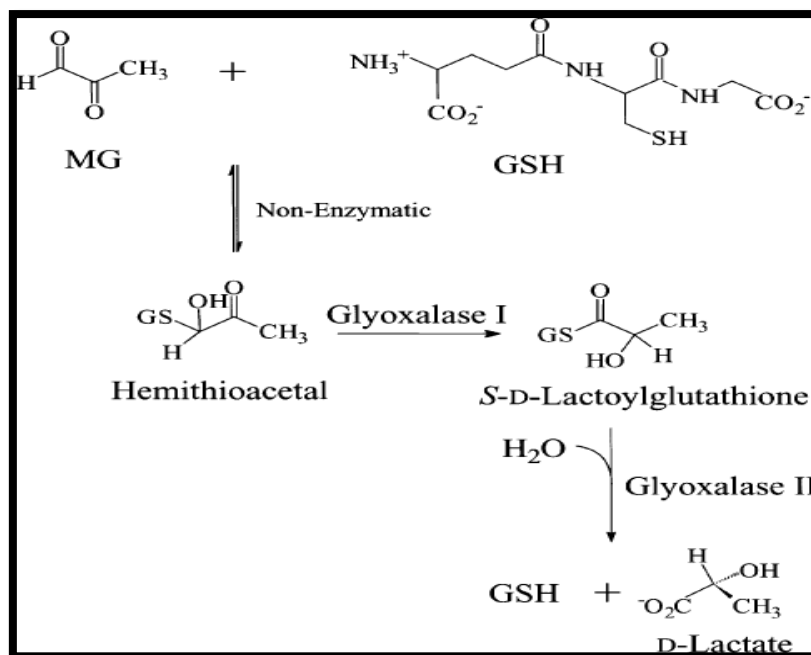
Primary renal cells were cultured in low and high glucose (5 mM and 25 mM) with and without Glo1 inducer in polystyrene flasks. After 4 days of incubation, cells were collected by trypsinisation, counted and sedimented by centrifugation (150 x g, 5 min). Cell pellets were rinsed by using ice-cold PBS three times. Cell pellets (*ca.* 1-2 x 10<sup>6</sup> cells) were re-suspended in 100 µl sodium phosphate buffer (10 mM, pH 7.0), sonicated on ice (110 W, 30 s) and the membranes sedimented by centrifugation (20,000 g, 30 min, 4 °C). Supernatants were transferred and stored at -80 °C.

#### 2.3.2.1 Activity of glyoxalase 1

The activity of Glo1 was determined by following the initial rate of formation of S-D-lactoylglutathione from the Hemithioacetal formed non-enzymatically from MG and GSH, monitored spectrophotometrically at 240 nm;  $\Delta\epsilon_{240} = 2.86 \text{ mM}^{-1} \text{ cm}^{-1}$  (Allen et al., 1993)-Figure 2.4. Hemithioacetal was pre-formed by the pre-incubation of 100 µl MG (20 mM) with 100 µl GSH (20 mM) at 37 °C for 10 min in 500 µl sodium phosphate buffer (100 mM, pH 6.6) and 280 µl water using 1 ml quartz cuvette. The cell lysate (20 µl) was added and absorbance at wavelength of 240 nm was followed for 5 min. The activity of Glo1 was determined from the initial increase in absorbance and deduced with correction for blank. Glo1 activity is expressed in units per mg protein, where one unit of Glo1 activity is the amount of enzyme which catalyses the formation of 1 µmol S-D-lactoylglutathione per minute under assay conditions (Allen et al., 1993).

#### 2.3.2.2 Activity of glyoxalase 2

Glo2 activity is determined by calculating the initial rate of hydrolysis of S-D-lactoylglutathione to GSH and D-lactate-Figure 2.4. The hydrolysis of S-D-lactoylglutathione is monitored spectrophotometrically at wavelength of 240 nm for which the change in molar absorption coefficient is  $\Delta\epsilon_{240} = 3.10 \text{ mM}^{-1} \text{ cm}^{-1}$  (Allen et al., 1993). Using 1 ml quartz cuvette, S-D-Lactoylglutathione (0.3 mM, 100 µl, 4°C) was incubated in Tris-HCl buffer (50 mM, 500 µl, pH 7.4, 37°C) and water (37 °C, 380 µl). The cell lysate (20 µl) was added and the absorbance was monitored for the duration of 5 min at 37°C. Glo2 activity is provided in units per mg of protein or per million cells, where one unit is the amount of enzyme that catalyses the hydrolysis of 1 µmol S-D-lactoylglutathione per min under assay conditions (Allen et al., 1993).



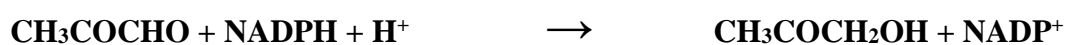
**Figure 2.4: The catalytic reactions of the glyoxalase system.**

From (Clugston et al., 2004).

### 2.3.2.3 Methylglyoxal reductase activity

NADPH-dependent aldoketo reductase is involved in the metabolism of MG and converts it to hydroxyacetone. AKR isozymes 1A4, 1B1 (aldose reductase) and 1B3 metabolise MG (Baba et al., 2009). MG reductase activity is calculated by monitoring the initial rate of oxidation of NADPH by cell lysates in the presence of MG and NADPH, and monitored spectrophotometrically at 340 nm;  $\Delta\epsilon_{340} = -6.20 \text{ mM}^{-1}\text{cm}^{-1}$ .

#### MG reductase

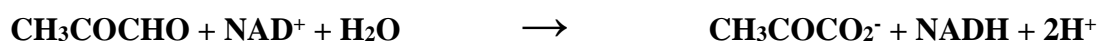


Using 1 ml quartz cuvette, MG (1 mM, 50  $\mu\text{l}$ , 4°C) was incubated with NADPH (0.1 mM, 100  $\mu\text{l}$ , 4°C) in sodium phosphate buffer (50 mM, pH 7.4, 500  $\mu\text{l}$  and 37 °C), water (380  $\mu\text{l}$ , 37 °C) then cell lysate, or lysate buffer blank, added to a final volume of 1 ml. The solution was mixed by inversion and the absorbance at 340 nm monitored for 5 min. The activity of MG reductase is measured in units where one unit catalyses the reduction of 1  $\mu\text{mol}$  of MG per min under assay conditions.

### 2.3.2.4 Methylglyoxal dehydrogenase activity

NAD<sup>+</sup>-dependent MG dehydrogenase converts MG to pyruvate (Monder, 1967). The methylglyoxal dehydrogenase activity is determined by following the initial rate of reduction of NAD<sup>+</sup> by sample extraction in the presence of MG and NAD<sup>+</sup>, and followed spectrophotometrically at 340 nm;  $\Delta\epsilon_{340} = 6.20 \text{ mM}^{-1}\text{cm}^{-1}$ .

#### MG dehydrogenase



Cell lysate, or lysate buffer for blanks, was added to MG (1 mM, 50  $\mu\text{l}$ , 4°C) and NAD<sup>+</sup> (0.1 Mm, 100  $\mu\text{l}$ , 4°C) in sodium phosphate buffer (50 mM, pH 7.4, 500  $\mu\text{l}$  and 37 °C) and water (380  $\mu\text{l}$ , 37 °C), then sample mixed well by inversion. The reaction was monitored for absorbance at 340 nm for 5 min. The activity of MG dehydrogenase is measured in units where one unit catalyses the oxidation of 1  $\mu\text{mol}$  of MG per minute under assay conditions.

## 2.4 Immunoblotting for Glo1

Expression level of Glo1 protein in primary hRPTECs was measured by Western blotting and normalised to  $\beta$ -actin.

### 2.4.1 Sample preparations

Primary hRPTECs were incubated in 7.2 mM glucose and 25 mM glucose conditions. After 4 days of culturing, cells were harvested, washed using PBS and collected as mentioned in cell culture section. Cell pellets were resuspended in 100  $\mu\text{l}$  sodium phosphate buffer (10 mM, pH 7.0), containing phosphatase and protease inhibitor (1 in 100). Samples were sonicated (110 W, 30 s) and left on ice for 10 min. Cell lysate suspension was centrifuged (20,000 g, 30 min, 4°C) to sediment all cell membranes and the supernatant was stored at -80°C until the analysis.

BCA assay was conducted to measure total protein concentration in each sample. Twenty micrograms of protein extract were prepared for loading onto the gel wells. Samples were mixed with the loading buffer (4x Laemmli buffer) to a final volume. Protein denaturation was conducted by heating the samples at 95°C, 5 min prior loading onto the gel.

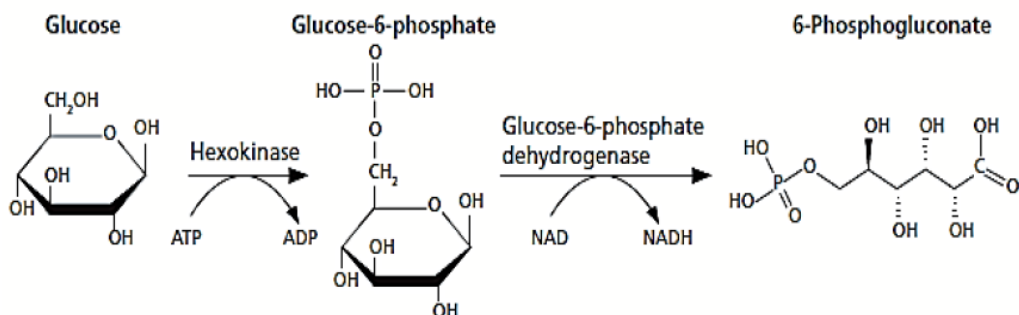
### **2.4.2 Western blotting**

The separation of protein extracts was conducted using 4–20% precast polyacrylamide gels (4-20% criterion™ TGX stain-free™ gel), where gels were placed into the Criterion electrophoresis cell (Bio-rad). Electrophoresis running buffer (25 mM Tris, 192 mM glycine, 0.1% SDS, pH 8.3) was diluted 1-fold, then the mixture was poured into the electrophoresis cell in order for proteins to separate via SDS-PAGE. An aliquot of each sample (15 µl) and pre-stained protein ladder (10 µl) was loaded to the wells. Samples were electrophoresed on the SDS-PAGE gel at 150 V for 60 minutes. Finally, the migrated proteins on the gel were transferred to the sandwich layer of semi-dry transfer using pre-cut blotting transfer packs that consist of filter paper and PVDF membrane. Protein transferring was performed using the Trans-Blot Turbo transfer system (Bio-rad) at 2.5A; 25V constant for 15 min.

The transfer membrane had been initially blocked by 5% (w/v) dried milk protein in Tris-buffered saline and Tween-20 (TBS-T buffer; 150 mM NaCl, 10 mM Tris/HCl pH 7.6 and 0.05% Tween-20). After blocking, the membrane was probed by primary antibody (anti Glo1 rat, 1/3000; anti β-actin mouse, 1/1000) incubated in 1% (w/v) dried milk protein in TBS-T buffer at 4°C for overnight. The following day the membrane was washed using TBS-T buffer for 10 min for 3 cycles. This was followed by the second probing with secondary antibody (anti-rat, 1/10000 dilution) at room temperature for 60 minutes, followed by washing three times using TBS-T and developed by detection reagents for ECL. The bands were photographed using G:BOX Chemi systems (Syngene). Glo1 bands were quantified relative to a reference loading control of β-actin using ImageQuant densitometry software.

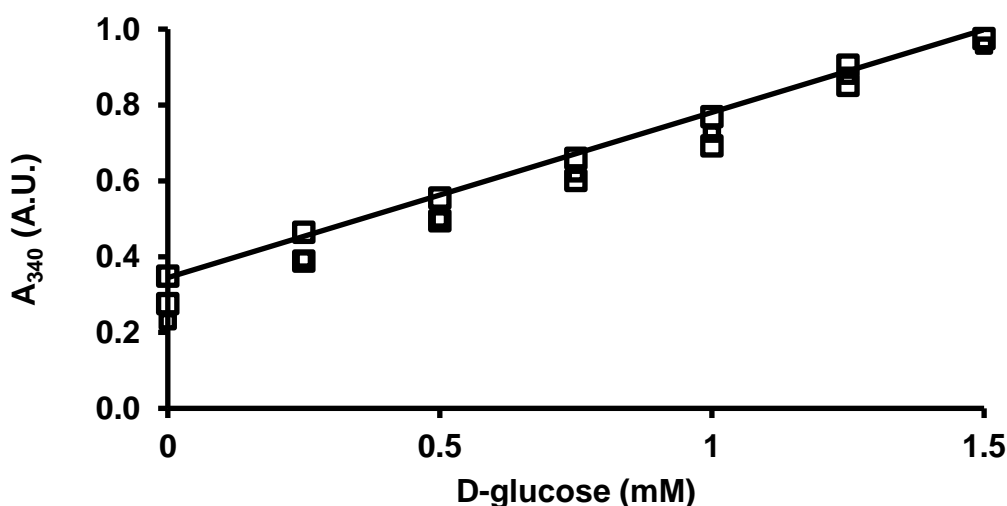
### **2.5 D-Glucose assay**

The glucose levels in the culture media were determined using a commercially available end-point enzymatic assay (consisting of 1.5 mM NAD<sup>+</sup>, 1 mM ATP, 1 unit/ml hexokinase (HK) and 1 unit/ml glucose-6-phosphate (G6P) dehydrogenase) and 1 mg/ml D-glucose standard (Sigma Aldrich). The chemical basis of this enzymatic reaction is indicated in Figure 2.5.



**Figure 2.5: Reaction scheme for detection of glucose via hexokinase and glucose 6 phosphate dehydrogenase.**

NADH is produced in this reaction and measured by endpoint measurement using the spectrophotometer at 340 nm. As equimolar amounts of glucose are phosphorylated in this reaction per NAD<sup>+</sup> reduced to NADH, the increase in absorbance at 340 nm is directly proportional to the concentration of glucose. Aliquots of standard and diluted sample (25  $\mu$ l) were mixed with assay reagent (225  $\mu$ l) in each well of a microplate. Then the plate was incubated at room temperature for 15 min before measuring the absorbance at 340 nm. A standard curve was constructed from 0.25 — 1.50 mM, and samples were diluted consequently with distilled water to ensure that the measured concentration was within the standard curve range-Figure 2.6.

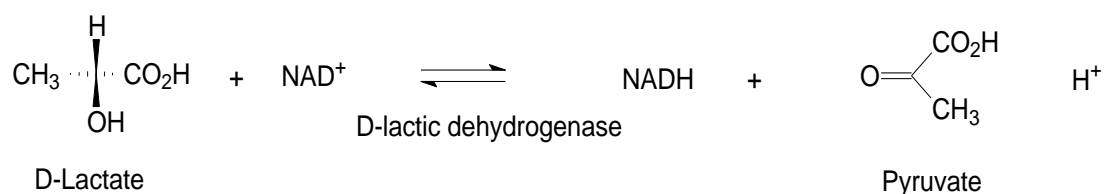


**Figure 2.6: Calibration curve for D-glucose.**

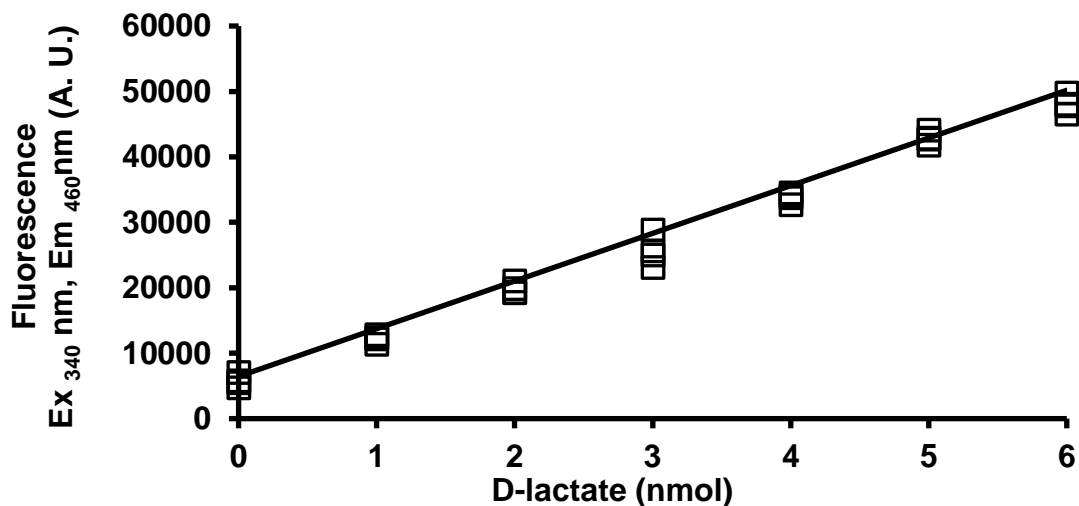
Linear regression equation:  $A_{340} \text{ (A.U.)} = (0.344 \pm 0.0143) \times \text{D-glucose (mM)}$ ;  $R^2 = 0.99$  ( $n = 21$ ).

## 2.6 D-lactate assay

Formation of D-lactate was determined by using end-point enzymatic fluorometric assay (McLellan et al., 1992), in the culture medium at the second and final day of the culture period at 37°C. D-Lactate crosses cell membranes through a specific lactate transporter, the inorganic anion exchange system and also by non-ionic passive diffusion. D-Lactate is converted to pyruvate by the D-lactic dehydrogenase enzyme, and the increase in accumulation of NADH is measured by fluorescence ( $\lambda_{\text{excitation}} = 340\text{nm}$  and  $\lambda_{\text{emission}} = 460\text{nm}$ ).



Samples were prepared by adding ice cold Perchloric acid (PCA) (1ml, 0.6M) to the culture medium (500  $\mu\text{l}$ ) for deproteinisation. Then the mixture was vortexed and left on ice for 10 min to complete protein precipitation. Samples were centrifuged (7000 x g, 4°C, 5 min) to sediment the protein precipitate. An aliquot of the supernatant (700  $\mu\text{l}$ ) was neutralized to pH 7 by adding potassium bicarbonate (200  $\mu\text{l}$ , 2 M), mixed and centrifuged again (7000 x g, 4°C, 10 min) to sediment the potassium perchlorate precipitate. The supernatant was saturated in  $\text{CO}_2$  and degassed by placing in centrifugal evaporator at room temperature for 5 min. A 100  $\mu\text{l}$  volume of degassed deproteinised extract or D-lactate standard solution was added in duplicate to the 96-well black microplates containing glycine hydrazine buffer (100  $\mu\text{l}$ ; 1.2 M glycine, 0.5 M hydrazine hydrate, 2.5 mM DETAPAC, pH 9.2) and  $\text{NAD}^+$  (4 mM, 25  $\mu\text{l}$ ). The reaction was started by adding D-lactate dehydrogenase enzyme (25  $\mu\text{l}$ , 250 units per ml). The microplate was incubated at 37°C in the dark for 2 h. Each sample has its own control without the enzyme and used as blank. Standard curves for calibration were constructed in the range of 0-6 nmol D-lactate/well as shown in Figure 2.7.



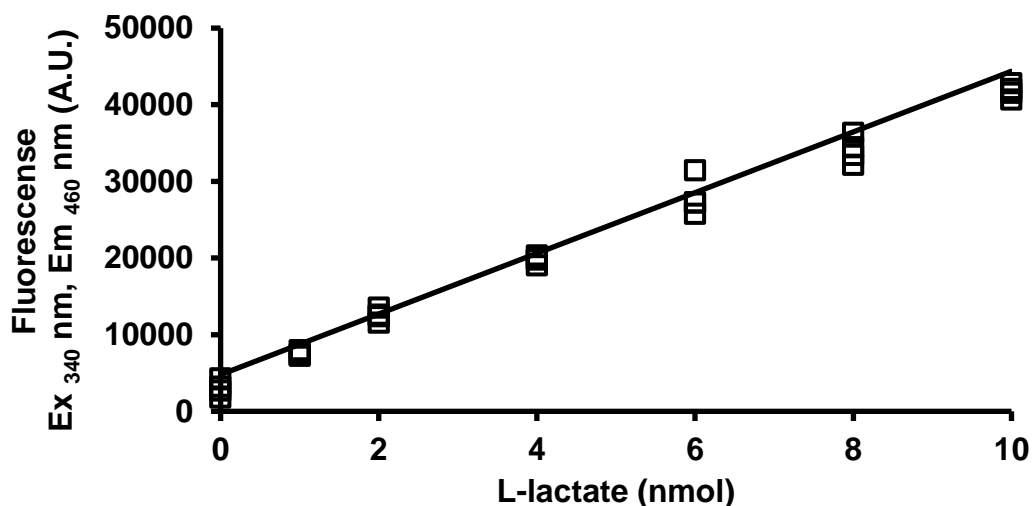
**Figure 2.7: Calibration curve for D-lactate assay.**

Equation of the regression line: Fluorescence (arbitrary units) =  $(5246 \pm 182) \times$  D-lactate (nmol);  $R^2 = 0.99$  (n=28).

## 2.7 L-lactate assay

The method to measure the concentration of L-lactate in culture medium was similar to that of D-lactate described above. A standard curve was produced using L-lactate standards and the enzyme L-lactate dehydrogenase was used (instead of the D-lactate dehydrogenase used for the D-lactate assay). The standard curve range was selected to ensure that the range used was linear and a time-course was achieved to establish the optimal incubation length. Since cellular levels of L-lactate are higher than D-lactate, media samples were diluted 10-fold with water to ensure that concentrations measured were within the standard curve range – See Figure 2.8.





**Figure 2.8: Calibration curve for L-lactate.**

Linear regression equation: Fluorescence (arbitrary units) =  $(3958 \pm 120) \times \text{L-lactate (nmol)}$ ;  $R^2 = 0.98$  ( $n = 28$ ).

## 2.8 Proteomics of cytosolic protein methodology

Human renal cells were cultured in normal and high glucose concentration for 4 days with and without Glo1 inducer. Quantities of *ca.*  $1.5 \times 10^6$  cells were harvested after trypsinisation, sedimentation and washing with PBS as described previously, and stored at  $-80^\circ\text{C}$  prior to further analysis. Cell pellets were suspended in  $400\ \mu\text{l}$  volumes of  $10\ \text{mM}$  sodium phosphate buffer,  $\text{pH } 7.0$  supplemented by phosphatase and protease inhibitor cocktail (1 in 100) and sonicated on ice ( $110\ \text{W}$ ,  $30\ \text{s}$ ), followed by centrifugation ( $20,000 \times g$ ,  $30\ \text{min}$ ,  $4^\circ\text{C}$ ) to sediment the membranes. The supernatant was recovered and protein concentration was measured using BCA assay.

An aliquot of the lysate ( $500\ \mu\text{g}$  protein level) was washed using argon-purged optima water by microspin ultrafilter ( $10\ \text{kDa}$  cut-off) in four consecutive cycles of dilution and concentration and then centrifuged ( $14,000g$ ,  $20\ \text{min}$ ,  $4^\circ\text{C}$ ). Protein concentrations were measured again using the BCA assay and aliquots ( $300\ \mu\text{g}$  protein) were digested by the trypsin/lys-C via the digestion method described below.

### 2.8.1 Filter Aided Sample Preparation (FASP Protocol)

An aliquot of cytosolic protein extract ( $300\ \mu\text{g}$  protein) for each sample was dissolved in  $8\ \text{M}$  of urea buffer to a total volume of  $400\ \mu\text{l}$ , the mixture was then vortexed and left at room temperature for 5 minutes. Samples were added to the filter unit and centrifuged ( $8000 \times g$ ,  $20$

min, room temperature), buffer was exchanged by 8 M of urea and centrifuged (8000 x g, 20 min, room temperature). Urea buffer was exchanged into 50 mM ammonium bicarbonate (ABC) to a total volume of 400 µl and centrifuged (8000 x g, 20 min, room temperature) over three cycles.

Proteins were reduced and alkylated by dissolving in 400 µl of 10 mM Tris-(2-carboxyethyl) phosphine hydrochloride (TCEP) and 40 mM of 2-chloroacetamide (CAA) in ABC, the mixture was incubated for 30 min at room temperature. The TCEP and CAA were removed by centrifugation (8000 g, 20 min, room temperature). Then the filter was washed 3 times via centrifugation by adding 400 µl of 50 mM ABC (8000 x g, 20 min, room temperature).

### **2.8.2 Protocol of Lys-C-Trypsin protease digestion of cytosolic protein**

For protein digestion, an aliquot of trypsin in ABC, 2 µg trypsin per 100 µg protein, was added to each sample and incubated at 37°C overnight. Filters were transferred to fresh collection tubes for peptide elution and centrifuged (8000 x g, 20 min, room temperature) and the flowthrough was collected. Peptide elution steps were conducted using 400 µl of distilled water and centrifuged (8000 x g, 20 min, room temperature). Samples were stored at -20 °C prior to further analysis.

### **2.8.3 C<sub>18</sub> Stage tip**

Following digestion, samples were subsequently desalted using a C<sub>18</sub> spin column (C<sub>18</sub> membrane). Prior sample loading, each column was prepared using the following procedures: the column was washed with 50 µl of 100% methanol and centrifuged (2000 rpm, 2 min), equilibrated with 50 µl of 100% acetonitrile and centrifuged (2000 rpm, 2 min), then equilibrated with aqueous solution (50 µl of 2% acetonitrile 0.1% Trifluoroacetic acid-TFA) and centrifuged (2000 rpm, 2 min). In each step, the Stage tip was kept wet and above the flowthrough, and each membrane was checked for any leaks. Then the pH value of each sample was determined and adjusted to a value between 1.5-2 using 1% TFA.

Samples of 50 µg of peptides were diluted in 2% acetonitrile /0.1% TFA to optimal final volumes 100-150 µl per spin and tip, and centrifuged (2000 rpm, 10 min), with the flowthrough being retained. Samples were washed with 50 µl of ethyl acetate/1% TFA and centrifuged (2000 rpm, 4 min), followed by washing with 50 µl of 2% acetonitrile/0.1% TFA and centrifuged (2000 rpm, 4 min). Peptides were eluted into fresh collection tubes in 20 µl of 60-

80% acetonitrile (2000 rpm, 2 min). Acetonitrile was removed by Speed vacuum for 15 minutes and then peptides were resuspended in 40  $\mu$ l of 2% acetonitrile /0.1% TFA and sonicated in a water bath. Samples were stored in -20°C prior to MS analysis.

#### **2.8.4 Peptide separation, protein quantitation and identifications**

The prepared cell lysate samples were submitted to the Mass Spectrometry and Proteomics Facility at School of Life Sciences, University of Warwick for label-free proteomic quantitation analysis. Nanoflow reversed phase liquid chromatography was conducted for protein identification using the Orbitrap mass spectrometer supplied by a micro spray source working in positive ion mode. For proteomics studies, the following column was used: an Acclaim PepMap  $\mu$ -pre-column cartridge (trap), 300  $\mu$ m i.d. x 5 mm, 5  $\mu$ m particle size, 100 Å pore size, fitted to an Acclaim PepMap RSLC 75  $\mu$ m i.d. x 50 cm, 2  $\mu$ m particle size, 100 Å pore size main column (Thermo Scientific). The columns were installed on an Ultimate 3000 RSLCnano system (Dionex). Each sample extract was subjected to analysis by the injection of an aliquot of (5  $\mu$ l). Following samples injection, the peptide fractions were eluted off of the trap onto the analytical column. Mobile phases used were: A - 0.1 % formic acid in water, and B - 0.1 % formic acid in acetonitrile. The flow rate was adjusted at 0.3  $\mu$ l/min. The proportion of Solvent B was increased from 3 % to 35 % in 125 to 220 min, depending on the complexity of the sample, to confirm that the peptides are separated. This is followed by increase in mobile phase B from 35 % to 80 % in 5 min prior to being brought back rapidly to 3 % in 1 min, then the column was equilibrated by the same solvent at 3 % for 15 min before the next sample was applied. Peptides were eluted (300 nl min<sup>-1</sup>) using a Triversa Nanomate nanospray source (Advion Biosciences, NY) into a Thermo Orbitrap Fusion (Q-OT-qIT, Thermo Scientific) mass spectrometer. Data survey scans of peptide precursors from 350 to 1500 m/z were conducted at 120K resolution (at 200 m/z) with automatic gain control (AGC)  $4 \times 10^5$ . Precursor ions with charge state 2 - 7 were isolated (isolation at 1.6 Th [Thomson units; m/z =1] in the quadrupole) and exposed to high energy collision dissociation (HCD) fragmentation. The collision-induced dissociation technique was programmed at 35 % to induce fragmentation energy. Rapid scan MS analysis in the ion trap was applied, the AGC was programmed at  $1 \times 10^4$  where the maximum injection time was 200 ms. The dynamic exclusion time was adjusted to 45 s with a 10ppm tolerance around the selected precursor and its isotopes. Monoisotopic precursor selection was set on. The mass spectrometry was run in top speed mode by 2 s cycles. Sequence outputs from the MS/MS data was processed through converting the raw (.raw) files

into a merged file (.mgf) using MSConvert in ProteoWizard Toolkit (version 3.0.5759) (Kessner et al., 2008). The resulting .mgf files were used to search against protein sequence databases.

### **2.8.5 Proteomic Data analysis**

Data were searched using the MASCOT (Matrix Science, version 2.5.0) search engine against *Homo sapiens* database (<http://www.uniprot.org/>). Mascot was set up to search assuming that the digestion enzyme was trypsin, to identify false positive peptides. The search parameter used looked for product ions and precursor mass:  $\pm 5$  ppm and  $\pm 0.8$  Da, with allowance made for six trypsin missed-cleavages, fixed modification of cysteine through carbamidomethylation, MG-H1 and methionine oxidation. Only fully tryptic peptide matches were included. Scaffold (version 4.8.9, Proteome Software Inc.) was used for validating MS/MS based peptides and protein identification. Peptide identifications were accepted if they could reach 95% probability false discovery rate FDR given by the software logarithms and containing at least 2 identified peptides. Protein prophet algorithms were used to assign protein probabilities (Nesvizhskii et al., 2003).

### **2.8.6 Statistical analysis**

All experimental studies were conducted in triplicate or more. All the statistical analyses such as mean, confidence score, standards deviation, and Student's t-test were performed using the statistical programme analysis of Perseus (version 1.6.12.0). Significance was asserted for  $P < 0.05$ . Functional enrichment analyses of differentially expressed proteins were studied using the g:Profiler (<https://biit.cs.ut.ee/gprofiler>) online software system and also REVIGO (<http://revigo.irb.hr/>).

### 3 Results

In this Chapter, all the experimental results studying the effect of hyperglycaemia on primary human renal cells are outlined in Section 3.1 and further presented and examined in detail later in the sections that follow.

#### 3.1 Characterisation of the effects of high glucose concentration on primary human renal cells *in vitro*

To examine the effects of low and high glucose concentration on the metabolism and function of primary human renal cells, the following experimental cultures were established with either 5.5 or 7.2 mM glucose (indicated as the “low glucose concentration”; LG conditions) or with 25.0 mM glucose (indicated as the “high glucose concentration”; HG conditions). The supplemented growth medium for human renal proximal tubular epithelial (hRPTE) cells from a commercial supplier was medium containing 7.2 mM glucose. Moreover, the mean human blood glucose level in a healthy subject is about 5.5 to 7.8 mM (Danaei et al., 2011, ADA, 2006), while in diabetic conditions it is typically around 25.0 mM on the basis of previous studies (Ho et al., 2000, Ido et al., 2002). Primary renal cells, hRPTE and Mesangial cells (MCs) were therefore maintained in 7.2 and 5.5 mM glucose respectively as low glucose concentration and 25.0 mM glucose as high glucose conditions and incubated for four days with changes of medium on the second day of culturing.

Growth and viability of hRPTE and MCs incubated in LG and HG concentration was studied for 6 days. The viable cell number increased progressively throughout the period of culture as judged by Trypan blue exclusion test, which was > 98% in the two culture conditions. Hyperglycaemia alone directly enhances the proliferation of both cell types.

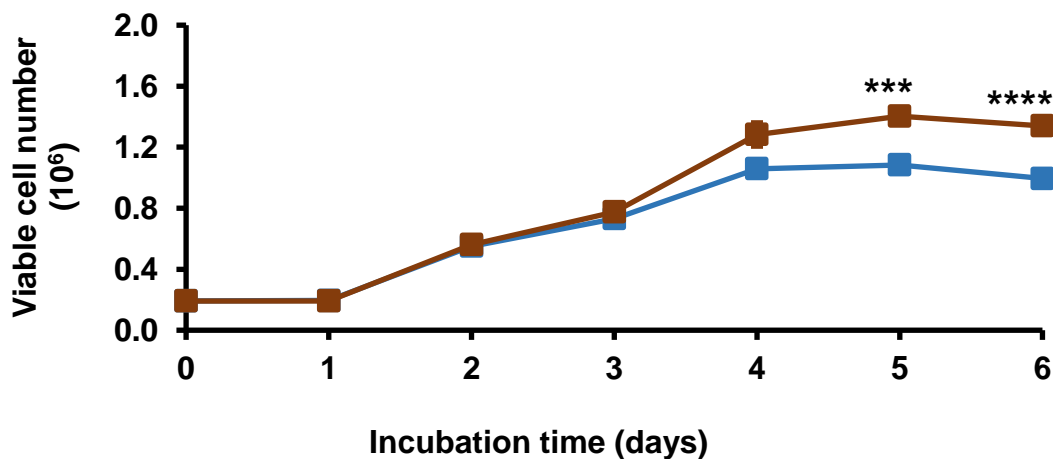
The effect of hyperglycaemia on the glyoxalase system has been studied in hRPTE cultured in LG and HG conditions. The activity of Glo1 under LG was  $728 \pm 142$  mU per mg protein and decreased by 39% after 4 days of culturing under HG conditions. This was further supported by measuring protein content of Glo1 which was decreased by 32% in the HG cultured cells, as compared to LG cultured controls.

Hyperglycaemia decreased Glo1 activity in hRPTE and therefore it is possible that dicarbonyl stress is induced under these conditions. This was studied by endpoint enzymatic assay of the levels of D-glucose intake, D-lactate formation (indicating increased flux of MG formation) and L-lactate flux formation in cell culture medium following culture for 2 days in

medium containing 7.2 mM glucose and 25 mM glucose. Under HG conditions, it was expected that glucose consumption and metabolism by hRPTE would increase. When hRPTECs were cultured in HG medium for two days, D-glucose intake increased by 2.5-fold compared with the LG conditions. Because MG is hard to measure precisely due to its highly reactive nature, D-lactate flux – the surrogate indication of MG flux of formation, was measured and found to be increased in HG by 2.6-fold in hRPTE cells compared to low glucose controls. This indicated dicarbonyl stress was induced in these cells by HG conditions, a model for hyperglycaemia *in vivo*.

### 3.1.1 Effects of high glucose concentration on growth and viability of hRPTE cells *in vitro*

To assess whether different concentrations of glucose influence primary hRPTE cells *in vitro*, cells were incubated in low glucose medium (7.2 mM) and medium with increased glucose concentrations (25.00 mM) for 6 days. The viable cell number increased progressively during the period of culture. At the 6th day of culturing, viable cell number had increased from  $0.192 \times 10^6$  at seeding to  $0.995 \pm 0.01 \times 10^6$  cells in 7.2 mM glucose and  $1.34 \pm 0.01 \times 10^6$  cells in 25.0 mM glucose. Trypan blue exclusion test for viability was used and it indicated  $> 98.5\%$  viability in all culture conditions. Growth curves are presented in the form shown in Figure 3.1, and this figure illustrates viable cell number over a period of 6 days. The growth rate of hRPTE cells in 7.2 mM glucose and 25.0 mM glucose was similar until the 4th day when the mean cell growth was higher by 21.3% in medium containing 25.0 mM compared to the 7.2 mM glucose cultures. At the 5th day of culturing, the rate of hRPTE cell growth in the low glucose concentration tended to slow and stopped at the last day, while it continued to increase in the high glucose cultures (by 29.5% compared to the low glucose cultures). Mean population doubling time was for 7.2 mM glucose,  $1.39 \pm 0.63$  days, and for 25.0 mM glucose,  $1.34 \pm 0.66$  days. Population doubling time indicated by the commercial supplier, Lonza (Slough, UK), was 1.08 days, the average rate here was slower than the given growth rate by Lonza.

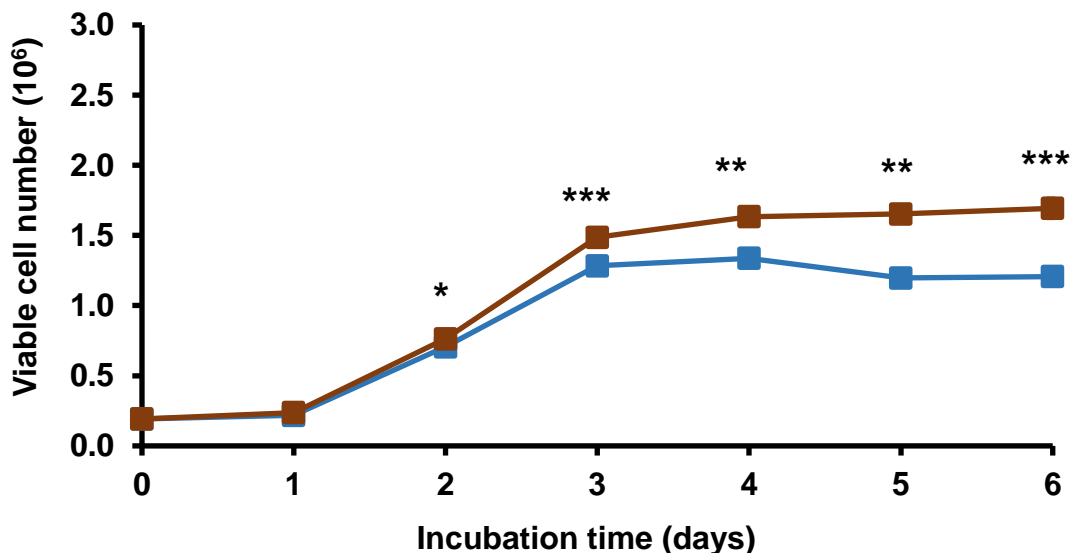


**Figure 3.1: Growth curve of hRPTE cells in media containing 7.2 mM and 25.0 mM glucose *in vitro*.**

Primary hRPTE cells ( $20000 \text{ cells/cm}^2$ ) were incubated in basal media with 0.5 % FBS at the glucose concentrations indicated for 6 days. Data are expressed as mean  $\pm$  SD ( $n = 3$ ). Significance: \*\*\* and \*\*\*\* denote  $P < 0.001$  and  $P < 0.0001$  respectively (Student's *t*-test) with respect to low glucose control. Key: 7.2 mM glucose —■— and 25.0 mM glucose —■—.

### 3.1.2 Effect of high glucose concentration on growth and viability of MCs *in vitro*

The cellular-growth curve for MCs was established, evaluating the growth characteristics of these cells under hyperglycaemic condition for 6 days of culturing. At the starting day of seeding, the cell number was  $0.192 \times 10^6$ . This number increased to  $1.20 \pm 0.02 \times 10^6$  cells in 5.5 mM glucose and  $1.69 \pm 0.06 \times 10^6$  cells in 25.0 mM glucose by end of the 6 day incubation period. Figure 3.2 shows that after the 3<sup>rd</sup> and 4<sup>th</sup> day of incubation, cells treated with 25.0 mM showed a significant increase in number compared to low glucose treatment by levels of 15.8% and 22.2% ( $P < 0.001$ ) and ( $P < 0.01$ ) respectively. Growth rates showed a progressive increase until stopping at day 5 of culturing for both glucose concentrations. In consequent experiments, for MCs cultured for 3 days the mean population doubling time was: 5.5 mM glucose,  $1.16 \pm 0.57$  days, and 25.0 mM glucose,  $1.09 \pm 0.49$  days ( $n = 4$ ).



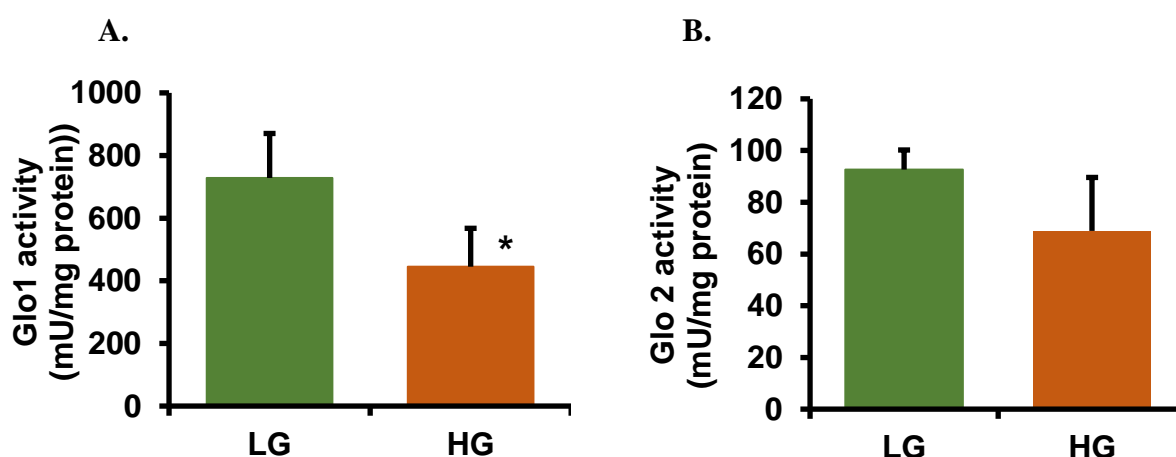
**Figure 3.2:** Growth curve of MCs cells in media containing 5.5 mM and 25.0 mM glucose *in vitro*.

Primary MCs ( $20000 \text{ cells/cm}^2$ ) were incubated in MCM media with 2 % FBS, and the above glucose concentrations indicated, for 6 days. Data are expressed as mean  $\pm$  SD ( $n = 4$ ). Key: 5.5 mM glucose —■— and 25.0 mM glucose —■—. Significance: \*  $P < 0.05$ , \*\*  $P < 0.01$  and \*\*\*  $P < 0.001$  (Student's *t*-test) with respect to low glucose control.



### 3.1.3 Characterisation of the glyoxalase system of hRPTE cells incubated in low and high glucose conditions *in vitro*

Activities of both the Glo1 and Glo2 enzymes were measured in hRPTE cells cultured in LG and HG conditions. The activity of Glo1 in LG was  $728 \pm 142$  mU per mg protein ( $n = 4$ ). This decreased by 39% after 4 days of culture under hyperglycaemic conditions ( $P < 0.05$ ) – see Table 3.1 and Figure 3.3A. Meanwhile the activity of Glo2 was not significantly changed after incubation for 4 days in HG conditions, and it was determined as  $92.6 \pm 7.58$  mU per mg protein ( $n = 4$ ) in LG conditions – see Table 3.1 and Figure 3.3B.



**Figure 3.3: Enzymatic activities of the glyoxalase system in hRPTE cells *in vitro*.**

Activities of (A) Glo1, (B) Glo2 in hRPTE cells were cultured in medium containing low glucose concentration (7.2 mM) and high glucose concentration (25 mM) for 3 days. Data are expressed as mean  $\pm$  SD ( $n = 4$ ). Significance: \*,  $P < 0.05$  (Student's *t-test*) with respect to low glucose control.

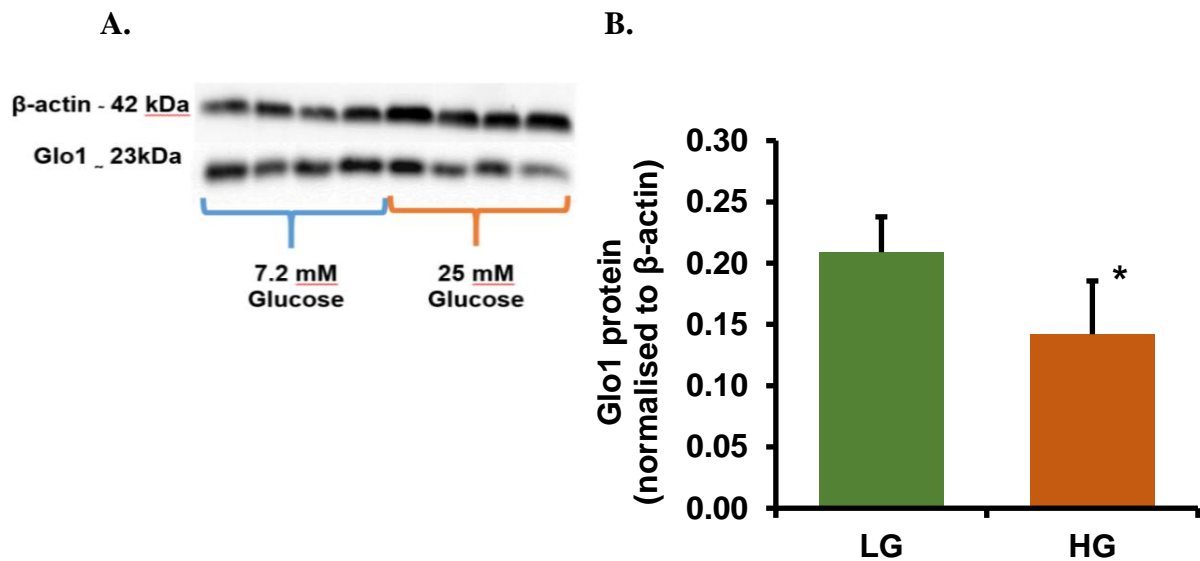
**Table 3.1: Values of Glo1 and Glo2 activity in hRPTE cells incubated in media containing low and high glucose *in vitro***

Analyte	LG (7.2 mM)	HG (25 mM)
Glo1 activity (mU/mg protein)	$728 \pm 142$	$445 \pm 122$ *
Glo2 activity (mU/mg protein)	$92.6 \pm 7.58$	$68.9 \pm 20.7$

Data are mean  $\pm$  SD,  $n = 4$ . Significance: \*,  $P < 0.05$  (*t-test*), with respect to low glucose control.

### 3.1.4 Glyoxalase 1 protein content of hRPTE cells incubated in low and high glucose concentration *in vitro*

The levels of Glo1 protein in the primary hRPTE cells incubated in LG and HG conditions was measured semi-quantitatively by Western blotting. Cells were incubated for 4 days and cell lysates were electrophoresed and immunoblotted for Glo1 protein measurement via densitometry relative to beta-actin signal. The Glo1 protein content of hRPTE cells measured by this method was decreased by 32% in the HG cultured cells, as compared to LG cultured controls ( $P < 0.05$ ). See Figure 3.4.



**Figure 3.4: Glyoxalase 1 protein content of hRPTE cells incubated in high glucose (25 mM) *in vitro*.**

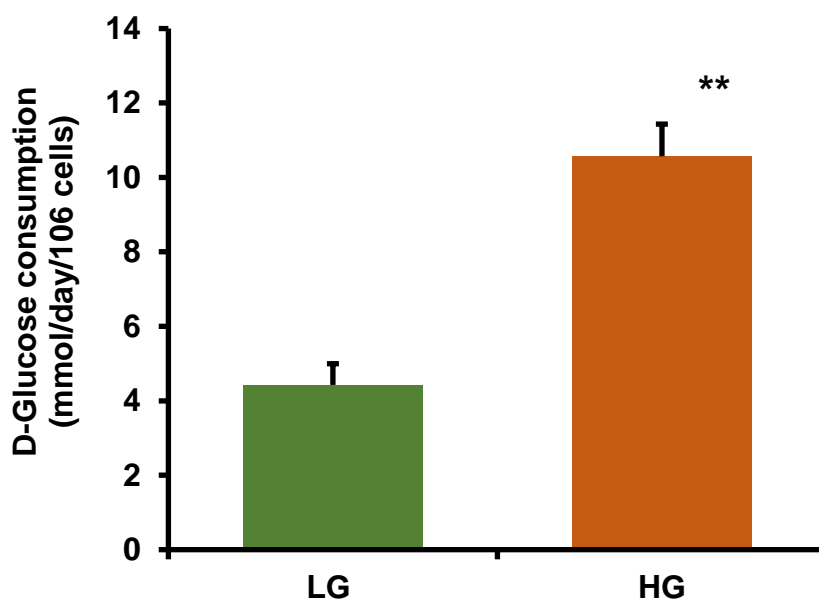
(A) Glo1 protein blot, (B) Glo1 protein blot interpretation. hRPTE cells were cultured in medium containing 7.2 mM and 25 mM glucose for 4 days. Data are expressed as mean  $\pm$  SD ( $n = 4$ ). Significance: \*  $P < 0.05$  (Student's *t*-test) with respect to low glucose control. Key: LG, low glucose concentration (7.2 mM); HG, high glucose concentration (25 mM).

## 3.2 Metabolism of methylglyoxal by renal cells in high glucose *in vitro*

### 3.2.1 Effect of high glucose concentration on D-glucose consumption, D-lactate and L-lactate formation in hRPTE cells *in vitro*

#### 3.2.1.1 Consumption of D-glucose by hRPTE cells incubated in low and high glucose *in vitro*.

Net glucose consumption by hRPTE cells was measured by determining the decrease in glucose concentration in the culture medium over a period of culturing. hRPTE cells were cultured in LG and HG concentrations for 2 days. Media samples were collected and glucose concentration was measured as described in Materials and Methods (Chapter 2). When glucose consumption was measured over 2 days of hRPTE cell culture in high glucose, there was a 2.4-fold increase in glucose consumption, compared to low glucose control ( $P < 0.01$ ) – see Figure 3.5. The anaerobic glycolysis pathway of metabolizing excessive glucose increases the flux of triosephosphate and subsequently the flux of MG formation. To assess whether there is increased flux of MG from the catabolism of glucose in high glucose conditions, the flux of D-lactate and L-lactate was measured.



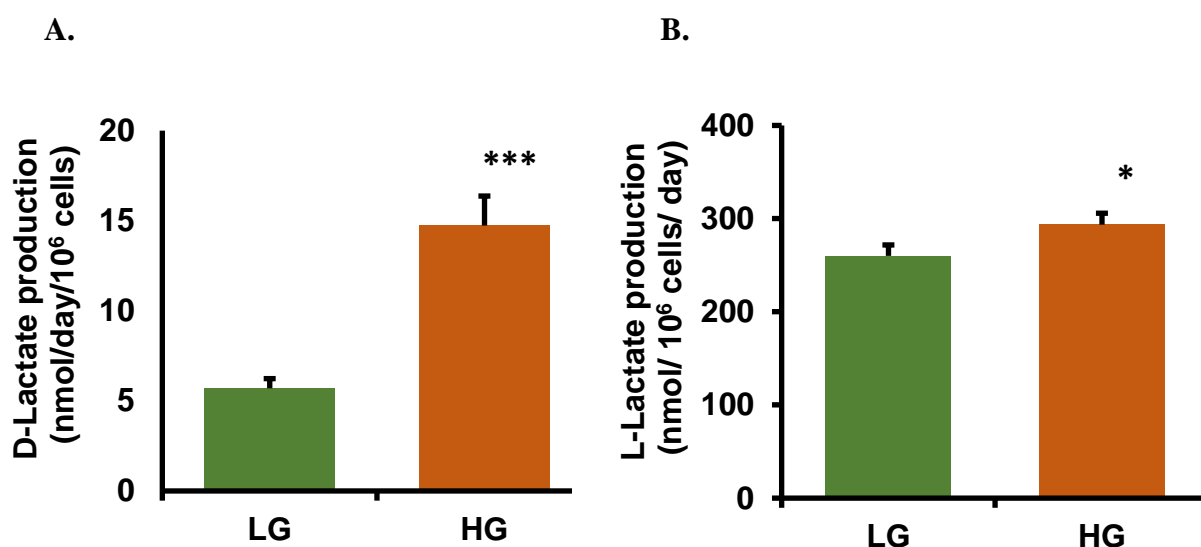
**Figure 3.5: Consumption of D-glucose by hRPTE cells incubated in high glucose *in vitro*.** hRPTE cells were cultured in medium containing 7.2 mM and 25 mM glucose for 2 days. Data are expressed as mean  $\pm$  SD,  $n = 4$ . Significance: \*\*,  $P < 0.01$  (Student's *t*-test) with respect to low glucose control. Key: LG, low glucose (7.2 mM); HG, high glucose (25 mM).

### **3.2.1.2 Flux of formation of D-lactate and L-lactate in hRPTE cells cultured in low and high glucose conditions *in vitro***

D-lactate is formed in human cells as respond to increased MG formation, and since more than 99% of MG produced is metabolised by the glyoxalase system, the main source of D-lactate is the glyoxalase system, D-lactate is usually present in human cells at low levels compared to L-lactate. As MG is difficult to measure directly due to its highly reactive nature, its end metabolite D-lactate can be used as a surrogate indicator of MG fluxes.

Primary hRPTE cells were cultured in LG and HG concentration for 2 days. The level of D-lactate and was measured in the media samples at baseline and after 2 days of culturing. The flux of D-lactate formation was analysed by subtracting the determined level of D-lactate at baseline from that at the second day. Data was normalised to cell number and days of culturing – to yield a measure of D-lactate flux as a function of nmol/million cells/day. The rate of D-Lactate metabolism in hRPTE cells is extremely low and the activity of other enzymes can catalyse the conversion of MG, such as MG reductase and MG dehydrogenase - although this is thought to be very low in these cells (Table 4.1), and therefore the main metabolic fate of MG is its conversion to D-lactate. The rate of D-lactate formation in high glucose cultures was determined as  $14.70 \pm 1.75$  nmol/day/million cells, and this is a 2.6-fold increase ( $P < 0.001$ ) in the rate of D-lactate formation by hRPTE cells in control conditions, suggesting that HG may increase MG in hRPTE cells – see Figure 3.6A and Table 3.2.

L-lactate is formed by cells as a consequence of anaerobic glycolysis and is rapidly metabolised to pyruvate. As mentioned above for D-lactate, determination of L-lactate formation is a qualitative indicator of glycolytic activity, while underestimation of L-lactate formation is common due to its rapid metabolism. The formation of L-lactate was 45-fold higher than that of D-lactate and was increased 11.5 % in cultures of hRPTE cells incubated with high glucose concentration ( $P < 0.05$ ) – see Figure 3.6B.



**Figure 3.6: Flux of formation of D-lactate and L-lactate in hRPTE cells cultured in low and high glucose conditions *in vitro*.**

hRPTE cells were cultured in medium containing 7.2 mM and 25 mM glucose for 2 days. (A) D-lactate production in hRPTE cells, (B) L-lactate production in hRPTE cells. Data are expressed as mean  $\pm$  S.D, n = 4. Significance: \*, P<0.05 and \*\*\*, P<0.001 (Student's *t-test*) with respect to low glucose control. Key: LG, low glucose (7.2 mM); HG, high glucose (25 mM).

**Table 3.2: Values of different analytical assays performed on hRPTE cells medium contains high and low glucose *in vitro*.**

Analyte	Culture Medium	
	LG (7.2 mM)	HG (25 mM)
D-Glucose consumption (mmol/day/10 <sup>6</sup> cells)	9.22 $\pm$ 1.19	22.0 $\pm$ 1.80**
D-Lactate production (nmol/day/10 <sup>6</sup> cells)	5.70 $\pm$ 0.77	14.6 $\pm$ 1.75***
L-Lactate production (nmol/day/10 <sup>6</sup> cells)	260 $\pm$ 11.7	293 $\pm$ 12.3*

Data are expressed as mean  $\pm$  SD, n = 4. Significance: \*, P<0.05, \*\*, P<0.01 and \*\*\*, P<0.001 (*t-test*) with respect to low glucose (control). Key: LG, low glucose (7.2 mM); HG, high glucose (25 mM).

## 4 Results

This chapter outlined the effect of Glo1 inducer treatment (tRSV-HSP) 10  $\mu\text{M}$  on human renal cell dysfunction in high glucose cultures *in vitro*, and whether this treatment can reverse cell dysfunction and dicarbonyl stress. Section 4.1 outlines the main findings.

### 4.1 Characterisation of the effects of the Glo1 inducer tRSV-HSP on the human renal cells incubated in high glucose concentration *in vitro*

Previously, the Thornalley research team had discovered that coformulation of tRSV and HSP increased the expression and activity of Glo1 through activation of the Nuclear factor 2 (Nrf2). After conducting a screen for over 100 nutritional bioactive compounds with Nrf2 activator activity, it was found that tRSV caused the highest maximum GLO1-ARE transcriptional activity response (Xue et al., 2016). This was confirmed by Cheng *et al.* demonstrating that 10  $\mu\text{M}$  tRSV induced increases in Glo1 protein in human hepatoma cells *in vitro* (Cheng et al., 2012). While HSP has the lowest half-maximal effective concentration ( $\text{EC}_{50}$ ) for GLO1-ARE transcriptional activity, the values for tRSV activating Glo1 were:  $\text{EC}_{50} = 2.52 \pm 0.19 \mu\text{M}$  and  $E_{\text{max}} 100 \pm 2\%$ . For HSP,  $\text{EC}_{50} = 0.59 \pm 0.01 \mu\text{M}$  and  $E_{\text{max}} 24.4 \pm 0.1\%$  (Xue et al., 2016). In one of the clinical studies to investigate the efficacy of HSP, an oral administration of 150 mg HSP reached a peak plasma concentration of 6.7  $\mu\text{M}$  (Takumi et al., 2012). This result indicates that the HSP compound is capable of inducing Glo1 in clinical trials with low maximal effect. After oral administration of a 500 mg dose, plasma tRSV reached a peak concentration of 0.3  $\mu\text{M}$  (Boocock et al., 2007). To improve Glo 1 inducer efficacy, Xue *et al.*, assessed the pharmacological combination of tRSV and HSP by analysing the GLO1-ARE transcriptional response of 5  $\mu\text{M}$  HSP with 0.625 – 10  $\mu\text{M}$  tRSV. The study concluded that HSP combined with tRSV reduced the  $\text{EC}_{50}$  of tRSV by 2-fold to  $1.46 \pm 0.10 \mu\text{M}$  while maintaining the  $E_{\text{max}}$ . This suggests the use of tRSV-HSP together leads to synergy rather than using each compound alone (Xue et al., 2016).

In this study, the effect of Glo1 inducer was studied on the growth and viability of the primary cells. The results showed a significant inhibition effect of tRSV-HSP (10  $\mu\text{M}$ ) on cell growth in both cell types with no evidence of increase in non-viable cell number. Furthermore, another experiment was conducted to study the effect of each compound, and it was found that tRSV alone arrested cell growth. Both types of primary renal cells showed similar sensitivity to tRSV (10  $\mu\text{M}$ ) by reduction in cell proliferation by 48% and 53% in hRPTECs and MCs

respectively. Resveratrol has been commonly studied in both *in vivo* and *in vitro* studies as a potent anti-proliferation, pro-apoptosis, anti-carcinogenic, and antioxidant agent.

The effect of tRSV-HSP combination on glyoxalase system and dicarbonyl stress of hRPTECs and MCs in normal and hyperglycaemia conditions was studied. The results showed significant increase in Glo1 activity in hRPTECs by tRSV-HSP treatment in comparison with the control treatments. Incubation of hRPTECs with Glo1 inducer increased Glo1 activity by 13% and 16% in LG and HG conditions, respectively. While in MCs the activity of Glo1 showed significant increase by 1.6-fold just in HG treatment. In both cell types the activities of MG reductase and MG dehydrogenase were below the limit of detection. Hence, metabolism by the glyoxalase system is expected to be the main fate for MG metabolism in these cells.

The ability of Glo1 inducers, a synergistic combination tRSV-HSP, to counter dicarbonyl stress in hRPTECs and MCs *in vitro* was studied, by measuring glucose consumption, D- and L-lactate formation in hRPTECs and MCs. In hRPTECs all these parameters were increased under hyperglycaemic conditions, Glo1 inducer treatment showed no significant change on glucose consumption or D-lactate levels, while the level of L-lactate formation was corrected by Glo1 inducer by 45% and 34% respectively in LG and HG conditions. While in MCs, D-glucose consumption increased under HG conditions by 3-fold, and Glo1 inducer showed a minor decrease that did not reach a significant value, and the flux formation of D-lactate was significantly reduced by 18% in Glo1 inducer treatment under hyperglycaemic conditions, although L-lactate levels did not change significantly. The increased formation of D-lactate indirectly indicated increased MG formation in these cells, and this further supported the principle of high glycolytic activity by the decreased activity of Glo1 in hyperglycaemia.

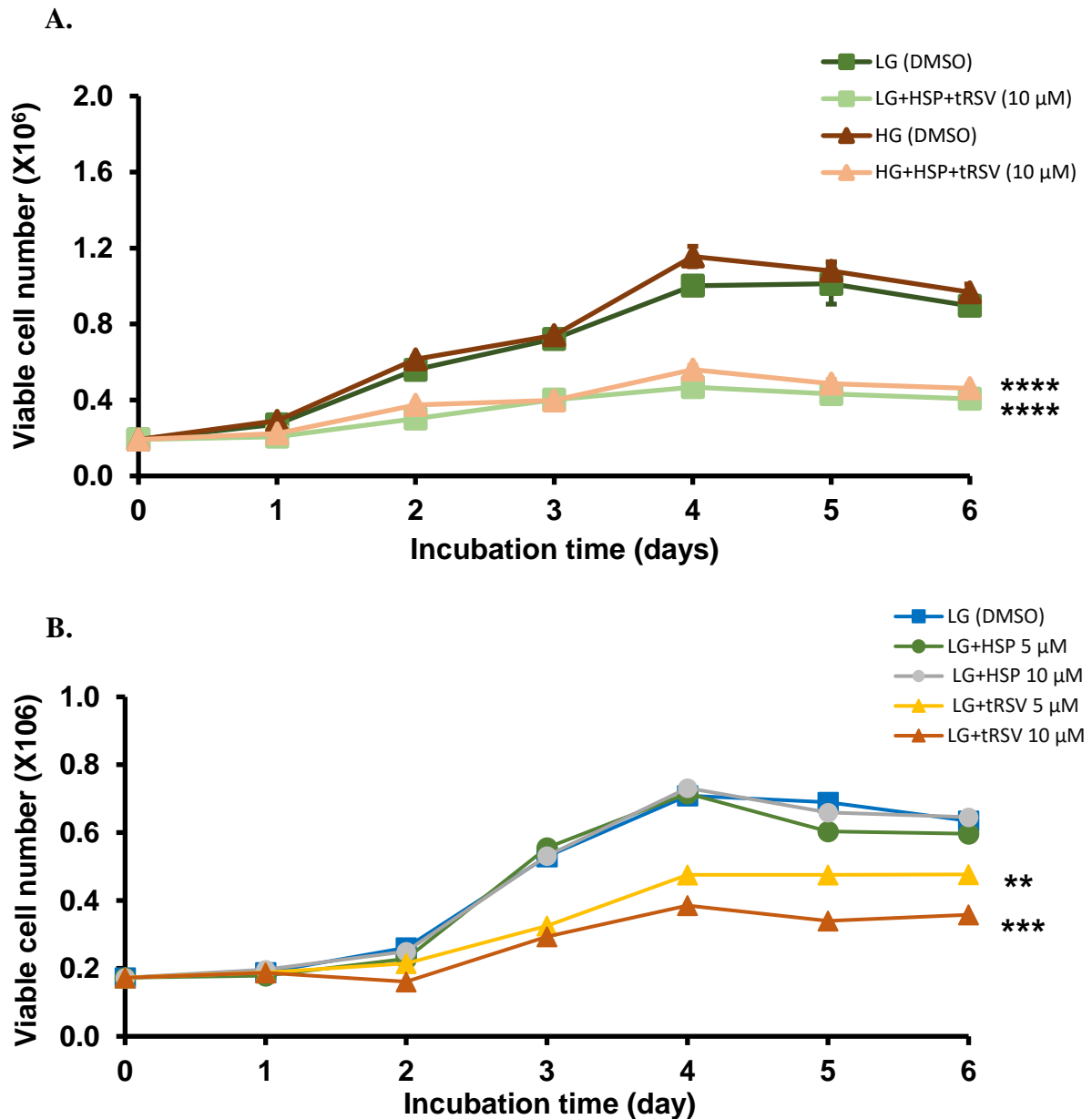
#### **4.1.1 Growth and viability of hRPTE cells incubated in 7.2 mM and 25.0 mM glucose concentration with and without Glo1 inducer *in vitro***

Growth and viability of hRPTE cells incubated in 7.2 mM and 25.0 mM glucose with and without Glo1 inducer was studied. Cell growth curves were established for viable cell number against time over 6 days to determine the type of growth pattern of hRPTE cells incubated with and without tRSV-HSP (10  $\mu$ M) – see Figure 4.1A. The viable cell number increased by 79% throughout the period of culture in low glucose. At the 6<sup>th</sup> day of culturing, the viable cell number had increased from  $0.192 \times 10^6$  at seeding to:  $0.93 \pm 0.037 \times 10^6$  cells in 7.2 mM glucose,  $0.95 \pm 0.025 \times 10^6$  cells in 25.0 mM glucose, then  $0.41 \pm 0.001 \times 10^6$  cells in 7.2 mM glucose + 10  $\mu$ M Glo1 inducer, and finally  $0.46 \pm 0.026 \times 10^6$  cells in 25.0 mM glucose + 10  $\mu$ M Glo1 inducer.

A significant decrease in cell confluence was observed under the microscope on the second day of treatment with tRSV-HSP (10  $\mu$ M). This was confirmed by Trypan blue exclusion tests when cell number in Glo1 inducer treated cells showed 44.8% and 38.7% decreases compared to control low and high glucose conditions, respectively ( $P < 0.0001$ ), with no evidence of increase in non-viable cell number. This significant change was stable during the experiment and by the 6<sup>th</sup> day, cells showed a significant decrease in number by 55.8 and 51.6% comparing to the control of low and high glucose treatment, respectively ( $P < 0.0001$ ).

To further examine the effect of each compound of Glo1 inducer, growth and viability of hRPTE cells was studied with and without tRSV and HSP at the concentration of 5 and 10  $\mu$ M under normal glucose conditions. As shown in Figure 4.1B, a significant decrease was noticeable in cell number between the tRSV-treated cells and controls after day 3 of treatment. Decrease in cell number was 34.1% and 48.5 % in tRSV-treated cells by 5 $\mu$ M and 10  $\mu$ M treatments, respectively as an average in the last three days of culturing. These results demonstrated the potent inhibitory effect of tRSV on the growth of hRPTE cells in a relatively short treatment time of study.





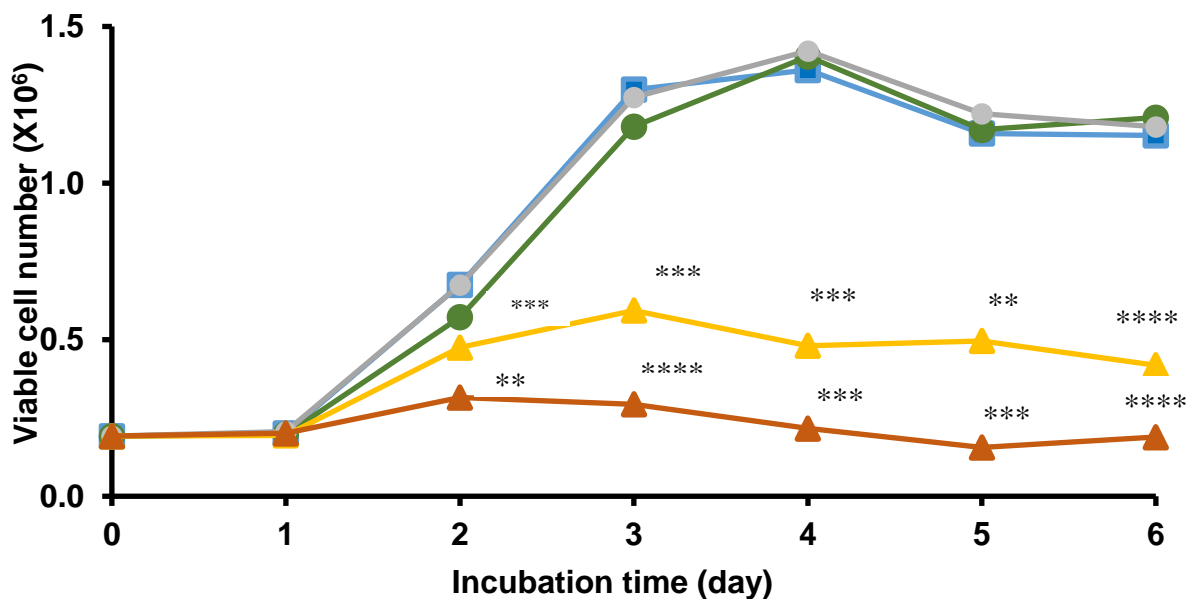
**Figure 4.1: Growth curve of hRPTE cells with and without tRSV-HSP (5 and 10 μM) combination and individually *in vitro*.**

**A.** Primary hRPTE cells (20000 cells/cm<sup>2</sup>) were incubated in basal media with 0.5 % FBS and glucose concentrations of (7.2 mM) or (25.00 mM), with and without tRSV-HSP (10 μM). Data are mean ± SD (n = 3) Significance: \*\*\*\* P<0.0001 (*t*-test) with respect to control.

**B.** Primary hRPTE cells (20000 cells/cm<sup>2</sup>) were incubated in basal media with 0.5 % FBS and the glucose concentrations indicated for 6 days, with and without HSP (5 μM), (10 μM) and tRSV (5 μM and 10 μM). Data are expressed as mean ± SD (n = 4) Significance: \*\* P<0.01 and \*\*\* P<0.001 (*t*-test) with respect to low glucose control.

#### 4.1.2 Growth and viability of MCs incubated in 5.5 mM glucose with and without HSP and tRSV *in vitro*

Primary MCs (20000 cells/cm<sup>2</sup>) were seeded in 6 well plates and incubated in MCM medium containing 5.5 mM glucose with and without the following treatments individually: HSP 5  $\mu$ M, 10  $\mu$ M, tRSV 5  $\mu$ M and 10  $\mu$ M for 6 days and the viable cell number was counted in all the study groups. The viable cell number of control and HSP-treated cells increased throughout the culture period and showed a steady increase with no significant change between these groups. Addition of tRSV decreased cell growth to a similar extent in both 5  $\mu$ M and 10  $\mu$ M tRSV groups – see Figure 4.2. Decreases in cell number were observed on the second day of treatment by 29.6% and 53.3% with 5  $\mu$ M and 10  $\mu$ M tRSV, ( $P < 0.001$  and  $P < 0.01$ ) respectively. Reduction in cell number continued steadily during time of the incubation and showed an average of 61% and 85% after treatment of the cells with 5  $\mu$ M and 10  $\mu$ M tRSV in the last three days of culturing – see Figure 4.2.



**Figure 4.2: Growth curve of MCs in media containing 5.5 mM glucose with and without 5  $\mu$ M and 10  $\mu$ M HSP and tRSV.**

Primary MCs (20000 cells/cm<sup>2</sup>) were incubated in MCM media with 2% FBS with and without HSP and tRSV, 5 and 10  $\mu$ M for 6 days. Data are expressed as mean  $\pm$  SD ( $n = 3$ ). Key: 5.5 mM glucose  $\blacksquare$ , 5.5 mM glucose + HSP (5  $\mu$ M)  $\bullet$ , 5.5 mM glucose + HSP (10  $\mu$ M)  $\bullet$ , 5.5 mM glucose + tRSV (5  $\mu$ M)  $\blacktriangle$  and 5.5 mM glucose + tRSV (10  $\mu$ M)  $\blacktriangle$ . Significance: \*\*  $P < 0.01$ , \*\*\*  $P < 0.001$ , \*\*\*\*  $P < 0.0001$  (Student's  $t$ -test) with respect to control.

### 4.1.3 Effect of Glo1 inducer on enzymatic activity related to dicarbonyl metabolism in hRPTE cells *in vitro*

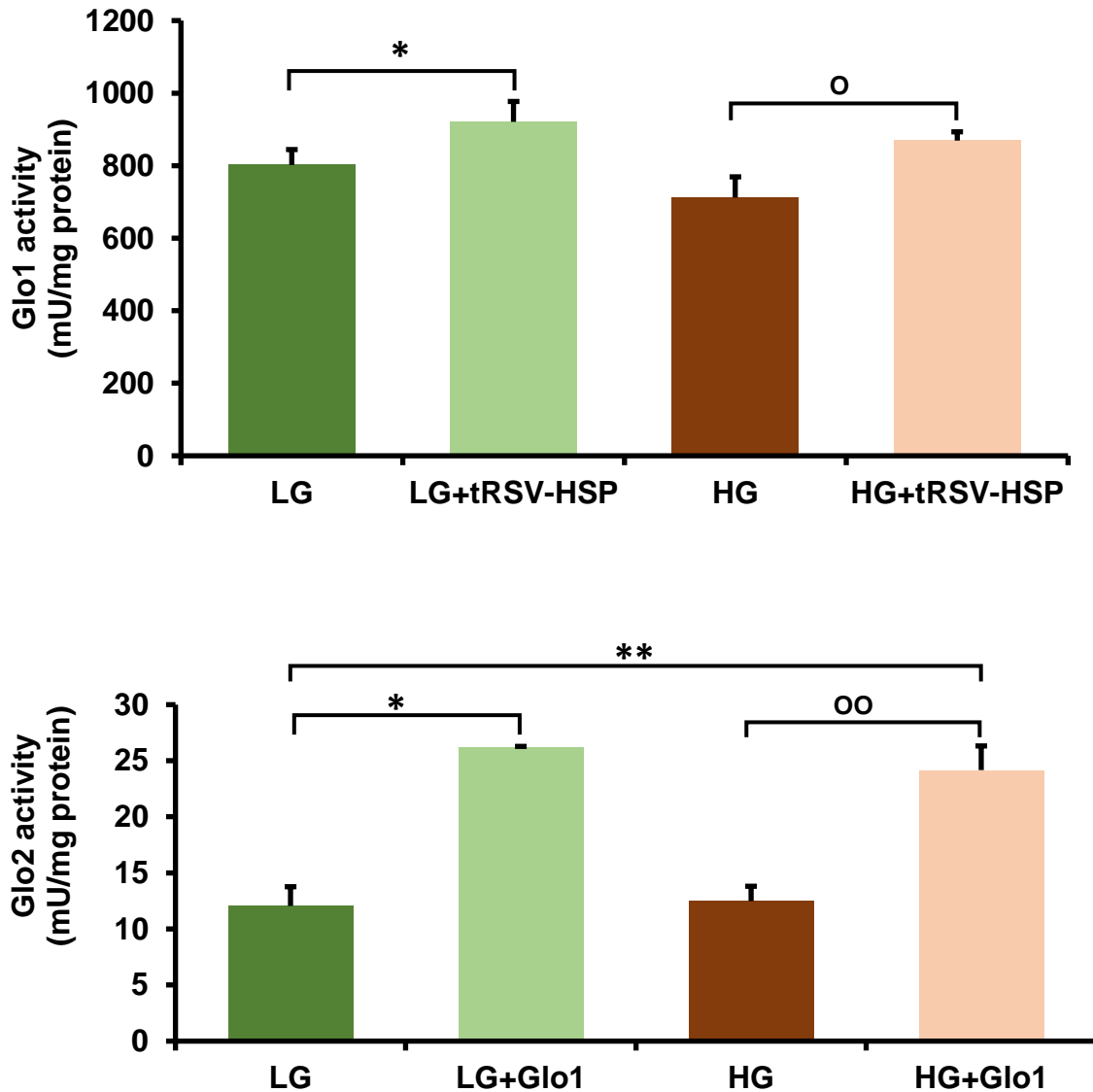
Activities of Glo1 and Glo2 were measured in primary hRPTE cells cultured in low and high glucose concentrations with and without 10  $\mu$ M tRSV+HSP for 4 days.

Incubation of hRPTE cells with tRSV+HSP in 7.2 mM glucose produced significant increase in both Glo1 and Glo2 activities by 12.9% ( $P < 0.05$ ) and 53.9% ( $P < 0.05$ ) above the 7.2 mM glucose control value. When cells were incubated in high, 25 mM glucose in the culture medium, activity of Glo1 was decreased by 12.6%, compared with the low, 7.2 mM glucose conditions but this did not reach significance ( $P = 0.09$ ), it is likely that dicarbonyl stress is induced by the hyperglycaemic conditions. This was investigated by assay of the levels of D- and L-lactate consumption. Decreases in Glo1 and Glo2 activities were reversed by incubation with Glo1 inducer by 15.7% and 48.4% ( $P < 0.05$ ) and ( $P < 0.01$ ) respectively with respect to 25 mM glucose controls. The activity of Glo1 in tRSV+HSP conditions under hyperglycaemic conditions (25 mM glucose) showed a 7.74 % increase compared to 7.2 mM glucose controls but this did not reach significance ( $P = 0.07$ ). This suggests that tRSV+HSP treatment could increase the activity of Glo1 in hyperglycaemic conditions and prevent a deficit of Glo1 activity - Figure 4.3 and Table 4.1. Metabolism of MG by MG reductase and MG dehydrogenase is another pathway beside the glyoxalase pathway that can degrade MG and other endogenous toxic metabolites into non-harmful D-lactate. In hRPTE cells the activities of MG reductase and MG dehydrogenase were below the limit of detection. Therefore, metabolism by glyoxalase system is expected to be the main fate for MG metabolism in hRPTE cells – see Table 4.1.

**Table 4.1: Effect of Glo1 inducers on Glo1 and Glo2 activity in hRPTE cells *in vitro***

Analyte (mU/mg protein)	7.2 mM Glc	7.2 mM Glc + Glo1 inducer	25 mM Glc	25 mM Glc + Glo1 inducer
<b>Glo1 activity</b>	802 $\pm$ 43	921 $\pm$ 56 *	733 $\pm$ 79	869 $\pm$ 24 <sup>o</sup>
<b>Glo2 activity</b>	12.1 $\pm$ 1.72	26.2 $\pm$ 0.111*	12.5 $\pm$ 1.33	24.2 $\pm$ 2.16 <sup>oo</sup>
<b>MG reductase</b>	<LOD	<LOD	<LOD	<LOD
<b>MG dehydrogenase</b>	<LOD	<LOD	<LOD	<LOD

Data are expressed as mean  $\pm$  SD, n = 3. Significance: \*  $P < 0.05$  (Student's *t*-test) with respect to low glucose control; <sup>o</sup> and <sup>oo</sup>,  $P < 0.05$  and  $P < 0.01$ , respectively with respect to high glucose control (Student's *t*-test).



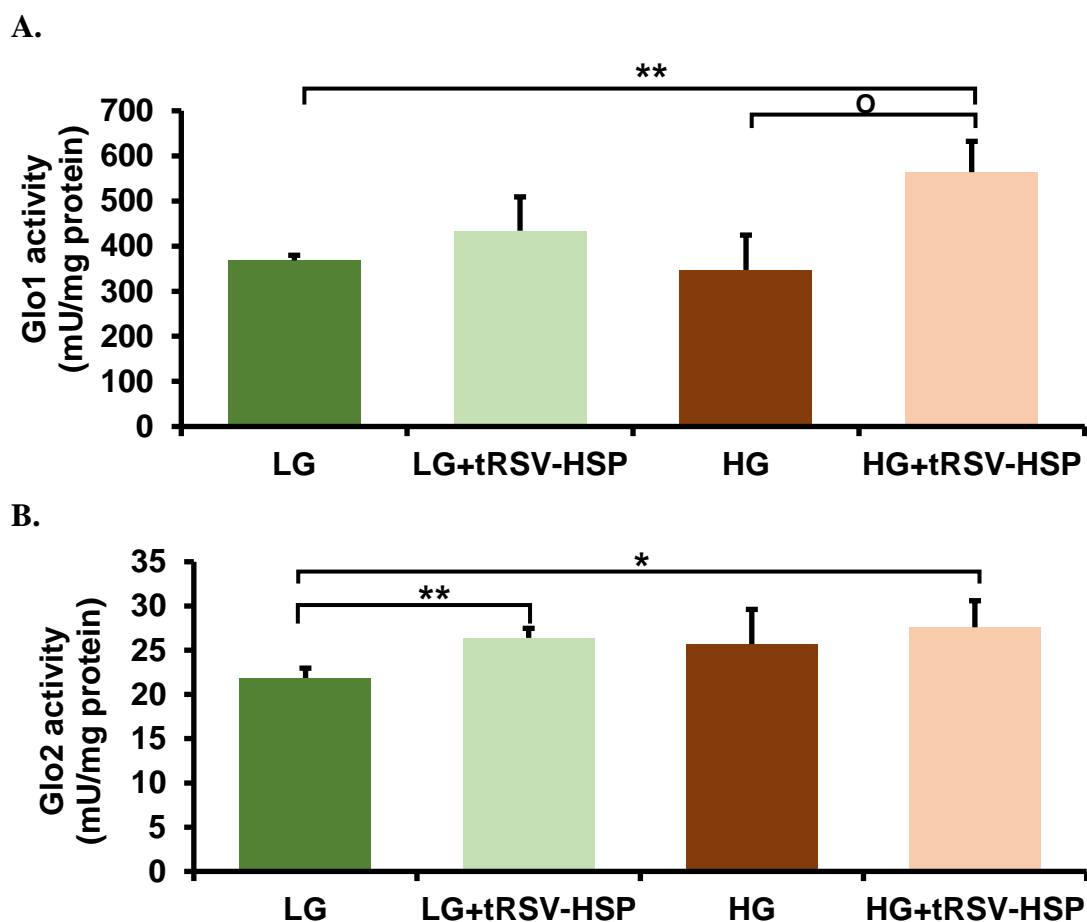
**Figure 4.3 : Enzymatic activities of glyoxalase system in hRPTE cells *in vitro*.**

Activities of (A) Glo1, (B) Glo2 in hRPTE cells cultured in medium containing low (7.2 mM) and high glucose concentration (25 mM) with and without tRSV-HSP (10 $\mu$ M) for 4 days. Data are expressed as mean  $\pm$  SD (n = 3). Significance: \* and \*\* P<0.05 P<0.01 respectively, (Student's *t-test*) with respect to low glucose control; <sup>°</sup> and <sup>°°</sup>, P<0.05 and P<0.01, respectively, with respect to high glucose control (Student's *t-test*).

#### **4.1.4 Effect of Glo1 inducer on enzymatic activity related to dicarbonyl metabolism in MCs *in vitro***

The activity of Glo1 and Glo2 was measured in primary MCs cultured in MCM medium containing 5.5 mM and 25 mM glucose concentrations, with and without 10  $\mu$ M tRSV+HSP after incubation for 4 days. There was no significant change in Glo1 activity in cells incubated with tRSV+HSP in 5.5 mM glucose, this was not expected under LG conditions. While treatment of the cells with tRSV+HSP combined with 25 mM glucose conditions increased the activity of Glo1 significantly - by 38.5% ( $P<0.05$ ) with respect to 25 mM glucose conditions. The same treatment showed a significant increase by 34.7% ( $P<0.01$ ) in activity above the 5.5mM glucose value. Under the 25 mM glucose conditions, there was no significant change in Glo1 activity after 4 days of incubation compared with 5.5 mM glucose conditions – see Table 4.2 and Figure 4.4.

The activity of the second enzyme of the glyoxalase pathway, Glo2, showed a significant increase by 26.4 % ( $P<0.01$ ) in cells incubated with tRSV+HSP in 5.5 mM glucoses conditions with respect to 5.5 mM glucose-only controls, while the activities of MG reductase and MG dehydrogenase in MCs were below the limit of detection.



**Figure 4.4: Enzymatic activities of the glyoxalase system in MCs cells *in vitro*.**

Activities of (A) Glo1 and (B) Glo2 in MCs. The cells were cultured in medium containing low glucose (LG - 5.5 mM) and high glucose (HG - 25 mM) with and without tRSV-HSP (10 $\mu$ M) for 4 days. Data are expressed as mean  $\pm$  SD (n = 3). Significance: \* and \*\*\*, P<0.05 and P<0.001, respectively (Student's *t-test*) with respect to low and high glucose control. °, P<0.05 with respect to high glucose control (Student's *t-test*).

**Table 4.2: Effect of Glo1 inducers on Glo1 and Glo2 activity in MCs *in vitro***

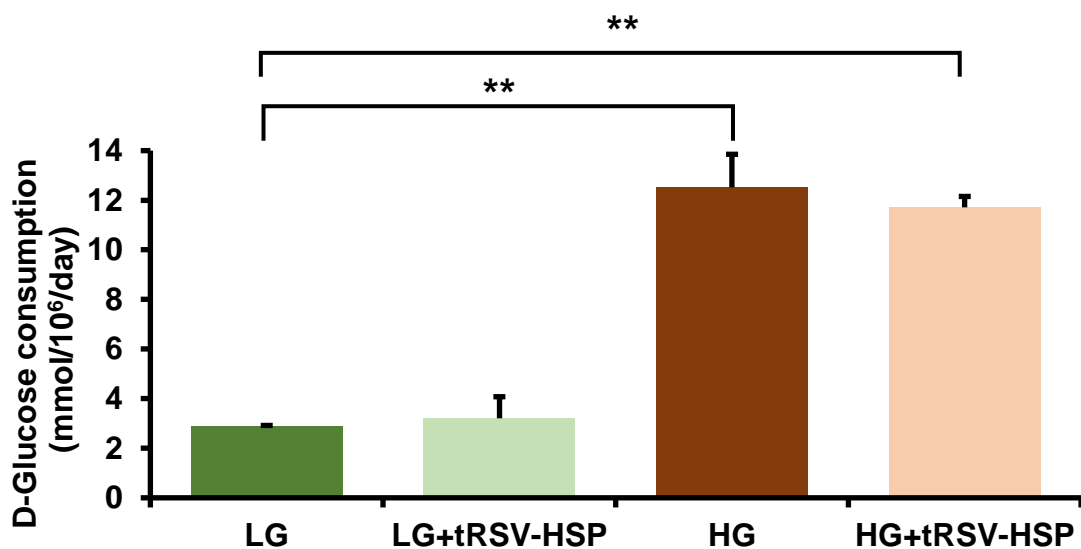
Analyte (mU/mg protein)	LG	LG + Glo1 inducer	HG	HG+ Glo1 inducer
Glo1 activity	368 $\pm$ 11.4	434 $\pm$ 75.1	347 $\pm$ 77.3	564 $\pm$ 68.3 ***°
Glo2 activity	21.9 $\pm$ 1.11	26.4 $\pm$ 1.08**	25.7 $\pm$ 3.91	27.6 $\pm$ 3 *
MG reductase	<LOD	<LOD	<LOD	<LOD
MG dehydrogenase	<LOD	<LOD	<LOD	<LOD

Data are expressed as mean  $\pm$  SD, n = 3. Significance: \* and \*\*, P<0.05 and P<0.01 (*t-test*) with respect to low glucose control; °, P<0.05 with respect to high glucose control (*t-test*).

## 4.2 Characterisation of the effect of Glo1 inducer on the D-glucose consumption, D-lactate and L-lactate formation by hRPTE cells in hyperglycaemia *in vitro*

### 4.2.1 Effect of Glo1 inducers on the consumption of D-Glucose by hRPTE cells *in vitro*

Glucose uptake by hRPTE cells was measured in the medium of cultured cells incubated in 7.2 mM glucose (LG) and 25 mM glucose (HG), with and without the Glo1 inducers (tRSV+HSP at 10  $\mu$ M) for 2 days. Glo1 inducer supplementation did not significantly change glucose consumption in either of the LG and HG conditions, while in HG conditions glucose consumption was increased by 71% with respect to the LG controls ( $P < 0.01$ ) – see Figure 4.5.



**Figure 4.5:** Effect of Glo1 inducers on consumption of D-glucose by hRPTE cells *in vitro*. hRPTE cells were cultured in medium containing 7.2 mM (LG) and 25 mM glucose (HG) with and without 10  $\mu$ M tRSV+HSP for 2 days. Data are expressed as mean  $\pm$  SD, n = 4. Significance: \*\*  $P < 0.01$  (Student's *t*-test) with respect to low glucose control.

#### 4.2.2 Effect of Glo1 inducers on flux of formation of D-lactate and L-lactate by hRPTE cells in hyperglycaemia *in vitro*

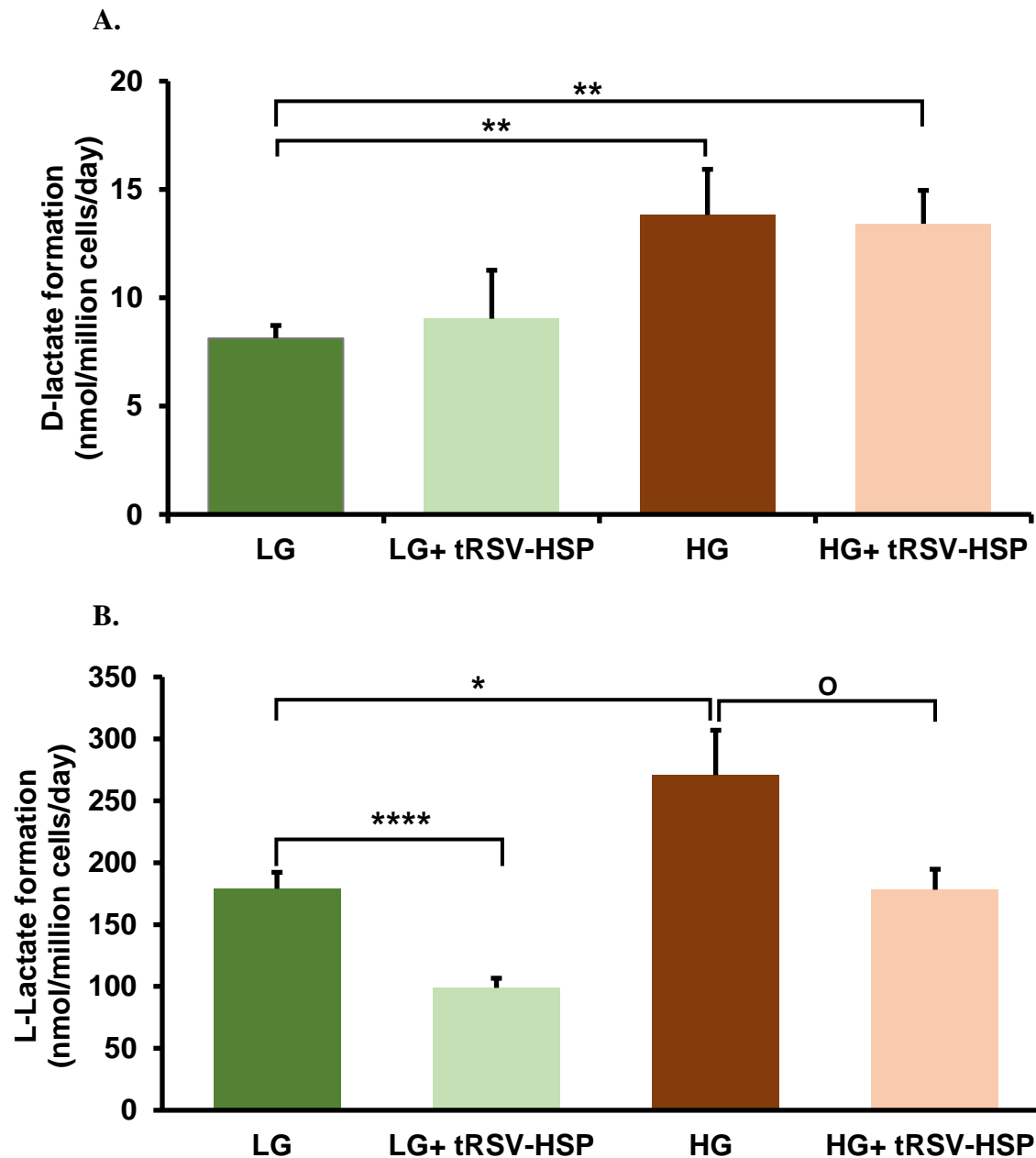
Primary hRPTE cells were cultured in 7.2 mM glucose and 25 mM glucose for 2 days with and without 10  $\mu$ M tRSV+HSP. The flux of formation of D-lactate was increased significantly in hPDLF cells in HG condition by 70 % (P<0.01), and in HG with tRSV+HSP by 65% (P<0.01) compared with LG control – see Figure 4.6 and Table 4.3. However, in the presence of Glo1 inducer, the flux of D-lactate formation in LG conditions did not change significantly. Table 4.3 illustrates the formation of L-lactate in hRPTE cells, the flux of L-lactate formation was increased significantly in HG conditions - by 51% (P<0.05) compared to LG cultures. The Glo1 inducers had a significant effect on the formation of L-lactate on both LG and HG cultures, leading to decreases by 45% and 34% (P<0.0001) and (P<0.05) respectively.

**Table 4.3: Effect of Glo1 inducers on formation of D-lactate and L-lactate in hRPTE cells *in vitro***

Analyte	Culture medium			
	LG	LG + Glo1 inducer	HG	HG + Glo1 inducer
<b>D-Lactate production (nmol/day/10<sup>6</sup> cells)</b>	8.13 $\pm$ 0.59	9.0 $\pm$ 2.24	13.8 $\pm$ 2.11**	13.4 $\pm$ 1.54**
<b>L-Lactate production (nmol/day/10<sup>6</sup> cells)</b>	179 $\pm$ 13.2	98.8 $\pm$ 7.77 ****	271 $\pm$ 36.2 *	178 $\pm$ 16.5 <sup>o</sup>

Data are expressed as mean  $\pm$  SD, n = 4. Significance: \*, \*\*, and \*\*\*\*, P<0.05, P<0.01 and P<0.0001, respectively, compared to low glucose control; <sup>o</sup>, P<0.05 compared to high glucose control (Students *t-test*).





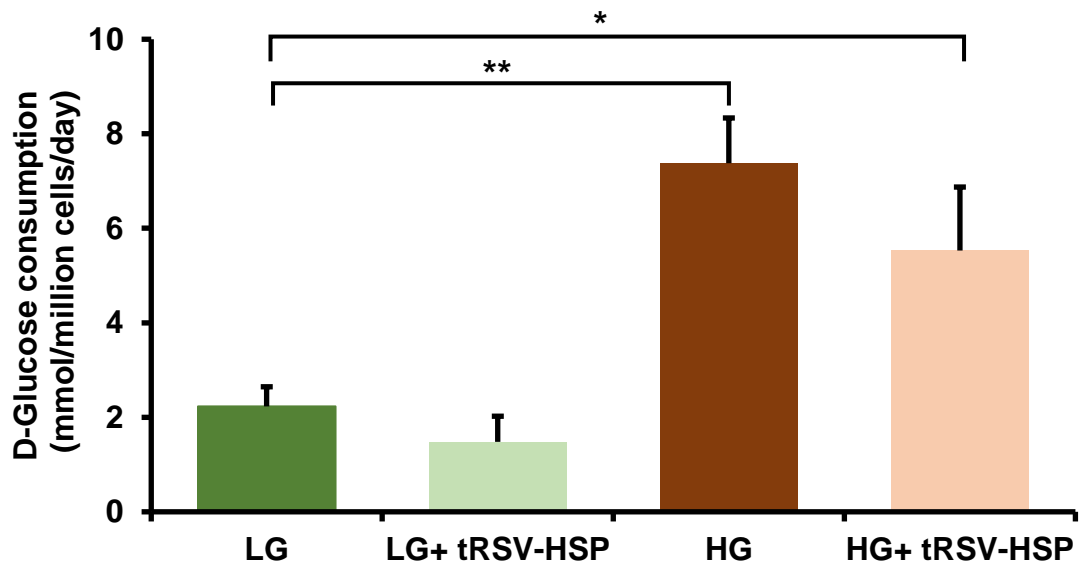
**Figure 4.6: Flux of formation of D-lactate and L-lactate in hRPTE cells cultured in low and high glucose conditions with and without Glo1 inducer *in vitro*.**

hRPTE cells were cultured in medium containing 7.2 mM and 25 mM glucose with and without tRSV-HSP (10 $\mu$ M) for 2 days. (A) D-lactate production in hRPTE cells, (B) L-lactate production in hRPTE cells. Data are expressed as mean  $\pm$  S.D, n = 4. Significance: \*, \*\*and \*\*\*\*, P<0.05, P<0.01 and P<0.0001 (Students *t-test*) with respect to low glucose control.  $\circ$ , P<0.05 with respect to high glucose control (Students *t-test*).

### 4.3 Characterisation of the effect of Glo1 inducer on the D-glucose consumption, D-lactate and L-lactate formation by MCs in hyperglycaemia *in vitro*

#### 4.3.1 Effect of Glo1 inducers on the consumption of D-Glucose by MCs *in vitro*

Glucose consumption was measured in MC cultures. Cells were cultured, as previously described in Chapter 2, in 5.5 mM glucose (LG) and 25 mM glucose (HG) with and without Glo1 inducers (10  $\mu$ M) tRSV-HSP combination. Addition of 10  $\mu$ M tRSV-HSP to the culture of LG and HG, did not change glucose consumption significantly. However, in the HG cultures, glucose consumption was increased by 3.3-fold with respect to the LG cultures ( $P < 0.01$ ) – see Figure 4.7.

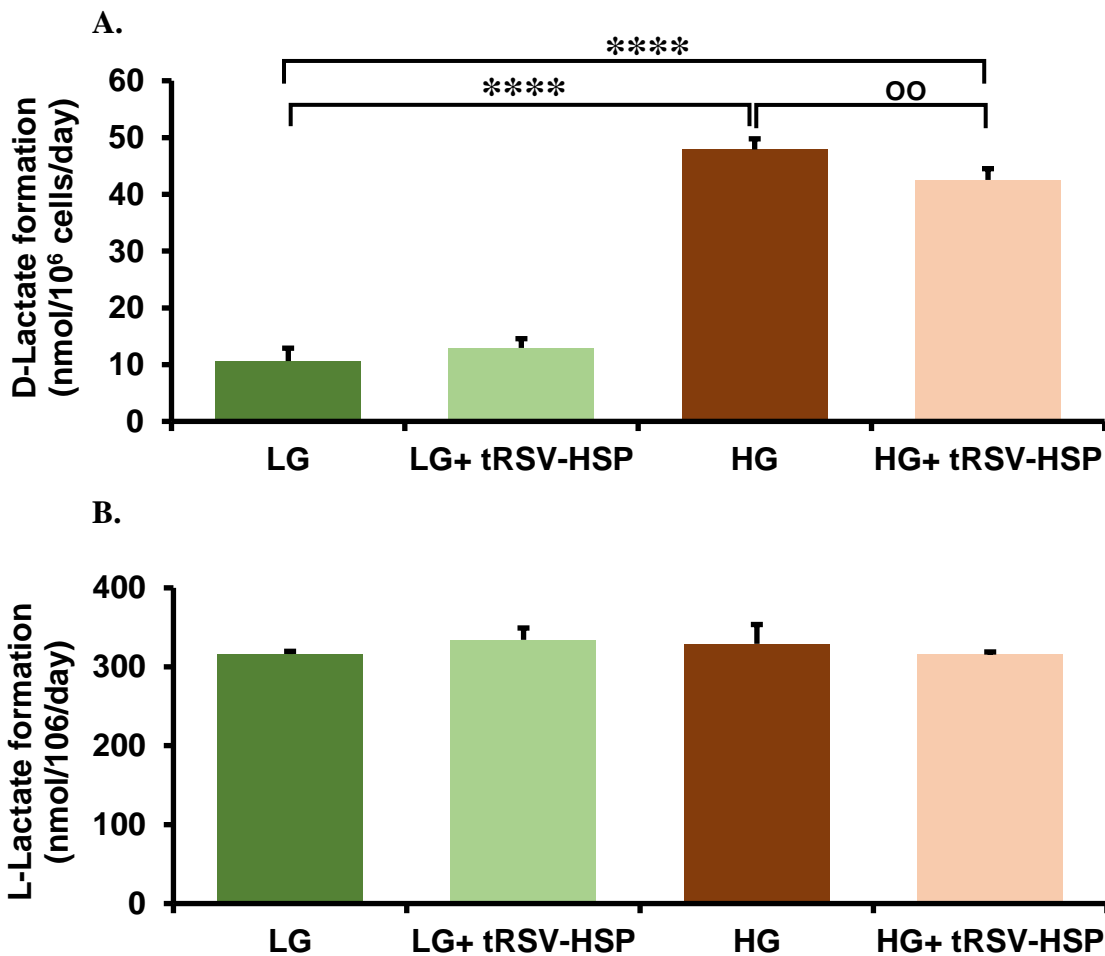


**Figure 4.7: Effect of Glo1 inducers on consumption of D-glucose by MCs *in vitro*.**

MCs were cultured in medium containing 5.5 mM (LG) and 25 mM glucose (HG) with and without 10  $\mu$ M tRSV+HSP for 2 days. Data are expressed as mean  $\pm$  SD,  $n = 4$ . Significance: \* and\*\*,  $P < 0.05$  and  $P < 0.01$  (Students *t-test*) with respect to low glucose control.

### 4.3.2 Effect of Glo1 inducers on flux of formation of D-lactate and L-lactate by MCs in hyperglycaemia *in vitro*

Primary MCs were cultured in 5.5 mM glucose and 25 mM glucose for 2 days with and without 10  $\mu$ M tRSV-HSP. The flux of formation of D-lactate was increased significantly in MCs in high glucose without tRSV-HSP - by 4.2-fold ( $P < 0.0001$ ), also in high glucose with tRSV-HSP - by 3.4-fold ( $P < 0.0001$ ) compared with the low glucose controls. However, in the presence of tRSV-HSP, the flux of D-lactate formation in the HG cultures was decreased significantly - by 18% ( $P < 0.01$ ), while the level of L-lactate did not show any significant change in any of the treatments – see Figure 4.8 and Table 4.4.



**Figure 4.8: Flux of formation of D-lactate and L-lactate in MCs cultured in low and high glucose conditions with and without Glo1 inducer *in vitro*.**

MCs were cultured in medium containing 5.5 mM and 25 mM glucose with and without tRSV-HSP (10 $\mu$ M) for 2 days. (A) D-lactate production in MCs, (B) L-lactate production in MCs. Data are expressed as mean  $\pm$  S.D,  $n = 4$ . Significance: \*\*\*\*,  $P < 0.0001$  (Students *t*-test) with respect to low glucose control. °°,  $P < 0.01$  with respect to high glucose control (Students *t*-test). Key: LG, low glucose (5.5 mM); HG, high glucose (25 mM).

**Table 4.4: Effect of Glo1 inducers on formation of D-lactate and L-lactate in MCs *in vitro***

Analyte	Culture medium			
	LG	LG + Glo1 inducer	HG	HG + Glo1 inducer
<b>D-Lactate production (nmol/day/10<sup>6</sup> cells)</b>	10.6 ± 2.27	14.0 ± 1.64	43.8 ± 1.60****	36.0 ± 2.01**** <sup>oo</sup>
<b>L-Lactate production (nmol/day/10<sup>6</sup> cells)</b>	316 ± 3.5	334 ± 15	329 ± 24.5	316 ± 3.23

Data are expressed as mean ± SD, n = 4. Significance: \*\*\*\* P<0.0001, compared to low glucose control; <sup>oo</sup> P<0.01 compared to high glucose control (Students *t-test*).

## 5 Results

This chapter describes the study of the modification of cytosolic proteins in renal cells cultured in hyperglycaemia with and without Glo1 inducer, section 5.1 summarises the main results of the proteome analysis.

### 5.1 Studying the modification of cytosolic proteins in renal cells: high mass resolution proteomics analysis

Primary hRPTE cells and MCs were cultured in LG and HG concentration with and without tRSV-HSP (10 $\mu$ M) in triplicate for 4 days. High resolution mass spectrometry via Orbitrap peptide analysis was used following tryptic digestion of the cytosolic proteins – with subsequent identification of the tryptic peptides and any quantitative changes in specific regions of the cytosolic proteome. In this experiment the following software programmes were used for analysis of proteomics data obtained by the high-resolution Mass Spectrometry protocol.

#### 1. Scaffold

Scaffold (version Scaffold 4.8.9, Proteome Software Inc.) was used as a bioinformatics tool that performs validation of proteomics data. The outcomes from the mass spectrometry data processing were analysed by Scaffold where this software combines the output of many peptides and protein validation methods following the interrogation of multiple data-base search engines including MASCOT and SEQUEST. Each search engine is used to identify the acquired peptide molecular ion and fragment ion series spectra to produce reliable spectrum identifier tracking (Searle, 2010). MASCOT searches are based on MS2 and this data is essential for peptide and protein identification in Scaffold.

#### 2. Perseus

Quantified proteins, determined by label free quantification (LFQ) were transformed to logarithm (log 2) values using the Perseus software 1.6.12.0. This software is a statistical tool that interprets details of protein quantification, interaction and post-translational modification data, and provides tools to conduct high-dimensional data analysis including normalization, pattern recognition, time-series analysis, cross-omics comparisons, and multiple-hypothesis testing. Basic statistical analysis was performed, such as visual inspection of normal distribution, principal component analysis (PCA) to summarize variance between different treatments, and Volcano plots to represent statistically significant differences in changes of

protein abundance measurements made between different cell culture treatments (e.g. with and without tRSV+HSP), assessed by two-sided *t-tests* adjusted by a permutation-based FDR at 0.05%. This was followed by exporting data using Microsoft Excel to calculate *P-values* by a two-tailed *t-test* and calculating fold changes.

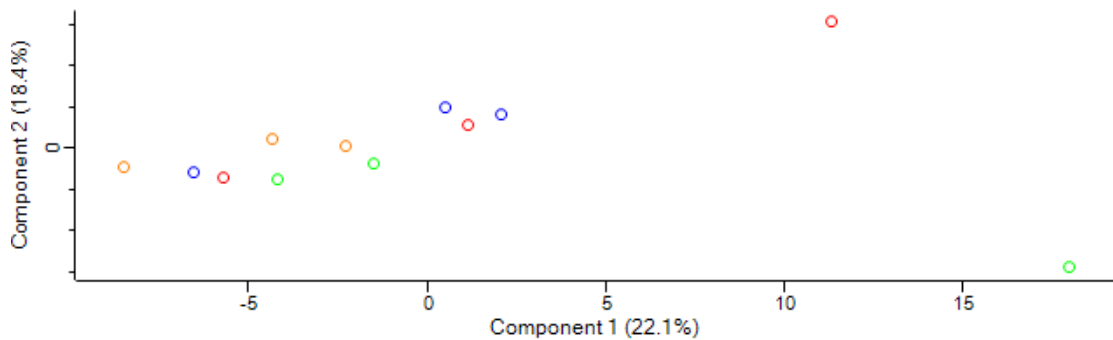
### **3. G: Profiler and REVIGO**

Functional enrichment analyses of differentially-expressed proteins were studied using g:Profiler (<https://biit.cs.ut.ee/gprofiler>), an online software system (Raudvere *et al.*, 2019). Protein validation was performed by a cumulative hypergeometric test with g:SCS (Set Counts and Sizes) correction, 64 method for multiple testing. Enriched terms obtained by g:Profiler were more summarised, reduced for redundant terms and visualised as a scatter plot using REVIGO (<http://revigo.irb.hr/>) (Supek *et al.*, 2011). Furthermore, default settings were applied for the REVIGO analysis.

Proteomics analysis of cytosolic extracts of hRPTE cells detected 725 proteins in all replicates of control and tRSV-HSP-treated cells, with no significant change between treatments. Meanwhile, the analysis of cytosolic extracts of MCs identified 1191 proteins in all replicates. The data indicated that high glucose incubations produced changes in 13 proteins identified, and upregulated proteins in HG treatment were linked to different cell functions such as cell morphology and the regulation of signal transduction pathways. The data showed that Glo1 inducer therapy upregulated antioxidant enzymes in MCs in LG conditions, with no significant upregulation or downregulation in HG conditions.

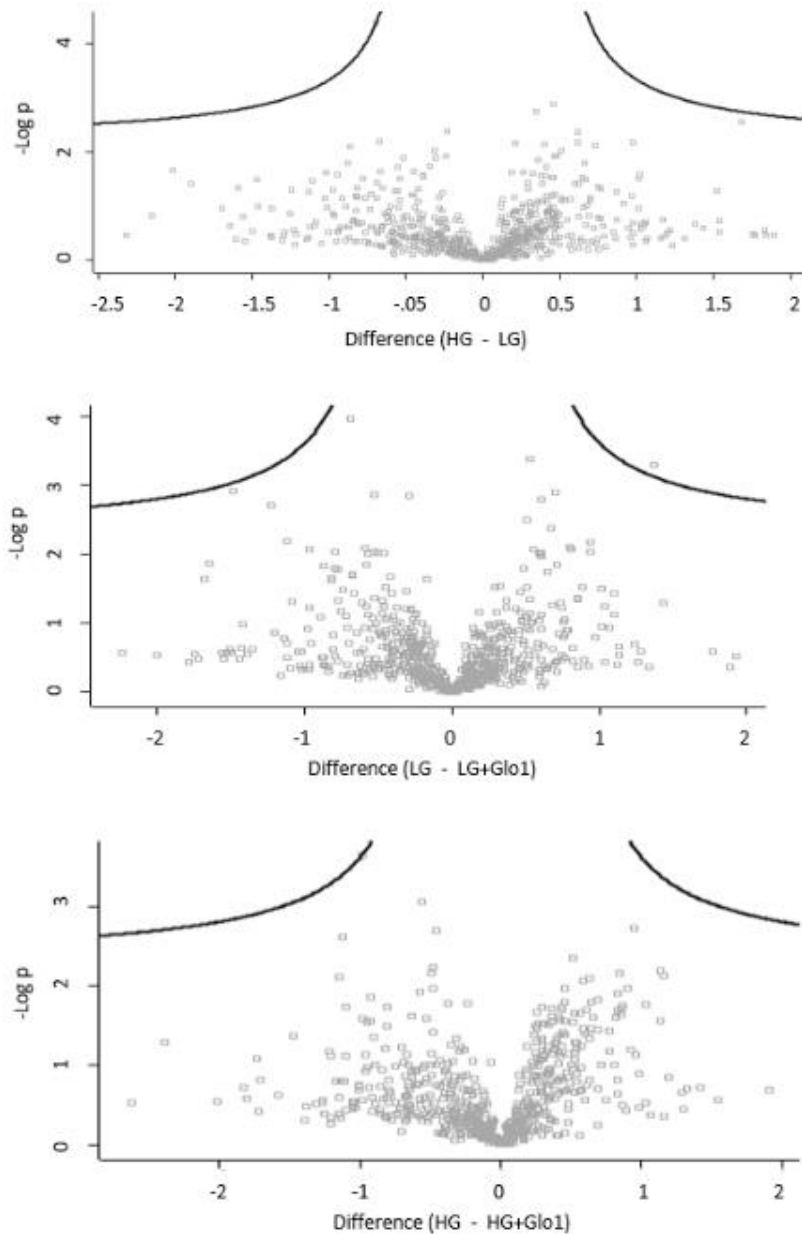
### 5.1.1 Studying the modification of cytosolic proteins in hRPTE: high mass resolution proteomics analysis

Proteomic analysis of primary hRPTE cells detected and resolved a total of 725 proteins in all replicates of cytoplasmic protein extract of control and tRSV-HSP-treated cells. This analysis detects proteins with limited total sequence coverage: the mean sequence coverage of proteins detected was 5.1%. Principal component analysis (PCA) was performed, to observe the clustering of gene expression data of different treatments (Figure 5.1). PCA is a statistical technique to visualise the variation present in a dataset with many variables.



**Figure 5.1: Principal component analysis (PCA) for all hRPTE cell samples.**

PCA shows the variance between the four conditions, low glucose 7.2 mM (green dots), low glucose + Glo1 inducer 10µM (blue dots), high glucose 25.00 mM (red dots), high glucose + Glo1 inducer 10µM (orange dots) incubated for 4 days. Data are expressed as mean  $\pm$  SD, n = 3.



**Figure 5.2: Comparison of protein profile of hRPTE cells cultured in low and high glucose conditions with and without Glo1 inducer *in vitro*.**

The Volcano plots (Figure 5.2) show differentially regulated proteins in response to Glo1 inducer and high glucose conditions. Human RPTE were cultured in medium containing 7.2 mM and 25.0 mM glucose with and without Glo1 inducer (10 $\mu$ M) for 4 days. Data are expressed as mean  $\pm$  SD, n = 3. Hyperbolic lines indicate the thresholds for statistical significance at  $P$  value  $< 0.05$ , above which any specific proteins (identified as each individual spots on the scatter) can be considered significantly differentially expressed. Proteins were quantified using label free quantitative mass spectrometry. Proteins were analysed by

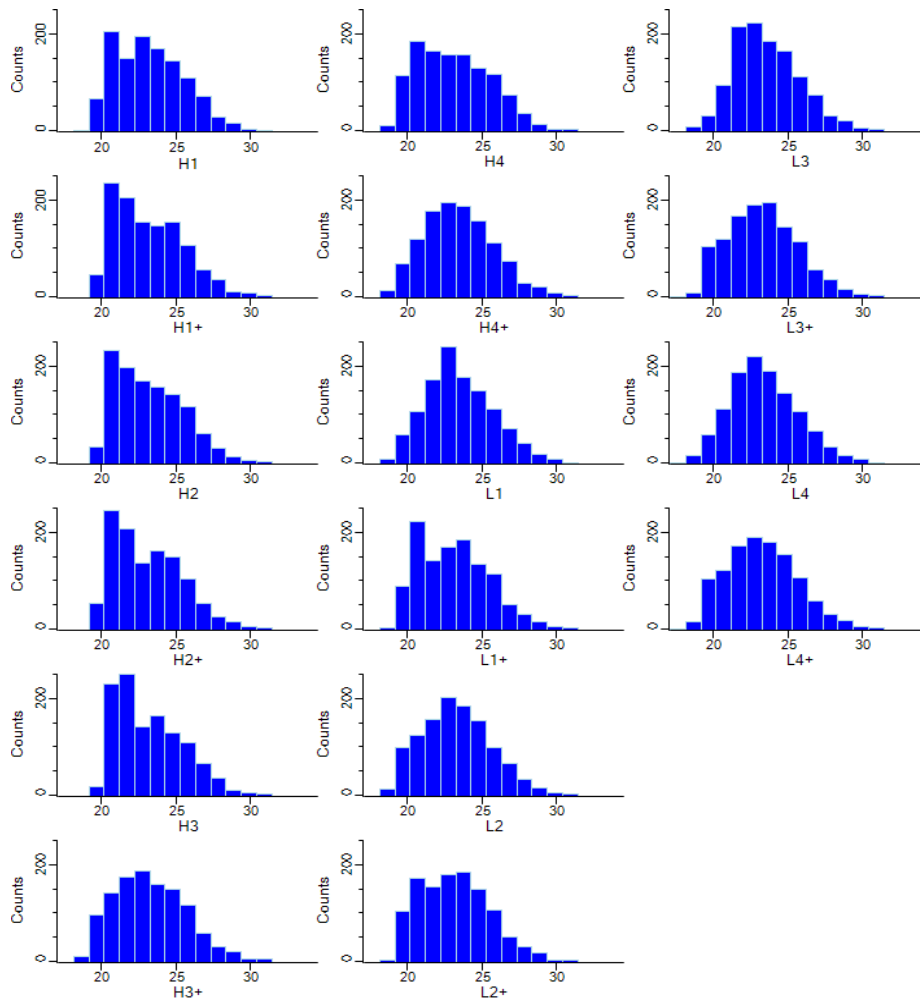


differentially expressed proteins (FDR) and significance (-Log p) using a false value of 0.05 and an S0 of 0.1. Proteins presented in grey did not reach statistical significance in change.

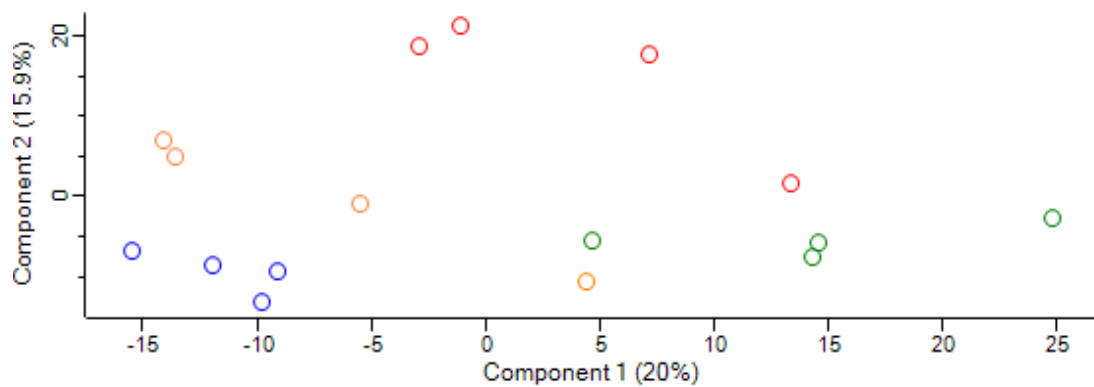
As seen in Figure 5.2, no protein species from the hRPTE cells were determined as being significantly differentially expressed between the treatments.

### **5.1.2 Studying the modification of cytosolic proteins in MCs: high mass resolution proteomics analysis**

Proteomic analysis of MCs identified 1191 protein species after filtering for valid values, and this number of proteins was used for the following analysis. Initially, data was subjected to normalisation by median value (Figure 5.3). Principal component analysis (PCA) was performed, to compute the variation of the data points distributed across the four groups of treatments (Figure 5.4). This Figure illustrates the variance between the four different treatments of MCs cultured in low and high glucose concentration, with and without the Glo1 inducer. PCA showed the largest variance between the two treatments of low glucose and low glucose+Glo1, in addition to the high degree of variance between high and low glucose treatment. However, there were no statistically significant differences between high glucose cultured cells treated with Glo1 inducer compared with high glucose without Glo1 inducer.



**Figure 5.3: Histograms of normalised protein abundance for all samples.**

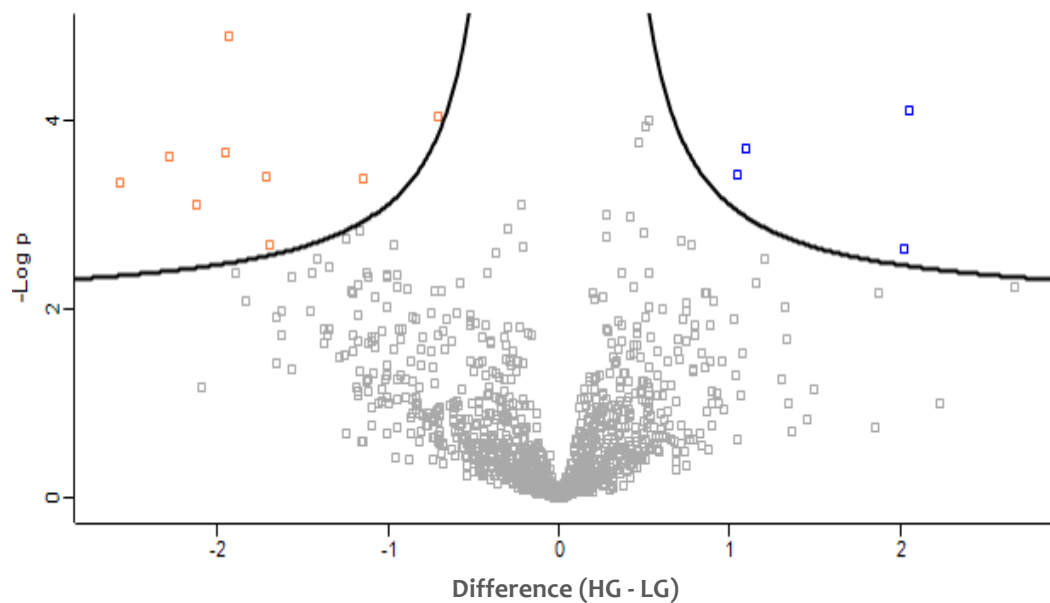


**Figure 5.4: Principal component analysis (PCA) for all MCs samples.**

PCA showed the variance between the four conditions, low glucose 5.5 mM (green dots), low glucose + Glo1 inducer 10  $\mu$ M (blue dots), high glucose 25 mM (red dots), high glucose + Glo1 inducer 10  $\mu$ M (orange dots) incubated for 4 days. Data are expressed as mean  $\pm$  SD, n = 4.

### 5.1.2.1 Differentially expressed proteins between low and high glucose cultures of MCs

The comparative analysis between low and high glucose treatment, demonstrated significantly differentially expressed protein species between the two conditions (Figure 5.5). Thirteen out of the 1191 detected proteins identified were changed significantly (FDR adjusted  $P$  value). This analysis detects proteins with limited total sequence coverage: the mean sequence coverage of proteins detected was 13.5%. Four proteins were up regulated in high glucose conditions ( $\log_2$  fold change  $\geq 1$ ), while nine cytosolic proteins were down regulated in MCs in high glucose ( $\log_2$  fold change  $\geq -1$ ). Pertinent proteins from these sets included Glutathione S-transferase Mu 1, an enzyme involved in the detoxification of electrophilic compounds, including carcinogens, environmental toxins, and products of oxidative stress, by conjugation with glutathione. A list of the down-regulated and up-regulated proteins are indicated in Table 5.3 and Table 5.4.

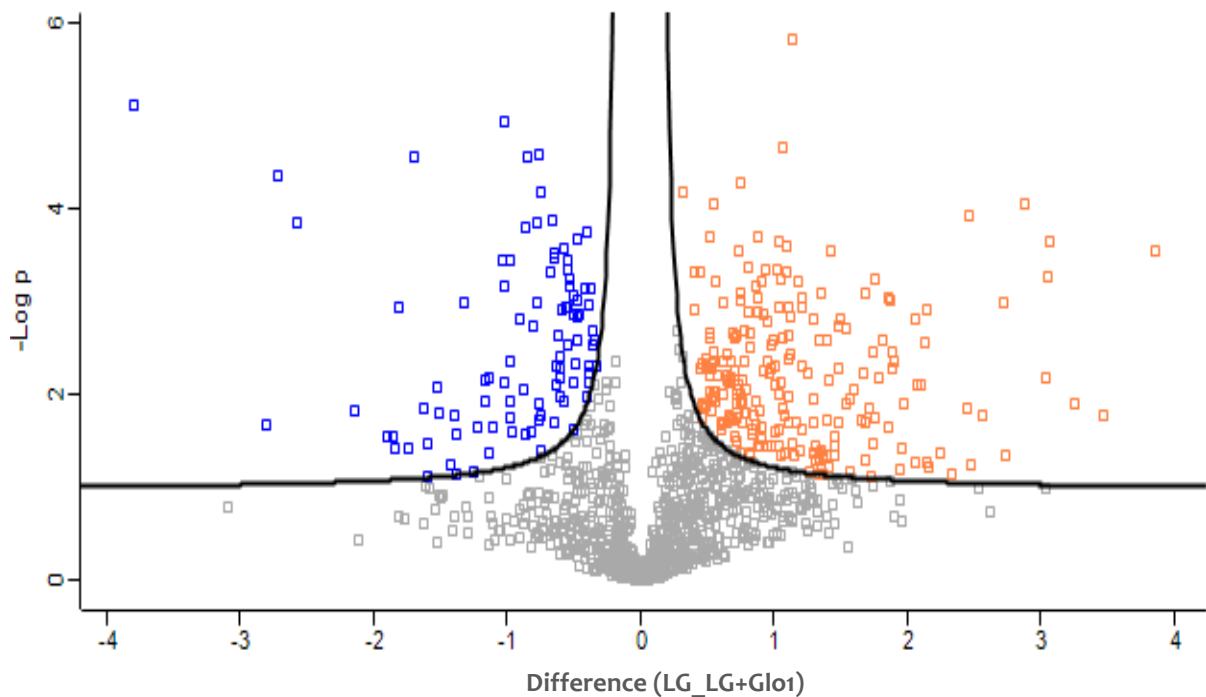


**Figure 5.5: Comparison of protein profiles from MCs cultured in low versus high glucose conditions *in vitro*.**

The above Volcano plot shows differentially-regulated proteins in response to the high glucose conditions. MCs were cultured in medium containing 5.5- and 25.0 mM glucose for 4 days. Data are mean  $\pm$  SD,  $n = 4$ . Proteins were quantified using label free quantitative mass spectrometry. Proteins were analysed by FDR and significance ( $-\log p$ ) determined using a false value of 0.05 and an  $S_0$  of 0.1. Proteins presented in blue are upregulated in high glucose culture while those in orange represent downregulated proteins. Proteins presented in grey did not reach statistical significance in change.

### 5.1.2.2 Differentially expressed proteins between Glo1 inducer treatment and controls in low glucose cultures of MCs

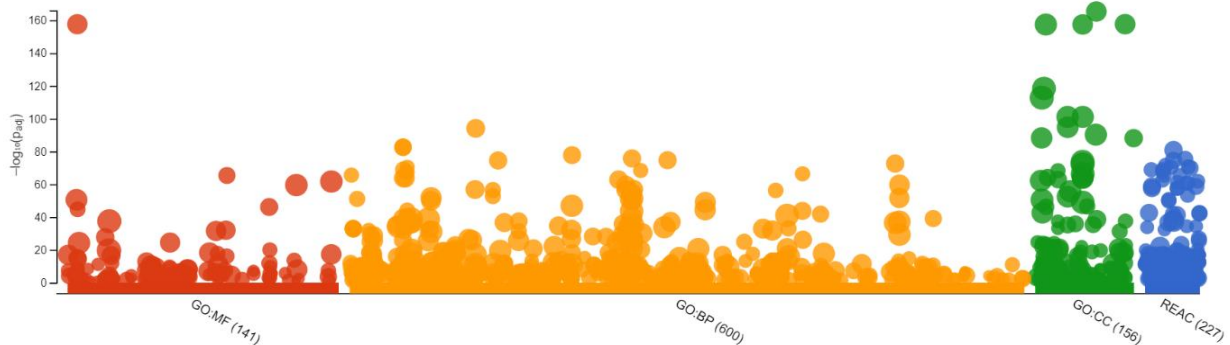
Ninety-six proteins were found to upregulated significantly in low glucose concentration cells treated with Glo1 inducer 10  $\mu$ M ( $\log_2$  fold change  $\geq -1$ ) compared with controls, while 225 proteins were down-regulated ( $\log_2$  fold change  $\geq 1$ ) (Figure 5.6). A list of the down- and upregulated proteins are indicated in Table 5.5 and Table 5.6.



**Figure 5.6: Comparison of protein profile of MCs cultured in low glucose condition with and without Glo1 inducer *in vitro*.**

The above Volcano plot shows differentially-regulated proteins in response to tRSV-HSP treatment. MCs were cultured in medium containing 5.5 mM glucose with and without tRSV-HSP (10 $\mu$ M) for 4 days and proteins were quantified using label free quantitative mass spectrometry. Proteins were analysed by FDR and statistical significance ( $-\log p$ ) was determined using a false value of 0.05 and an S0 of 0.1. Proteins presented in blue are upregulated) and orange are downregulated. Proteins presented in grey did not reach statistical significance in change.

Functional enrichment analysis of differentially expressed proteins was performed using g:Profiler (Figure 5.7). Using one of the comprehensive methods for interpreting the gene list, g:GOST. Data were provided from multiple sources such as: Gene Ontology (GO) Metabolic Function (MF), GO Biological Processes (BP), GO Cell Components (CC) and Reactome datasets – see Table 5.1.




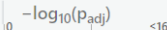
**Figure 5.7: Manhattan plot of Functional Enrichment Analysis of differentially expressed cytosolic proteins from MCs.**

Differentially expressed proteins were subjected to g:Profiler analysis. The software used Gene Ontology (GO) Metabolic Function (MF), GO Biological Processes (BP), GO Cell Components (CC) and Reactome datasets for the analysis, with each dataset being colour coded. The Manhattan plot showed that in GO:MF 141 terms were significantly enriched (dark red dots), in GO:BP 600 terms (dark yellow dots), and in GO:CC 156 terms (dark green dots). A set of 227 terms were significantly enriched in the Reactome data source. Each dot represents a single functional term and is size scaled according to the number of annotated genes in that term. The lighter coloured dots represent insignificant terms.


**Table 5.1: Functional enrichment analysis of differentially expressed proteins in MCs**

The top enriched functional analysis terms from the following data sources – GO:MO (A), GO:BF (B), GO:CC (C) and Reactome (D) – each term is shown with its ID and the associated adjusted *P* value. The *P* values in the table outputs are presented by a colour gradient scheme: yellow (insignificant) to purple/blue (highly significant).


**A) Gene ontology: Molecular Function**

Term name	Term ID	 P <sub>adj</sub>	
RNA binding	GO:0003723	$2.210 \times 10^{-158}$	
cadherin binding	GO:0045296	$4.380 \times 10^{-66}$	
heterocyclic compound binding	GO:1901363	$2.174 \times 10^{-62}$	
organic cyclic compound binding	GO:0097159	$3.147 \times 10^{-60}$	
nucleic acid binding	GO:0003676	$3.080 \times 10^{-51}$	
cell adhesion molecule binding	GO:0050839	$7.408 \times 10^{-47}$	
protein-containing complex binding	GO:0044877	$1.127 \times 10^{-32}$	
identical protein binding	GO:0042802	$3.038 \times 10^{-32}$	
structural molecule activity	GO:0005198	$1.926 \times 10^{-28}$	
enzyme binding	GO:0019899	$3.774 \times 10^{-25}$	
catalytic activity	GO:0003824	$6.318 \times 10^{-25}$	
small molecule binding	GO:0036094	$5.583 \times 10^{-19}$	
nucleoside phosphate binding	GO:1901265	$5.688 \times 10^{-18}$	
nucleotide binding	GO:0000166	$1.137 \times 10^{-17}$	
cytoskeletal protein binding	GO:0008092	$2.949 \times 10^{-17}$	
mRNA binding	GO:0003729	$1.005 \times 10^{-15}$	
actin binding	GO:0003779	$4.572 \times 10^{-15}$	
oxidoreductase activity	GO:0016491	$1.542 \times 10^{-13}$	
anion binding	GO:0043168	$1.660 \times 10^{-11}$	
hydrolase activity	GO:0016787	$4.094 \times 10^{-11}$	
purine nucleotide binding	GO:0017076	$6.918 \times 10^{-10}$	
purine ribonucleotide binding	GO:0032555	$7.434 \times 10^{-9}$	
ribonucleotide binding	GO:0032553	$8.989 \times 10^{-9}$	
carbohydrate derivative binding	GO:0097367	$1.313 \times 10^{-8}$	
protein domain specific binding	GO:0019904	$2.356 \times 10^{-8}$	
pyrophosphatase activity	GO:0016462	$3.417 \times 10^{-8}$	
ubiquitin-like protein ligase binding	GO:0044389	$3.522 \times 10^{-8}$	
hydrolase activity, acting on acid anhydrides, in phosphorus-containing anhydrides	GO:0016818	$4.459 \times 10^{-8}$	

## B) Gene ontology: Biological Processes


Term name	Term ID		P <sub>adj</sub>	$-\log_{10}(P_{adj})$
mRNA metabolic process	GO:0016071		$8.181 \times 10^{-95}$	
mRNA catabolic process	GO:0006402		$1.852 \times 10^{-83}$	
RNA catabolic process	GO:0006401		$3.280 \times 10^{-83}$	
nucleobase-containing compound catabolic process	GO:0034655		$1.668 \times 10^{-78}$	
cellular nitrogen compound catabolic process	GO:0044270		$1.712 \times 10^{-76}$	
heterocycle catabolic process	GO:0046700		$2.106 \times 10^{-75}$	
aromatic compound catabolic process	GO:0019439		$3.116 \times 10^{-75}$	
organic cyclic compound catabolic process	GO:1901361		$2.348 \times 10^{-73}$	
translation	GO:0006412		$1.566 \times 10^{-64}$	
peptide metabolic process	GO:0006518		$1.754 \times 10^{-64}$	
peptide biosynthetic process	GO:0043043		$1.642 \times 10^{-63}$	
organic substance catabolic process	GO:1901575		$2.018 \times 10^{-60}$	
cellular amide metabolic process	GO:0043603		$4.854 \times 10^{-60}$	
biological process involved in symbiotic interaction	GO:0044403		$1.127 \times 10^{-57}$	
viral process	GO:0016032		$1.626 \times 10^{-57}$	
amide biosynthetic process	GO:0043604		$3.808 \times 10^{-57}$	
cellular catabolic process	GO:0044248		$5.950 \times 10^{-55}$	
catabolic process	GO:0009056		$1.173 \times 10^{-52}$	
organonitrogen compound biosynthetic process	GO:1901566		$2.438 \times 10^{-52}$	
cellular macromolecule catabolic process	GO:0044265		$6.094 \times 10^{-51}$	
macromolecule catabolic process	GO:0009057		$1.236 \times 10^{-50}$	
establishment of localization in cell	GO:0051649		$1.053 \times 10^{-49}$	
cellular nitrogen compound metabolic process	GO:0034641		$1.306 \times 10^{-47}$	
cellular localization	GO:0051641		$3.737 \times 10^{-45}$	
establishment of protein localization to organelle	GO:0072594		$1.839 \times 10^{-44}$	
establishment of protein localization to membrane	GO:0090150		$1.710 \times 10^{-42}$	
protein targeting	GO:0006605		$5.709 \times 10^{-41}$	
small molecule metabolic process	GO:0044281		$1.590 \times 10^{-40}$	

### C) Gene Ontology: Cellular Component

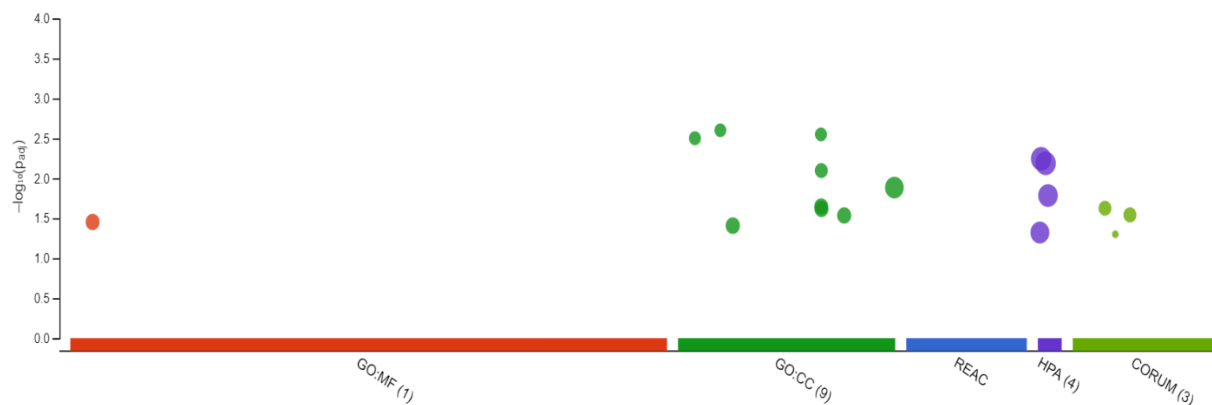
Term name	Term ID		P <sub>adj</sub>	$-\log_{10}(P_{adj})$
extracellular exosome	GO:0070062		$4.043 \times 10^{-166}$	
extracellular vesicle	GO:1903561		$2.126 \times 10^{-158}$	
extracellular organelle	GO:0043230		$3.179 \times 10^{-158}$	
cytosol	GO:0005829		$3.460 \times 10^{-158}$	
membrane-enclosed lumen	GO:0031974		$8.290 \times 10^{-102}$	
organelle lumen	GO:0043233		$8.290 \times 10^{-102}$	
vesicle	GO:0031982		$1.714 \times 10^{-95}$	
intracellular organelle lumen	GO:0070013		$5.588 \times 10^{-91}$	
extracellular space	GO:0005615		$5.498 \times 10^{-89}$	
ribonucleoprotein complex	GO:1990904		$7.458 \times 10^{-89}$	
focal adhesion	GO:0005925		$8.987 \times 10^{-65}$	
intracellular non-membrane-bounded organelle	GO:0043232		$9.614 \times 10^{-65}$	
non-membrane-bounded organelle	GO:0043228		$1.736 \times 10^{-64}$	
cell-substrate junction	GO:0030055		$1.475 \times 10^{-63}$	
extracellular region	GO:0005576		$6.736 \times 10^{-63}$	
protein-containing complex	GO:0032991		$1.612 \times 10^{-56}$	
nuclear lumen	GO:0031981		$3.902 \times 10^{-53}$	
nucleus	GO:0005634		$3.660 \times 10^{-51}$	
nucleoplasm	GO:0005654		$2.760 \times 10^{-43}$	
anchoring junction	GO:0070161		$2.852 \times 10^{-39}$	
secretory granule lumen	GO:0034774		$1.419 \times 10^{-36}$	
cytoplasmic vesicle lumen	GO:0060205		$4.457 \times 10^{-36}$	
vesicle lumen	GO:0031983		$7.841 \times 10^{-36}$	
nucleolus	GO:0005730		$9.318 \times 10^{-23}$	
secretory granule	GO:0030141		$7.177 \times 10^{-22}$	
supramolecular complex	GO:0099080		$9.962 \times 10^{-22}$	
cell junction	GO:0030054		$2.021 \times 10^{-20}$	
actin cytoskeleton	GO:0015629		$4.011 \times 10^{-20}$	



## D) Reactome

Term name	Term ID	 P <sub>adj</sub>	$-\log_{10}(P_{adj})$
Metabolism of RNA	REAC:R-HSA-89...	$1.352 \times 10^{-81}$	
Metabolism of amino acids and derivatives	REAC:R-HSA-71...	$2.658 \times 10^{-75}$	
Cellular responses to stress	REAC:R-HSA-22...	$1.766 \times 10^{-59}$	
Translation	REAC:R-HSA-72...	$2.283 \times 10^{-59}$	
Cellular responses to external stimuli	REAC:R-HSA-89...	$2.530 \times 10^{-58}$	
Axon guidance	REAC:R-HSA-42...	$2.565 \times 10^{-43}$	
Nervous system development	REAC:R-HSA-96...	$6.644 \times 10^{-42}$	
Metabolism	REAC:R-HSA-14...	$6.040 \times 10^{-39}$	
Metabolism of proteins	REAC:R-HSA-39...	$7.079 \times 10^{-38}$	
Infectious disease	REAC:R-HSA-56...	$1.640 \times 10^{-37}$	
Disease	REAC:R-HSA-16...	$1.006 \times 10^{-22}$	
Neutrophil degranulation	REAC:R-HSA-67...	$5.339 \times 10^{-20}$	
Developmental Biology	REAC:R-HSA-12...	$8.968 \times 10^{-15}$	
M Phase	REAC:R-HSA-68...	$3.931 \times 10^{-12}$	
Innate Immune System	REAC:R-HSA-16...	$3.433 \times 10^{-11}$	
Cell Cycle, Mitotic	REAC:R-HSA-69...	$2.307 \times 10^{-10}$	
Cell Cycle	REAC:R-HSA-16...	$1.328 \times 10^{-9}$	
Cell Cycle Checkpoints	REAC:R-HSA-69...	$9.998 \times 10^{-9}$	
RHO GTPase Effectors	REAC:R-HSA-19...	$6.123 \times 10^{-7}$	
Signaling by Interleukins	REAC:R-HSA-44...	$1.450 \times 10^{-6}$	
Metabolism of carbohydrates	REAC:R-HSA-71...	$1.565 \times 10^{-5}$	
MAPK family signaling cascades	REAC:R-HSA-56...	$3.435 \times 10^{-5}$	
Signaling by WNT	REAC:R-HSA-19...	$3.664 \times 10^{-5}$	
Diseases of signal transduction by growth factor recep...	REAC:R-HSA-56...	$1.237 \times 10^{-4}$	
Membrane Trafficking	REAC:R-HSA-19...	$2.464 \times 10^{-4}$	
Deubiquitination	REAC:R-HSA-56...	$5.259 \times 10^{-4}$	
Post-translational protein modification	REAC:R-HSA-59...	$6.959 \times 10^{-4}$	
Vesicle-mediated transport	REAC:R-HSA-56...	$1.628 \times 10^{-3}$	

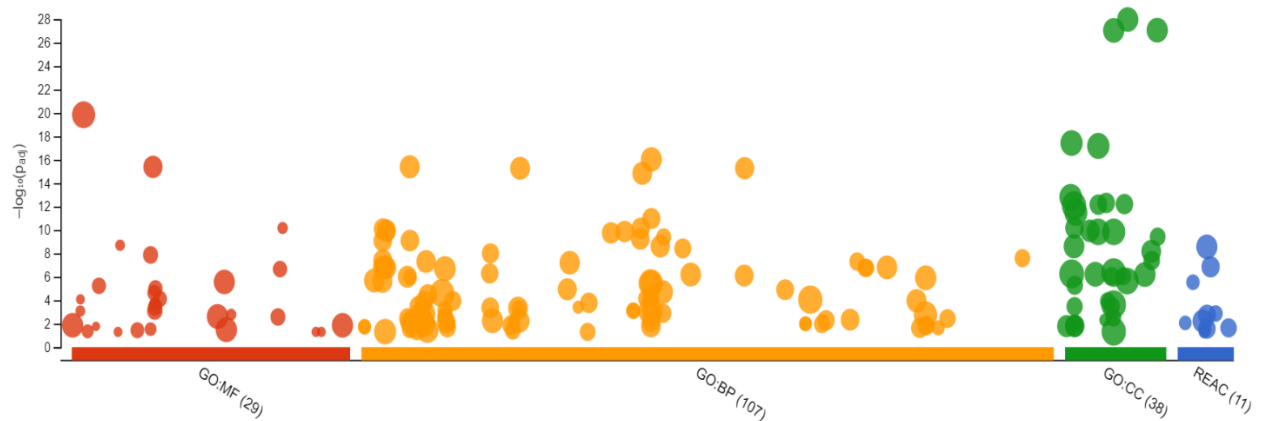
Differentially expressed proteins in HG compared with normal LG treatment showed 17 significantly enriched terms in GO:MF, relating to translation initiation factor activity (GO:0003743). In GO:CC there were 9 categories to be enriched with the three top terms being: eukaryotic 43S preinitiation complex (GO:0016282), translation preinitiation complex (GO:0070993) and U2 snRNP (GO:0005686). Human Protein Atlas (HPA) showed 4 significant enriched terms including: cerebellum; Purkinje cells [High] (HPA:0090163), epididymis; glandular cells [High] (HPA:0180053) and hippocampus; neuronal cells [High] (HPA:0250133). In CORUM, three terms were enriched, which are CDC5L complex (CORUM:1183), 17S U2 snRNP (CORUM:2755) and BANF1 homodimer protein (CORUM:1989)-Figure 5.8.



**Figure 5.8: Manhattan plot of Functional enrichment analysis of downregulated proteins of MCs in hyperglycaemia.**

Differentially expressed proteins were subjected to g:Profiler analysis. The software used Gene Ontology (GO) Metabolic Function (MF), GO Biological Processes (BP), GO Cell Components (CC), Human Protein Atlas (HPA), Comprehensive Resource of Mammalian Protein Complexes (CORUM) and Reactome datasets (REAC) for the analysis, with each dataset being colour coded. The Manhattan plot showed that in GO:MF, a single term was significantly enriched (dark red dots), in GO:CC 9 terms (dark green dots), in HPA 4 terms, and 3 terms were significantly enriched in the CORUM. Each dot represents a single functional term and is size scaled according to the number of annotated genes in that term. The lighter coloured dots represent insignificant terms.

Differentially expressed proteins in Glo1 inducer treatment showed 29 significantly enriched terms in GO:MF, with the most significant terms being catalytic activity (GO:0003824), oxidoreductase activity (GO:0016491) and peroxiredoxin activity (GO:0051920). In GO:BP, 107 terms were significantly enriched including small molecule metabolic process (GO:0044281), organic acid metabolic process (GO:0006082) and oxidation-reduction process (GO:0055114). GO:CC reported 38 categories that were enriched with extracellular exosomes (GO:0070062), extracellular vesicles (GO:1903561) and extracellular organelle (GO:0043230) and being the top three – see Figure 5.9. In the Reactome database, 11 terms were enriched, with the most significantly enriched terms including Metabolism (REAC:R-HSA-1430728), neutrophil degranulation (REAC:R-HAS-6798695) and the detoxification of reactive oxygen species (REAC:R-HSA-3299685) – see Table 5.2.



**Figure 5.9: Manhattan plot of Functional enrichment analysis of differentially expressed proteins of MCs treated by Glo1 inducer**


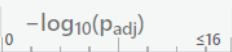
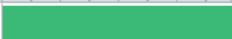



























Differentially expressed proteins were subjected to g:Profiler analysis. The software used Gene Ontology (GO) Metabolic Function (MF), GO Biological Processes (BP), GO Cell Components (CC) and Reactome datasets (REAC) for the analysis, with each dataset being colour coded. The Manhattan plot showed that in GO:MF 29 terms were significantly enriched (dark red dots), in GO:BP 107 terms (dark yellow dots), and in GO:CC 38 terms (dark green dots). 11 terms were significantly enriched in the Reactome data source. Each dot represents a single functional term and is size scaled according to the number of annotated genes in that term. The lighter coloured dots represent insignificant terms.

**Table 5.2: Functional enrichment analysis of differentially expressed proteins in MCs treated by Glo1 inducer.**

**A) Gene ontology: Molecular Function**

Term name	Term ID	Padj	$-\log_{10}(P_{adj})$
catalytic activity	GO:0003824	$1.416 \times 10^{-20}$	20.05
oxidoreductase activity	GO:0016491	$4.007 \times 10^{-16}$	15.80
peroxiredoxin activity	GO:0051920	$6.643 \times 10^{-11}$	10.82
thioredoxin peroxidase activity	GO:0008379	$1.979 \times 10^{-9}$	8.71
antioxidant activity	GO:0016209	$1.331 \times 10^{-8}$	7.88
NAD binding	GO:0051287	$2.141 \times 10^{-7}$	6.67
identical protein binding	GO:0042802	$2.687 \times 10^{-6}$	5.57
peroxidase activity	GO:0004601	$5.785 \times 10^{-6}$	5.24
oxidoreductase activity, acting on peroxide as acceptor	GO:0016684	$9.760 \times 10^{-6}$	5.01
oxidoreductase activity, acting on the aldehyde or oxo group of donors, NAD or NADP as acceptor	GO:0016620	$2.308 \times 10^{-5}$	4.63
oxidoreductase activity, acting on the aldehyde or oxo group of donors	GO:0016903	$7.579 \times 10^{-5}$	4.22
purine nucleobase binding	GO:0002060	$8.256 \times 10^{-5}$	4.19
oxidoreductase activity, acting on a sulfur group of donors, NAD(P) as acceptor	GO:0016668	$1.950 \times 10^{-4}$	3.71
oxidoreductase activity, acting on a sulfur group of donors	GO:0016667	$3.826 \times 10^{-4}$	3.42
oxidoreductase activity, acting on NAD(P)H	GO:0016651	$7.833 \times 10^{-4}$	3.11
nucleobase binding	GO:0002054	$8.195 \times 10^{-4}$	3.09
glyceraldehyde-3-phosphate dehydrogenase (NAD+) (non-phosphorylating) activity	GO:0043878	$1.633 \times 10^{-3}$	2.79
small molecule binding	GO:0036094	$2.412 \times 10^{-3}$	2.61
flavin adenine dinucleotide binding	GO:0050660	$2.626 \times 10^{-3}$	2.58
nucleotide binding	GO:0000166	$1.345 \times 10^{-2}$	1.87
nucleoside phosphate binding	GO:1901265	$1.356 \times 10^{-2}$	1.86
isocitrate dehydrogenase (NADP+) activity	GO:0004450	$1.659 \times 10^{-2}$	1.78
AMP binding	GO:0016208	$2.886 \times 10^{-2}$	1.54
anion binding	GO:0043168	$3.217 \times 10^{-2}$	1.49
disulfide oxidoreductase activity	GO:0015036	$3.563 \times 10^{-2}$	1.45
aldehyde dehydrogenase (NAD+) activity	GO:0004029	$4.407 \times 10^{-2}$	1.35
linear malto-oligosaccharide phosphorylase activity	GO:0102250	$4.962 \times 10^{-2}$	1.30
SHG alpha-glucan phosphorylase activity	GO:0102499	$4.962 \times 10^{-2}$	1.30


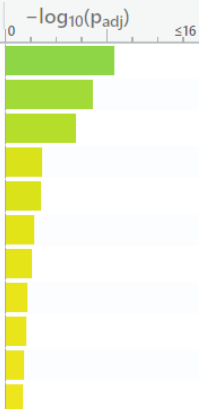











## B) Gene ontology: Biological Processes

Term name	Term ID 	P <sub>adj</sub>	$-\log_{10}(P_{adj})$ 
small molecule metabolic process	GO:0044281	$9.246 \times 10^{-17}$	
organic acid metabolic process	GO:0006082	$3.941 \times 10^{-16}$	
oxidation-reduction process	GO:0055114	$5.225 \times 10^{-16}$	
carboxylic acid metabolic process	GO:0019752	$5.300 \times 10^{-16}$	
oxoacid metabolic process	GO:0043436	$1.415 \times 10^{-15}$	
small molecule catabolic process	GO:0044282	$1.037 \times 10^{-11}$	
neutrophil degranulation	GO:0043312	$7.075 \times 10^{-11}$	
neutrophil activation involved in immune response	GO:0002283	$7.984 \times 10^{-11}$	
myeloid leukocyte mediated immunity	GO:0002444	$1.038 \times 10^{-10}$	
neutrophil mediated immunity	GO:0002446	$1.235 \times 10^{-10}$	
neutrophil activation	GO:0042119	$1.335 \times 10^{-10}$	
granulocyte activation	GO:0036230	$1.750 \times 10^{-10}$	
cell redox homeostasis	GO:0045454	$3.912 \times 10^{-10}$	
leukocyte degranulation	GO:0043299	$5.729 \times 10^{-10}$	
generation of precursor metabolites and energy	GO:0006091	$7.883 \times 10^{-10}$	
myeloid cell activation involved in immune response	GO:0002275	$8.165 \times 10^{-10}$	
regulated exocytosis	GO:0045055	$2.411 \times 10^{-9}$	
carboxylic acid catabolic process	GO:0046395	$3.691 \times 10^{-9}$	
organic acid catabolic process	GO:0016054	$9.655 \times 10^{-9}$	
cellular detoxification	GO:1990748	$2.526 \times 10^{-8}$	
myeloid leukocyte activation	GO:0002274	$3.890 \times 10^{-8}$	
exocytosis	GO:0006887	$4.799 \times 10^{-8}$	
cellular response to toxic substance	GO:0097237	$4.899 \times 10^{-8}$	
secretion by cell	GO:0032940	$6.159 \times 10^{-8}$	
leukocyte activation involved in immune response	GO:0002366	$1.328 \times 10^{-7}$	
cell activation involved in immune response	GO:0002263	$1.472 \times 10^{-7}$	
export from cell	GO:0140352	$1.534 \times 10^{-7}$	
detoxification	GO:0098754	$1.636 \times 10^{-7}$	

### C) Gene Ontology: Cellular Component

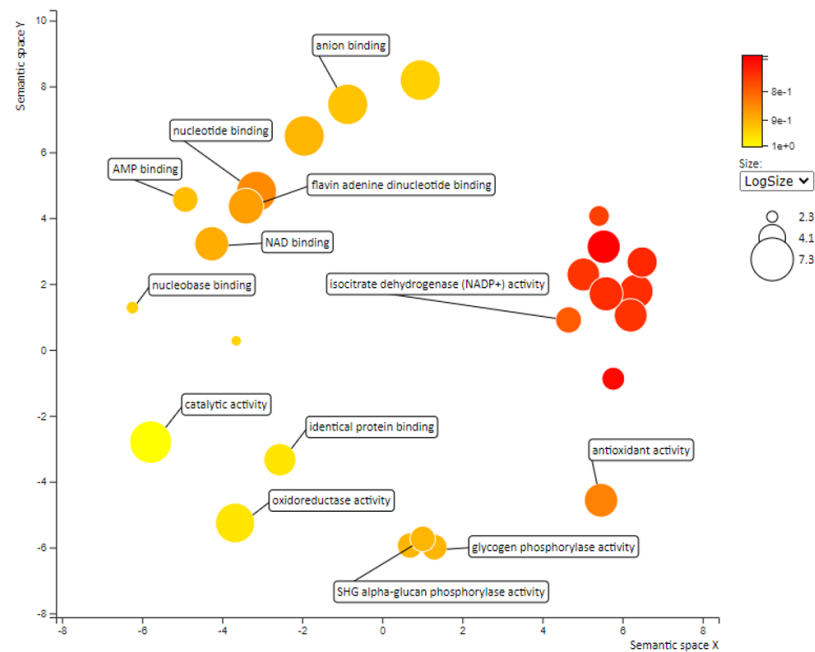
Term name	Term ID	P <sub>adj</sub>	$-\log_{10}(P_{adj})$
extracellular exosome	GO:0070062	$1.050 \times 10^{-28}$	28.0
extracellular vesicle	GO:1903561	$8.509 \times 10^{-28}$	27.1
extracellular organelle	GO:0043230	$8.924 \times 10^{-28}$	27.0
extracellular space	GO:0005615	$3.705 \times 10^{-18}$	17.4
vesicle	GO:0031982	$6.534 \times 10^{-18}$	17.2
extracellular region	GO:0005576	$1.515 \times 10^{-13}$	13.8
secretory granule lumen	GO:0034774	$4.825 \times 10^{-13}$	12.8
cytoplasmic vesicle lumen	GO:0060205	$6.059 \times 10^{-13}$	12.7
vesicle lumen	GO:0031983	$6.781 \times 10^{-13}$	12.6
cytosol	GO:0005829	$3.241 \times 10^{-12}$	11.5
mitochondrial matrix	GO:0005759	$6.505 \times 10^{-11}$	10.5
secretory granule	GO:0030141	$1.162 \times 10^{-10}$	10.0
membrane-enclosed lumen	GO:0031974	$1.413 \times 10^{-10}$	9.8
organelle lumen	GO:0043233	$1.413 \times 10^{-10}$	9.8
ficolin-1-rich granule lumen	GO:1904813	$3.721 \times 10^{-10}$	9.4
mitochondrion	GO:0005739	$2.440 \times 10^{-9}$	8.6
secretory vesicle	GO:0099503	$6.562 \times 10^{-9}$	8.2
ficolin-1-rich granule	GO:0101002	$4.003 \times 10^{-8}$	7.4
cytoplasmic vesicle	GO:0031410	$5.914 \times 10^{-7}$	6.8
intracellular vesicle	GO:0097708	$6.180 \times 10^{-7}$	6.7
melanosome	GO:0042470	$8.571 \times 10^{-7}$	6.6
pigment granule	GO:0048770	$8.571 \times 10^{-7}$	6.6
intracellular organelle lumen	GO:0070013	$2.291 \times 10^{-6}$	6.0
vacuolar lumen	GO:0005775	$5.236 \times 10^{-6}$	5.3
azurophil granule lumen	GO:0035578	$1.166 \times 10^{-4}$	3.9
azurophil granule	GO:0042582	$3.352 \times 10^{-4}$	3.5
primary lysosome	GO:0005766	$3.352 \times 10^{-4}$	3.5
lysosomal lumen	GO:0043202	$2.993 \times 10^{-3}$	3.2

## D) Reactome

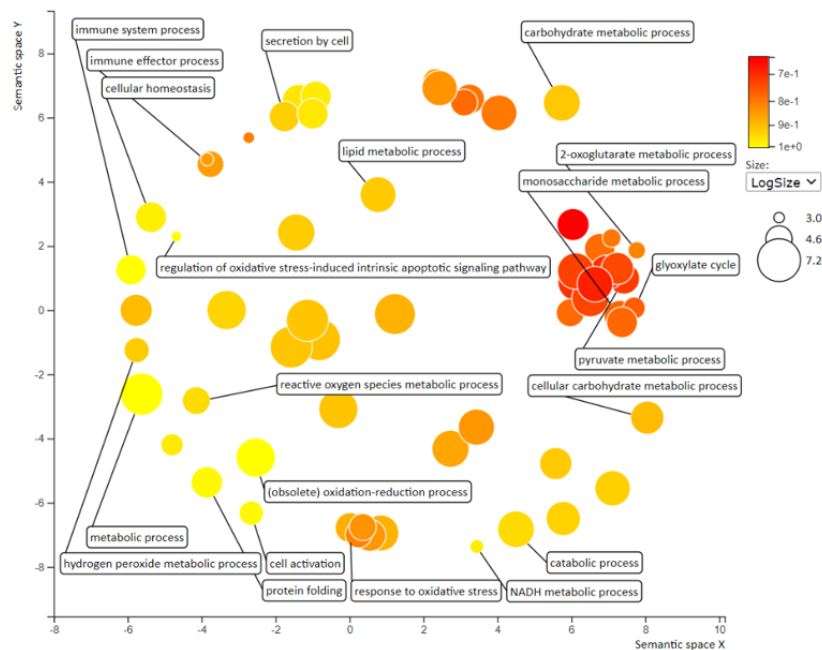
Term name	Term ID	 P <sub>adj</sub>	
			0 $-\log_{10}(P_{adj})$ $\leq 16$
Metabolism	REAC:R-HSA-1430728	$2.659 \times 10^{-9}$	
Neutrophil degranulation	REAC:R-HSA-6798695	$1.365 \times 10^{-7}$	
Detoxification of Reactive Oxygen Species	REAC:R-HSA-3299685	$2.836 \times 10^{-6}$	
Pyruvate metabolism and Citric Acid (TCA) cycle	REAC:R-HSA-71406	$1.335 \times 10^{-3}$	
Metabolism of amino acids and derivatives	REAC:R-HSA-71291	$1.768 \times 10^{-3}$	
Innate Immune System	REAC:R-HSA-168249	$5.854 \times 10^{-3}$	
Citric acid cycle (TCA cycle)	REAC:R-HSA-71403	$8.439 \times 10^{-3}$	
The citric acid (TCA) cycle and respiratory electron transport	REAC:R-HSA-1428517	$2.238 \times 10^{-2}$	
Metabolism of carbohydrates	REAC:R-HSA-71387	$2.590 \times 10^{-2}$	
Lysine catabolism	REAC:R-HSA-71064	$3.578 \times 10^{-2}$	
Keratan sulfate degradation	REAC:R-HSA-2022857	$4.625 \times 10^{-2}$	

The output (data) analysed by g:Profiler were then subjected to REVIGO analysis to facilitate interpretation through reducing redundancy, to obtain and summarise significantly enriched GO terms. The results then are shown on a scatter plot for identifying related GO terms based on how closely sets of points clusters together. In Glo1 inducer treatment, REVIGO analysis of enriched terms from the GO:MF dataset revealed that major clusters were catalytic activity, oxidoreductase activity and peroxiredoxin activity (Figure 5.10A). Analysis of enriched terms from the GO:BP dataset revealed the following main clusters: small molecule metabolic process, organic acid metabolic process and oxidation-reduction process (Figure 5.10B).

### A) GO:MF terms enriched in Glo1 inducer



### B) GO: BP terms enriched in Glo1 inducer



**Figure 5.10: GO enrich terms in MCs treated by Glo1 inducer summarised by REVIGO.**

Concise presentation of (A) GO:MF and (B) GO: BP terms enriched in MCs treated by Glo1 inducer treatment. Similarities on the scatter plot reflect their closeness in the GO semantic similarity. Circle colour corresponds to the significance obtained using g:Profiler, while the size indicates the frequency of the GO term in the GOA database (circles of more general terms are larger).



**Table 5.3: Proteins in the cytoplasmic extract increased significantly in abundance in MCs by treatment with high glucose concentration.**

<b>Protein accession number</b>	<b>Protein name</b>	<b>Gene name</b>	<b>Unique peptide</b>	<b>Percentage sequence coverage</b>	<b>Fold increase</b>
P08134	RHO related GTP-binding protein	RHOC	5	49.2	1.10
P63313	Thymosin Beta 10	TMSB10	9	97.7	1.08
O60256	Phosphoribosyl Pyrophosphate Synthetase Associated Protein 2	PRPSAP2	4	32.2	1.05
P28072	Proteasome Subunit Beta type-6	PSMB6	7	21.3	1.05

Data are mean  $\pm$  SD, n = 4.

**Table 5.4: Proteins in the cytoplasmic extract decreased significantly in abundance in MCs by treatment with high glucose concentration.**

<b>Protein accession number</b>	<b>Protein name</b>	<b>Gene name</b>	<b>Unique peptide</b>	<b>Percentage sequence coverage</b>	<b>Fold decrease</b>
O75531	Barrier to autointegration factor 1	BANF1	7	68.5	0.879
Q06323	Proteasome activator complex subunit 1	PSME1	12	53.8	0.885
P09488	Glutathione S-transferase Mu 1	GSTM1	1	44.0	0.900
Q14257	Reticulocalbin 2	RCN2	12	42.6	0.904
P41567	Eukaryotic translation initiation factor 1	EIF1	1	41.3	0.906
P09661	U2 small nuclear ribonucleoprotein A	SNRPA1	5	33.3	0.907
O75821	Eukaryotic translation initiation factor 3 subunit G	EIF3G	0	30.6	0.914
P62805	Histone H4	HIST1H4A	17	81.6	0.948
P62316	Small nuclear ribonucleoprotein Sm D2	SNRPD2	8	61.9	0.974

Data are mean  $\pm$  SD, n = 4.

**Table 5.5: Cytosolic proteins upregulated significantly in MCs treated by Glo1 inducer in normal glucose condition.**

<b>Protein accession number</b>	<b>Protein name</b>	<b>Gene name</b>	<b>Unique peptide</b>	<b>Percentage sequence coverage</b>	<b>Fold increase</b>
P07602	Prosaposin	PSAP	10	22.3	1.19
Q8IV08	Phospholipase D3	PLD3	7	21.2	1.14
Q9UBR2	Cathepsin Z	CTSZ	29	45.7	1.14
P22570	NADPH:adrenodoxin oxidoreductase, mitochondrial	FDXR	11	39.7	1.12
O95810	Serum deprivation-response protein	SDPR	10	31.1	1.10
P06737	Glycogen phosphorylase	PYGL	34	45.3	1.09
Q13011	Delta (3,5)-Delta (2,4)-dienoyl-CoA isomerase, mitochondrial	ECH1	6	23.8	1.09
P12277	Creatine kinase B-type	CKB	9	35.4	1.09
Q15274	Nicotinate-nucleotide pyrophosphorylase [carboxylating]	QPRT	6	23.2	1.09
Q16881	Thioredoxin reductase 1	TXNRD1	2	36.9	1.08
P26440	Isovaleryl-CoA dehydrogenase	IVD	5	14.6	1.08
P19367	Hexokinase-1	HK1	13	24.5	1.07
P50453	Serpin B9	SERPINB9	13	41.5	1.07
P0CG29	Glutathione S-transferase theta-2	GSTT2	8	41.8	1.07
E9PMS6	LIM domain only protein 7	LMO7	1	53.5	1.07
Q9Y570	Protein phosphatase methylesterase 1	PPME1	1	49.3	1.07
Q86V21	Acetoacetyl-CoA synthetase	AACS	12	18.8	1.07
Q8NCN5	Pyruvate dehydrogenase phosphatase regulatory subunit, mitochondrial	PDPR	12	20.8	1.07
Q96AT1	Uncharacterized protein KIAA1143	KIAA1143	2	36.9	1.07
P21980	Protein-glutamine gamma-glutamyltransferase 2	TGM2	42	54.6	1.06
P05091	Aldehyde dehydrogenase	ALDH2	10	35.4	1.06
P38117	Electron transfer flavoprotein subunit beta	ETFB	13	50.2	1.06
Q6X734	NIF3-like protein 1	NIF3L1	7	38.5	1.06

Q86TX2	Acyl-coenzyme A thioesterase 1	ACOT1	2	23.0	1.06
P21266	Glutathione S-transferase Mu 3	GSTM3	17	65.3	1.06
Q9UI42	Carboxypeptidase A4	CPA4	11	47.5	1.05
Q16822	Phosphoenolpyruvate carboxykinase [GTP], mitochondrial	PCK2	7	32.8	1.05
P13804	Electron transfer flavoprotein subunit alpha, mitochondrial	ETF A	11	47.1	1.05
P48735	Isocitrate dehydrogenase [NADP], mitochondrial	IDH2	16	38.3	1.05
P11177	Pyruvate dehydrogenase E1 component subunit beta, mitochondrial	PDHB	4	33.7	1.04
Q53FA7	Quinone oxidoreductase PIG3	TP53I3	6	41.0	1.04
P16278	Beta-galactosidase	GLB1	9	19.1	1.04
P52926	High mobility group protein HMGI-C	HMGA2	5	34.7	1.04
P15559	NAD(P)H dehydrogenase [quinone] 1	NQO1	11	47.5	1.04
O94760	N(G), N(G)-dimethylarginine dimethyl amino hydrolase 1	DDAH1	6	67.7	1.04
Q9Y617	Phosphoserine aminotransferase	PSAT1	1	53.5	1.04
P05783	Keratin, type I cytoskeletal 18	KRT18	12	52.1	1.04
P42574	Caspase-3	CASP3	6	23.8	1.04
P09936	Ubiquitin carboxyl-terminal hydrolase isozyme L1	UCHL1	0	67.3	1.04
P30084	Enoyl-CoA hydratase, mitochondrial	ECHS1	15	57.6	1.04
Q9NR45	Sialic acid synthase	NANS	32	42.6	1.04
P30048	Thioredoxin-dependent peroxide reductase, mitochondrial	PRDX3	13	53.9	1.04
P00441	Superoxide dismutase [Cu-Zn]	SOD1	8	71.4	1.03
P49748	Very long-chain specific acyl-CoA dehydrogenase, mitochondrial	ACADVL	20	43.1	1.03
P07339	Cathepsin D	CTSD	0	45.3	1.03
P04792	Heat shock protein beta-1	HSPB1	18	77.6	1.03
P30041	Peroxiredoxin-6	PRDX6	21	71.0	1.03
Q9UJ70	N-acetyl-D-glucosamine kinase	NAGK	10	22.3	1.03
P30044	Peroxiredoxin-5, mitochondrial	PRDX5	11	57.5	1.03
Q06210	Glutamine--fructose-6-phosphate aminotransferase [isomerizing] 1	GFPT1	28	50.6	1.03

P30040	Endoplasmic reticulum resident protein 29	ERP29	13	49.4	1.03
P32119	Peroxiredoxin-2	PRDX2	14	42.4	1.03
P36871	Phosphoglucomutase-1	PGM1	29	45.7	1.03
P00387	NADH-cytochrome b5 reductase 3	CYB5R3	10	36.2	1.03
P07686	Beta-hexosaminidase subunit beta	HEXB	19	35.3	1.03
P31949	Protein S100-A11	S100A11	7	56.2	1.03
Q9BRA2	Thioredoxin domain-containing protein 17	TXNDC17	4	46.6	1.03
Q6NZI2	Polymerase I and transcript release factor	PTRF	21	46.4	1.03
P19105	Myosin regulatory light chain 12A	MYL12A	4	55.4	1.03
P11216	Glycogen phosphorylase, brain form	PYGB	50	57.9	1.02
P07741	Adenine phosphoribosyltransferase	APRT	3	44.4	1.02
P14324	Farnesyl pyrophosphate synthase	FDPS	3	17.2	1.02
P46063	ATP-dependent DNA helicase Q1	RECQL	16	28.5	1.02
D6RA82	Annexin	ANXA3	1	49.3	1.02
P49189	4-trimethylaminobutyraldehyde dehydrogenase	ALDH9A1	21	43.9	1.02
Q9H488	GDP-fucose protein O-fucosyltransferase 1	POFUT1	5	14.6	1.02
P62937	Peptidyl-prolyl cis-trans isomerase A	PPIA	12	84.2	1.02
P08758	Annexin A5	ANXA5	25	66.2	1.02
P15586	N-acetylglucosamine-6-sulfatase	GNS	11	24.0	1.02
O75368	SH3 domain-binding glutamic acid-rich-like protein	SH3BGRL	10	85.1	1.02
Q9H7C9	Mth938 domain-containing protein	AAMDC	0	45.3	1.02
P31150	Rab GDP dissociation inhibitor alpha	GDI1	16	55.3	1.02
O75874	Isocitrate dehydrogenase [NADP] cytoplasmic	IDH1	24	54.6	1.02
P02751	Fibronectin	FN1	38	22.1	1.02
Q06830	Peroxiredoxin-1	PRDX1	7	68.8	1.02
Q13162	Peroxiredoxin-4	PRDX4	13	64.9	1.02
Q14019	Coactosin-like protein	COTL1	16	62.7	1.02

P59998	Actin-related protein 2/3 complex subunit 4	ARPC4	1	27.6	1.02
P49419	Alpha-aminoadipic semialdehyde dehydrogenase	ALDH7A1	4	46.6	1.02
P07237	Protein disulfide-isomerase	P4HB	15	64.4	1.02
P11021	Endoplasmic reticulum chaperone BiP	HSPA5	60	66.4	1.02
Q92820	Gamma-glutamyl hydrolase	GGH	9	35.8	1.02
P23284	Peptidyl-prolyl cis-trans isomerase B	PPIB	25	70.4	1.02
P14618	Pyruvate kinase PKM	PKM	5	82.9	1.02
P30101	Protein disulfide-isomerase A3	PDIA3	40	63.2	1.02
P00491	Purine nucleoside phosphorylase	PNP	3	45.3	1.02
P15121	Aldose reductase	AKR1B1	10	41.1	1.02
Q99798	Aconitate hydratase	ACO2	32	42.6	1.02
P04181	Ornithine aminotransferase	OAT	22	50.1	1.01
P41250	Glycine--tRNA ligase	GARS	41	46.8	1.01
P40925	Malate dehydrogenase, cytoplasmic	MDH1	18	52.1	1.01
O60701	UDP-glucose 6-dehydrogenase	UGDH	20	60.7	1.01
P12081	Histidine--tRNA ligase, cytoplasmic	HARS	1	49.1	1.01
P09622	Dihydrolipoyl dehydrogenase	DLD	15	30.5	1.01
P36957	Dihydrolipoyllysine-residue succinyltransferase component of 2-oxoglutarate dehydrogenase complex, mitochondrial	DLST	15	40.2	1.01
P23526	Adenosylhomocysteinase	AHCY	25	49.5	1.01

**Table 5.6: Cytosolic proteins downregulated significantly in MCs treated by Glo1 inducer in normal glucose condition.**

<b>Protein accession number</b>	<b>Protein name</b>	<b>Gene name</b>		<b>Percentage sequence coverage</b>	<b>Fold increase</b>
P40429	60S ribosomal protein L13a	RPL13A	8	50.7	0.987
P11940	Polyadenylate-binding protein 1	PABPC1	6	43.6	0.984
P26373	60S ribosomal protein L13	RPL13	14	53.6	0.983
Q92598	Heat shock protein 105 kDa	HSPH1	7	60.5	0.983
P35269	General transcription factor IIF subunit 1	GTF2F1	19	34.6	0.982
P46777	60S ribosomal protein L5	RPL5	13	55.2	0.982
Q14195	Dihydropyrimidinase-related protein 3	DPYSL3	23	57.5	0.982
Q9BUJ2	Heterogeneous nuclear ribonucleoprotein U-like protein 1	HNRNPUL1	2	39.6	0.982
P62910	60S ribosomal protein L32	RPL32	7	47.4	0.981
O15067	Phosphoribosylformylglycinamide synthase	PFAS	27	21.7	0.981
P07355	Annexin A2	ANXA2	22	71.7	0.981
P43034	Platelet-activating factor acetylhydrolase IB subunit alpha	PAFAH1B1	20	47.8	0.981
P61586	Transforming protein RhoA	RHOA	7	57.0	0.981
Q15075	Early endosome antigen 1	EEA1	77	57.7	0.981
P07910	Heterogeneous nuclear ribonucleoproteins C1/C2	HNRNPC	2	72.1	0.980
P48681	Nestin	NES	76	48.7	0.980
P62701	40S ribosomal protein S4, X isoform	RPS4X	16	68.1	0.980
Q99879	Histone H2B	H2BFS	3	59.5	0.980
Q9H910	Hematological and neurological expressed 1-like protein	HN1L	0	81.6	0.980
O75347	Tubulin-specific chaperone A	TBCA	0	77.8	0.979
P13639	Elongation factor 2	EEF2	63	55.2	0.979
P62424	60S ribosomal protein L7a	RPL7A	8	48.1	0.979
Q14444	Caprin-1	CAPRIN1	23	33.6	0.979

Q01844	RNA-binding protein EWS	EWSR1	10	23.5	0.978
P63279	SUMO-conjugating enzyme UBC9	UBE2I	10	45.7	0.978
O43396	Thioredoxin-like protein 1	TXNL1	12	57.1	0.978
P27695	DNA-(apurinic or apyrimidinic site) lyase, mitochondrial	APEX1	12	48.7	0.978
P52565	Rho GDP-dissociation inhibitor 1	ARHGDI1	1	54.9	0.978
Q16643	Drebrin	DBN1	35	53.0	0.978
Q9UKY7	Protein CDV3 homolog	CDV3	11	81.8	0.978
P08133	Annexin A6	ANXA6	6	64.6	0.977
P62913	60S ribosomal protein L11	RPL11	15	52.8	0.977
Q01105	Protein SET	SET	8	44.5	0.977
Q96C19	EF-hand domain-containing protein D2	EFHD2	7	46.7	0.977
Q9UHD9	Ubiquilin-2	UBQLN2	8	29.5	0.977
Q9Y383	Putative RNA-binding protein Luc7-like 2	LUC7L2	10	29.5	0.976
P61221	ATP-binding cassette sub-family E member 1	ABCE1	20	37.9	0.976
P63104	14-3-3 protein zeta/delta	YWHAZ	19	71.8	0.976
P61981	14-3-3 protein gamma	YWHAG	12	63.6	0.975
P62917	60S ribosomal protein L8	RPL8	12	37.7	0.975
Q02878	60S ribosomal protein L6	RPL6	25	50.3	0.975
Q15942	Zyxin	ZYX	14	44.6	0.975
Q07955	Serine/arginine-rich splicing factor 1	SRSF1	19	55.3	0.974
P08238	Heat shock protein HSP 90-beta	HSP90AB1	12	54.8	0.974
P31943	Heterogeneous nuclear ribonucleoprotein H	HNRNPH1	3	53.0	0.973
P06748	Nucleophosmin	NPM1	18	52.0	0.972
P20700	Lamin-B1	LMNB1	32	51.0	0.972
S4R417	40S ribosomal protein S15	RPS15	2	57.6	0.971
E7EQT4	Apoptotic chromatin condensation inducer in the nucleus	ACIN1	2	28.9	0.971
P08621	U1 small nuclear ribonucleoprotein 70 kDa	SNRNP70	21	43.7	0.971

P10412	Histone H1.4	HIST1H1E	5	36.5	0.971
P18124	60S ribosomal protein L7	RPL7	21	48.4	0.971
P27348	14-3-3 protein theta	YWHAQ	16	61.2	0.971
P40222	Alpha-taxilin	TXLNA	28	54.8	0.971
P42677	40S ribosomal protein S27	RPS27	4	45.2	0.971
Q02952	A-kinase anchor protein 12	AKAP12	108	59.8	0.971
Q9UK76	Hematological and neurological expressed 1 protein	HN1	5	63.6	0.971
Q9Y4Z0	U6 snRNA-associated Sm-like protein LSM4	LSM4	3	30.2	0.971
O14776	Transcription elongation regulator 1	TCERG1	30	23.4	0.970
P25685	DnaJ homolog subfamily B member 1	DNAJB1	10	36.5	0.970
P31153	S-adenosylmethionine synthase isoform type-2	MAT2A	17	44.8	0.970
P52597	Heterogeneous nuclear ribonucleoprotein F	HNRNPF	14	48.4	0.970
Q13185	Chromobox protein homolog 3	CBX3	8	54.6	0.970
Q13428	Treacle protein	TCOF1	5	27.9	0.970
O43707	Alpha-actinin-4	ACTN4	48	71.9	0.969
P05388	60S acidic ribosomal protein P0	RPLP0	1	39.7	0.969
P07900	Heat shock protein HSP 90-alpha	HSP90AA1	16	47.1	0.969
P11047	Laminin subunit gamma-1	LAMC1	50	40.8	0.969
Q04917	14-3-3 protein eta	YWHAH	16	62.6	0.969
O96019	Actin-like protein 6A	ACTL6A	12	40.1	0.968
P39023	60S ribosomal protein L3	RPL3	0	51.1	0.968
P42167	Lamina-associated polypeptide 2, isoforms beta/gamma	TMPO	2	41.6	0.968
Q5SW79	Centrosomal protein of 170 kDa	CEP170	7	51.9	0.968
Q9UBE0	SUMO-activating enzyme subunit 1	SAE1	17	49.4	0.968
Q13148	TAR DNA-binding protein 43	TARDBP	2	20.0	0.967
P68400	Casein kinase II subunit alpha	CSNK2A1	12	46.0	0.967
Q15185	Prostaglandin E synthase 3	PTGES3	8	47.0	0.966



P84098	Ribosomal protein L19	RPL19	10	28.0	0.966
P61254	60S ribosomal protein L26	RPL26	5	71.7	0.966
Q00839	Heterogeneous nuclear ribonucleoprotein U	HNRNPU	15	53.8	0.966
Q09028	Histone-binding protein RBBP4	RBBP4	5	22.4	0.966
Q9GZU8	Protein FAM192A	FAM192A	15	50.8	0.966
O14979	Heterogeneous nuclear ribonucleoprotein D-like	HNRNPDL	16	39.9	0.965
O43493	Trans-Golgi network integral membrane protein 2	TGOLN2	11	24.8	0.965
P12270	Nucleoprotein TPR	TPR	104	45.0	0.964
P61956	Small ubiquitin-related modifier 2	SUMO2	4	33.7	0.964
Q02790	Peptidyl-prolyl cis-trans isomerase FKBP4	FKBP4	30	55.3	0.964
Q8NC51	Plasminogen activator inhibitor 1 RNA-binding protein	SERBP1	35	69.4	0.964
P49321	Nuclear autoantigenic sperm protein	NASP	32	49.6	0.963
Q86U42	Polyadenylate-binding protein 2	PABPN1	4	39.2	0.963
Q8WW12	PEST proteolytic signal-containing nuclear protein	PCNP	10	48.9	0.963
Q9NX55	Huntingtin-interacting protein K	HYPK	6	51.9	0.963
P27635	60S ribosomal protein L10	RPL10	2	54.5	0.962
P22626	Heterogeneous nuclear ribonucleoproteins A2/B1	HNRNPA2B1	29	65.2	0.962
Q07020	60S ribosomal protein L18	RPL18	9	45.7	0.962
Q15459	Splicing factor 3A subunit 1	SF3A1	13	21.7	0.962
Q9P258	Protein RCC2	RCC2	14	32.0	0.962
Q92841	Probable ATP-dependent RNA helicase DDX17	DDX17	24	50.5	0.961
O43583	Density-regulated protein	DENR	2	48.5	0.961
P26599	Polypyrimidine tract-binding protein 1	PTBP1	2	13.7	0.961
O60506	Heterogeneous nuclear ribonucleoprotein Q	SYNCRIP	26	51.5	0.960
P18206	Vinculin	VCL	62	55.6	0.960
P46778	60S ribosomal protein L21	RPL21	11	53.1	0.960
Q13435	Splicing factor 3B subunit 2	SF3B2	46	48.3	0.960

Q14103	Heterogeneous nuclear ribonucleoprotein D0	HNRNPD	0	47.9	0.960
P23588	Eukaryotic translation initiation factor 4B	EIF4B	46	62.2	0.959
P38159	RNA-binding motif protein, X chromosome	RBMX	3	58.6	0.959
P61006	Ras-related protein Rab-8A	RAB8A	6	46.9	0.959
Q12904	Aminoacyl tRNA synthase complex-interacting multifunctional protein 1	AIMP1	12	52.9	0.959
Q92945	Far upstream element-binding protein 2	KHSRP	26	46.4	0.959
Q99733	Nucleosome assembly protein 1-like 4	NAP1L4	2	30.7	0.959
Q9Y696	Chloride intracellular channel protein 4	CLIC4	17	76.7	0.959
O43670	BUB3-interacting and GLEBS motif-containing protein ZNF207	ZNF207	6	13.5	0.959
P29966	Myristoylated alanine-rich C-kinase substrate	MARCKS	14	54.8	0.958
P61313	60S ribosomal protein L15	RPL15	17	52.5	0.958
P67809	Nuclease-sensitive element-binding protein 1	YBX1	2	70.1	0.958
Q96AE4	Far upstream element-binding protein 1	FUBP1	16	50.8	0.958
P51991	Heterogeneous nuclear ribonucleoprotein A3	HNRNPA3	31	56.1	0.957
P61978	Heterogeneous nuclear ribonucleoprotein K	HNRNPK	3	47.1	0.957
Q8N543	Prolyl 3-hydroxylase OGFOD1	OGFOD1	13	27.5	0.957
P07942	Laminin subunit beta-1	LAMB1	37	23.1	0.956
O00422	Histone deacetylase complex subunit SAP18	SAP18	5	41.2	0.956
P12814	Alpha-actinin-1	ACTN1	4	68.6	0.956
P31942	Heterogeneous nuclear ribonucleoprotein H3	HNRNPH3	14	66.2	0.956
Q9C0C2	182 kDa tankyrase-1-binding protein	TNKS1BP1	54	40.0	0.956
Q9H773	dCTP pyrophosphatase 1	DCTPP1	8	44.7	0.956
Q12905	Interleukin enhancer-binding factor 2	ILF2	7	21.0	0.955
Q99729	Heterogeneous nuclear ribonucleoprotein A/B	HNRNPAB	15	51.6	0.955
Q9Y2V2	Calcium-regulated heat stable protein 1	CARHSP1	2	42.2	0.955
Q15257	Serine/threonine-protein phosphatase 2A activator	PPP2R4	7	32.4	0.954
Q92882	Osteoclast-stimulating factor 1	OSTF1	6	44.4	0.954

P22061	Protein-L-isoaspartate O-methyltransferase	PCMT1	8	40.8	0.953
Q9UHR5	SAP30-binding protein	SAP30BP	2	26.8	0.952
P33316	Deoxyuridine 5-triphosphate nucleotidohydrolase, mitochondrial	DUT	2	52.4	0.952
O43390	Heterogeneous nuclear ribonucleoprotein R	HNRNPR	19	38.9	0.950
F8W0J6	Nucleosome assembly protein 1-like 1	NAP1L1	0	36.7	0.949
P09651	Heterogeneous nuclear ribonucleoprotein A1	HNRNPA1	15	73.0	0.949
P23246	Splicing factor, proline- and glutamine-rich	SFPQ	39	52.6	0.949
P38919	Eukaryotic initiation factor 4A-III	EIF4A3	16	38.7	0.949
Q9BYG3	MKI67 FHA domain-interacting nucleolar phosphoprotein	NIFK	10	36.5	0.948
Q9Y2X3	Nucleolar protein 58	NOP58	10	20.4	0.948
P02786	Transferrin receptor protein 1, serum form	TFRC	3	28.0	0.947
P57081	tRNA (guanine-N (7)-)-methyltransferase non-catalytic subunit WDR4	WDR4	8	33.0	0.947
P52434	DNA-directed RNA polymerases I, II, and III subunit RPABC3	POLR2H	6	42.6	0.946
Q9BRP8	Partner of Y14 and mago	WIBG	8	50.5	0.945
O43290	U4/U6.U5 tri-snRNP-associated protein 1	SART1	26	38.0	0.944
Q16630	Cleavage and polyadenylation specificity factor subunit 6	CPSF6	16	36.2	0.943
O75934	Pre-mRNA-splicing factor SPF27	BCAS2	8	39.6	0.943
P16989	Y-box-binding protein 3	YBX3	14	59.1	0.943
Q15233	Non-POU domain-containing octamer-binding protein	NONO	26	61.1	0.943
Q7Z4V5	Hepatoma-derived growth factor-related protein 2	HDGFRP2	16	30.3	0.943
Q9BWJ5	Splicing factor 3B subunit 5	SF3B5	4	48.8	0.943
P23193	Transcription elongation factor A protein 1	TCEA1	6	51.5	0.942
P82094	TATA element modulatory factor	TMF1	33	37.1	0.942
O43809	Cleavage and polyadenylation specificity factor subunit 5	NUDT21	5	42.3	0.941
Q96C90	Protein phosphatase 1 regulatory subunit 14B	PPP1R14B	3	34.7	0.941
Q9Y2Z0	Suppressor of G2 allele of SKP1 homolog	SUGT1	15	55.3	0.941
Q99829	Copine-1	CPNE1	6	23.8	0.939

Q15287	RNA-binding protein with serine-rich domain 1	RNPS1	2	31.0	0.939
Q9H6F5	Coiled-coil domain-containing protein 86	CCDC86	14	47.2	0.939
Q6PKG0	La-related protein 1	LARP1	7	25.8	0.938
O75391	Sperm-associated antigen 7	SPAG7	2	44.5	0.937
P09497	Clathrin light chain B	CLTB	13	31.9	0.937
Q92769	Histone deacetylase 2	HDAC2	7	33.6	0.937
O15355	Protein phosphatase 1G	PPM1G	15	33.7	0.936
P22087	rRNA 2-O-methyltransferase fibrillar	FBL	5	41.7	0.936
Q96PK6	RNA-binding protein 14	RBM14	11	21.1	0.936
Q08209	Serine/threonine-protein phosphatase 2B catalytic subunit alpha isoform	PPP3CA	8	18.4	0.935
Q6Y7W6	PERQ amino acid-rich with GYF domain-containing protein 2	GIGYF2	5	20.4	0.935
O00159	Unconventional myosin-Ic	MYO1C	11	16.1	0.933
Q08211	ATP-dependent RNA helicase A	DHX9	27	23.9	0.933
D6RDG3	Transcription factor BTF3	BTF3	3	29.4	0.932
O75940	Survival of motor neuron-related-splicing factor 30	SMNDC1	8	43.7	0.932
Q8WWM7	Ataxin-2-like protein	ATXN2L	18	23.4	0.932
P40855	Peroxisomal biogenesis factor 19	PEX19	7	36.2	0.931
Q93052	Lipoma-preferred partner	LPP	15	32.0	0.931
P41227	N-alpha-acetyltransferase 10	NAA10	3	34.5	0.930
P62993	Growth factor receptor-bound protein 2	GRB2	15	62.2	0.930
Q8NFP7	Diphosphoinositol polyphosphate phosphohydrolase 3-alpha	NUDT10	1	48.2	0.930
O75534	Cold shock domain-containing protein E1	CSDE1	30	40.5	0.928
Q9Y2W1	Thyroid hormone receptor-associated protein 3	THRAP3	47	47.4	0.927
E7EQ69	N-alpha-acetyltransferase 50	NAA50	9	48.2	0.926
O43143	Pre-mRNA-splicing factor ATP-dependent RNA helicase DHX15	DHX15	20	26.4	0.926
P63167	Dynein light chain 1, cytoplasmic	DYNLL1	5	69.7	0.926
Q8IYB3	Serine/arginine repetitive matrix protein 1	SRRM1	2	31.8	0.925

Q9H307	Pinin	PNN	13	23.7	0.925
P19784	Casein kinase II subunit alpha	CSNK2A2	10	32.3	0.923
Q9NZB2	Constitutive coactivator of PPAR-gamma-like protein 1	FAM120A	22	25.5	0.923
P09874	Poly [ADP-ribose] polymerase 1	PARP1	25	28.0	0.922
Q16576	Histone-binding protein RBBP7	RBBP7	3	28.5	0.921
Q9NX46	Poly (ADP-ribose) glycohydrolase ARH3	ADPRHL2	10	35.8	0.921
Q9Y266	Nuclear migration protein nudC	NUDC	15	50.8	0.921
P49327	Fatty acid synthase	FASN	43	20.5	0.920
Q9NPD3	Exosome complex component RRP41	EXOSC4	3	29.0	0.919
Q9Y520	Protein PRRC2C	PRRC2C	2	27.9	0.919
Q92522	Histone H1x	H1FX	10	36.2	0.917
Q5JW30	Double-stranded RNA-binding protein Staufen homolog 1	STAU1	5	32.4	0.916
P43243	Matrin-3	MATR3	24	27.4	0.915
P35520	Cystathionine beta-synthase	CBS	10	20.1	0.915
P14866	Heterogeneous nuclear ribonucleoprotein L	HNRNPL	15	49.4	0.915
P54105	Methylosome subunit pICln	CLNS1A	3	26.9	0.914
P83916	Chromobox protein homolog 1	CBX1	8	54.6	0.914
Q9Y230	RuvB-like 2	RUVBL2	15	42.1	0.913
Q9BQ61	Uncharacterized protein C19orf43	C19orf43	10	42.0	0.908
Q9BXJ9	N-alpha-acetyltransferase 15, NatA auxiliary subunit	NAA15	18	26.4	0.906
P33176	Kinesin-1 heavy chain	KIF5B	31	46.4	0.906
P33992	DNA replication licensing factor MCM5;DNA helicase	MCM5	19	37.2	0.906
P49750	YLP motif-containing protein 1	YLPM1	7	23.3	0.903
Q9UKD2	mRNA turnover protein 4 homolog	MRT04	10	53.1	0.903
Q9GZL7	Ribosome biogenesis protein WDR12	WDR12	10	33.3	0.902
O43684	Mitotic checkpoint protein BUB3	BUB3	12	35.7	0.899
Q9BWU0	Kanadaplin	SLC4A1AP	14	29.9	0.896

Q9Y5S9	RNA-binding protein 8A	RBM8A	5	27	0.896
Q9HB07	UPF0160 protein MYG1, mitochondrial	C12orf10	9	31.9	0.891
Q15631	Translin	TSN	3	50.7	0.890
P47897	Glutamine--tRNA ligase	QARS	9	44.0	0.889
P60842	Eukaryotic initiation factor 4A-I	EIF4A1	2	31.0	0.888
Q9NR30	Nucleolar RNA helicase 2	DDX21	28	34.6	0.883
Q12906	Interleukin enhancer-binding factor 3	ILF3	26	49.7	0.877
Q13151	Heterogeneous nuclear ribonucleoprotein A0	HNRNPA0	10	30.5	0.874
O00193	Small acidic protein	SMAP	2	56.8	0.871
P83731	60S ribosomal protein L24	RPL24	10	47.1	0.871
Q96A72	Protein mago nashi homolog 2	MAGOHB	0	52.0	0.870
P17655	Calpain-2 catalytic subunit	CAPN2	20	28.4	0.850
Q15424	Scaffold attachment factor B1	SAFB	30	35.2	0.836

## 6 Discussion

DKD is one of the most common and important chronic inflammatory disease complications of diabetes and affects ~40% of diabetic patients. Epidemiological data confirm that diabetes is a major risk factor for kidney disease, and in many Western countries, diabetes is a common cause renal replacement treatment due to ESRD. Published studies found that 24 % of subjects who started renal replacement therapy were diabetic (Bell et al., 2015). Increased hyperglycaemia is linked to increased severity of DKD. The mechanisms that link hyperglycaemia to DKD are widely thought to involve factors that are responsible for inducing imbalance in the metabolic mechanisms involving glycation, oxidative and inflammatory pathways. Many studies point to a link between glycation and diabetes and its complications (Akram et al., 2020, Algerban, 2021), for instance, one of the early studies on glycation and diabetes by Thornalley found that the flux formation and concentration of the reactive glycating agent MG was linked to major diabetes complications (Thornalley 1988).

In hyperglycaemia, MG increases as a consequence of increased flux of glucose metabolism in cells expressing GLUT1, followed by downregulation of Glo1 expression, which is the major enzyme of MG breakdown/metabolism, and this potentiates downstream inflammation and stress pathways (for example cytokine release and hypoxic responses). In previous studies it was proven that in diabetes and diabetes complications, MG derived AGEs was significantly increased accompanied by decreased in Glo1 activity in some studies (Schumacher et al., 2018, Xue et al., 2016, Strom et al., 2021). Further experimental studies suggest that Glo1 overexpression could prevent the progress of diabetes complications such as DKD (Pereira et al., 2017, Peng et al., 2017a).

In this study I hypothesised that the Glo1 inducer, tRES-HESP can reverse or reduce markers of DKD progression in models of renal cell hyperglycaemia *in vitro*. The aim of this project has been to test this hypothesis using primary human renal cells and also to embark upon novel studies into the protein expression profiles of these cells using state-of-the-art label-free quantitative proteomics. This modern proteomics approach offers vital, new and in-depth information on the identification of the theoretically damaging protein expression profiles and characteristics in type 2 diabetes, and can potentially guide the future understanding and application of Glo1 inducer therapy for this major disease. Primary human cells used in this study, RPTECs and MCs have been acknowledged as valuable models of diabetic renal disease (Bessho et al., 2019, Wang et al., 2020a), and I have aimed to drive this area further through investigating aspects of dicarbonyl stress and proteomic analysis.

## 6.1 Effect of glucose concentration on growth and viability of primary human renal cells *in vitro*

Cellular responses to hyperglycaemia occur in various ways but ultimately lead to functional changes or the initiation of apoptosis. In this project I studied the effect of glucose concentration on the growth of both hRPTEC and MCs in primary culture. Concentration of 7.2 and 5.5 mM glucose was used as the “low glucose concentration” (LG) while concentration of 25.0 mM glucose was used as the “high glucose concentration” (HG; mimicking diabetic conditions found *in vivo*). Hyperglycaemia alone directly enhances the proliferation of the hRPTECs and MCs.

When hRPTECs are incubated in medium containing 7.2 mM or 25.0 mM glucose for 6 days without change of medium, the cells showed similar increase in growth in both concentrations over 3 days, until the fourth day where cell number increased slightly but significantly in the last two days of culturing in the HG cultures. At initial passage, hRPTECs maintained moderate growth characteristics with a mean population doubling time of 1.40 days in LG condition and 1.35 days in hyperglycaemic conditions. Therefore, in later experiments passages (3 – 5) were used, cells were sub-cultured and grown for up to 4 days with changing of the medium on the second day of culturing. This result was similar to a study that found that hyperglycaemia induced cellular hypertrophy rather than cell death in proximal tubular cells through activation of extracellular signal-related kinase which increased TGF- $\beta$  expression (Fujita et al., 2004). PTECs have a crucial role in renal pathology and carry out a wide range of systemic regulatory and endocrine roles, and also form a large portion of the kidney tissue mass. Previous studies have demonstrated that kidney enlargement is a hallmark pathological feature of DKD (Zafar and Naqvi, 2010, Han et al., 2019). The hRPTEC growth data in this thesis contrast with the previous study of Yuan *et al.*, who found that long time hyperglycaemia led to growth suppression of human proximal tubular epithelial cells (HK-2) through enhancing expression of the Inhibitor of growth 2 in the kidney of diabetes-induced mice and HK2 cells (Ma et al., 2020). There is further contrast in an older study by Park *et al.*, showing that in primary RPTECs, hyperglycaemia inhibited renal cell growth via induction of oxidative stress (Park et al., 2001).

I further demonstrate that increased glucose levels significantly enhance the proliferation of MCs. Culture of MCs herein for 6 days in LG and HG media did not produce a decrease in cell viability. However, growth rates showed a progressive increase under hyperglycemic conditions from the second day, where the average population doubling time



was 1.16 and 1.09 days when cells were cultured in LG and HG glucose conditions, respectively. In parallel with previous studies increased glucose levels enhance MC proliferation (Yano et al., 2009, Li et al., 2019a), and further evidence indicates also that long term diabetes-induced abnormal glomerular growth occurs as a result of upregulation of ECM formation, with accumulation of fibronectin and collagen, as well as increased activity of the growth factor TGF- $\beta$ 1 (Qiao et al., 2017). In other studies, hyperglycemia stimulated antiproliferative effects through increases in protein content without DNA replication, which is a key characteristic of glomerular hypertrophy (Masson et al., 2005, Wolf et al., 2001).

## **6.2 The effect of high glucose and dicarbonyl stress on the glyoxalase system in primary human renal cells *in vitro*.**

Glo1 has long been related to control of cell growth and diabetes. However, the activity of Glo1 in hRPTECs and MCs in LG concentration was determined as  $728 \pm 142$  and  $368 \pm 11.4$  mU per mg protein respectively; by way of reference point, the proportion of Glo1 is 110 mU per mg protein in human red blood cells (McLellan et al., 1994), while in primary cultured human aortal endothelial cells, the activity of the enzyme has been determined as 1,500 mU per mg (Thornalley et al., 2014). Activity of the Glo1 enzyme noticeably exceeds activities of both MG reductase and MG dehydrogenase, and this makes it the main component of the MG detoxification pathway. Meanwhile, the activity of Glo2 in LG conditions in hRPTECs and MCs was found to be relatively low at  $92.6 \pm 7.58$  mU and  $21.9 \pm 1.11$  per mg protein, respectively; as a reference point, it is around 64 mU per mg protein in human red blood cells (McLellan et al., 1994).

I anticipated the likely decrease in Glo1 activity of both hRPTECs and MCs in HG medium. However, the results in fact showed a slight decrease but did not reach statistically significant values in activity after 4 days of culturing. In the immunoprecipitation study I found a reduction in Glo1 protein in hRPTECs in HG culture, and Glo1 protein appeared to decrease significantly by 32% in the HG treated cells, as compared to LG cultured controls, suggesting increased proteolysis of Glo1 protein in the HG condition. It hence suggests that hRPTECs under HG condition activate a process of increased proteolysis which increases dicarbonyl stress and Glo1 destabilisation. Reduction in Glo 1 enzyme activity has been detected on both *in vivo* and *in vitro* studies in HG condition where it has been speculated as a result of reduced Glo1 expression or increased degradation (Bierhaus et al., 2006, Giacco et al., 2014, Thornalley et al., 2014), while one of the previous *in vitro* studies in cells in HG culture showed that the

activities of Glo1 and Glo2 and the cellular GSH concentration did not change in red blood cells (Thornalley, 1988). Similar to Thornalley's findings, an *in vivo* study showed that activity of both Glo1 and Glo2 enzymes in rats exhibiting mild hyperglycaemia did not change comparing with the control in blood samples, showing that Glo1 activity was 3 times of that of Glo2 (Skapare et al., 2012).

### **6.3 The effect of high glucose on dicarbonyl metabolism in primary human renal cells *in vitro*.**

In hyperglycaemic conditions, it was expected that glucose uptake and metabolism by hRPTE and MCs would increase. When cells were incubated in medium containing 25 mM glucose (HG) for two days, the consumption of D-glucose increased by 2.5-fold and 3.3-fold in hRPTEC and MCs respectively. This is consistent with previous studies suggesting that glucose consumption increases due to the higher concentration stimulating glucose uptake and increasing expression of glucose transporters (Bayar and Bildik, 2021, Han et al., 2015). To maintain glucose homeostasis in renal cells (non-insulin-dependent cells) under hyperglycaemic condition, these cells might increase expression of both GLUT 1 and GLUT2 as glucose transporters, as the main glucose transporter GLUT4 is not expressed in renal cells. This might cause increased glucose concentrations entering the cells (Lagranha et al., 2007, Machado et al., 2006). Therefore, in patients with diabetes, glucose reabsorption in the proximal tubule is enhanced, leading to hyperglycaemia and glomerular hyperfiltration (Vallon, 2011).

Consequently, the flux of net D-lactate formation increased under HG conditions by 2.6-fold and 4.2-fold in hRPTE and MCs, respectively. D-lactate measurements have been established as indirect methods to measure MG and several studies have linked the increase in D-lactate concentrations to hyperglycaemia (Chou et al., 2015, Hoffman et al., 2020) and the increased flux of MG formation (Chatterjee et al., 2013). MG is the main causal metabolite in hyperglycaemia which is generated mostly from triphosphate intermediates of glycolysis. Therefore, elevated glucose consumption by these cells will be linked to elevated triphosphate intermediates, increased degradation to MG, with the resulting increased production fluxes of D-lactate. One of the recent clinical studies found a correlation between elevated urinary D-lactate levels in diabetic patients and renal damage (Chou et al., 2015), implicating a relationship between raised MG flux and renal complications.

The levels of L-lactate are linked to glycolytic activity but are not considered as an indicator of disease risk. L-Lactate is produced under anaerobic glycolysis conditions from pyruvate and is converted to this in order for pyruvate to enter the citric acid cycle of aerobic glycolysis. L-Lactate concentration showed a significant increase by 11.5 % in hRPTECs under HG conditions, reflecting increased glycolytic activity. However, the flux of net L-lactate formation was unchanged in MCs in HG, suggesting that metabolic regulation and glucose handling may be different between these two renal cell types.

#### **6.4 Effect of Glo1 inducers on growth and viability of primary human renal cells *in vitro***

In the present study, a significant inhibition of cell growth was found in normal hRPTECs and MCs, after treated with a combination of tRSV-HSP (10  $\mu$ M) with no evidence of increase in non-viable cell number. The effect of each individual compound was studied and it was found that tRSV alone arrested cell growth. Both types of primary renal cells showed similar sensitivity to tRSV (10  $\mu$ M) by reduction in cell proliferation by 48% and 53% in hRPTECs and MCs respectively. Resveratrol has been widely studied in both *in vivo* and *in vitro* studies as a potent anti-proliferation, pro-apoptosis, anti-carcinogenic, and antioxidant agent (Shahidi and Ambigaipalan, 2015, Wong et al., 2010, Lin et al., 2013, Hudson et al., 2007). With respect to MCs, cell proliferation is a principle feature and diagnostic tool in several renal diseases and also in renal ageing (Verzola et al., 2008, Coemans et al., 2019). Recent studies involving natural compounds such as tRSV could be used as intervention strategies to treat these disorders. In this study further proteomics experiments on MCs highlight the possible efficacy of the tRSV-HSP combination.

#### **6.5 Effect of Glo1 inducers on the glyoxalase system in primary human renal cells *in vitro*.**

The use of tRSV as a dietary supplement has been studied widely regarding its potential beneficial effect to counter several diseases including obesity, cancer and diabetes (Wang et al., 2020b, Li et al., 2013b, Bhatt et al., 2012). Most studies have been conducted on experimental models, where translation of these studies into clinical practice was hard to approach – for instance, a meta-analysis review considering 16 intervention studies summarised the effect of tRSV on metabolic parameters including body weight, systolic blood pressure, HDL, total cholesterol, triglyceride and glucose levels, wherein 10

studies were on human subjects, and 6 on animal models (Asgary et al., 2019). The review showed that analysis of studies conducted on human subjects found that tRSV has significant effects on glucose concentrations at the dosage of > 500 mg over  $\geq$  10 weeks (Asgary et al., 2019). In addition, the European Food Safety Authority affirmed that tRSV supplementation at 150 mg/ day does not raise concerns of safety for adult (EFSA, 2016).

tRSV influences several aspects of metabolic syndrome including activation of the anti-apoptotic protein SIRT1, although this is restricted to higher concentrations of 50 – 100  $\mu$ M, which could be toxic (Milne et al., 2007). In addition, a metabolic aspect at the lower range of tRSV dosage (3 - 10  $\mu$ M) is the inhibition of phosphodiesterases, leading to elevated cellular cAMP and NAD<sup>+</sup>, and increased sirtuins (Park et al., 2012). The Thornalley group found that tRSV activated Nrf2, inducing expression of Glo1 at the tRSV concentration ranges of 1 – 10  $\mu$ M, and that HSP is an activator of Nrf2 at doses achievable clinically and extremely safely, and found to act synergistically as the combined preparation tRSV-HSP. The tRSV-HSP combination has been found to be an effective Glo1 inducer at clinically translatable doses and so far appears to be very safe (Xue et al., 2016). Recent findings found that tRSV activates Nrf2 through preventing nuclear acetylation that would otherwise inactivate Nrf2 (Xue et al., 2015a, Xue et al., 2015b). Meanwhile the mechanism of action of HSP in activation of Nrf2 might include induction and activation of protein kinase A, upstream of Fyn kinase that consequently drives Nrf2 translocational oscillations with increased expression of ARE-linked genes (Xue et al., 2015b).

The effect of the tRSV-HSP combination on dicarbonyl stress and function of hRPTECs and MCs in LG and HG conditions was therefore studied. Consistent with the results of both hRPTECs and MCs, Glo1 activity was significantly increased by Glo1 inducer treatment in comparison with the two control treatments. Incubation of hRPTECs with tRSV-HSP increased Glo1 activity by 13% and 16% in LG and HG conditions, respectively. While in MCs the activity of Glo1 showed significant increase by 1.6-fold in HG treatment. Glo1 inducer treatment may produce activities positive for upregulation of Glo1 under HG conditions which may be a potential inducer of Glo1 activity and return it to normal levels in hyperglycaemia in these cells. Similar to Glo1, Glo2 activity showed significant increases in both cell types in Glo1 inducer treatment under LG and HG conditions. Meanwhile no effects for Glo1 inducer were observed on MG reductase and MG dehydrogenase, suggesting that the effect is specific for Glo1 and Glo2. Several studies have shown the effective role of tRSV-HSP in metabolic health. Clinical studies of Xue et al., showed that tRSV-HSP in

combination increased activity and expression of Glo1 in highly obese participants with decreased fasting and postprandial glucose concentration, and improved arterial dilation (Xue et al., 2016). Recent *in vitro* study of Ashour *et al.*, showed similar effect, the study proved the reversal effect of Glo1 inducer (tRSV-HSP) on primary human periodontal ligament fibroblasts, Glo1 inducer combination showed a direct activation of Glo1 enzyme at a concentration of at 10  $\mu$ M, in 3 days culture with LG condition and prevented the decrease of Glo1 activity under hyperglycaemia (Ashour et al., 2020).

## **6.6 Effect of Glo1 inducers on dicarbonyl metabolism in primary human renal cells *in vitro*.**

I also studied the effect of the tRSV-HSP combination on glucose consumption, D- and L-lactate formation in hRPTECs and MCs. In hRPTECs while all these parameters were increased under HG treatment with respect to control treatment, and Glo1 inducer treatment showed no significant change on glucose consumption or D-lactate levels, while the level of L-lactate formation was corrected by Glo1 inducer by 45 and 34% respectively in LG and HG conditions.

In MCs, D-Glucose consumption increased under hyperglycaemic conditions by 3-fold, and this showed a minor decrease after treatment by Glo1 inducer but did not reach a significant value, and the flux formation of D-lactate was significantly reduced by 18% in Glo1 inducer treatment under hyperglycaemic, although L-lactate concentrations did not change significantly. The increased flux of D-lactate indicated increased flux of MG formation, and this further supported the principle of high glycolytic activity by the decreased activity of Glo1 under hyperglycaemia conditions.

As expected, D-lactate formation in both cell types was less when compared to L-lactate production, and it is widely accepted that the flux of D-lactate formation is nearly equivalent to the flux of MG formation. This indicates that MG flux formation represents a comparatively minor fate of glucose degradation under high glucose conditions and is correlated with the overall increased glucose metabolism in hyperglycaemia. Remarkably, both *in vitro* and clinical studies proved the protective role of Glo1 inducer treatment in countering dicarbonyl stress induced in diabetes, Nrf2 activators increase Glo1 activity and decrease cellular and extracellular levels of MG. *In vitro* study of Ashour et al., showed that tRSV-HSP combination corrected the increase in D-lactate formation of human periodontal cells cultured in high glucose concentration of 25 mM. The study also found an associated

correction by Glo1 inducer of MG formation, protein modification by MG under hyperglycaemia (Ashour et al., 2020). Clinical studies of Xue et al. were conducted on 29 overweight and obese subjects at phase 1 clinical trial using tRSV-HSP combination capsules at concentrations achieved clinically for 8 weeks, and the study showed that Glo1 inducer treatment increased expression and activity of Glo1 by 27% and decreased plasma MG by 237% also reduced total body MG-protein glycation by 214% (Xue et al., 2016). While the study of Ficek *et al.*, showed a weak correlation between D-Lactate concentration and severity of inflammation in the plasma of haemodialysis patients (Ficek et al., 2017).

## **6.7 The effect of high glucose concentration on the cytosolic proteome of renal cells *in vitro***

Prior to the proteomics analysis, I adapted pre-analytic methods to prevent sample heating and high pH drift in order to sustain sample analyte integrity. In this study, I have studied the cytosolic proteomes of both hRPTECs and MCs incubated in LG and HG conditions, plus with and without tRSV-HSP, using high resolution, label-free mass spectrometry proteomics analysis.

Cytoplasmic extracts of hRPTECs yielded 725 identifiable protein species, with no significant change in molecular components response to HG stress. This was surprising, given the anticipated level of physiological change induced by high glucose concentrations in the HG cultures. In the cytoplasmic extract of MCs, I detected and identified 1191 proteins. Given that the extracted protein was prepared by sonication, it was expected to include soluble protein from both cytosol and other intracellular organelles, although the lysis procedure would remove the plasma membrane proteome upstream of analysis. A relatively small number of changes in proteome expression up to the subtle but consistent and statistically significant 1.10-fold level found in MCs incubated under HG conditions, where 13 of the 1191 proteins changed significantly. Of these 13 there were 4 upregulated proteins and 9 downregulated.

In this study RhoC was especially interesting as a protein upregulated in MCs under hyperglycaemic conditions. RhoC is a small GTP-binding protein that localises to the cytoplasm and plasma membrane and is involved in different cell functions such as cell morphology and the regulation of signal transduction pathways. High expression of RhoC is linked to cell proliferation and triggering tumours malignancy (Di Zhang et al., 2014). In addition, recent evidence demonstrates that Rho GTPase proteins are implicated in

tumorigenesis by activation of NF- $\kappa$ B signalling (Shaverdashvili et al., 2019). In the meta-analysis study of Gorski *et al.*, RhoC was one of the 10 identified genes that were positively associated with kidney development, cardiac septum development and glucose metabolism (Gorski et al., 2017). The mechanism of action involved matrix upregulation, and the study of Peng *et al.*, showed that HG concentrations of 30 mM induced fibronectin upregulation in MCs and kidney of STZ-induced diabetic rats (Peng et al., 2008). Another recent *in vivo* study found that oxidative stress in hyperglycaemia upregulates the RhoA/Rho pathway causing smooth muscle disturbances (Mahavadi et al., 2017), although implications in renal disease have yet to be established.

Another upregulated protein in HG conditions for MCs was Thymosin Beta 10 (TMSB10) which is a member of the beta-thymosin family of peptides. This protein is found to be implicated in the malignant processes of many cancers, and previous studies showed that overexpression of Thymosin Beta 10 correlates with hepatocellular, renal carcinoma and pancreatic cancer (Xiao et al., 2019, Song et al., 2019, Li et al., 2009). This result indirectly suggests that hyperglycaemia and possibly increased MG formation may induce cell proliferation, migration, stimulation of apoptotic resistance and hence develop the chemoresistance in tumour cells – with possible connections to renal cancer.

Proteasome Subunit Beta type-6 (PSMB6) was also upregulated in HG treatment in MCs. PSMB6 is a component of the 20S proteasome and plays major roles in the maintenance of cellular protein homeostasis via degrading damaged proteins that could affect cellular functions. In contrast with previous studies, hyperglycaemia significantly decreased proteasome activities by 20% leading to apoptosis in beta cells of diabetic rats (Broca et al., 2014). Another clinical study showed that PSMA6 protein was downregulated in diabetic patients with nephropathy compared with healthy control (Feng et al., 2018).

Also, HG conditions in this study of MCs leads to Glutathione S-transferase Mu (GST-Mu) being downregulated. GST-Mu exists as cytosolic and membrane-bound forms of GST that exhibit detoxification responses to carcinogens, toxins and oxidative stress factors in healthy and also pathophysiological conditions like diabetes. One of the recent studies conducted on T2DM patients found a significant correlation between GST-Mu null genotype and susceptibility to diabetic nephropathy (Hashemi-Soteh et al., 2020). In addition, some studies demonstrated that diabetes is associated with GST Mu downregulation and protein expression, and that this could be used as an indicator enzyme to analyse the effect of

oxidative stress caused by hyperglycaemia (Sadi et al., 2013, Sadi et al., 2015). This finding provides some affirmative validation of the proteomics approach used here to study the MCs.

Reticulocalbin 2 (RCN2) was also found to be downregulated under HG condition - this is a calcium-binding protein reported to be involved in cell differentiation, although its function remains unclear. However, some studies have highlighted the correlation between RCN2 and diabetes - a study of Chang *et al.*, showed that the expression of RCN2 was significantly higher in the femoropopliteal artery plaques of diabetic patients and also human aortic vascular cells under hyperglycaemic conditions (Chang et al., 2019). The proteomic studies I have carried out suggest a downregulation in MCs (cells of different lineage to vascular endothelium) and indicate that further understanding of this gene in diabetic conditions is needed.

## **6.8 The effect of Glo 1 inducer on the cytosolic proteome of MCs *in vitro***

The highest increase abundance change was caused by Glo1 inducer in comparison to LG control treatment in MCs. We observed significant changes in the protein cargo of Glo1 inducer treatment, wherein 96 protein species were upregulated and 225 were downregulated. Gene ontology (GO)-enriched terms in molecular function showed differentially expressed proteins between control and Glo1 inducer treatment, where upregulated proteins in Glo1 inducer were associated with cellular catalytic, oxidoreductase and peroxiredoxin activities. This was supported by Reactome database analysis which revealed that the most significantly enriched terms were associated with metabolism, cellular response to chemical stress, detoxification of ROS also the innate immune system.

One of the functional categories of metabolism, including carbohydrate derivate metabolism, emphasises the impact of Glo1 inducer treatment in carbohydrate metabolism. Acyl-CoA thioesterase 1 (ACOT1) is a cytosolic enzyme that the proteomics data showed to be upregulated in Glo1 inducer treatment. This enzyme is expressed mainly in the liver and kidney and it plays a vital role in fatty acid and lipid metabolism. The role of ACOT1 in DKD remains unclear, while in one of the latest renal carcinoma studies using three online cancer datasets, the study concluded that ACOT enzymes including ACOT1 were found to be significantly downregulated in Clear cell renal cell carcinoma, which can be used as renal cancer diagnostic marker (Xu et al., 2020a). In contrast, within an *in vivo* study, knockdown of ACOT1 protected against diabetes and insulin resistance in mice within a diet-induced diabetes model (Zhang et al., 2012), indicating that further research is required to pinpoint



the function of this protein in human vs mouse metabolic disease. The result of our study indicated that Glo1 might be a regulator of ACOT1 deficiency in renal cell expansion.

Hexokinase 1 (HK1) is another protein that was upregulated by Glo1 inducer. This enzyme is one of the three main hexokinase family members that localizes on the mitochondrial membrane and is involved in the first step of glucose metabolism to produce glucose-6-phosphate (G6P). Increased regulation of HK1 might serve to sustain viability and proliferation via glucose metabolism, where elevated glucose metabolism prevents cell death by activating protein kinase C. In contrast to my proteomics data, the study of Dai *et al.*, tRSV showed inhibition in cell growth and stimulation of apoptosis via downregulating the expression of HK2 as a major regulator of tumour glycolysis (Dai *et al.*, 2015). However, this focused on glycolysis in malignant cells which may differ considerably to primary cells with regard to gene regulation and metabolic function.

Another potentially significant protein, pyruvate dehydrogenase E1 subunit beta, was also found to be upregulated by Glo1 inducer treatment. This enzyme is responsible for conversion of pyruvate to the final products of Acetyl-CoA and CO<sub>2</sub>, providing the crucial link between glycolysis and the tricarboxylic acid cycle. Deficiency of pyruvate dehydrogenase enzymes is characterized by the accumulation of lactic acid (as L-lactate) in the body. Studies from Huang *et al.*, found that starvation and chemical-induced diabetes leads to downregulation of the Pyruvate dehydrogenase complex, and this was linked to stable changes in pyruvate dehydrogenase phosphatase 2 expression in rat heart and kidney (Huang *et al.*, 2003).

Pyruvate kinase M1-2 was found also to be upregulated by Glo1 inducer treatment. This enzyme is one of the main enzymes of glycolysis, drives the catalysis of phosphoenolpyruvate to produce pyruvate and is responsible for producing ATP through glycolysis. This enzyme acts in a different way to mitochondrial respiration, whereby it produces energy independently of O<sub>2</sub> consumption and may provide support to some tumours under hypoxic conditions. This finding within these proteomic studies might support the effective role of tRSV as a chemoprevention agent, where protection against renal carcinoma might be considered. A recent study showed that elevated glycolytic enzymes in renal glomeruli of DKD, in particular pyruvate kinase M2, are linked to protection of renal function in both T1DM and T2DM (Gordin *et al.*, 2019). Therefore, this observed upregulation of pyruvate kinase M1-2 in the proteome profile of MCs treated with tRSV-HESP would appear

to be consistent with therapeutic potential for this Glo1 inducer in treatment and prevention of DKD.

Glo1 inducer treatment also showed ontological and functional upregulation in the detoxification of ROS genes. Thioredoxin reductase 1 (TXNRD1) is one of the enzymes upregulated by Glo1 inducer and this enzyme reduces thioredoxins to play a vital role in cellular protection against ROS. It was previously claimed that TXNRD1 can be a major target for the reduction of nephrotoxicity against chemotherapeutic-induced tissue damage (Cheng et al., 2020).

Superoxide dismutase 1 (SOD1) is another key upregulated enzyme in the Glo1 inducer treatment group. It is a major antioxidant enzyme within many cells, located in the cytoplasm with high abundance in the liver and kidney. SOD enzymes have long been hypothesised to participate in protection against DKD through reducing oxidative damage. GST-Mu gene expression was also found to be increased by Glo1 inducer under LG conditions. Previous studies by Sadi *et al.*, found that RSV treatment normalised the activities of SOD1, SOD2 and GST-Mu in diabetic liver of STZ-induced diabetic rats (Sadi et al., 2015). The proteomics data here support this overall phenomenon and in future, it would be very interesting to probe the function of these enzymes in kidney *in vivo*, especially in the context of the Glo1 inducer treatment.

Peroxiredoxins (PRDX) were also found to be upregulated by Glo1 treatment in the proteomics analyses of MCs. PRDXs are a family of antioxidant enzymes found to be upregulated by Glo1 inducer therapy including PRDX 1,2,3,4,5 & 6, and these enzymes play an important role in regulating cytokine-induced peroxide concentrations in cells and facilitate signal transduction. PRDX 5 has been reported to play a dominant role in protecting against kidney fibrosis via maintaining collagen formation in a rat model of renal fibrosis (Choi et al., 2016).

## 7 Conclusion and further work

### 7.1 Conclusion

This PhD project has been comprised of the following parts:

- (i) To characterise the metabolic function of the glyoxalase system and dicarbonyl metabolism in primary human renal cell cultures models of hyperglycaemia.
- (ii) To study the impact of the Glo1 inducer, tRES-HESP, on human renal cell dysfunction in hyperglycaemia *in vitro*.
- (iii) To characterise quantitatively the intrinsic protein expression profiles of primary human proximal tubular epithelial and mesangial cells via label-free proteomics, also to examine the impact of hyperglycaemic conditions on protein expression.
- (iv) To characterise quantitatively the impact of the Glo1 inducer, tRES-HESP, on the protein expression profiles of the primary proximal tubular epithelial and mesangial cells, both in the context of normoglycaemia and hyperglycaemia.

I studied the effect of hyperglycaemia on glyoxalase enzyme system and metabolism of methylglyoxal in human renal cells through culturing in 25 mM D-glucose. High glucose concentration was linked to a decrease in Glo1 activity and Glo1 protein level, suggesting increased Glo1 degradation under hyperglycaemia. This was supported by increased levels of D-lactate and higher L-lactate formation under high glucose conditions compared to low glucose. High glucose concentration was also characterised by increase glucose uptake by renal cells which was shown in this study. Noteworthy is that Resveratrol (10  $\mu$ M) induced marked growth inhibition in both renal cell types as a key regulator of apoptosis, this supported the important role of Resveratrol in chemoprevention and cancer treatment studies.

Treatment of renal cells, hRPTECs by Glo1 inducers resveratrol and hesperetin (10  $\mu$ M) protected the cells against decrease in the Glo1, Glo2 activity in hyperglycaemia *in vitro*. The treatment did not show any drastic change in D-Glucose consumption and D-lactate formation, while L-lactate formation was shown to be corrected by Glo1 inducer under hyperglycaemic conditions. In MCs, Glo1 inducer was shown to induce both Glo1, Glo2 activities. However, the flux formation of D-lactate as a marker of methylglyoxal was reduced in high glucose primary MCs after treatment with tRSV-HSP. Thus, Glo1 induction may contribute to health and well-being and Glo1 inducers may prevent the development of DKD in patients with diabetes.

In addition, proteomics studies showed that Glo1 inducer treatment upregulated antioxidant enzymes in MCs in normal glucose conditions. With no significant regulation under hyperglycaemia, these findings demonstrated the effective role of Glo1 inducer (tRSV-HSP) in increasing antioxidant activity in the MCs following maintenance of glucose level within the normal range.

Genetic approaches can be used to up- or downregulate Glo1 to induce/inhibit its expression. Glo1 function is known to be compromised in diabetes and its complications. Thus, Glo1 overexpression studies had been carried out using pre-clinical models and showed development in nephropathy, retinopathy and neuropathy complications. One of the genetic studies using Glo1 transgenic mice showed that Glo1 overexpression prevented diabetes-induced MG modification of glomerular proteins, oxidative stress, and the development of DKD (Giacco et al., 2014). Meanwhile in cancer studies, Glo1 was found to be overexpressed and causes resistance to anticancer agents. The silencing of this gene may lead to potent therapeutic agents, using genetic target modulation such as siRNA-Glo1 (Peng et al, 2017b) and CRISPR/Cas9 gene editing technologies (Jandova et al., 2020).

## **7.2 Limitations**

As with all studies, there were certain limitations in this thesis which included the challenge of culturing of the primary cells, conducting large number of replicates reach 16 samples of the four different treatment on the same batch, stock solution stability, long term sample stability (storage) and freeze-thaw stability. However, statistically significant trends were elucidated in the growth dynamics, Glo1 activity and MG flux within key experiments. The thesis also pioneered the use of proteomics analysis for primary human renal cells in the context of Glo1 inducer treatment. While the results showed promising trends in protein expression changes in MCs, the fold changes were largely very subtle – although the identified changes satisfied statistical significance thresholds. It was surprising to not see significant changes in protein expression for Glo1 inducer treatment in the hRPTECs, but this could highlight the possibility that MCs are more responsive to tRSV-HESP, which may be more pharmacologically relevant.

Another surprising observation was the lack of significant change in protein expression observed in the Glo1-inducer study of cells in high glucose conditions. This of course may be due to metabolic shifts in high glucose leading to unresponsiveness to tRSV-HESP, but one other technical factor may be involved. All prototypic proteomics experiments

use trypsin as the gold standard protease for generating peptides for MS analysis, cleaving proteins at Lysine and Arginine sites. However, in high glucose and dicarbonyl stress environments, the possible glycation events might lead to modification of some Lysine and Arginine residues and subsequent changes in peptide signal. A future alternative might be to incorporate protein digestion by Glu-C Protease as a pre-analysis step and calibrate the proteomics analysis accordingly.

### **7.3 Further work**

In this study I studied the effect of hyperglycaemia on primary renal cells (proximal tubular epithelial and mesangial cells) *in vitro* and effective role of Glo1 inducer against dicarbonyl stress. However, I did not examine the protein damage markers and AGEs on these cells under hyperglycaemic conditions. The experiments on renal cells needs to be followed up with further research studying the role of glycation on DKD and it would be fascinating to expand the proteomics work to incorporate samples recovered from *in vivo* material. Finally, it will be crucial to investigate glyoxalase system, Glo1 inducers, dicarbonyl stress and glycation on different cell lines derived from kidney tissues (for example podocytes and also native kidney tissue extracts) and examine its effective role on other kidney diseases – for example glomerulonephritis.

## 8 References

- ABBATE, M., ZOJA, C. & REMUZZI, G. 2006. How does proteinuria cause progressive renal damage? *Journal of the American Society of Nephrology*, 17, 2974-2984.
- ABEDIN, M. & KING, N. 2010. Diverse evolutionary paths to cell adhesion. *Trends in cell biology*, 20, 734-742.
- ABORDO, E. A., MINHAS, H. S. & THORNALLEY, P. J. 1999. Accumulation of  $\alpha$ -oxoaldehydes during oxidative stress: a role in cytotoxicity. *Biochemical pharmacology*, 58, 641-648.
- ADA 2006. Standards of Medical Care in Diabetes–2006. *Diabetes care*, S4-S42.
- ADA 2017. 2. Classification and Diagnosis of Diabetes. *Diabetes Care*, 40, S11-S24.
- ADA 2020a. 2. Classification and Diagnosis of Diabetes: Standards of Medical Care in Diabetes 2020. *Diabetes Care*, 43
- ADA 2020b. 11. Microvascular and : Standards of Medical Care in Diabetes– 2020. *Diabetes Care*, 43, S135-S151.
- AEBERSOLD, R. & MANN, M. 2003. Mass spectrometry-based proteomics. *Nature*, 422, 198-207.
- AGALOU, S., AHMED, N., BABAEI-JADIDI, R., DAWNAY, A. & THORNALLEY, P. J. 2005. Profound mishandling of protein glycation degradation products in uremia and dialysis. *Journal of the American Society of Nephrology*, 16, 1471-1485.
- AHMED, N., AHMED, U., THORNALLEY, P., WATTS, R., TARR, J., HAIGH, R. & WINYARD, P. Profound increase in proteolytic products of glycated and oxidised proteins in synovial fluid and plasma in osteoarthritis and rheumatoid arthritis, corrected by TNF-alpha antibody therapy in rheumatoid arthritis. *Rheumatology*, 2006. OXFORD UNIV PRESS GREAT CLARENDON ST, OXFORD OX2 6DP, ENGLAND, I53-I53.
- AHMED, N., AHMED, U., THORNALLEY, P. J., HAGER, K., FLEISCHER, G. & MÜNCH, G. 2005a. Protein glycation, oxidation and nitration adduct residues and free adducts of cerebrospinal fluid in Alzheimer's disease and link to cognitive impairment. *Journal of neurochemistry*, 92, 255-263.
- AHMED, N., BABAEI-JADIDI, R., HOWELL, S., BEISSWENGER, P. & THORNALLEY, P. 2005b. Degradation products of proteins damaged by glycation, oxidation and nitration in clinical type 1 diabetes. *Diabetologia*, 48, 1590-1603.

- AHMED, N. & THORNALLEY, P. 2007. Advanced glycation endproducts: what is their relevance to diabetic complications? *Diabetes, Obesity and Metabolism*, 9, 233-245.
- AHMED, N., THORNALLEY, P. J., LÜTHEN, R., HÄUSSINGER, D., SEBEKOVA, K., SCHINZEL, R., VOELKER, W. & HEIDLAND, A. 2004. Processing of protein glycation, oxidation and nitrosation adducts in the liver and the effect of cirrhosis. *Journal of hepatology*, 41, 913-919.
- AHMED, U., DOBLER, D., LARKIN, S. J., RABBANI, N. & THORNALLEY, P. J. 2008. Reversal of Hyperglycemia-Induced Angiogenesis Deficit of Human Endothelial Cells by Overexpression of Glyoxalase I In Vitro. *Annals of the New York Academy of Sciences*, 1126, 262-264.
- AKRAM, Z., ALQAHTANI, F., ALQAHTANI, M., AL-KHERAIF, A. A. & JAVED, F. 2020. Levels of advanced glycation end products in gingival crevicular fluid of chronic periodontitis patients with and without type-2 diabetes mellitus. *Journal of periodontology*, 91, 396-402.
- ALBANI, D., POLITO, L., BATELLI, S., DE MAURO, S., FRACASSO, C., MARTELLI, G., COLOMBO, L., MANZONI, C., SALMONA, M. & CACCIA, S. 2009. The SIRT1 activator resveratrol protects SK-N-BE cells from oxidative stress and against toxicity caused by  $\alpha$ -synuclein or amyloid- $\beta$  (1-42) peptide. *Journal of neurochemistry*, 110, 1445-1456.
- ALHOWAISH, A. K. 2013. Economic costs of diabetes in Saudi Arabia. *Journal of Family and Community Medicine*, 20, 1.
- ALI, O. 2010. Type 1 diabetes mellitus: epidemiology, genetics, pathogenesis, and clinical manifestations. In: *PORETSKY, L. (ed.) Principles of Diabetes Mellitus. 2 ed.* New York: Springer US.
- ALLEN, R. E., LO, T. W. & THORNALLEY, P. J. Purification and characterisation of glyoxalase II from human red blood cells. *The FEBS Journal*, 213, 1261-1267.
- ALQERBAN, A. 2021. Levels of proinflammatory chemokines and advanced glycation end products in patients with type-2 diabetes mellitus undergoing fixed orthodontic treatment. *The Angle Orthodontist*, 91, 105-110.
- ALY, T. A., IDE, A., JAHROMI, M. M., BARKER, J. M., FERNANDO, M. S., BABU, S. R., YU, L., MIAO, D., ERLICH, H. A. & FAIN, P. R. 2006. Extreme genetic risk for type 1A diabetes. *Proceedings of the National Academy of Sciences*, 103, 14074-14079.
- ANDERSON, M. M., HAZEN, S. L., HSU, F. F. & HEINECKE, J. W. 1997. Human neutrophils employ the myeloperoxidase-hydrogen peroxide-chloride system to convert hydroxy-amino acids into glycolaldehyde, 2-hydroxypropanal, and acrolein. A mechanism for the generation of highly reactive alpha-hydroxy and alpha,beta-

- unsaturated aldehydes by phagocytes at sites of inflammation. *Journal of Clinical Investigation*, 99, 424-432.
- ANDERSON, N. L. & ANDERSON, N. G. 1998. Proteome and proteomics: new technologies, new concepts, and new words. *Electrophoresis*, 19, 1853-1861.
- ANTHARAVALLY, B. S., MALLIA, K. A., ROSENBLATT, M. M., SALUNKHE, A. M., ROGERS, J. C., HANEY, P. & HAGHDOOST, N. 2011. Efficient removal of detergents from proteins and peptides in a spin column format. *Analytical biochemistry*, 416, 39-44.
- ARAI, M., YUZAWA, H., NOHARA, I., OHNISHI, T., OBATA, N., IWAYAMA, Y., HAGA, S., TOYOTA, T., UJIKE, H. & ARAI, M. 2010. Enhanced carbonyl stress in a subpopulation of schizophrenia. *Archives of general psychiatry*, 67, 589-597.
- ARMSTRONG, D. G., WROBEL, J. & ROBBINS, J. M. 2007. Guest Editorial: are diabetes-related wounds and amputations worse than cancer? *International wound journal*, 4, 286-287.
- ASGARY, S., KARIMI, R., MOMTAZ, S., NASERI, R. & FARZAEI, M. H. 2019. Effect of resveratrol on metabolic syndrome components: A systematic review and meta-analysis. *Reviews in Endocrine and Metabolic Disorders*, 20, 173-186.
- ASHBURNER, J. M., GO, A. S., CHANG, Y., FANG, M. C., FREDMAN, L., APPLEBAUM, K. M. & SINGER, D. E. 2016. Effect of diabetes and glycemic control on ischemic stroke risk in AF patients: ATRIA study. *Journal of the American College of Cardiology*, 67, 239-247.
- ASHOUR, A., XUE, M., AL-MOTAWA, M., THORNALLEY, P. J. & RABBANI, N. 2020. Glycolytic overload-driven dysfunction of periodontal ligament fibroblasts in high glucose concentration, corrected by glyoxalase 1 inducer. *BMJ Open Diabetes Research and Care*, 8, e001458.
- ASWAR, M., KUTE, P., MAHAJAN, S., MAHAJAN, U., NERURKAR, G. & ASWAR, U. 2014. Protective effect of hesperetin in rat model of partial sciatic nerve ligation induced painful neuropathic pain: an evidence of anti-inflammatory and anti-oxidative activity. *Pharmacology Biochemistry and Behavior*, 124, 101-107.
- ATKINSON, M. A., EISENBARTH, G. S. & MICHELS, A. W. 2014. Type 1 diabetes. *The Lancet*, 383, 69-82.
- BABA, S. P., BARSKI, O. A., AHMED, Y., O'TOOLE, T. E., CONKLIN, D. J., BHATNAGAR, A. & SRIVASTAVA, S. 2009. Reductive metabolism of AGE precursors: a metabolic route for preventing AGE accumulation in cardiovascular tissue. *Diabetes*, 58, 2486-2497.



- BAIGENT, C., LANDRAY, M. J., REITH, C., EMBERSON, J., WHEELER, D. C., TOMSON, C., WANNER, C., KRANE, V., CASS, A. & CRAIG, J. 2011. The effects of lowering LDL cholesterol with simvastatin plus ezetimibe in patients with chronic kidney disease (Study of Heart and Renal Protection): a randomised placebo-controlled trial. *The Lancet*, 377, 2181-2192.
- BARAJAS, L. 1997. CELL-SPECIFIC PROTEIN AND GENE EXPRESSION IN THE JUXTAGLOMERULAR APPARATUS. *Clinical and experimental pharmacology and physiology*, 24, 520-526.
- BARATI, M. T., MERCHANT, M. L., KAIN, A. B., JEVANS, A. W., MCLEISH, K. R. & KLEIN, J. B. 2007. Proteomic analysis defines altered cellular redox pathways and advanced glycation end-product metabolism in glomeruli of db/db diabetic mice. *American Journal of Physiology-Renal Physiology*, 293, F1157-F1165.
- BARGER, J. L., KAYO, T., VANN, J. M., ARIAS, E. B., WANG, J., HACKER, T. A., WANG, Y., RAEDERSTORFF, D., MORROW, J. D. & LEEUWENBURGH, C. 2008. A low dose of dietary resveratrol partially mimics caloric restriction and retards aging parameters in mice. *PloS one*, 3, e2264.
- BAUR, J. A., PEARSON, K. J., PRICE, N. L., JAMIESON, H. A., LERIN, C., KALRA, A., PRABHU, V. V., ALLARD, J. S., LOPEZ-LLUCH, G. & LEWIS, K. 2006. Resveratrol improves health and survival of mice on a high-calorie diet. *Nature*, 444, 337-342.
- BAUR, J. A. & SINCLAIR, D. A. 2006. Therapeutic potential of resveratrol: the in vivo evidence. *Nature reviews Drug discovery*, 5, 493-506.
- BAYAR, İ. & BILDIK, A. 2021. Investigation of glucose catabolism in hypoxic Mcf 7 breast cancer culture. *Cytotechnology*, 1-16.
- BELL, S., FLETCHER, E., BRADY, I., LOOKER, H., LEVIN, D., JOSS, N., TRAYNOR, J., METCALFE, W., CONWAY, B. & LIVINGSTONE, S. 2015. Scottish Diabetes Research Network and Scottish Renal Registry. End-stage renal disease and survival in people with diabetes: a national database linkage study. *QJM*, 108, 127-34.
- BENJAMIN, E. J., MUNTNER, P., ALONSO, A., BITTENCOURT, M. S., CALLAWAY, C. W., CARSON, A. P., CHAMBERLAIN, A. M., CHANG, A. R., CHENG, S. & DAS, S. R. 2019. Heart disease and stroke Statistics-2019 update a report from the American Heart Association. *Circulation*, 139, e56-e528.
- BESSHO, R., TAKIYAMA, Y., TAKIYAMA, T., KITSUNAI, H., TAKEDA, Y., SAKAGAMI, H. & OTA, T. 2019. Hypoxia-inducible factor-1 $\alpha$  is the therapeutic target of the SGLT2 inhibitor for diabetic nephropathy. *Scientific reports*, 9, 1-12.
- BEYAN, H., RIESE, H., HAWA, M. I., BERETTA, G., DAVIDSON, H. W., HUTTON, J. C., BURGER, H., SCHLOSSER, M., SNIEDER, H. & BOEHM, B. O. 2012. Glycotoxin

and autoantibodies are additive environmentally determined predictors of type 1 diabetes: a twin and population study. *Diabetes*, 61, 1192-1198.

BHATT, J. K., THOMAS, S. & NANJAN, M. J. 2012. Resveratrol supplementation improves glycemic control in type 2 diabetes mellitus. *Nutrition research*, 32, 537-541.

BIDER-CANFIELD, Z., MARTINEZ, M., WANG, X., YU, W., BAUTISTA, M., BROOKEY, J., PAGE, K., BUCHANAN, T. & XIANG, A. 2017. Maternal obesity, gestational diabetes, breastfeeding and childhood overweight at age 2 years. *Pediatric obesity*, 12, 171-178.

BIERHAUS, A., FLEMING, T., STOYANOV, S., LEFFLER, A., BABES, A., NEACSU, C., SAUER, S. K., EBERHARDT, M., SCHNÖLZER, M. & LASITSCHKA, F. 2012. Methylglyoxal modification of Nav1.8 facilitates nociceptive neuron firing and causes hyperalgesia in diabetic neuropathy. *Nature medicine*, 18, 926-933.

BIERHAUS, A., STOYANOV, S., HAAG, G.-M., KONRADE, I., HUMPERT, P. M., THORNALLEY, P., THORPE, S. R. & NAWROTH, P. P. RAGE-deficiency reduces diabetes-associated impairment of glyoxalase-1 in neuronal cells. *Diabetes*, 2006. AMER DIABETES ASSOC 1701 N BEAUREGARD ST, ALEXANDRIA, VA 22311-1717 USA, A511-A511.

BILOUS, R. 2008. Microvascular disease: what does the UKPDS tell us about diabetic nephropathy? *Diabetic medicine*, 25, 25-29.

BIRKENMEIER, G., STEGEMANN, C., HOFFMANN, R., GÜNTHER, R., HUSE, K. & BIRKEMEYER, C. 2010. Posttranslational modification of human glyoxalase 1 indicates redox-dependent regulation. *PloS one*, 5, e10399.

BODANSKY, H., DEAN, B., BOTTAZZO, G., GRANT, P., MCNALLY, J., HAMBLING, M. & WALES, J. 1986. Islet-cell antibodies and insulin autoantibodies in association with common viral infections. *The Lancet*, 328, 1351-1353.

BÖHM, F. & PERNOW, J. 2007. The importance of endothelin-1 for vascular dysfunction in cardiovascular disease. *Cardiovascular research*, 76, 8-18.

BONDARENKO, P. V., CHELIUS, D. & SHALER, T. A. 2002. Identification and relative quantitation of protein mixtures by enzymatic digestion followed by capillary reversed-phase liquid chromatography– tandem mass spectrometry. *Analytical chemistry*, 74, 4741-4749.

BOOCOCK, D. J., FAUST, G. E., PATEL, K. R., SCHINAS, A. M., BROWN, V. A., DUCHARME, M. P., BOOTH, T. D., CROWELL, J. A., PERLOFF, M. & GESCHER, A. J. 2007. Phase I dose escalation pharmacokinetic study in healthy volunteers of resveratrol, a potential cancer chemopreventive agent. *Cancer Epidemiology and Prevention Biomarkers*, 16, 1246-1252.

- BORA, S., ADOLE, P. S., MOTUPALLI, N., PANDIT, V. R. & VINOD, K. V. 2020. Association between carbonyl stress markers and the risk of acute coronary syndrome in patients with type 2 diabetes mellitus—A pilot study. *Diabetes & Metabolic Syndrome: Clinical Research & Reviews*, 14, 1751-1755.
- BOSMAN, F. T. & STAMENKOVIC, I. 2003. Functional structure and composition of the extracellular matrix. *The Journal of pathology*, 200, 423-428.
- BRADFORD, M. M. 1976. A rapid and sensitive method for the quantitation of microgram quantities of protein utilizing the principle of protein-dye binding. *Analytical biochemistry*, 72, 248-254.
- BRANDT, R. B., SIEGEL, S. A., WATERS, M. G. & BLOCH, M. H. 1980. Spectrophotometric assay for D(-)-lactate in plasma. *Analytical biochemistry*, 102, 39-46.
- BRASNYÓ, P., MOLNÁR, G. A., MOHÁS, M., MARKÓ, L., LACZY, B., CSEH, J., MIKOLÁS, E., SZIJÁRTÓ, I. A., MÉREI, A. & HALMAI, R. 2011. Resveratrol improves insulin sensitivity, reduces oxidative stress and activates the Akt pathway in type 2 diabetic patients. *British Journal of Nutrition*, 106, 383-389.
- BRENNER, B. M., COOPER, M. E., DE ZEEUW, D., KEANE, W. F., MITCH, W. E., PARVING, H.-H., REMUZZI, G., SNAPINN, S. M., ZHANG, Z. & SHAHINFAR, S. 2001. Effects of losartan on renal and cardiovascular outcomes in patients with type 2 diabetes and nephropathy. *New England journal of medicine*, 345, 861-869.
- BROCA, C., VARIN, E., ARMANET, M., TOURREL-CUZIN, C., BOSCO, D., DALLE, S. & WOJTUSCISZYN, A. 2014. Proteasome dysfunction mediates high glucose-induced apoptosis in rodent beta cells and human islets. *PLoS One*, 9, e92066.
- BROPHY, P., CROWLEY, P. & BARRETT, J. 1990. Relative distribution of glutathione transferase, glyoxalase I and glyoxalase II in helminths. *International journal for parasitology*, 20, 259-261.
- BROUWERS, O., NIESSEN, P., HAENEN, G., MIYATA, T., BROWNLEE, M., STEHOUWER, C., DE MEY, J. & SCHALKWIJK, C. 2010. Hyperglycaemia-induced impairment of endothelium-dependent vasorelaxation in rat mesenteric arteries is mediated by intracellular methylglyoxal levels in a pathway dependent on oxidative stress. *Diabetologia*, 53, 989-1000.
- BROUWERS, O., NIESSEN, P. M., FERREIRA, I., MIYATA, T., SCHEFFER, P. G., TEERLINK, T., SCHRAUWEN, P., BROWNLEE, M., STEHOUWER, C. D. & SCHALKWIJK, C. G. 2011. Overexpression of glyoxalase-I reduces hyperglycemia-induced levels of advanced glycation end products and oxidative stress in diabetic rats. *Journal of Biological Chemistry*, 286, 1374-1380.

- BROUWERS, O., NIESSEN, P. M., MIYATA, T., ØSTERGAARD, J. A., FLYVBJERG, A., PEUTZ-KOOTSTRA, C. J., SIEBER, J., MUNDEL, P. H., BROWNLEE, M. & JANSSEN, B. J. 2014. Glyoxalase-1 overexpression reduces endothelial dysfunction and attenuates early renal impairment in a rat model of diabetes. *Diabetologia*, 57, 224-235.
- BROWNLEE, M. 2005. The pathobiology of diabetic complications. *Diabetes*, 54, 1615-1625.
- BURCHFIEL, C. M., CURB, J. D., RODRIGUEZ, B. L., ABBOTT, R. D., CHIU, D. & YANO, K. 1994. Glucose intolerance and 22-year stroke incidence. The Honolulu Heart Program. *Stroke*, 25, 951-957.
- BURNS, J., YOKOTA, T., ASHIHARA, H., LEAN, M. E. & CROZIER, A. 2002. Plant foods and herbal sources of resveratrol. *Journal of agricultural and food chemistry*, 50, 3337-3340.
- BURTON, C. & HARRIS, K. 1996. The role of proteinuria in the progression of chronic renal failure. *American journal of kidney diseases*, 27, 765-775.
- BUSH, P. & NORTON, S. 1985. S-(Nitrocarbonyl) glutathiones: potent competitive inhibitors of mammalian glyoxalase II. *Journal of medicinal chemistry*, 28, 828-830.
- CAMERON, A. D., OLIN, B., RIDDERSTRÖM, M., MANNERVIK, B. & JONES, T. A. 1997. Crystal structure of human glyoxalase I—evidence for gene duplication and 3D domain swapping. *The EMBO Journal*, 16, 3386-3395.
- CAMERON, A. D., RIDDERSTRÖM, M., OLIN, B. & MANNERVIK, B. 1999. Crystal structure of human glyoxalase II and its complex with a glutathione thiolester substrate analogue. *Structure*, 7, 1067-1078.
- CAMPBELL-THOMPSON, M., ATKINSON, M., BUTLER, A., CHAPMAN, N., FRISK, G., GIANANI, R., GIEPMANS, B., VON HERRATH, M., HYÖTY, H. & KAY, T. 2013. The diagnosis of insulinitis in human type 1 diabetes. *Diabetologia*, 56, 2541-2543.
- CAPIRALLA, H., VINGTDEUX, V., ZHAO, H., SANKOWSKI, R., AL-ABED, Y., DAVIES, P. & MARAMBAUD, P. 2012. Resveratrol mitigates lipopolysaccharide- and A $\beta$ -mediated microglial inflammation by inhibiting the TLR4/NF- $\kappa$ B/STAT signaling cascade. *Journal of neurochemistry*, 120, 461-472.
- CARBALLO-VILLALOBOS, A., GONZÁLEZ-TRUJANO, M., ALVARADO-VÁZQUEZ, N. & LÓPEZ-MUÑOZ, F. 2017. Pro-inflammatory cytokines involvement in the hesperidin antihyperalgesic effects at peripheral and central levels in a neuropathic pain model. *Inflammopharmacology*, 25, 265-269.
- CAUCHI, S., EL ACHHAB, Y., CHOQUET, H., DINA, C., KREMPER, F., WEITGASSER, R., NEJJARI, C., PATSCH, W., CHIKRI, M. & MEYRE, D. 2007. TCF7L2 is

reproducibly associated with type 2 diabetes in various ethnic groups: a global meta-analysis. *Journal of molecular medicine*, 85, 777-782.

CHACHAY, V. S., KIRKPATRICK, C. M., HICKMAN, I. J., FERGUSON, M., PRINS, J. B. & MARTIN, J. H. 2011. Resveratrol—pills to replace a healthy diet? *British journal of clinical pharmacology*, 72, 27-38.

CHANG, T. K., CHEN, J. & LEE, W. B. 2001. Differential Inhibition and Inactivation of Human CYP1 Enzymes by trans-Resveratrol: Evidence for Mechanism-Based Inactivation of CYP1A2. *Journal of Pharmacology and Experimental Therapeutics*, 299, 874-882.

CHANG, Y.-T., WU, J.-L., HSU, C.-C., WANG, J.-D. & SUNG, J.-M. 2014. Diabetes and end-stage renal disease synergistically contribute to increased incidence of cardiovascular events: a nationwide follow-up study during 1998–2009. *Diabetes care*, 37, 277-285.

CHANG, Z., YAN, G., YAN, H., ZHENG, J. & LIU, Z. 2019. Reticulocalbin 2 enhances osteogenic differentiation of human vascular smooth muscle cells in diabetic conditions. *Life sciences*, 233, 116746.

CHATTERJEE, S., WEN, J. & CHEN, A. 2013. Electrochemical determination of methylglyoxal as a biomarker in human plasma. *Biosensors and Bioelectronics*, 42, 349-354.

CHELIUS, D. & BONDARENKO, P. V. 2002. Quantitative profiling of proteins in complex mixtures using liquid chromatography and mass spectrometry. *Journal of proteome research*, 1, 317-323.

CHEN, F., WOLLMER, M. A., HOERNDLI, F., MÜNCH, G., KUHLA, B., ROGAEV, E. I., TSOLAKI, M., PAPASSOTIROPOULOS, A. & GÖTZ, J. 2004. Role for glyoxalase I in Alzheimer's disease. *Proceedings of the National Academy of Sciences*, 101, 7687-7692.

CHEN, Y.-J., KONG, L., TANG, Z.-Z., ZHANG, Y.-M., LIU, Y., WANG, T.-Y. & LIU, Y.-W. 2019. Hesperetin ameliorates diabetic nephropathy in rats by activating Nrf2/ARE/glyoxalase 1 pathway. *Biomedicine & Pharmacotherapy*, 111, 1166-1175.

CHENG, A.-S., CHENG, Y.-H., CHIOU, C.-H. & CHANG, T.-L. 2012. Resveratrol upregulates Nrf2 expression to attenuate methylglyoxal-induced insulin resistance in Hep G2 cells. *Journal of agricultural and food chemistry*, 60, 9180-9187.

CHENG, P., LIU, H., LI, Y., PI, P., JIANG, Y., ZANG, S., LI, X., FU, A., REN, X. & XU, J. 2020. Inhibition of thioredoxin reductase 1 correlates with platinum-based chemotherapeutic induced tissue injury. *Biochemical pharmacology*, 175, 113873.

- CHOI, E. J. 2008. Antioxidative effects of hesperetin against 7, 12-dimethylbenz (a) anthracene-induced oxidative stress in mice. *Life sciences*, 82, 1059-1064.
- CHOI, H.-I., MA, S. K., BAE, E. H., LEE, J. & KIM, S. W. 2016. Peroxiredoxin 5 protects TGF- $\beta$  induced fibrosis by inhibiting Stat3 activation in rat kidney interstitial fibroblast cells. *PloS one*, 11, e0149266.
- CHOLEAU, C., MAITRE, J., ELIE, C., BARAT, P., BERTRAND, A., LE, C. T., NICOLINO, M., TUBIANA-RUFI, N., LEVY-MARCHAL, C. & CAHANÉ, M. 2015. Ketoacidosis at time of diagnosis of type 1 diabetes in children and adolescents: effect of a national prevention campaign. *Archives de pediatrie: organe officiel de la Societe francaise de pediatrie*, 22, 343-351.
- CHOU, C.-K., LEE, Y.-T., CHEN, S.-M., HSIEH, C.-W., HUANG, T.-C., LI, Y.-C. & LEE, J.-A. 2015. Elevated urinary D-lactate levels in patients with diabetes and microalbuminuria. *Journal of pharmaceutical and biomedical analysis*, 116, 65-70.
- CHOUDHARY, C., KUMAR, C., GNAD, F., NIELSEN, M. L., REHMAN, M., WALTHER, T. C., OLSEN, J. V. & MANN, M. 2009. Lysine acetylation targets protein complexes and co-regulates major cellular functions. *Science*, 325, 834-840.
- CLELLAND, J. D. & THORNALLEY, P. J. 1991. S-2-hydroxyacylglutathione-derivatives: enzymatic preparation, purification and characterisation. *Journal of the Chemical Society, Perkin Transactions 1*,
- CLUGSTON, SUSAN L., YAJIMA, R. & HONEK, JOHN F. 2004. Investigation of metal binding and activation of Escherichia coli glyoxalase I: kinetic, thermodynamic and mutagenesis studies. *Biochem. J.*, 377, 309.
- COEMANS, M., VAN LOON, E., LERUT, E., GILLARD, P., SPRANGERS, B., SENEV, A., EMONDS, M.-P., VAN KEER, J., CALLEMEYN, J. & DANIÉLS, L. 2019. Occurrence of diabetic nephropathy after renal transplantation despite intensive glycemic control: an observational cohort study. *Diabetes care*, 42, 625-634.
- COHEN, J. S. 2006. Statin therapy after stroke or transient ischemic attack. *The New England journal of medicine*, 355, 2368; 2371.
- COLAFELLA, K. M. M., BOVÉE, D. M. & DANSER, A. J. 2019. The renin-angiotensin-aldosterone system and its therapeutic targets. *Experimental eye research*, 186, 107680.
- CONBOY, C. M., SPYROU, C., THORNE, N. P., WADE, E. J., BARBOSA-MORAIS, N. L., WILSON, M. D., BHATTACHARJEE, A., YOUNG, R. A., TAVARÉ, S. & LEES, J. A. 2007. Cell cycle genes are the evolutionarily conserved targets of the E2F4 transcription factor. *PloS one*, 2, e1061.

- CONNOR, H., WOODS, H. & LEDINGHAM, J. 1983. Comparison of the kinetics and utilisation of D (-)-and L (+)-sodium lactate in normal man. *Annals of nutrition and metabolism*, 27, 481-487.
- CONSTANT, J. 1997. Alcohol, ischemic heart disease, and the French paradox. *Clinical cardiology*, 20, 420-424.
- CORDELL, P. A., FUTERS, T. S., GRANT, P. J. & PEASE, R. J. 2004. The human hydroxyacylglutathione hydrolase (HAGH) gene encodes both cytosolic and mitochondrial forms of glyoxalase II. *Journal of Biological Chemistry*, 279, 28653-28661.
- COUNET, C., CALLEMIEN, D. & COLLIN, S. 2006. Chocolate and cocoa: New sources of trans-resveratrol and trans-piceid. *Food Chemistry*, 98, 649-657.
- CUSI, K., MAEZONO, K., OSMAN, A., PENDERGRASS, M., PATTI, M. E., PRATIPANAWATR, T., DEFRONZO, R. A., KAHN, C. R. & MANDARINO, L. J. 2000. Insulin resistance differentially affects the PI 3-kinase–and MAP kinase–mediated signaling in human muscle. *The Journal of clinical investigation*, 105, 311-320.
- CYBULSKY, A. V., TAKANO, T., PAPILLON, J. & BIJIAN, K. 2005. Role of the endoplasmic reticulum unfolded protein response in glomerular epithelial cell injury. *Journal of Biological Chemistry*, 280, 24396-24403.
- CZAJKA, A. & MALIK, A. N. 2016. Hyperglycemia induced damage to mitochondrial respiration in renal mesangial and tubular cells: Implications for diabetic nephropathy. *Redox biology*, 10, 100-107.
- DABELEA, D., REWERS, A., STAFFORD, J. M., STANDIFORD, D. A., LAWRENCE, J. M., SAYDAH, S., IMPERATORE, G., D'AGOSTINO, R. B., MAYER-DAVIS, E. J. & PIHOKER, C. 2014. Trends in the prevalence of ketoacidosis at diabetes diagnosis: the SEARCH for diabetes in youth study. *Pediatrics*, 133, e938-e945.
- DAI, W., WANG, F., LU, J., XIA, Y., HE, L., CHEN, K., LI, J., LI, S., LIU, T. & ZHENG, Y. 2015. By reducing hexokinase 2, resveratrol induces apoptosis in HCC cells addicted to aerobic glycolysis and inhibits tumor growth in mice. *Oncotarget*, 6, 13703.
- DAKIN, H. & DUDLEY, H. 1913. An enzyme concerned with the formation of hydroxy acids from ketonic aldehydes. *Journal of Biological Chemistry*, 14, 155-157.
- DANAEI, G., FINUCANE, M. M., LU, Y., SINGH, G. M., COWAN, M. J., PACIOREK, C. J., LIN, J. K., FARZADFAR, F., KHANG, Y.-H. & STEVENS, G. A. 2011. National, regional, and global trends in fasting plasma glucose and diabetes prevalence since 1980: systematic analysis of health examination surveys and epidemiological studies with 370 country-years and 2·7 million participants. *The lancet*, 378, 31-40.

- DANIELSSON, A., ÖST, A., LYSTEDT, E., KJOLHEDE, P., GUSTAVSSON, J., NYSTROM, F. H. & STRÅLFORS, P. 2005. Insulin resistance in human adipocytes occurs downstream of IRS1 after surgical cell isolation but at the level of phosphorylation of IRS1 in type 2 diabetes. *The FEBS journal*, 272, 141-151.
- DARLING, T. N. & BLUM, J. J. 1988. D-Lactate production by *Leishmania braziliensis* through the glyoxalase pathway. *Molecular and biochemical parasitology*, 28, 121-127.
- DCCT 1993. The effect of intensive treatment of diabetes on the development and progression of long-term complications in insulin-dependent diabetes mellitus. *New England journal of medicine*, 329, 977-986.
- DE HEMPTINNE, V., RONDAS, D., TOEPOEL, M. & VANCOMPERNOLLE, K. 2009. Phosphorylation on Thr-106 and NO-modification of glyoxalase I suppress the TNF-induced transcriptional activity of NF- $\kappa$ B. *Molecular and cellular biochemistry*, 325, 169-178.
- DE HEMPTINNE, V., RONDAS, D., VANDEKERCKHOVE, J. & VANCOMPERNOLLE, K. 2007. Tumour necrosis factor induces phosphorylation primarily of the nitric-oxide-responsive form of glyoxalase I. *Biochemical Journal*, 407, 121-128.
- DE HOFFMANN, E. & STROOBANT, V. 2007. Tandem mass spectrometry. *Mass spectrometry principles and applications, 3rd Edition, John Wiley & Sons Ltd., West Sussex, England*, 189-215.
- DE LIGT, M., BERGMAN, M., FUENTES, R. M., ESSERS, H., MOONEN-KORNIPS, E., HAVEKES, B., SCHRAUWEN-HINDERLING, V. B. & SCHRAUWEN, P. 2020. No effect of resveratrol supplementation after 6 months on insulin sensitivity in overweight adults: a randomized trial. *The American journal of clinical nutrition*, 112, 1029-1038.
- DE VRESE, M. & BARTH, C. 1991. Postprandial plasma D-lactate concentrations after yogurt ingestion. *Zeitschrift für Ernährungswissenschaft*, 30, 131-137.
- DE VRIESE, A. S., VERBEUREN, T. J., VAN DE VOORDE, J., LAMEIRE, N. H. & VANHOUTTE, P. M. 2000. Endothelial dysfunction in diabetes. *British journal of pharmacology*, 130, 963-974.
- DE ZEEUW, D., AGARWAL, R., AMDAHL, M., AUDHYA, P., COYNE, D., GARIMELLA, T., PARVING, H.-H., PRITCHETT, Y., REMUZZI, G. & RITZ, E. 2010. Selective vitamin D receptor activation with paricalcitol for reduction of albuminuria in patients with type 2 diabetes (VITAL study): a randomised controlled trial. *The Lancet*, 376, 1543-1551.
- DE ZEEUW, D. & HEERSPINK, H. J. 2016. Unmet need in diabetic nephropathy: failed drugs or trials? *The Lancet Diabetes & Endocrinology*, 4, 638-640.



- DEFRONZO, R., FLEMING, G. A., CHEN, K. & BICSAK, T. A. 2016. Metformin-associated lactic acidosis: current perspectives on causes and risk. *Metabolism*, 65, 20-29.
- DELPierre, G., RIDER, M. H., COLLARD, F., STROOBANT, V., VANSTAPEL, F., SANTOS, H. & VAN SCHAFTINGEN, E. 2000. Identification, cloning, and heterologous expression of a mammalian fructosamine-3-kinase. *Diabetes*, 49, 1627-1634.
- DEMARIN, V., LOVRENČIĆ-HUZJAN, A., TRKANJEC, Z., VUKOVIĆ, V., VARGEK SOLTER, V., ŠERIĆ, V., LUŠIĆ, I., KADOJIĆ, D., BIELEN, I. & TUŠKAN-MOHAR, L. 2006. Recommendations for stroke management 2006 update. *Acta Clinica Croatica*, 45, 219-285.
- DHANYA, R. & JAYAMURTHY, P. 2020. In vitro evaluation of antidiabetic potential of hesperidin and its aglycone hesperetin under oxidative stress in skeletal muscle cell line. *Cell biochemistry and function*, 38, 419-427.
- DI PINO, A., CURRENTI, W., URBANO, F., SCICALI, R., PIRO, S., PURRELLO, F. & RABUAZZO, A. 2017. High intake of dietary advanced glycation end-products is associated with increased arterial stiffness and inflammation in subjects with type 2 diabetes. *Nutrition, Metabolism and Cardiovascular Diseases*, 27, 978-984.
- DI ZHANG, J.-Y. Z., DAI, S.-D., LIU, S.-L., LIU, Y., TANG, N. & WANG, E.-H. 2014. Co-expression of delta-catenin and RhoA is significantly associated with a malignant lung cancer phenotype. *International journal of clinical and experimental pathology*, 7, 3724.
- DIANA SHERIFALI, R. & ROBYN, L. 2018. Diabetes Canada clinical practice guidelines expert committee. *Canadian Journal of Diabetes*, 42, S6-S9.
- DING, H.-W., HUANG, A.-L., ZHANG, Y.-L., LI, B., HUANG, C., MA, T.-T., MENG, X.-M. & LI, J. 2017. Design, synthesis and biological evaluation of hesperetin derivatives as potent anti-inflammatory agent. *Fitoterapia*, 121, 212-222.
- DO, G. M., JUNG, U. J., PARK, H. J., KWON, E. Y., JEON, S. M., MCGREGOR, R. A. & CHOI, M. S. 2012. Resveratrol ameliorates diabetes-related metabolic changes via activation of AMP-activated protein kinase and its downstream targets in db/db mice. *Molecular nutrition & food research*, 56, 1282-1291.
- DOBLER, D., AHMED, N., SONG, L., EBOIGBODIN, K. E. & THORNALLEY, P. J. 2006. Increased dicarbonyl metabolism in endothelial cells in hyperglycemia induces anoikis and impairs angiogenesis by RGD and GFOGER motif modification. *Diabetes*, 55, 1961-1969.
- DONNELLY, R., EMSLIE-SMITH, A. M., GARDNER, I. D. & MORRIS, A. D. 2000. ABC of arterial and venous disease: vascular complications of diabetes. *BMJ*, 320, 1062-6.

- DRAGANI, B., COCCO, R., RIDDERSTRÖM, M., STENBERG, G., MANNERVIK, B. & ACETO, A. 1999. Unfolding and refolding of human glyoxalase II and its single-tryptophan mutants. *Journal of molecular biology*, 291, 481-490.
- DRONAVALLI, S., DUKA, I. & BAKRIS, G. L. 2008. The pathogenesis of diabetic nephropathy. *Nature clinical practice Endocrinology & metabolism*, 4, 444-452.
- DRURY, D. R. & WICK, A. N. 1965. Chemistry and metabolism of L (+) and D (-) lactic acids. *Annals of the New York Academy of Sciences*, 119, 1061-1069.
- DUPUIS, J., LANGENBERG, C., PROKOPENKO, I., SAXENA, R., SORANZO, N., JACKSON, A. U., WHEELER, E., GLAZER, N. L., BOUATIA-NAJI, N. & GLOYN, A. L. 2010. New genetic loci implicated in fasting glucose homeostasis and their impact on type 2 diabetes risk. *Nature genetics*, 42, 105-116.
- DUTTON, G. R. & LEWIS, C. E. 2015. The Look AHEAD Trial: implications for lifestyle intervention in type 2 diabetes mellitus. *Progress in cardiovascular diseases*, 58, 69-75.
- EFSA 2016. Safety of synthetic trans-resveratrol as a novel food pursuant to Regulation (EC) No 258/97. *EFSA Journal*, 14, 4368.
- EISENBARTH, G. S. 1986. Type I diabetes mellitus. *New England journal of medicine*, 314, 1360-1368.
- EKNOYAN, G., LAMEIRE, N., ECKARDT, K., KASISKE, B., WHEELER, D., LEVIN, A., STEVENS, P., BILOUS, R., LAMB, E. & CORESH, J. 2013. KDIGO 2012 clinical practice guideline for the evaluation and management of chronic kidney disease. *Kidney Int*, 3, 5-14.
- EMBDEN, G., DEUTICKE, H. J., AND KRAFT, G. 1932. *Ober die intermediären Vorgänge bei der Glykolyse in der Muskulatur*, Klin. Wochensh. 12,213-215.
- EWASCHUK, J. B., NAYLOR, J. M. & ZELLO, G. A. 2005. D-lactate in human and ruminant metabolism. *The Journal of nutrition*, 135, 1619-1625.
- FAN, X., SELL, D. R., ZHANG, J., NEMET, I., THEVES, M., LU, J., STRAUCH, C., HALUSHKA, M. K. & MONNIER, V. M. 2010. Anaerobic vs aerobic pathways of carbonyl and oxidant stress in human lens and skin during aging and in diabetes: A comparative analysis. *Free Radical Biology and Medicine*, 49, 847-856.
- FANG, X., SCHUMMER, M., MAO, M., YU, S., TABASSAM, F. H., SWABY, R., HASEGAWA, Y., TANYI, J. L., LAPUSHIN, R., EDER, A., JAFFE, R., ERICKSON, J. & MILLS, G. B. 2002. Lysophosphatidic acid is a bioactive mediator in ovarian

- cancer. *Biochimica et Biophysica Acta (BBA) - Molecular and Cell Biology of Lipids*, 1582, 257-264.
- FARVID, M. S., HOMAYOUNI, F., AMIRI, Z. & ADELMANESH, F. 2011. Improving neuropathy scores in type 2 diabetic patients using micronutrients supplementation. *Diabetes research and clinical practice*, 93, 86-94.
- FELDMAN, E. L., CALLAGHAN, B. C., POP-BUSUI, R., ZOCHODNE, D. W., WRIGHT, D. E., BENNETT, D. L., BRIL, V., RUSSELL, J. W. & VISWANATHAN, V. 2019. Diabetic neuropathy. *Nature Reviews Disease Primers*, 5, 1-18.
- FENG, X., LIU, X., LUO, Q. & LIU, B. F. 2008. Mass spectrometry in systems biology: an overview. *Mass spectrometry reviews*, 27, 635-660.
- FENG, Y., JIN, M.-Y., LIU, D.-W. & WEI, L. 2018. Proteasome subunit- $\alpha$  type-6 protein is post-transcriptionally repressed by the microRNA-4490 in diabetic nephropathy. *Bioscience reports*, 38.
- FENN, J. B., MANN, M., MENG, C. K., WONG, S. F. & WHITEHOUSE, C. M. 1989. Electrospray ionization for mass spectrometry of large biomolecules. *Science*, 246, 64-71.
- FICEK, J., WYSKIDA, K., FICEK, R., WAJDA, J., KLEIN, D., WITKOWICZ, J., ROTKEGEL, S., SPIECHOWICZ-ZATON, U., KOCEMBA-DYCZEK, J. & CIEPAŁ, J. 2017. Relationship between plasma levels of zonulin, bacterial lipopolysaccharides, D-lactate and markers of inflammation in haemodialysis patients. *International urology and nephrology*, 49, 717-725.
- FINCK, B. N., HAN, X., COURTOIS, M., AIMOND, F., NERBONNE, J. M., KOVACS, A., GROSS, R. W. & KELLY, D. P. 2003. A critical role for PPAR $\alpha$ -mediated lipotoxicity in the pathogenesis of diabetic cardiomyopathy: modulation by dietary fat content. *Proceedings of the National Academy of Sciences*, 100, 1226-1231.
- FINEBERG, D., JANDELEIT-DAHM, K. A. & COOPER, M. E. 2013. Diabetic nephropathy: diagnosis and treatment. *Nature Reviews Endocrinology*, 9, 713-723.
- FIORETTO, P., STEFFES, M. W., BARBOSA, J., RICH, S. S., MILLER, M. E. & MAUER, M. 1999. Is diabetic nephropathy inherited? Studies of glomerular structure in type 1 diabetic sibling pairs. *Diabetes*, 48, 865-9.
- FONG, D. S., AIELLO, L., GARDNER, T. W., KING, G. L., BLANKENSHIP, G., CAVALLERANO, J. D., FERRIS, F. L. & KLEIN, R. 2004. Retinopathy in diabetes. *Diabetes care*, 27, s84-s87.

- FONSECA, V. & JOHN-KALARICKAL, J. 2010. Type 2 diabetes mellitus: epidemiology, genetics, pathogenesis, and clinical manifestations. *In: PORETSKY, L. (ed.) Principles of diabetes mellitus*. 2nd ed. New York: Springer.
- FORBES, J. M. & COOPER, M. E. 2013. Mechanisms of diabetic complications. *Physiological reviews*, 93, 137-188.
- FOWLER, M. J. 2011. Microvascular and macrovascular complications of diabetes. *Clinical Diabetes*, 29, 116-122.
- FRANCIOSO, A., LAŠTOVIČKOVÁ, L., MOSCA, L., BOFFI, A., BONAMORE, A. & MACONE, A. 2019. Gas Chromatographic–Mass Spectrometric Method for the Simultaneous Determination of Resveratrol Isomers and 2, 4, 6-Trihydroxyphenanthrene in Red Wines Exposed to UV-Light. *Journal of agricultural and food chemistry*, 67, 11752-11757.
- FUJITA, H., OMORI, S., ISHIKURA, K., HIDA, M. & AWAZU, M. 2004. ERK and p38 mediate high-glucose-induced hypertrophy and TGF- $\beta$  expression in renal tubular cells. *American Journal of Physiology-Renal Physiology*, 286, F120-F126.
- GARCIA-HERMOSO, A., SAAVEDRA, J. M., ESCALANTE, Y., SANCHEZ-LOPEZ, M. & MARTINEZ-VIZCAINO, V. 2014. Endocrinology and adolescence: aerobic exercise reduces insulin resistance markers in obese youth: a meta-analysis of randomized controlled trials. *European journal of endocrinology*, 171, R163-R171.
- GARCIA-MORALES, E., LAZARO-MARTINEZ, J., MARTINEZ-HERNANDEZ, D., ARAGÓN-SÁNCHEZ, J., BENEIT-MONTESINOS, J. & GONZÁLEZ-JURADO, M. 2011. Impact of diabetic foot related complications on the Health Related Quality of Life (HRQol) of patients-a regional study in Spain. *The international journal of lower extremity wounds*, 10, 6-11.
- GENOVESE, F., MANRESA, A. A., LEEMING, D. J., KARSDAL, M. A. & BOOR, P. 2014. The extracellular matrix in the kidney: a source of novel non-invasive biomarkers of kidney fibrosis? *Fibrogenesis & tissue repair*, 7, 1-14.
- GEOFFRION, M., DU, X., IRSHAD, Z., VANDERHYDEN, B. C., COURVILLE, K., SUI, G., D'AGATI, V. D., OTT-BRASCHI, S., RABBANI, N. & THORNALLEY, P. J. 2014. Differential effects of glyoxalase 1 overexpression on diabetic atherosclerosis and renal dysfunction in streptozotocin-treated, apolipoprotein E-deficient mice. *Physiological reports*, 2, e12043.
- GEPTS, W. & LECOMPTE, P. M. 1981. The pancreatic islets in diabetes. *The American journal of medicine*, 70, 105-115.
- GERSTEIN, H., MILLER, M., BYINGTON, R., GOFF, D. J., BIGGER, J., BUSE, J., CUSHMAN, W., GENUTH, S., ISMAIL-BEIGI, F. & GRIMM, R. J. 2008. Action to

Control Cardiovascular Risk in Diabetes Study, Group. *Effects of intensive glucose lowering in type 2, 2545-59.*

GIACCO, F., DU, X., D'AGATI, V. D., MILNE, R., SUI, G., GEOFFRION, M. & BROWNLEE, M. 2014. Knockdown of glyoxalase 1 mimics diabetic nephropathy in nondiabetic mice. *Diabetes*, 63, 291-299.

GIOVANNA, L., FRANCESCA, V. & ROBERTO, P. 2012. RAAS inhibition and renal protection. *Current pharmaceutical design*, 18, 971-980.

GIUNTI, S., BARIT, D. & COOPER, M. E. 2006. Mechanisms of diabetic nephropathy. *Hypertension*, 48, 519-526.

GO, A. S., CHERTOW, G. M., FAN, D., MCCULLOCH, C. E. & HSU, C.-Y. 2004. Chronic kidney disease and the risks of death, cardiovascular events, and hospitalization. *New England Journal of Medicine*, 351, 1296-1305.

GOH, K. P., LEE, H. Y., LAU, D. P., SUPAAT, W., CHAN, Y. H. & KOH, A. F. Y. 2014. Effects of resveratrol in patients with type 2 diabetes mellitus on skeletal muscle SIRT1 expression and energy expenditure. *International journal of sport nutrition and exercise metabolism*, 24, 2-13.

GOLDBERG, D. M., YAN, J., NG, E., DIAMANDIS, E. P., KARUMANCHIRI, A., SOLEAS, G. & WATERHOUSE, A. L. 1995. A global survey of trans-resveratrol concentrations in commercial wines. *American journal of enology and viticulture*, 46, 159-165.

GORDIN, D., SHAH, H., SHINJO, T., ST-LOUIS, R., QI, W., PARK, K., PANIAGUA, S. M., POBER, D. M., WU, I.-H. & BAHNAM, V. 2019. Characterization of glycolytic enzymes and pyruvate kinase M2 in type 1 and 2 diabetic nephropathy. *Diabetes care*, 42, 1263-1273.

GORSKI, M., VAN DER MOST, P. J., TEUMER, A., CHU, A. Y., LI, M., MIJATOVIC, V., NOLTE, I. M., COCCA, M., TALIUN, D. & GOMEZ, F. 2017. 1000 Genomes-based meta-analysis identifies 10 novel loci for kidney function. *Scientific reports*, 7, 1-11.

GUERIN-DUBOURG, A., COURNOT, M., PLANESSE, C., DEBUSSCHE, X., MEILHAC, O., RONDEAU, P. & BOURDON, E. 2017. Association between fluorescent advanced glycation end-products and vascular complications in type 2 diabetic patients. *BioMed research international*, 2017.

GUNDERSON, E., GREENSPAN, L., FAITH, M., HURSTON, S., QUESENBERRY JR, C. & INVESTIGATORS, S. O. S. 2018. Breastfeeding and growth during infancy among offspring of mothers with gestational diabetes mellitus: a prospective cohort study. *Pediatric obesity*, 13, 492-504.

- HA, H. & LEE, H. B. 2005. Reactive oxygen species amplify glucose signalling in renal cells cultured under high glucose and in diabetic kidney. *Nephrology*, 10, S7-S10.
- HAMBLETON, I. R., JONNALAGADDA, R., DAVIS, C. R., FRASER, H. S., CHATURVEDI, N. & HENNIS, A. J. 2009. All-cause mortality after diabetes-related amputation in Barbados: a prospective case-control study. *Diabetes care*, 32, 306-307.
- HAMBSCH, B., CHEN, B. G., BRENNDÖRFER, J., MEYER, M., AVRABOS, C., MACCARRONE, G., LIU, R. H., EDER, M., TURCK, C. W. & LANDGRAF, R. 2010. Methylglyoxal-mediated anxiolysis involves increased protein modification and elevated expression of glyoxalase 1 in the brain. *Journal of neurochemistry*, 113, 1240-1251.
- HAN, H. J., LEE, Y. J., PARK, S. H., LEE, J. H. & TAUB, M. 2005. High glucose-induced oxidative stress inhibits Na<sup>+</sup>/glucose cotransporter activity in renal proximal tubule cells. *American Journal of Physiology-Renal Physiology*, 288, F988-F996.
- HAN, J., ZHANG, L., GUO, H., WYSHAM, W. Z., ROQUE, D. R., WILLSON, A. K., SHENG, X., ZHOU, C. & BAE-JUMP, V. L. 2015. Glucose promotes cell proliferation, glucose uptake and invasion in endometrial cancer cells via AMPK/mTOR/S6 and MAPK signaling. *Gynecologic oncology*, 138, 668-675.
- HAN, P., WANG, Y., ZHAN, H., WENG, W., YU, X., GE, N., WANG, W., SONG, G., YI, T. & LI, S. 2019. Artemether ameliorates type 2 diabetic kidney disease by increasing mitochondrial pyruvate carrier content in db/db mice. *American journal of translational research*, 11, 1389.
- HÄNNINEN, A., JALKANEN, S., SALMI, M., TOIKKANEN, S., NIKOLAKAROS, G. & SIMELL, O. 1992. Macrophages, T cell receptor usage, and endothelial cell activation in the pancreas at the onset of insulin-dependent diabetes mellitus. *The Journal of clinical investigation*, 90, 1901-1910.
- HANSEN, H. P., TAUBER-LASSEN, E., JENSEN, B. R. & PARVING, H.-H. 2002. Effect of dietary protein restriction on prognosis in patients with diabetic nephropathy. *Kidney international*, 62, 220-228.
- HAR, R., SCHOLEY, J., DANEMAN, D., MAHMUD, F., DEKKER, R., LAI, V., ELIA, Y., FRITZLER, M., SOCHETT, E. & REICH, H. 2013. The effect of renal hyperfiltration on urinary inflammatory cytokines/chemokines in patients with uncomplicated type 1 diabetes mellitus. *Diabetologia*, 56, 1166-1173.
- HARIKUMAR, K. B. & AGGARWAL, B. B. 2008. Resveratrol: a multitargeted agent for age-associated chronic diseases. *Cell cycle*, 7, 1020-1035.
- HASHEMI-SOTEH, M. B., AMIRI, A. A., REZAEI, M. R. S., AMIRI, A. A., AHRARI, R., AMIRI, A. A. & DANESHVAR, F. 2020. Evaluation of glutathione S-transferase

polymorphism in Iranian patients with type 2 diabetic microangiopathy. *Egyptian Journal of Medical Human Genetics*, 21, 1-8.

HAUSENBLAS, H. A., SCHOULDA, J. A. & SMOLIGA, J. M. 2015. Resveratrol treatment as an adjunct to pharmacological management in type 2 diabetes mellitus—systematic review and meta-analysis. *Molecular nutrition & food research*, 59, 147-159.

HEIDARI, F., RABIZADEH, S., RAJAB, A., HEIDARI, F., MOUODI, M., MIRMIRANPOUR, H., ESTEGHAMATI, A. & NAKHJAVANI, M. 2020. Advanced glycation end-products and advanced oxidation protein products levels are correlates of duration of type 2 diabetes. *Life Sciences*, 260, 118422.

HELMKE, K., OTTEN, A., WILLEMS, W., BROCKHAUS, R., MUELLER-ECKHARDT, G., STIEF, T., BERTRAMS, J., WOLF, H. & FEDERLIN, K. 1986. Islet cell antibodies and the development of diabetes mellitus in relation to mumps infection and mumps vaccination. *Diabetologia*, 29, 30-33.

HENRIKSEN, E. J., DIAMOND-STANIC, M. K. & MARCHIONNE, E. M. 2011. Oxidative stress and the etiology of insulin resistance and type 2 diabetes. *Free Radical Biology and Medicine*, 51, 993-999.

HIMO, F. & SIEGBAHN, P. E. 2001. Catalytic mechanism of glyoxalase I: a theoretical study. *Journal of the American Chemical Society*, 123, 10280-10289.

HO, F. M., LIU, S. H., LIAU, C. S., HUANG, P. J. & LIN-SHIAU, S. Y. 2000. High glucose-induced apoptosis in human endothelial cells is mediated by sequential activations of c-Jun NH2-terminal kinase and caspase-3. *Circulation*, 101, 2618-2624.

HOFFMAN, W. H., ISHIKAWA, T., BLUM, J., TANI, N., IKEDA, T. & ARTLETT, C. M. 2020. Soluble Receptor for Glycation End-products Concentration Increases Following the Treatment of Severe Diabetic Ketoacidosis. *Journal of clinical research in pediatric endocrinology*, 12, 160.

HOLMAN, R. R., PAUL, S. K., BETHEL, M. A., MATTHEWS, D. R. & NEIL, H. A. W. 2008. 10-year follow-up of intensive glucose control in type 2 diabetes. *New England Journal of Medicine*, 359, 1577-1589.

HOLT, R. I., COCKRAM, C., FLYVBJERG, A. & GOLDSTEIN, B. J. 2011. *Textbook of diabetes*, John Wiley & Sons.

HONEYMAN, M. C., COULSON, B. S., STONE, N. L., GELLERT, S. A., GOLDWATER, P. N., STEELE, C. E., COUPER, J. J., TAIT, B. D., COLMAN, P. G. & HARRISON, L. C. 2000. Association between rotavirus infection and pancreatic islet autoimmunity in children at risk of developing type 1 diabetes. *Diabetes*, 49, 1319-1324.

- HOOPER, N., TISDALE, M. & THORNALLEY, P. 1987. Glyoxalase activity during differentiation of human leukaemia cells in vitro. *Leukemia research*, 11, 1141-1148.
- HOOPER, N. I., TISDALE, M. J. & THORNALLEY, P. J. 1988. Modification of the glyoxalase system in human HL60 promyelocytic leukemia cells during differentiation to neutrophils in vitro. *Biochimica et Biophysica Acta (BBA)-General Subjects*, 966, 362-369.
- HOPE, S. V., WIENAND-BARNETT, S., SHEPHERD, M., KING, S. M., FOX, C., KHUNTI, K., ORAM, R. A., KNIGHT, B. A., HATTERSLEY, A. T. & JONES, A. G. 2016. Practical Classification Guidelines for Diabetes in patients treated with insulin: a cross-sectional study of the accuracy of diabetes diagnosis. *British Journal of General Practice*, 66, e315-e322.
- HOPKINS, F. G. & MORGAN, E. 1945. On the distribution of glyoxalase and glutathione. *Biochemical Journal*, 39, 320.
- HOVE, H. 1998. Lactate and short-chain fatty acid production in the human colon: implications for D-lactic acidosis, shortbowel syndrome, antibiotic-associated diarrhea, colonic cancer, and inflammatory bowel disease. *Dan. Med. Bull.*, 45, 15-33.
- HU, Y., TENG, W., LIU, L., CHEN, K., LIU, L., HUA, R., CHEN, J., ZHOU, Y. & CHEN, L. 2015. Prevalence and risk factors of diabetes and diabetic retinopathy in Liaoning province, China: a population-based cross-sectional study. *PloS one*, 10, e0121477.
- HUANG, B., WU, P., POPOV, K. M. & HARRIS, R. A. 2003. Starvation and diabetes reduce the amount of pyruvate dehydrogenase phosphatase in rat heart and kidney. *Diabetes*, 52, 1371-1376.
- HUDSON, T. S., HARTLE, D. K., HURSTING, S. D., NUNEZ, N. P., WANG, T. T., YOUNG, H. A., ARANY, P. & GREEN, J. E. 2007. Inhibition of prostate cancer growth by muscadine grape skin extract and resveratrol through distinct mechanisms. *Cancer Research*, 67, 8396-8405.
- HUMPHREYS, A., BRAVIS, V., KAUR, A., WALKEY, H. C., GODSLAND, I. F., MISRA, S., JOHNSTON, D. G. & OLIVER, N. S. 2019. Individual and diabetes presentation characteristics associated with partial remission status in children and adults evaluated up to 12 months following diagnosis of type 1 diabetes: an ADDRESS-2 (After Diagnosis Diabetes Research Support System-2) study analysis. *Diabetes research and clinical practice*, 155, 107789.
- HURST, W. J., GLINSKI, J. A., MILLER, K. B., APGAR, J., DAVEY, M. H. & STUART, D. A. 2008. Survey of the trans-resveratrol and trans-piceid content of cocoa-containing and chocolate products. *Journal of agricultural and food chemistry*, 56, 8374-8378.
- HWANG, P. T., KWON, O.-D., KIM, H.-J., KIM, B.-G., KIM, S.-H., JANG, Y.-W., KIM, P.-K., HAN, G.-Y. & KIM, C.-W. 2013. Hyperglycemia decreases the expression of ATP



- synthase  $\beta$  subunit and enolase 2 in glomerular epithelial cells. *The Tohoku journal of experimental medicine*, 231, 45-56.
- HYÖTY, H. & TAYLOR, K. 2002. The role of viruses in human diabetes. *Diabetologia*, 45, 1353-1361.
- IDF 2019. IDF Diabetes Atlas. 9th ed. Brussels, Belgium. *International Diabetes Federation*.
- IDF 2020. International Diabetes Federation. Diabetes and cardiovascular disease.
- IDO, Y., CARLING, D. & RUDERMAN, N. 2002. Hyperglycemia-induced apoptosis in human umbilical vein endothelial cells: inhibition by the AMP-activated protein kinase activation. *Diabetes*, 51, 159-167.
- IMAMURA, M., TAKAHASHI, A., YAMAUCHI, T., HARA, K., YASUDA, K., GRARUP, N., ZHAO, W., WANG, X., HUERTA-CHAGOYA, A. & HU, C. 2016. Genome-wide association studies in the Japanese population identify seven novel loci for type 2 diabetes. *Nature communications*, 7, 1-12.
- INOUE, Y. & KIMURA, A. 1992. Purification and characterization of glyoxalase II from *Hansenula mrakii*. *Journal of fermentation and bioengineering*, 73, 271-276.
- ISKENDER, H., DOKUMACIOGLU, E., SEN, T. M., INCE, I., KANBAY, Y. & SARAL, S. 2017. The effect of hesperidin and quercetin on oxidative stress, NF- $\kappa$ B and SIRT1 levels in a STZ-induced experimental diabetes model. *Biomedicine & pharmacotherapy*, 90, 500-508.
- IZAGUIRRE, G., KIKONYOGO, A. & PIETRUSZKO, R. 1998. Methylglyoxal as substrate and inhibitor of human aldehyde dehydrogenase: comparison of kinetic properties among the three isozymes. *Comparative Biochemistry and Physiology Part B: Biochemistry and Molecular Biology*, 119, 747-754.
- JANDOVA, J., PERER, J., HUA, A., SNELL, J.A. & WONDRAK, G.T., 2020. Genetic target modulation employing CRISPR/Cas9 identifies glyoxalase 1 as a novel molecular determinant of invasion and metastasis in A375 human malignant melanoma cells in vitro and in vivo. *Cancers*, 12(6), p.1369.
- JAHAN, S., SINGH, S., SRIVASTAVA, A., KUMAR, V., KUMAR, D., PANDEY, A., RAJPUROHIT, C., PUROHIT, A., KHANNA, V. & PANT, A. 2018. PKA-GSK3 $\beta$  and  $\beta$ -catenin signaling play a critical role in trans-resveratrol mediated neuronal differentiation in human cord blood stem cells. *Molecular Neurobiology*, 55, 2828-2839.
- JAIN, M. & PARMAR, H. S. 2011. Evaluation of antioxidative and anti-inflammatory potential of hesperidin and naringin on the rat air pouch model of inflammation. *Inflammation Research*, 60, 483-491.

- JAMES, P. A., OPARIL, S., CARTER, B. L., CUSHMAN, W. C., DENNISON-HIMMELFARB, C., HANDLER, J., LACKLAND, D. T., LEFEVRE, M. L., MACKENZIE, T. D. & OGEDEGBE, O. 2014. 2014 evidence-based guideline for the management of high blood pressure in adults: report from the panel members appointed to the Eighth Joint National Committee (JNC 8). *Jama*, 311, 507-520.
- JOWETT, M. & QUASTEL, J. H. 1933. The glyoxalase activity of the red blood cell: the function of glutathione. *Biochemical Journal*, 27, 486.
- JU, Y., SU, Y., CHEN, Q., MA, K., JI, T., WANG, Z., LI, W. & LI, W. 2019. Protective effects of Astragaloside IV on endoplasmic reticulum stress-induced renal tubular epithelial cells apoptosis in type 2 diabetic nephropathy rats. *Biomedicine & Pharmacotherapy*, 109, 84-92.
- JUNG, H., JOO, J., JEON, Y., LEE, J., IN, J., KIM, D., KANG, E., KIM, Y., LIM, Y., KANG, J. & CHOI, J. 2011. Advanced glycation end products downregulate glucokinase in mice. *Diabetes/Metabolism Research and Reviews*, 27, 557-563.
- JUNG, U. J., LEE, M.-K., JEONG, K.-S. & CHOI, M.-S. 2004. The hypoglycemic effects of hesperidin and naringin are partly mediated by hepatic glucose-regulating enzymes in C57BL/KsJ-db/db mice. *The Journal of nutrition*, 134, 2499-2503.
- KANAZE, F., BOUNARTZI, M., GEORGARAKIS, M. & NIOPAS, I. 2007. Pharmacokinetics of the citrus flavanone aglycones hesperetin and naringenin after single oral administration in human subjects. *European journal of clinical nutrition*, 61, 472-477.
- KANG, M., KANG, E., RYU, H., HONG, Y., HAN, S. S., PARK, S. K., HYUN, Y. Y., SUNG, S. A., KIM, S. W. & YOO, T.-H. 2021. Measured sodium excretion is associated with CKD progression: results from the KNOW-CKD study. *Nephrology Dialysis Transplantation*, 36, 512-519.
- KAPRIO, J., TUOMILEHTO, J., KOSKENVUO, M., ROMANOV, K., REUNANEN, A., ERIKSSON, J., STENGÅRD, J. & KESÄNIEMI, Y. 1992. Concordance for type 1 (insulin-dependent) and type 2 (non-insulin-dependent) diabetes mellitus in a population-based cohort of twins in Finland. *Diabetologia*, 35, 1060-1067.
- KARACHALIAS, N., BABAEI-JADIDI, R., AHMED, N. & THORNALLEY, P. 2003. Accumulation of fructosyl-lysine and advanced glycation end products in the kidney, retina and peripheral nerve of streptozotocin-induced diabetic rats. *Biochemical Society Transactions*, 31, 1423-1425.
- KARACHALIAS, N., BABAEI-JADIDI, R., RABBANI, N. & THORNALLEY, P. J. 2010. Increased protein damage in renal glomeruli, retina, nerve, plasma and urine and its prevention by thiamine and benfotiamine therapy in a rat model of diabetes. *Diabetologia*, 53, 1506-1516.

- KARACHALIAS, N., BABEI-JADIDI, R., AHMED, N., BAYNES, K. & THORNALLEY, P. 2005. Urinary D-lactate as a marker of biochemical dysfunction linked to the development of diabetic microvascular complications: A80. *Diabetic Medicine*, 22.
- KARAS, M., BACHMANN, D., BAHR, U. & HILLENKAMP, F. 1987. Matrix-assisted ultraviolet laser desorption of non-volatile compounds. *International journal of mass spectrometry and ion processes*, 78, 53-68.
- KARAS, M. & HILLENKAMP, F. 1988. Laser desorption ionization of proteins with molecular masses exceeding 10,000 daltons. *Analytical chemistry*, 60, 2299-2301.
- KAZEMIRAD, H. & KAZERANI, H. R. 2020. Cardioprotective effects of resveratrol following myocardial ischemia and reperfusion. *Molecular Biology Reports*, 47, 5843-5850.
- KELLEY, D. E., MINTUN, M. A., WATKINS, S. C., SIMONEAU, J.-A., JADALI, F., FREDRICKSON, A., BEATTIE, J. & THÉRIAULT, R. 1996. The effect of non-insulin-dependent diabetes mellitus and obesity on glucose transport and phosphorylation in skeletal muscle. *The Journal of clinical investigation*, 97, 2705-2713.
- KENNEDY, A., OVERMAN, A., LAPOINT, K., HOPKINS, R., WEST, T., CHUANG, C.-C., MARTINEZ, K., BELL, D. & MCINTOSH, M. 2009. Conjugated linoleic acid-mediated inflammation and insulin resistance in human adipocytes are attenuated by resveratrol. *Journal of lipid research*, 50, 225-232.
- KERTES, P. J. & JOHNSON, T. M. 2007. *Evidence-based eye care*, Lippincott Williams & Wilkins.
- KESSNER, D., CHAMBERS, M., BURKE, R., AGUS, D. & MALLICK, P. 2008. ProteoWizard: open source software for rapid proteomics tools development. *Bioinformatics*, 24, 2534-2536.
- KHAN, M. K. 2014. Zill-E-Huma, Dangles O. A comprehensive review on flavanones, the major citrus polyphenols. *Journal of Food Composition and Analysis*, 33, 85-104.
- KIM, H. S. 2020. Risk of Stroke according to the Duration of Diabetes Mellitus with Hypertension. *Korean Journal of Clinical Laboratory Science*, 52, 188-193.
- KIM, N.-S., SEKINE, S., KIUCHI, N. & KATO, S. 1995. cDNA cloning and characterization of human glyoxalase I isoforms from HT-1080 cells. *The Journal of Biochemistry*, 117, 359-361.
- KISSELA, B. M., KHOURY, J., KLEINDORFER, D., WOO, D., SCHNEIDER, A., ALWELL, K., MILLER, R., EWING, I., MOOMAW, C. J. & SZAFLARSKI, J. P.

2005. Epidemiology of ischemic stroke in patients with diabetes: the greater Cincinnati/Northern Kentucky Stroke Study. *Diabetes care*, 28, 355-359.
- KNIGHT, B. A., SHIELDS, B. M., BROOK, A., HILL, A., BHAT, D. S., HATTERSLEY, A. T. & YAJNIK, C. S. 2015. Lower circulating B12 is associated with higher obesity and insulin resistance during pregnancy in a non-diabetic white British population. *PLoS One*, 10, e0135268.
- KONDOH, Y., KAWASE, M., KAWAKAMI, Y. & OHMORI, S. 1992a. Concentrations of D-lactate and its related metabolic intermediates in liver, blood, and muscle of diabetic and starved rats. *Research in experimental medicine*, 192, 407-414.
- KONDOH, Y., KAWASE, M. & OHMORI, S. 1992b. D-lactate concentrations in blood, urine and sweat before and after exercise. *European journal of applied physiology and occupational physiology*, 65, 88-93.
- KOSKA, J., SAREMI, A., HOWELL, S., BAHN, G., DE COURTEN, B., GINSBERG, H., BEISSWENGER, P. J. & REAVEN, P. D. 2018. Advanced glycation end products, oxidation products, and incident cardiovascular events in patients with type 2 diabetes. *Diabetes care*, 41, 570-576.
- KOUSHKI, M., DASHATAN, N. A. & MESHKANI, R. 2018. Effect of resveratrol supplementation on inflammatory markers: a systematic review and meta-analysis of randomized controlled trials. *Clinical therapeutics*, 40, 1180-1192. e5.
- KRUSZYNSKA, Y. T. & OLEFSKY, J. M. 1996. Cellular and molecular mechanisms of non-insulin dependent diabetes mellitus. *Journal of investigative medicine: the official publication of the American Federation for Clinical Research*, 44, 413-428.
- KURZ, A., RABBANI, N., WALTER, M., BONIN, M., THORNALLEY, P., AUBURGER, G. & GISPERT, S. 2011. Alpha-synuclein deficiency leads to increased glyoxalase I expression and glycation stress. *Cellular and Molecular Life Sciences*, 68, 721-733.
- KWAK, M.-K., WAKABAYASHI, N., ITOH, K., MOTOHASHI, H., YAMAMOTO, M. & KENSLER, T. W. 2003. Modulation of gene expression by cancer chemopreventive dithiolethiones through the Keap1-Nrf2 pathway Identification of novel gene clusters for cell survival. *Journal of Biological Chemistry*, 278, 8135-8145.
- LAAKSO, M. & KUUSISTO, J. 2014. Insulin resistance and hyperglycaemia in cardiovascular disease development. *Nature Reviews Endocrinology*, 10, 293-302.
- LAGOUGE, M., ARGMANN, C., GERHART-HINES, Z., MEZIANE, H., LERIN, C., DAUSSIN, F., MESSADEQ, N., MILNE, J., LAMBERT, P. & ELLIOTT, P. 2006. Resveratrol improves mitochondrial function and protects against metabolic disease by activating SIRT1 and PGC-1 $\alpha$ . *Cell*, 127, 1109-1122.

- LAGRANHA, C. J., FIORINO, P., CASARINI, D. E., SCHAAN, B. D. A. & IRIGOYEN, M. C. 2007. Molecular bases of diabetic nephropathy. *Arquivos Brasileiros de Endocrinologia & Metabologia*, 51, 901-912.
- LAIOS, K., KARAMANOU, M., SARIDAKI, Z. & ANDROUTSOS, G. 2012. Aretaeus of Cappadocia and the first description of diabetes. *Hormones*, 11, 109-113.
- LAITEERAPONG, N., KARTER, A. J., LIU, J. Y., MOFFET, H. H., SUDORE, R., SCHILLINGER, D., JOHN, P. M. & HUANG, E. S. 2011. Correlates of quality of life in older adults with diabetes: the diabetes & aging study. *Diabetes care*, 34, 1749-1753.
- LAL, S., RANDALL, W. C., TAYLOR, A. H., KAPPLER, F., WALKER, M., BROWN, T. R. & SZWERGOLD, B. S. 1997. Fructose-3-phosphate production and polyol pathway metabolism in diabetic rat hearts. *Metabolism*, 46, 1333-1338.
- LANE, R., HARWOOD, A., WATSON, L. & LENG, G. C. 2017. Exercise for intermittent claudication. *Cochrane Database of Systematic Reviews*.
- LANSDOWN, A. J., BARTON, J., WARNER, J., WILLIAMS, D., GREGORY, J. W., HARVEY, J., LOWES, L. & GROUP, B. 2012. Prevalence of ketoacidosis at diagnosis of childhood onset Type 1 diabetes in Wales from 1991 to 2009 and effect of a publicity campaign. *Diabetic medicine*, 29, 1506-1509.
- LARKIN, J. R., ZHANG, F., GODFREY, L., MOLOSTVOV, G., ZEHNDER, D., RABBANI, N. & THORNALLEY, P. J. 2012. Glucose-induced down regulation of thiamine transporters in the kidney proximal tubular epithelium produces thiamine insufficiency in diabetes. *PLoS One*, 7, e53175.
- LARSEN, K., ARONSSON, A.-C., MARMSTÅL, E. & MANNERVIK, B. 1985. Immunological comparison of glyoxalase I from yeast and mammals and quantitative determination of the enzyme in human tissues by radioimmunoassay. *Comparative biochemistry and physiology. B, Comparative biochemistry*, 82, 625-638.
- LEAHY, J. L. 2005. Pathogenesis of type 2 diabetes mellitus. *Archives of medical research*, 36, 197-209.
- LEE, J.-H., SONG, M.-Y., SONG, E.-K., KIM, E.-K., MOON, W. S., HAN, M.-K., PARK, J.-W., KWON, K.-B. & PARK, B.-H. 2009. Overexpression of SIRT1 protects pancreatic  $\beta$ -cells against cytokine toxicity by suppressing the nuclear factor- $\kappa$ B signaling pathway. *Diabetes*, 58, 344-351.
- LEE, M., SAVER, J. L., HONG, K.-S., SONG, S., CHANG, K.-H. & OVBIAGELE, B. 2012. Effect of pre-diabetes on future risk of stroke: meta-analysis. *Bmj*, 344.

- LEE, S.-M., YANG, H., TARTAR, D., GAO, B., LUO, X., YE, S., ZAGHOUBANI, H. & FANG, D. 2011. Prevention and treatment of diabetes with resveratrol in a non-obese mouse model of type 1 diabetes. *Diabetologia*, 54, 1136-1146.
- LEU, J. P. & ZONSZEIN, J. 2010. Diagnostic criteria and classification of diabetes. *Principles of diabetes mellitus*. Springer.
- LEVEY, A. & INKER, L. 2017. Assessment of glomerular filtration rate in health and disease: a state of the art review. *Clinical Pharmacology & Therapeutics*, 102, 405-419.
- LEWIS, G. & MAXWELL, A. 2014. Risk factor control is key in diabetic nephropathy. *The Practitioner*, 258, 13-7, 2.
- LI, C. & SCHLUESENER, H. 2017. Health-promoting effects of the citrus flavanone hesperidin. *Critical reviews in food science and nutrition*, 57, 613-631.
- LI, M., ZHANG, Y., ZHAI, Q., FEURINO, L. W., FISHER, W. E., CHEN, C. & YAO, Q. 2009. Thymosin beta-10 is aberrantly expressed in pancreatic cancer and induces JNK activation. *Cancer investigation*, 27, 251-256.
- LI, Q., PARK, K., LI, C., RASK-MADSEN, C., MIMA, A., QI, W., MIZUTANI, K., HUANG, P. & KING, G. L. 2013a. Induction of vascular insulin resistance and endothelin-1 expression and acceleration of atherosclerosis by the overexpression of protein kinase C- $\beta$  isoform in the endothelium. *Circulation research*, 113, 418-427.
- LI, W., MA, J., MA, Q., LI, B., HAN, L., LIU, J., XU, Q., DUAN, W., YU, S. & WANG, F. 2013b. Resveratrol inhibits the epithelial-mesenchymal transition of pancreatic cancer cells via suppression of the PI-3K/Akt/NF- $\kappa$ B pathway. *Current medicinal chemistry*, 20, 4185-4194.
- LI, X., WANG, L. & MA, H. 2019a. Betaine alleviates high glucose-induced mesangial cell proliferation by inhibiting cell proliferation and extracellular matrix deposition via the AKT/ERK1/2/p38 MAPK pathway. *Molecular medicine reports*, 20, 1754-1760.
- LI, Y., KANDHARE, A. D., MUKHERJEE, A. A. & BODHANKAR, S. L. 2019b. Acute and sub-chronic oral toxicity studies of hesperidin isolated from orange peel extract in Sprague Dawley rats. *Regulatory Toxicology and Pharmacology*, 105, 77-85.
- LIMPHONG, P., MCKINNEY, R. M., ADAMS, N. E., BENNETT, B., MAKAROFF, C. A., GUNASEKERA, T. & CROWDER, M. W. 2009. Human glyoxalase II contains an Fe (II) Zn (II) center but is active as a mononuclear Zn (II) enzyme. *Biochemistry*, 48, 5426-5434.
- LIN, C.-Y., HSIAO, W.-C., WRIGHT, D. E., HSU, C.-L., LO, Y.-C., HSU, G.-S. W. & KAO, C.-F. 2013. Resveratrol activates the histone H2B ubiquitin ligase, RNF20, in MDA-MB-231 breast cancer cells. *Journal of Functional Foods*, 5, 790-800.

- LIPPI, G., FRANCHINI, M., FAVALORO, E. J. & TARGHER, G. Moderate red wine consumption and cardiovascular disease risk: beyond the “French paradox”. *Seminars in thrombosis and hemostasis*, 2010. Thieme Medical Publishers, 059-070.
- LIU, H., SADYGOV, R. G. & YATES, J. R. 2004. A model for random sampling and estimation of relative protein abundance in shotgun proteomics. *Analytical chemistry*, 76, 4193-4201.
- LIU, H., ZHANG, S., ZHAO, L., ZHANG, Y., LI, Q., CHAI, X. & ZHANG, Y. 2016. Resveratrol enhances cardiomyocyte differentiation of human induced pluripotent stem cells through inhibiting canonical WNT signal pathway and enhancing serum response factor-miR-1 Axis. *Stem cells international*, 2016.
- LIU, W. J., SHEN, T. T., CHEN, R. H., WU, H.-L., WANG, Y. J., DENG, J. K., CHEN, Q. H., PAN, Q., FU, C.-M. H. & TAO, J.-L. 2015. Autophagy-lysosome pathway in renal tubular epithelial cells is disrupted by advanced glycation end products in diabetic nephropathy. *Journal of Biological Chemistry*, 290, 20499-20510.
- LIU, Y., SUN, Z., XU, D., LIU, J., LI, X., WU, X., ZHANG, Y., WANG, Q., HUANG, C. & MENG, X. 2017. Hesperidin derivative-11 inhibits fibroblast-like synoviocytes proliferation by activating Secreted frizzled-related protein 2 in adjuvant arthritis rats. *European journal of pharmacology*, 794, 173-183.
- LIYANAGE, T., NINOMIYA, T., JHA, V., NEAL, B., PATRICE, H. M., OKPECHI, I., ZHAO, M.-H., LV, J., GARG, A. X. & KNIGHT, J. 2015. Worldwide access to treatment for end-stage kidney disease: a systematic review. *The Lancet*, 385, 1975-1982.
- LO, T. W., SELWOOD, T. & THORNALLEY, P. J. 1994. The reaction of methylglyoxal with aminoguanidine under physiological conditions and prevention of methylglyoxal binding to plasma proteins. *Biochemical pharmacology*, 48, 1865-1870.
- LO, T. W. & THORNALLEY, P. J. 1992. Inhibition of proliferation of human leukaemia 60 cells by diethyl esters of glyoxalase inhibitors in vitro. *Biochemical pharmacology*, 44, 2357-2363.
- LOHMANN, K. 1932. A study of the enzymatic transformation of synthetic methylglyoxal to lactic acid. *Biochem. Z*, 254, 332-354.
- LOIDL-STÄHLHOFEN, A. & SPITELIER, G. 1994.  $\alpha$ -Hydroxyaldehydes, products of lipid peroxidation. *Biochimica et Biophysica Acta (BBA) - Lipids and Lipid Metabolism*, 1211, 156-160.
- LOWRY, O. H., ROSEBROUGH, N. J., FARR, A. L. & RANDALL, R. J. 1951. Protein measurement with the Folin phenol reagent. *Journal of biological chemistry*, 193, 265-275.

- LUCAS, I. K. & KOLODZIEJ, H. 2015. Trans-resveratrol induces apoptosis through ROS-triggered mitochondria-dependent pathways in A549 human lung adenocarcinoma epithelial cells. *Planta medica*, 81, 1038-1044.
- LYLES, G. A. & CHALMERS, J. 1992. The metabolism of aminoacetone to methylglyoxal by semicarbazide-sensitive amine oxidase in human umbilical artery. *Biochemical pharmacology*, 43, 1409-1414.
- LYONS, M. M., YU, C., TOMA, R., CHO, S. Y., REIBOLDT, W., LEE, J. & VAN BREEMEN, R. B. 2003. Resveratrol in raw and baked blueberries and bilberries. *Journal of Agricultural and Food Chemistry*, 51, 5867-5870.
- MA, Y., YAN, R., WAN, Q., LV, B., YANG, Y., LV, T. & XIN, W. 2020. Inhibitor of growth 2 regulates the high glucose-induced cell cycle arrest and epithelial-to-mesenchymal transition in renal proximal tubular cells. *Journal of physiology and biochemistry*, 76, 373-382.
- MACARULLA, M., ALBERDI, G., GÓMEZ, S., TUEROS, I., BALD, C., RODRÍGUEZ, V., MARTÍNEZ, J. & PORTILLO, M. 2009. Effects of different doses of resveratrol on body fat and serum parameters in rats fed a hypercaloric diet. *Journal of physiology and biochemistry*, 65, 369-376.
- MACHADO, U. F., SCHAAN, B. D. & SERAPHIM, P. M. 2006. Glucose transporters in the metabolic syndrome. *Arquivos brasileiros de endocrinologia e metabologia*, 50, 177-189.
- MACHOWSKA, A., SUN, J., QURESHI, A. R., ISOYAMA, N., LEURS, P., ANDERSTAM, B., HEIMBURGER, O., BARANY, P., STENVINKEL, P. & LINDHOLM, B. 2016. Plasma pentosidine and its association with mortality in patients with chronic kidney disease. *PLoS one*, 11, e0163826.
- MACLEOD, A. K., MCMAHON, M., PLUMMER, S. M., HIGGINS, L. G., PENNING, T. M., IGARASHI, K. & HAYES, J. D. 2009. Characterization of the cancer chemopreventive NRF2-dependent gene battery in human keratinocytes: demonstration that the KEAP1–NRF2 pathway, and not the BACH1–NRF2 pathway, controls cytoprotection against electrophiles as well as redox-cycling compounds. *Carcinogenesis*, 30, 1571-1580.
- MAHAJAN, A., TALIUN, D., THURNER, M., ROBERTSON, N. R., TORRES, J. M., RAYNER, N. W., PAYNE, A. J., STEINTHORSDDOTTIR, V., SCOTT, R. A. & GRARUP, N. 2018. Fine-mapping type 2 diabetes loci to single-variant resolution using high-density imputation and islet-specific epigenome maps. *Nature genetics*, 50, 1505-1513.
- MAHAVADI, S., SRIWAI, W., MANION, O., GRIDER, J. R. & MURTHY, K. S. 2017. Diabetes-induced oxidative stress mediates upregulation of RhoA/Rho kinase pathway and hypercontractility of gastric smooth muscle. *PloS one*, 12, e0178574.



- MAHMOUD, A. M. 2014. Hesperidin protects against cyclophosphamide-induced hepatotoxicity by upregulation of PPAR $\gamma$  and abrogation of oxidative stress and inflammation. *Canadian journal of physiology and pharmacology*, 92, 717-724.
- MALLIKA, P., TAN, A., AZIZ, S., ASOK, T., ALWI, S. S. & INTAN, G. 2010. Diabetic retinopathy and the effect of pregnancy. *Malaysian family physician: the official journal of the Academy of Family Physicians of Malaysia*, 5, 2.
- MALLONE, R. & VAN ENDERT, P. 2008. T cells in the pathogenesis of type 1 diabetes. *Current diabetes reports*, 8, 101-106.
- MANACH, C., MORAND, C., GIL-IZQUIERDO, A., BOUTELOUP-DEMANGE, C. & REMESY, C. 2003. Bioavailability in humans of the flavanones hesperidin and naringin after the ingestion of two doses of orange juice. *European journal of clinical nutrition*, 57, 235-242.
- MANTHEY, J. A. & GROHMANN, K. 1998. Flavonoids of the orange subfamily Aurantioideae. *Flavonoids in the Living System*, 85-101.
- MASANIA, J., MALCZEWSKA-MALEC, M., RAZNY, U., GORALSKA, J., ZDZIENICKA, A., KIEC-WILK, B., GRUCA, A., STANCEL-MOZWILLO, J., DEMBINSKA-KIEC, A. & RABBANI, N. 2016. Dicarbonyl stress in clinical obesity. *Glycoconjugate Journal*, 33, 581-589.
- MASON, R. M. & WAHAB, N. A. 2003. Extracellular matrix metabolism in diabetic nephropathy. *Journal of the American Society of Nephrology*, 14, 1358-1373.
- MASSON, E., WIERNSPERGER, N., LAGARDE, M. & BAWAB, S. E. 2005. Glucosamine induces cell-cycle arrest and hypertrophy of mesangial cells: implication of gangliosides. *Biochemical Journal*, 388, 537-544.
- MCCANCE, D. R., DYER, D. G., DUNN, J. A., BAILIE, K. E., THORPE, S. R., BAYNES, J. W. & LYONS, T. J. 1993. Maillard reaction products and their relation to complications in insulin-dependent diabetes mellitus. *The Journal of clinical investigation*, 91, 2470-2478.
- MCDONALD, S. P., MARSHALL, M. R., JOHNSON, D. W. & POLKINGHORNE, K. R. 2009. Relationship between dialysis modality and mortality. *Journal of the American Society of Nephrology*, 20, 155-163.
- MCLELLAN, A., PHILLIPS, S. & THORNALLEY, P. 1992. Fluorimetric assay of D-lactate. *Analytical biochemistry*, 206, 12-16.
- MCLELLAN, A. C., PHILLIPS, S. A. & THORNALLEY, P. J. 1993. The assay of SD-lactoylglutathione in biological systems. *Analytical biochemistry*, 211, 37-43.

- MCLELLAN, A. C. & THORNALLEY, P. J. 1991. Optimisation of non-denaturing polyacrylamide gel electrophoretic analysis of glyoxalase I phenotypes in clinical blood samples. *Clinica chimica acta*, 204, 137-143.
- MCLELLAN, A. C. & THORNALLEY, P. J. 1992. Synthesis and chromatography of 1, 2-diamino-4, 5-dimethoxybenzene, 6, 7-dimethoxy-2-methylquinoxaline and 6, 7-dimethoxy-2, 3-dimethylquinoxaline for use in a liquid chromatographic fluorimetric assay of methylglyoxal. *Analytica chimica acta*, 263, 137-142.
- MCLELLAN, A. C., THORNALLEY, P. J., BENN, J. & SONKSEN, P. H. 1994. Glyoxalase system in clinical diabetes mellitus and correlation with diabetic complications. *Clinical Science*, 87, 21-29.
- MEGGER, D. A., BRACHT, T., MEYER, H. E. & SITEK, B. 2013. Label-free quantification in clinical proteomics. *Biochimica et Biophysica Acta (BBA)-Proteins and Proteomics*, 1834, 1581-1590.
- MÉNDEZ-DEL VILLAR, M., GONZALEZ-ORTIZ, M., MARTÍNEZ-ABUNDIS, E., PEREZ-RUBIO, K. G. & LIZARRAGA-VALDEZ, R. 2014. Effect of resveratrol administration on metabolic syndrome, insulin sensitivity, and insulin secretion. *Metabolic syndrome and related disorders*, 12, 497-501.
- MEYERHOF, O. 1933. Intermediate products and the last stages of carbohydrate breakdown in the metabolism of muscle and in alcoholic fermentation. *Nature*, 132, 337-340.
- MILNE, J. C., LAMBERT, P. D., SCHENK, S., CARNEY, D. P., SMITH, J. J., GAGNE, D. J., JIN, L., BOSS, O., PERNI, R. B. & VU, C. B. 2007. Small molecule activators of SIRT1 as therapeutics for the treatment of type 2 diabetes. *Nature*, 450, 712-716.
- MINER, J. H. 2012. The glomerular basement membrane. *Experimental cell research*, 318, 973-978.
- MONDER, C. 1967.  $\alpha$ -Keto aldehyde dehydrogenase, an enzyme that catalyzes the enzymic oxidation of methylglyoxal to pyruvate. *Journal of Biological Chemistry*, 242, 4603-4609.
- MORCOS, M., DU, X., HUTTER, A., PFISTERER, F., THORNALLEY, P., BAYNES, J., THORPE, S., EL BAKI, R., AHMED, N. & MIFTARI, N. Life extension in *Caenorhabditis elegans* by overexpression of glyoxalase I-The connection to protein damage by glycation, oxidation and nitration. *Free Radical Research*, 2005. TAYLOR & FRANCIS LTD S43-S43.
- MORTENSEN, P. B., HOVE, H., CLAUSEN, M. R. & HOLTUG, K. 1991. Fermentation to short-chain fatty acids and lactate in human faecal batch cultures intra-and inter-individual variations versus variations caused by changes in fermented saccharides. *Scandinavian journal of gastroenterology*, 26, 1285-1294.

- MOUSAVI, S. B., TAVAZOE, M., HAYATI, F. & SAMETZADEH, M. 2010. Arterio-Venous fistula recirculation in hemodialysis: causes and prevalences. *Shiraz E Medical Journal*, 11, 219-224.
- MOUSAVI, S. S. B., ANSARI, M. J. A. & CHERAGHIAN, B. 2011. Outcome of patients on haemodialysis in Khuzestan, Iran. *NDT plus*, 4, 143.
- MOVAHED, A., NABIPOUR, I., LIEBEN LOUIS, X., THANDAPILLY, S. J., YU, L., KALANTARHORMOZI, M., REKABPOUR, S. J. & NETTICADAN, T. 2013. Antihyperglycemic effects of short term resveratrol supplementation in type 2 diabetic patients. *Evidence-Based complementary and alternative medicine*, 2013.
- MURATA, K., INOUE, Y., SAIKUSA, T., WATANABE, K., FUKUDA, Y., MAKOTO, S. & KIMURA, A. 1986. Metabolism of  $\alpha$ -ketoaldehydes in yeasts: Inducible formation of methylglyoxal reductase and its relation to growth arrest of *Saccharomyces cerevisiae*. *Journal of fermentation technology*, 64, 1-4.
- NAJAFIAN, B., FOGO, A. B., LUSCO, M. A. & ALPERS, C. E. 2015. AJKD atlas of renal pathology: Diabetic nephropathy. *American Journal of Kidney Diseases*, 66, e37-e38.
- NAJAFIAN, B. & MAUER, M. 2009. Progression of diabetic nephropathy in type 1 diabetic patients. *Diabetes research and clinical practice*, 83, 1-8.
- NAKAMURA, T., USHIYAMA, C., SUZUKI, S., HARA, M., SHIMADA, N., EBIHARA, I. & KOIDE, H. 2000. Urinary excretion of podocytes in patients with diabetic nephropathy. *Nephrology Dialysis Transplantation*, 15, 1379-1383.
- NATH, K. A. 1992. Tubulointerstitial changes as a major determinant in the progression of renal damage. *American Journal of Kidney Diseases*, 20, 1-17.
- NEHRING, I., CHMITORZ, A., REULEN, H., VON KRIES, R. & ENSENAUER, R. 2013. Gestational diabetes predicts the risk of childhood overweight and abdominal circumference independent of maternal obesity. *Diabetic medicine*, 30, 1449-1456.
- NEMET, I., VARGA-DEFTERDAROVIC, L. & TURK, Z. 2006. Methylglyoxal in food and living organisms. *Molecular nutrition & food research*, 50, 1105-1117.
- NESVIZHSHKII, A. I., KELLER, A., KOLKER, E. & AEBERSOLD, R. 2003. A statistical model for identifying proteins by tandem mass spectrometry. *Analytical chemistry*, 75, 4646-4658.
- NEUBERG, C. 1913. The destruction of lactic aldehyde and methylglyoxal by animal organs. *Biochem Z*, 49, 502-506.
- NEUBERG, C. & KOBEL, M. 1929. Die isolierung von methylglyoxal bei der Milchsäuregärung. *Biochem. Z*, 207, 232-262.

- NEWTON, C. A. & RASKIN, P. 2004. Diabetic ketoacidosis in type 1 and type 2 diabetes mellitus: clinical and biochemical differences. *Archives of internal medicine*, 164, 1925-1931.
- NEZU, U., KAMIYAMA, H., KONDO, Y., SAKUMA, M., MORIMOTO, T. & UEDA, S. 2013. Effect of low-protein diet on kidney function in diabetic nephropathy: meta-analysis of randomised controlled trials. *BMJ open*, 3.
- NG, M. C., SHRINER, D., CHEN, B. H., LI, J., CHEN, W.-M., GUO, X., LIU, J., BIELINSKI, S. J., YANEK, L. R. & NALLS, M. A. 2014. Meta-analysis of genome-wide association studies in African Americans provides insights into the genetic architecture of type 2 diabetes. *PLoS Genet*, 10, e1004517.
- NISHIMURA, C., FURUE, M., ITO, T., OMORI, Y. & TANIMOTO, T. 1993. Quantitative determination of human aldose reductase by enzyme-linked immunosorbent assay: Immunoassay of human aldose reductase. *Biochemical pharmacology*, 46, 21-28.
- NISHINAKA, T. & YABE-NISHIMURA, C. 2005. Transcription factor Nrf2 regulates promoter activity of mouse aldose reductase (AKR1B3) gene. *Journal of pharmacological sciences*, 97, 43-51.
- NOBLE, J. A. & VALDES, A. M. 2011. Genetics of the HLA region in the prediction of type 1 diabetes. *Current diabetes reports*, 11, 533.
- NORGREN, L., HIATT, W. R., DORMANDY, J. A., NEHLER, M. R., HARRIS, K. A. & FOWKES, F. G. R. 2007. Inter-society consensus for the management of peripheral arterial disease (TASC II). *Journal of vascular surgery*, 45, S5-S67.
- OH, M. S., URIBARRI, J., ALVERANGA, D., LAZAR, I., BAZILINSKI, N. & CARROLL, H. J. 1985. Metabolic utilization and renal handling of D-lactate in men. *Metabolism*, 34, 621-625.
- OHMORI, S. & IWAMOTO, T. 1988. Sensitive determination of D-lactic acid in biological samples by high-performance liquid chromatography. *Journal of Chromatography B: Biomedical Sciences and Applications*, 431, 239-247.
- OHMORI, S., NOSE, Y., OGAWA, H., TSUYAMA, K., HIROTA, T., GOTO, H., YANO, Y., KONDOH, Y., NAKATA, K. & TSUBOI, S. 1991. Fluorimetric and high-performance liquid chromatographic determination of D-lactate in biological samples. *Journal of Chromatography B: Biomedical Sciences and Applications*, 566, 1-8.
- ONG, S.-E. & MANN, M. 2005. Mass spectrometry-based proteomics turns quantitative. *Nature chemical biology*, 1, 252-262.

- ORSO, F., CORÀ, D., UBEZIO, B., PROVERO, P., CASELLE, M. & TAVERNA, D. 2010. Identification of functional TFAP2A and SP1 binding sites in new TFAP2A-modulated genes. *BMC genomics*, 11, 1-26.
- OZOUGWU, J., OBIMBA, K., BELONWU, C. & UNAKALAMBA, C. 2013. The pathogenesis and pathophysiology of type 1 and type 2 diabetes mellitus. *Journal of Physiology and Pathophysiology*, 4, 46-57.
- PACE-ASCIAK, C. R., HAHN, S., DIAMANDIS, E. P., SOLEAS, G. & GOLDBERG, D. M. 1995. The red wine phenolics trans-resveratrol and quercetin block human platelet aggregation and eicosanoid synthesis: implications for protection against coronary heart disease. *Clinica chimica acta*, 235, 207-219.
- PAK, C., MCARTHUR, R., EUN, H.-M. & YOON, J.-W. 1988. Association of cytomegalovirus infection with autoimmune type 1 diabetes. *The Lancet*, 332, 1-4.
- PALMER, N. D., MCDONOUGH, C. W., HICKS, P. J., ROH, B. H., WING, M. R., AN, S. S., HESTER, J. M., COOKE, J. N., BOSTROM, M. A. & RUDOCK, M. E. 2012. A genome-wide association search for type 2 diabetes genes in African Americans. *PLoS one*, 7, e29202.
- PALSAMY, P. & SUBRAMANIAN, S. 2009. Modulatory effects of resveratrol on attenuating the key enzymes activities of carbohydrate metabolism in streptozotocin–nicotinamide-induced diabetic rats. *Chemico-biological interactions*, 179, 356-362.
- PALSAMY, P. & SUBRAMANIAN, S. 2010. Ameliorative potential of resveratrol on proinflammatory cytokines, hyperglycemia mediated oxidative stress, and pancreatic  $\beta$ -cell dysfunction in streptozotocin-nicotinamide-induced diabetic rats. *Journal of cellular physiology*, 224, 423-432.
- PALSAMY, P. & SUBRAMANIAN, S. 2011. Resveratrol protects diabetic kidney by attenuating hyperglycemia-mediated oxidative stress and renal inflammatory cytokines via Nrf2–Keap1 signaling. *Biochimica et Biophysica Acta (BBA)-Molecular Basis of Disease*, 1812, 719-731.
- PANCHAUD, A., AFFOLTER, M., MOREILLON, P. & KUSSMANN, M. 2008. Experimental and computational approaches to quantitative proteomics: status quo and outlook. *Journal of proteomics*, 71, 19-33.
- PAPADEMETRIOU, V., LOVATO, L., DOUMAS, M., NYLEN, E., MOTTI, A., COHEN, R. M., APPELEGATE, W. B., PUNTAKEE, Z., YALE, J. F. & CUSHMAN, W. C. 2015. Chronic kidney disease and intensive glycemic control increase cardiovascular risk in patients with type 2 diabetes. *Kidney international*, 87, 649-659.
- PARCHWANI, D. N. & UPADHYAH, A. A. 2012. Diabetic nephropathy: Progression and pathophysiology. *Int J Med Sci Public Health*, 1, 59-70.

- PARK, S.-H., CHOI, H.-J., LEE, J.-H., WOO, C.-H., KIM, J.-H. & HAN, H.-J. 2001. High glucose inhibits renal proximal tubule cell proliferation and involves PKC, oxidative stress, and TGF- $\beta$ 1. *Kidney international*, 59, 1695-1705.
- PARK, S.-J., AHMAD, F., PHILP, A., BAAR, K., WILLIAMS, T., LUO, H., KE, H., REHMANN, H., TAUSSIG, R. & BROWN, A. L. 2012. Resveratrol ameliorates aging-related metabolic phenotypes by inhibiting cAMP phosphodiesterases. *Cell*, 148, 421-433.
- PARRA, E., BELOW, J., KRITHIKA, S., VALLADARES, A., BARTA, J., COX, N., HANIS, C., WACHER, N., GARCIA-MENA, J. & HU, P. 2011. Genome-wide association study of type 2 diabetes in a sample from Mexico City and a meta-analysis of a Mexican-American sample from Starr County, Texas. *Diabetologia*, 54, 2038-2046.
- PARSA, A., KAO, W. L., XIE, D., ASTOR, B. C., LI, M., HSU, C.-Y., FELDMAN, H. I., PAREKH, R. S., KUSEK, J. W. & GREENE, T. H. 2013. APOL1 risk variants, race, and progression of chronic kidney disease. *New England Journal of Medicine*, 369, 2183-2196.
- PARVING, H.-H., BRENNER, B. M., MCMURRAY, J. J., DE ZEEUW, D., HAFFNER, S. M., SOLOMON, S. D., CHATURVEDI, N., PERSSON, F., DESAI, A. S. & NICOLAIDES, M. 2012. Cardiorenal end points in a trial of aliskiren for type 2 diabetes. *New England Journal of Medicine*, 367, 2204-2213.
- PARVING, H.-H., SMIDT, U., FRIISBERG, B., BONNEVIE-NIELSEN, V. & ANDERSEN, A. 1981. A prospective study of glomerular filtration rate and arterial blood pressure in insulin-dependent diabetics with diabetic nephropathy. *Diabetologia*, 20, 457-461.
- PAUL, B., MASI, I., DEOPUJARI, J. & CHARPENTIER, C. 1999. Occurrence of resveratrol and pterostilbene in age-old darakchasava, an ayurvedic medicine from India. *Journal of ethnopharmacology*, 68, 71-76.
- PAVENSTÄDT, H., KRIZ, W. & KRETZLER, M. 2003. Cell biology of the glomerular podocyte. *Physiological reviews*, 83, 253-307.
- PEARSON, K. J., BAUR, J. A., LEWIS, K. N., PESHKIN, L., PRICE, N. L., LABINSKY, N., SWINDELL, W. R., KAMARA, D., MINOR, R. K. & PEREZ, E. 2008. Resveratrol delays age-related deterioration and mimics transcriptional aspects of dietary restriction without extending life span. *Cell metabolism*, 8, 157-168.
- PEMBERTON, K. & BARRETT, J. 1989. The detoxification of xenobiotic compounds by *Onchocerca gutturosa* (Nematoda: Filarioidea). *International journal for parasitology*, 19, 875-878.
- PENG, F., WU, D., GAO, B., INGRAM, A. J., ZHANG, B., CHORNEYKO, K., MCKENZIE, R. & KREPINSKY, J. C. 2008. RhoA/Rho-kinase contribute to the pathogenesis of diabetic renal disease. *Diabetes*, 57, 1683-1692.

- PENG, Z., YANG, X., QIN, J., YE, K., WANG, X., SHI, H., JIANG, M., LIU, X. & LU, X. 2017A. Glyoxalase-1 overexpression reverses defective proangiogenic function of diabetic adipose-derived stem cells in streptozotocin-induced diabetic mice model of critical limb ischemia. *Stem cells translational medicine*, 6, 261-271.
- PENG, H.T., CHEN, J., LIU, T.Y., WU, Y.Q., LIN, X.H., LAI, Y.H. & HUANG, Y.F., 2017b. Up-regulation of the tumor promoter Glyoxalase-1 indicates poor prognosis in breast cancer. *International journal of clinical and experimental pathology*, 10 (11), p.10852.
- PERALTA, C. A., BIBBINS-DOMINGO, K., VITTINGHOFF, E., LIN, F., FORNAGE, M., KOPP, J. B. & WINKLER, C. A. 2016. APOL1 genotype and race differences in incident albuminuria and renal function decline. *Journal of the American Society of Nephrology*, 27, 887-893.
- PERCHE, O., VERGNAUD-GAUDUCHON, J., MORAND, C., DUBRAY, C., MAZUR, A. & VASSON, M.-P. 2014. Orange juice and its major polyphenol hesperidin consumption do not induce immunomodulation in healthy well-nourished humans. *Clinical Nutrition*, 33, 130-135.
- PEREIRA, A., FERNANDES, R., CRISÓSTOMO, J., SEIÇA, R. M. & SENA, C. M. 2017. The Sulforaphane and pyridoxamine supplementation normalize endothelial dysfunction associated with type 2 diabetes. *Scientific reports*, 7, 1-13.
- PERES, G. B., SCHOR, N. & MICHELACCI, Y. M. 2017. Impact of high glucose and AGEs on cultured kidney-derived cells. Effects on cell viability, lysosomal enzymes and effectors of cell signaling pathways. *Biochimie*, 135, 137-148.
- PETERS, T. 1962. The biosynthesis of rat serum albumin I. Properties of rat albumin and its occurrence in liver cell fractions. *Journal of Biological Chemistry*, 237, 1181-1185.
- PETERSON, J. J., BEECHER, G. R., BHAGWAT, S. A., DWYER, J. T., GEBHARDT, S. E., HAYTOWITZ, D. B. & HOLDEN, J. M. 2006a. Flavanones in grapefruit, lemons, and limes: A compilation and review of the data from the analytical literature. *Journal of food composition and analysis*, 19, S74-S80.
- PETERSON, J. J., DWYER, J. T., BEECHER, G. R., BHAGWAT, S. A., GEBHARDT, S. E., HAYTOWITZ, D. B. & HOLDEN, J. M. 2006b. Flavanones in oranges, tangerines (mandarins), tangors, and tangelos: a compilation and review of the data from the analytical literature. *Journal of Food Composition and Analysis*, 19, S66-S73.
- PHILLIPS, S. A. & THORNALLEY, P. J. 1993. The formation of methylglyoxal from triose phosphates. *The FEBS Journal*, 212, 101-105.
- PIERCE, M., KEEN, H. & BRADLEY, C. 1995. Risk of Diabetes in Offspring of Parents with Non-insulin-dependent Diabetes. *Diabetic medicine*, 12, 6-13.

- PILMORE, H., DOGRA, G., ROBERTS, M., HEERSPINK, H., NINOMIYA, T., HUXLEY, R. & PERKOVIC, V. 2014. Cardiovascular disease in patients with chronic kidney disease. *Nephrology (Carlton)* 19, 3–10.
- PINHO-RIBEIRO, F. A., HOHMANN, M. S., BORGHI, S. M., ZARPELON, A. C., GUAZELLI, C. F., MANCHOPE, M. F., CASAGRANDE, R. & VERRI JR, W. A. 2015. Protective effects of the flavonoid hesperidin methyl chalcone in inflammation and pain in mice: role of TRPV1, oxidative stress, cytokines and NF- $\kappa$ B. *Chemico-biological interactions*, 228, 88-99.
- PLANTINGA, L. C., MILLER III, E. R., STEVENS, L. A., SARAN, R., MESSER, K., FLOWERS, N., GEISS, L. & POWE, N. R. 2009. Blood pressure control among persons without and with chronic kidney disease: US trends and risk factors 1999–2006. *Hypertension*, 54, 47-56.
- POHER, A.-L., ARSENIJEVIC, D., ASRIH, M., DULLOO, A. G., JORNAYVAZ, F. R., ROHNER-JEANRENAUD, F. & VEYRAT-DUREBEX, C. 2016. Preserving of postnatal leptin signaling in obesity-resistant Lou/C rats following a perinatal high-fat diet. *PloS one*, 11, e0162517.
- POPOV, N., SCHMITT, M., SCHULZECK, S. & MATTHIES, H. 1975. Reliable micromethod for determination of the protein content in tissue homogenates. *Acta biologica et medica Germanica*, 34, 1441-1446.
- PORETSKY, L. 2010. *Principles of diabetes mellitus*, Springer.
- POURGHASEM, M., SHAFI, H. & BABAZADEH, Z. 2015. Histological changes of kidney in diabetic nephropathy. *Caspian journal of internal medicine*, 6, 120.
- QI, Q., STILP, A. M., SOFER, T., MOON, J.-Y., HIDALGO, B., SZPIRO, A. A., WANG, T., NG, M. C., GUO, X. & CHEN, Y.-D. I. 2017. Genetics of type 2 diabetes in US Hispanic/Latino individuals: results from the Hispanic Community Health Study/Study of Latinos (HCHS/SOL). *Diabetes*, 66, 1419-1425.
- QIAO, Y., GAO, K., WANG, Y., WANG, X. & CUI, B. 2017. Resveratrol ameliorates diabetic nephropathy in rats through negative regulation of the p38 MAPK/TGF- $\beta$ 1 pathway. *Experimental and therapeutic medicine*, 13, 3223-3230.
- RABBANI, N., ANTONYSUNIL, A., ROSSING, K., ROSSING, P., TARNOW, L., PARVING, H. & THORNALLEY, P. 2011a. Effect of Irbesartan treatment on plasma and urinary protein glycation, oxidation and nitration markers in patients with type 2 diabetes and microalbuminuria. *Amino Acids*, 42, 1627-1639.
- RABBANI, N., GODFREY, L., XUE, M., SHAHEEN, F., GEOFFRION, M., MILNE, R. & THORNALLEY, P. 2011b. Conversion of low density lipoprotein to the pro-atherogenic form by methylglyoxal with increased arterial proteoglycan binding and aortal retention. *Diabetes*, 60, 1973-1980.



- RABBANI, N., GODFREY, L., XUE, M., SHAHEEN, F., GEOFFRION, M., MILNE, R. & THORNALLEY, P. J. 2011c. Glycation of LDL by methylglyoxal increases arterial atherogenicity: a possible contributor to increased risk of cardiovascular disease in diabetes. *Diabetes*, 60, 1973-1980.
- RABBANI, N., SEBEKOVA, K., SEBEKOVA JR, K., HEIDLAND, A. & THORNALLEY, P. 2007. Accumulation of free adduct glycation, oxidation, and nitration products follows acute loss of renal function. , 72, 1113-1121.
- RABBANI, N. & THORNALLEY, P. J. 2012a. Dicarbonyls (Glyoxal, Methylglyoxal, and 3-Deoxyglucosone). *Uremic Toxins*, 177-192.
- RABBANI, N. & THORNALLEY, P. J. 2012b. Glycation research in amino acids: a place to call home. *Amino Acids*, 42, 1087-96.
- RABBANI, N. & THORNALLEY, P. J. 2015. Dicarbonyl stress in cell and tissue dysfunction contributing to ageing and disease. *Biochemical and biophysical research communications*, 458, 221-226.
- RABBANI, N. & THORNALLEY, P. J. 2016. Glycation of proteins. *Analysis of Protein Post-Translational Modifications by Mass Spectrometry*, 307.
- RABBANI, N. & THORNALLEY, P. J. 2018. Advanced glycation end products in the pathogenesis of chronic kidney disease. *Kidney International*, 93, 803-813.
- RABBANI, N. & THORNALLEY, P. J. 2019. Glyoxalase 1 modulation in obesity and diabetes. *Antioxidants & redox signaling*, 30, 354-374.
- RABBANI, N., XUE, M. & THORNALLEY, P. J. 2014. Activity, regulation, copy number and function in the glyoxalase system. *Biochemical Society transactions*, 42, 419-424.
- RABBANI, N., XUE, M. & THORNALLEY, P. J. 2016. Methylglyoxal-induced dicarbonyl stress in aging and disease: first steps towards glyoxalase 1-based treatments. *Clinical Science*, 130, 1677-1696.
- RABBANI, N., XUE, M. & THORNALLEY, P. J. 2021. Dicarbonyl stress, protein glycation and the unfolded protein response. *Glycoconjugate Journal*, 1-10.
- RACKER, E. 1951. The mechanism of action of glyoxalase. *Journal of Biological Chemistry*, 190, 685-696.
- RAHBAR, S. 1968. An abnormal hemoglobin in red cells of diabetics. *Clinica chimica acta*, 22, 296-298.
- RAMAN, R., GANESAN, S., PAL, S. S., KULOTHUNGAN, V. & SHARMA, T. 2014. Prevalence and risk factors for diabetic retinopathy in rural India. *Sankara Nethralaya*

Diabetic Retinopathy Epidemiology and Molecular Genetic Study III (SN-DREAMS III), report no 2. *BMJ Open Diabetes Research and Care*, 2, e000005.

- RANGANATHAN, S., CIACCIO, P. J., WALSH, E. S. & TEW, K. D. 1999. Genomic sequence of human glyoxalase-I: analysis of promoter activity and its regulation. *Gene*, 240, 149-155.
- RAUDVERE, U., KOLBERG, L., KUZMIN, I., ARAK, T., ADLER, P., PETERSON, H. & VILO, J. 2019. g: Profiler: a web server for functional enrichment analysis and conversions of gene lists (2019 update). *Nucleic acids research*, 47, W191-W198.
- REDONDO, M. J., JEFFREY, J., FAIN, P. R., EISENBARTH, G. S. & ORBAN, T. 2008. Concordance for islet autoimmunity among monozygotic twins. *New England Journal of Medicine*, 359, 2849-2850.
- REICHARD, G., SKUTCHES, C., HOELDTKE, R. & OWEN, O. 1986. Acetone metabolism in humans during diabetic ketoacidosis. *Diabetes*, 35, 668-674.
- REIDY, K., KANG, H. M., HOSTETTER, T. & SUSZTAK, K. 2014. Molecular mechanisms of diabetic kidney disease. *The Journal of clinical investigation*, 124, 2333.
- REKHA, S. S., PRADEEPKIRAN, J. A. & BHASKAR, M. 2019. Bioflavonoid hesperidin possesses the anti-hyperglycemic and hypolipidemic property in STZ induced diabetic myocardial infarction (DMI) in male Wister rats. *Journal of Nutrition & Intermediary Metabolism*, 15, 58-64.
- RIDDERSTRÖM, M., SACCUCCI, F., HELLMAN, U., BERGMAN, T., PRINCIPATO, G. & MANNERVIK, B. 1996. Molecular cloning, heterologous expression, and characterization of human glyoxalase II. *Journal of Biological Chemistry*, 271, 319-323.
- RIMANDO, A. M., KALT, W., MAGEE, J. B., DEWEY, J. & BALLINGTON, J. R. 2004. Resveratrol, pterostilbene, and piceatannol in vaccinium berries. *Journal of agricultural and food chemistry*, 52, 4713-4719.
- RIZZA, S., MUNIYAPPA, R., IANTORNO, M., KIM, J.-A., CHEN, H., PULLIKOTIL, P., SENESE, N., TESAURO, M., LAURO, D. & CARDILLO, C. 2011. Citrus polyphenol hesperidin stimulates production of nitric oxide in endothelial cells while improving endothelial function and reducing inflammatory markers in patients with metabolic syndrome. *The Journal of Clinical Endocrinology & Metabolism*, 96, E782-E792.
- ROCHA, K., SOUZA, G., EBAID, G. X., SEIVA, F., CATANEO, A. & NOVELLI, E. 2009. Resveratrol toxicity: effects on risk factors for atherosclerosis and hepatic oxidative stress in standard and high-fat diets. *Food and Chemical Toxicology*, 47, 1362-1367.

- ROE, N. D. & REN, J. 2012. Nitric oxide synthase uncoupling: a therapeutic target in cardiovascular diseases. *Vascular pharmacology*, 57, 168-172.
- ROOHBAKHSH, A., PARHIZ, H., SOLTANI, F., REZAAEE, R. & IRANSHAHI, M. 2015. Molecular mechanisms behind the biological effects of hesperidin and hesperetin for the prevention of cancer and cardiovascular diseases. *Life sciences*, 124, 64-74.
- RUZICKA, M., QUINN, R. R., MCFARLANE, P., HEMMELGARN, B., PRASAD, G. R., FEBER, J., NESRALLAH, G., MACKINNON, M., TANGRI, N. & MCCORMICK, B. 2014. Canadian Society of Nephrology commentary on the 2012 KDIGO clinical practice guideline for the management of blood pressure in CKD. *American Journal of Kidney Diseases*, 63, 869-887.
- SADI, G., BALOĞLU, M. C. & PEKTAŞ, M. B. 2015. Differential gene expression in liver tissues of streptozotocin-induced diabetic rats in response to resveratrol treatment. *PLoS one*, 10, e0124968.
- SADI, G., KARTAL, D. İ. & GÜRAY, T. 2013. Regulation of Glutathione S-Transferase Mu with type 1 diabetes and its regulation with antioxidants.
- SADYGOV, R. G., COCIORVA, D. & YATES, J. R. 2004. Large-scale database searching using tandem mass spectra: looking up the answer in the back of the book. *Nature methods*, 1, 195-202.
- SAEEDI, P., PETERSOHN, I., SALPEA, P., MALANDA, B., KARURANGA, S., UNWIN, N., COLAGIURI, S., GUARIGUATA, L., MOTALA, A. A. & OGURTSOVA, K. 2019. Global and regional diabetes prevalence estimates for 2019 and projections for 2030 and 2045: Results from the International Diabetes Federation Diabetes Atlas. *Diabetes research and clinical practice*, 157, 107843.
- SALTI, T., KHAZIM, K., HADDAD, R., CAMPISI-PINTO, S., BAR-SELA, G. & COHEN, I. 2020. Glucose induces IL-1 $\alpha$ -dependent inflammation and extracellular matrix proteins expression and deposition in renal tubular epithelial cells in diabetic kidney disease. *Frontiers in immunology*, 11, 1270.
- SANDERS, T. H., MCMICHAEL, R. W. & HENDRIX, K. W. 2000. Occurrence of resveratrol in edible peanuts. *Journal of agricultural and food chemistry*, 48, 1243-1246.
- SANTARIUS, T., BIGNELL, G. R., GREENMAN, C. D., WIDAA, S., CHEN, L., MAHONEY, C. L., BUTLER, A., EDKINS, S., WARIS, S. & THORNALLEY, P. J. 2010. GLO1—a novel amplified gene in human cancer. *Genes, Chromosomes and Cancer*, 49, 711-725.
- SATCHELL, S. C. & BRAET, F. 2009. Glomerular endothelial cell fenestrations: an integral component of the glomerular filtration barrier. *American Journal of Physiology-Renal Physiology*, 296, F947-F956.

- SAVELIEV, S., BRATZ, M., ZUBAREV, R., SZAPACS, M., BUDAMGUNTA, H. & URH, M. 2013. Trypsin/Lys-C protease mix for enhanced protein mass spectrometry analysis. *Nature Methods*, 10, 1134.
- SCHALKWIJK, C. G., BAIDOSHVILI, A., STEHOUWER, C. D., VAN HINSBERGH, V. W. & NIESSEN, H. W. 2004. Increased accumulation of the glycooxidation product N $\epsilon$ -(carboxymethyl) lysine in hearts of diabetic patients: generation and characterisation of a monoclonal anti-CML antibody. *Biochimica et Biophysica Acta (BBA)-Molecular and Cell Biology of Lipids*, 1636, 82-89.
- SCHEIJEN, J. L. & SCHALKWIJK, C. G. 2014. Quantification of glyoxal, methylglyoxal and 3-deoxyglucosone in blood and plasma by ultra performance liquid chromatography tandem mass spectrometry: evaluation of blood specimen. *Clinical Chemistry and Laboratory Medicine (CCLM)*, 52, 85-91.
- SCHIMANDLE, C. M. & VANDER JAGT, D. L. 1979. Isolation and kinetic analysis of the multiple forms of glyoxalase-I from human erythrocytes. *Archives of biochemistry and biophysics*, 195, 261-268.
- SCHMATZ, R., MAZZANTI, C. M., SPANEVELLO, R., STEFANELLO, N., GUTIERRES, J., MALDONADO, P. A., CORRÊA, M., DA ROSA, C. S., BECKER, L. & BAGATINI, M. 2009a. Ectonucleotidase and acetylcholinesterase activities in synaptosomes from the cerebral cortex of streptozotocin-induced diabetic rats and treated with resveratrol. *Brain research bulletin*, 80, 371-376.
- SCHMATZ, R., SCHETINGER, M. R. C., SPANEVELLO, R. M., MAZZANTI, C. M., STEFANELLO, N., MALDONADO, P. A., GUTIERRES, J., DE CARVALHO CORRÊA, M., GIROTTO, E. & MORETTO, M. B. 2009b. Effects of resveratrol on nucleotide degrading enzymes in streptozotocin-induced diabetic rats. *Life Sciences*, 84, 345-350.
- SCHNURR, T. M., JAKUPOVIĆ, H., CARRASQUILLA, G. D., ÄNGQUIST, L., GRARUP, N., SØRENSEN, T. I., TJØNNELAND, A., OVERVAD, K., PEDERSEN, O. & HANSEN, T. 2020. Obesity, unfavourable lifestyle and genetic risk of type 2 diabetes: A case-cohort study. *Diabetologia*, 63, 1324-1332.
- SCHRIER, R. W., ESTACIO, R. O., ESLER, A. & MEHLER, P. 2002. Effects of aggressive blood pressure control in normotensive type 2 diabetic patients on albuminuria, retinopathy and strokes. *Kidney international*, 61, 1086-1097.
- SCHROIJEN, M., VAN DE LUIJTGAARDEN, M., NOORDZIJ, M., RAVANI, P., JARRAYA, F., COLLART, F., PRÜTZ, K., FOGARTY, D., LEIVESTAD, T. & PRISCHL, F. 2013. Survival in dialysis patients is different between patients with diabetes as primary renal disease and patients with diabetes as a co-morbid condition. *Diabetologia*, 56, 1949-1957.

- SCHUMACHER, D., MORGENSTERN, J., OGUCHI, Y., VOLK, N., KOPF, S., GROENER, J. B., NAWROTH, P. P., FLEMING, T. & FREICHEL, M. 2018. Compensatory mechanisms for methylglyoxal detoxification in experimental & clinical diabetes. *Molecular metabolism*, 18, 143-152.
- SCHWEDLER, S. B., METZGER, T., SCHINZEL, R. & WANNER, C. 2002. Advanced glycation end products and mortality in hemodialysis patients. *Kidney international*, 62, 301-310.
- SCOTT, R. A., SCOTT, L. J., MÄGI, R., MARULLO, L., GAULTON, K. J., KAAKINEN, M., PERVJAKOVA, N., PERS, T. H., JOHNSON, A. D. & EICHER, J. D. 2017. An expanded genome-wide association study of type 2 diabetes in Europeans. *Diabetes*, 66, 2888-2902.
- SCOTT, R. P. & QUAGGIN, S. E. 2015. The cell biology of renal filtration. *Journal of cell biology*, 209, 199-210.
- SEARLE, B. C. 2010. Scaffold: a bioinformatic tool for validating MS/MS-based proteomic studies. *Proteomics*, 10, 1265-1269.
- ŠEBEKOVÁ, K., KRAJČOVIČOVÁ-KUDLÁČKOVÁ, M., SCHINZEL, R., FAIST, V., KLVANOVÁ, J. & HEIDLAND, A. 2001. Plasma levels of advanced glycation end products in healthy, long-term vegetarians and subjects on a western mixed diet. *European journal of nutrition*, 40, 275-281.
- SEETHO, I. W. & WILDING, J. P. 2014. The clinical management of diabetes mellitus. *Clin Biochem Metab Clin Asp*, 305-32.
- SEINO, Y., NANJO, K., TAJIMA, N., KADOWAKI, T., KASHIWAGI, A., ARAKI, E., ITO, C., INAGAKI, N., IWAMOTO, Y. & KASUGA, M. 2010. Report of the committee on the classification and diagnostic criteria of diabetes mellitus. *Diabetology International*, 1, 2-20.
- SELVIN, E., MARINOPOULOS, S., BERKENBLIT, G., RAMI, T., BRANCATI, F. L., POWE, N. R. & GOLDEN, S. H. 2004. Meta-analysis: glycosylated hemoglobin and cardiovascular disease in diabetes mellitus. *Annals of internal medicine*, 141, 421-431.
- SERENA, G., CAMHI, S., STURGEON, C., YAN, S. & FASANO, A. 2015. The role of gluten in celiac disease and type 1 diabetes. *Nutrients*, 7, 7143-7162.
- SHAGIRTHA, K. & PARI, L. 2011. Hesperetin, a citrus flavonone, protects potentially cadmium induced oxidative testicular dysfunction in rats. *Ecotoxicology and environmental safety*, 74, 2105-2111.

- SHAHIDI, F. & AMBIGAIPALAN, P. 2015. Phenolics and polyphenolics in foods, beverages and spices: Antioxidant activity and health effects—A review. *Journal of functional foods*, 18, 820-897.
- SHAKIBAEI, M., HARIKUMAR, K. B. & AGGARWAL, B. B. 2009. Resveratrol addiction: to die or not to die. *Molecular nutrition & food research*, 53, 115-128.
- SHAKIL-UR-REHMAN, S., KARIMI, H. & GILLANI, S. A. 2017. Effects of supervised structured aerobic exercise training program on fasting blood glucose level, plasma insulin level, glycemic control, and insulin resistance in type 2 diabetes mellitus. *Pakistan journal of medical sciences*, 33, 576.
- SHANG, J., CHEN, L.-L., XIAO, F.-X., SUN, H., DING, H.-C. & XIAO, H. 2008. Resveratrol improves non-alcoholic fatty liver disease by activating AMP-activated protein kinase. *Acta Pharmacologica Sinica*, 29, 698-706.
- SHANIJA, S., ADOLE, P. S., VINOD, K. V. & SAYA, R. P. 2018. Assessment of serum εN-carboxymethyllysine and soluble receptor of advanced glycation end product levels among type 2 diabetes mellitus patients with and without acute coronary syndrome. *International Journal of Medical Science and Public Health*, 7, 879-884.
- SHARMA, S., MISRA, C. S., ARUMUGAM, S., ROY, S., SHAH, V., DAVIS, J. A., SHIRUMALLA, R. K. & RAY, A. 2011. Antidiabetic activity of resveratrol, a known SIRT1 activator in a genetic model for type-2 diabetes. *Phytotherapy Research*, 25, 67-73.
- SHAVERDASHVILI, K., PADLO, J., WEINBLATT, D., JIA, Y., JIANG, W., RAO, D., LACZKÓ, D., WHELAN, K. A., LYNCH, J. P. & MUIR, A. B. 2019. KLF4 activates NFκB signaling and esophageal epithelial inflammation via the Rho-related GTP-binding protein RHOF. *PloS one*, 14, e0215746.
- SHAW, J. E., ZIMMET, P. Z., DE COURTEN, M., DOWSE, G. K., CHITSON, P., GAREEBOO, H. A., HEMRAJ, F., FAREED, D., TUOMILEHTO, J. & ALBERTI, K. 1999. Impaired fasting glucose or impaired glucose tolerance. What best predicts future diabetes in Mauritius? *Diabetes Care*, 22, 399-402.
- SHEN, M. Y., HSIAO, G., LIU, C. L., FONG, T. H., LIN, K. H., CHOU, D. S. & SHEU, J. R. 2007. Inhibitory mechanisms of resveratrol in platelet activation: pivotal roles of p38 MAPK and NO/cyclic GMP. *British journal of haematology*, 139, 475-485.
- SHEVCHENKO, G., MUSUNURI, S., WETTERHALL, M. & BERGQUIST, J. 2012. Comparison of extraction methods for the comprehensive analysis of mouse brain proteome using shotgun-based mass spectrometry. *Journal of proteome research*, 11, 2441-2451.
- SHINOHARA, M., THORNALLEY, P., GIARDINO, I., BEISSWENGER, P., THORPE, S. R., ONORATO, J. & BROWNLEE, M. 1998. Overexpression of glyoxalase-I in bovine

endothelial cells inhibits intracellular advanced glycation endproduct formation and prevents hyperglycemia-induced increases in macromolecular endocytosis. *The Journal of clinical investigation*, 101, 1142-1147.

SHISHODIA, S. & AGGARWAL, B. B. 2006. Resveratrol: a polyphenol for all seasons. *Resveratrol in Health and Disease*, 1, 1-15.

SIEMANN, E. & CREASY, L. 1992. Concentration of the phytoalexin resveratrol in wine. *American Journal of Enology and Viticulture*, 43, 49-52.

SIEMIONOW, M. & DEMIR, Y. 2004. Diabetic neuropathy: Pathogenesis and treatment. A review. *Journal of reconstructive microsurgery*, 20, 241-252.

SIMAS, J. N., MENDES, T. B., PACCOLA, C. C., VENDRAMINI, V. & MIRAGLIA, S. M. 2017. Resveratrol attenuates reproductive alterations in type 1 diabetes-induced rats. *International Journal of Experimental Pathology*, 98, 312-328.

SINGH, C. K., NDIAYE, M. A., CHHABRA, G., MINTIE, C. A. & AHMAD, N. 2019. Molecular analysis of chemopreventive effects of grape antioxidants resveratrol and quercetin in transgenic adenocarcinoma of the mouse prostate. *AACR*.

SKAPARE, E., KONRADE, I., LIEPINSH, E., MAKRECKA, M., ZVEJNIECE, L., SVALBE, B., VILSKERSTS, R. & DAMBROVA, M. 2012. Glyoxalase 1 and glyoxalase 2 activities in blood and neuronal tissue samples from experimental animal models of obesity and type 2 diabetes mellitus. *The Journal of Physiological Sciences*, 62, 469-478.

SKYLER, J. S. 2015. Prevention and reversal of type 1 diabetes—past challenges and future opportunities. *Diabetes care*, 38, 997-1007.

SMITH, P. K., KROHN, R. I., HERMANSON, G., MALLIA, A., GARTNER, F., PROVENZANO, M., FUJIMOTO, E., GOEKE, N., OLSON, B. & KLENK, D. 1985. Measurement of protein using bicinchoninic acid. *Analytical biochemistry*, 150, 76-85.

SOLEAS, G. J., DIAMANDIS, E. P. & GOLDBERG, D. M. 1997. Resveratrol: a molecule whose time has come? And gone? *Clinical biochemistry*, 30, 91-113.

SOMMER, A., FISCHER, P., KRAUSE, K., BOETTCHER, K., BROPHY, P. M., WALTER, R. D. & LIEBAU, E. 2001. A stress-responsive glyoxalase I from the parasitic nematode *Onchocerca volvulus*. *Biochemical Journal*, 353, 445-452.

SONG, C., SU, Z. & GUO, J. 2019. Thymosin  $\beta$  10 is overexpressed and associated with unfavorable prognosis in hepatocellular carcinoma. *Bioscience reports*, 39.

- SPIESS, B. D., ARMOUR, S., HORROW, J., KAPLAN, J. A., KOCH, C. G., KARKOUTI, K. & BODY, S. C. 2018. Transfusion medicine and coagulation disorders. *Kaplan's Essentials of Cardiac Anesthesia for Cardiac Surgery*. Elsevier Inc.
- STEEN, H. & MANN, M. 2004. The ABC's (and XYZ's) of peptide sequencing. *Nature reviews Molecular cell biology*, 5, 699-711.
- STEWART, C. P., CHRISTIAN, P., SCHULZE, K. J., ARGUELLO, M., LECLERQ, S. C., KHATRY, S. K. & WEST JR, K. P. 2011. Low maternal vitamin B-12 status is associated with offspring insulin resistance regardless of antenatal micronutrient supplementation in rural Nepal. *The Journal of nutrition*, 141, 1912-1917.
- STØRLING, J. & POCIOT, F. 2017. Type 1 diabetes candidate genes linked to pancreatic islet cell inflammation and beta-cell apoptosis. *Genes*, 8, 72.
- STRATMANN, B., ENGELBRECHT, B., ESPELAGE, B. C., KLUSMEIER, N., TIEMANN, J., GAWLOWSKI, T., MATTERN, Y., EISENACHER, M., MEYER, H. E. & RABBANI, N. 2016. Glyoxalase 1-knockdown in human aortic endothelial cells—effect on the proteome and endothelial function estimates. *Scientific reports*, 6.
- STROBER, W. 2001. Trypan blue exclusion test of cell viability. *Current protocols in immunology*, A3. B. 1-A3. B. 3.
- STROM, A., STRASSBURGER, K., SCHMUCK, M., SHEVALYE, H., DAVIDSON, E., ZIVEHE, F., BÖNHOF, G., REIMER, R., BELGARDT, B.-F. & FLEMING, T. 2021. Interaction between magnesium and methylglyoxal in diabetic polyneuropathy and neuronal models. *Molecular Metabolism*, 43, 101114.
- STUMVOLL, M., GOLDSTEIN, B. J. & VAN HAEFTEN, T. W. 2005. Type 2 diabetes: principles of pathogenesis and therapy. *The Lancet*, 365, 1333-1346.
- SU, H.-C., HUNG, L.-M. & CHEN, J.-K. 2006. Resveratrol, a red wine antioxidant, possesses an insulin-like effect in streptozotocin-induced diabetic rats. *American Journal of Physiology-Endocrinology and Metabolism*, 290, E1339-E1346.
- SUCKLING, R. J., HE, F. J. & MACGREGOR, G. A. 2010. Altered dietary salt intake for preventing and treating diabetic kidney disease. *The Cochrane Library*.
- SUGIURA, T., TAKASE, H., OHTE, N. & DOHI, Y. 2018. Dietary salt intake is a significant determinant of impaired kidney function in the general population. *Kidney and Blood Pressure Research*, 43, 1245-1254.
- SUPEK, F., BOŠNJAK, M., ŠKUNCA, N. & ŠMUC, T. 2011. REVIGO summarizes and visualizes long lists of gene ontology terms. *PloS one*, 6, 1-9.



- SUSZTAK, K., RAFF, A. C., SCHIFFER, M. & BÖTTINGER, E. P. 2006. Glucose-induced reactive oxygen species cause apoptosis of podocytes and podocyte depletion at the onset of diabetic nephropathy. *Diabetes*, 55, 225-233.
- SZENT-GYORGYI, A., EGYUD, L. & MCLAUGHLIN, J. A. 1967. Keto-aldehydes and cell division. *Science*, 155, 539-543.
- SZENT-GYORGYI, A., HEGYELI, A. & MCLAUGHLIN, J. A. 1963. Cancer therapy: a possible new approach. *Science*, 140, 1391-1392.
- SZKUDELSKA, K., NOGOWSKI, L. & SZKUDELSKI, T. 2009. Resveratrol, a naturally occurring diphenolic compound, affects lipogenesis, lipolysis and the antilipolytic action of insulin in isolated rat adipocytes. *The Journal of steroid biochemistry and molecular biology*, 113, 17-24.
- SZKUDELSKA, K., NOGOWSKI, L. & SZKUDELSKI, T. 2011. Resveratrol and genistein as adenosine triphosphate-depleting agents in fat cells. *Metabolism*, 60, 720-729.
- SZKUDELSKI, T. 2001. The mechanism of alloxan and streptozotocin action in B cells of the rat pancreas. *Physiological research*, 50, 537-546.
- SZYPOWSKA, A., RAMOTOWSKA, A., GRZECHNIK-GRYZIAK, M., SZYPOWSKI, W., PASIERB, A. & PIECHOWIAK, K. 2016. High frequency of diabetic ketoacidosis in children with newly diagnosed type 1 diabetes. *Journal of diabetes research*, 2016.
- TAKAOKA, M. 1940. Of the phenolic substances of white hellebore (*Veratrum grandiflorum* Loes. fil.). *Journal of Faculty of Sciences Hokkaido Imperial University*, 3, 1-16.
- TAKUMI, H., NAKAMURA, H., SIMIZU, T., HARADA, R., KOMETANI, T., NADAMOTO, T., MUKAI, R., MUROTA, K., KAWAI, Y. & TERAOKA, J. 2012. Bioavailability of orally administered water-dispersible hesperetin and its effect on peripheral vasodilatation in human subjects: implication of endothelial functions of plasma conjugated metabolites. *Food & function*, 3, 389-398.
- TALESA, V., ROSI, G., BISTONI, F., MARCONI, P., NORTON, S. & PRINCIPATO, G. 1990. Presence of a plant-like glyoxalase II in *Candida albicans*. *Biochemistry international*, 21, 397-403.
- TAMADON, M.-R. & BELADI-MOUSAVI, S. S. 2013. Erythropoietin; a review on current knowledge and new concepts. , 2, 119-121.
- TANAKA, K., WAKI, H., IDO, Y., AKITA, S., YOSHIDA, Y., YOSHIDA, T. & MATSUO, T. 1988. Protein and polymer analyses up to m/z 100 000 by laser ionization time-of-flight mass spectrometry. *Rapid communications in mass spectrometry*, 2, 151-153.

- TAPP, R. J., SHAW, J. E., HARPER, C. A., DE COURTEN, M. P., BALKAU, B., MCCARTY, D. J., TAYLOR, H. R., WELBORN, T. A. & ZIMMET, P. Z. 2003. The prevalence of and factors associated with diabetic retinopathy in the Australian population. *Diabetes care*, 26, 1731-1737.
- TARIQ, A., AKRAM, M. U., SHAUKAT, A. & KHAN, S. A. 2013. Automated detection and grading of diabetic maculopathy in digital retinal images. *Journal of digital imaging*, 26, 803-812.
- TATE, S. S. 1975. Interaction of  $\gamma$ -glutamyl transpeptidase with S-acyl derivatives of glutathione. *FEBS letters*, 54, 319-322.
- THIES, R. S., MOLINA, J. M., CIARALDI, T. P., FREIDENBERG, G. R. & OLEFSKY, J. M. 1990. Insulin-receptor autophosphorylation and endogenous substrate phosphorylation in human adipocytes from control, obese, and NIDDM subjects. *Diabetes*, 39, 250-259.
- THIMMULAPPA, R. K., MAI, K. H., SRISUMA, S., KENSLER, T. W., YAMAMOTO, M. & BISWAL, S. 2002. Identification of Nrf2-regulated genes induced by the chemopreventive agent sulforaphane by oligonucleotide microarray. *Cancer research*, 62, 5196-5203.
- THORNALLEY, P. 2003a. The enzymatic defence against glycation in health, disease and therapeutics: a symposium to examine the concept. *Biochem Soc Trans*, 31, 1341-2.
- THORNALLEY, P. 2003b. Glyoxalase I—structure, function and a critical role in the enzymatic defence against glycation. .
- THORNALLEY, P., GRESKOWIAK, M. & DELLA BIANCA, V. 1990. Potentiation of secretion from neutrophils by Sd-lactoylglutathione. *Med. Sci. Res.*, 18, 813.
- THORNALLEY, P., HOOPER, N., JENNINGS, P., FLORKOWSKI, C., JONES, A., LUNEC, J. & BARNETT, A. 1989. The human red blood cell glyoxalase system in diabetes mellitus. *Diabetes research and clinical practice*, 7, 115-120.
- THORNALLEY, P. & TISDALE, M. 1988. Inhibition of proliferation of human promyelocytic leukaemia HL60 cells by SD-lactoylglutathione in vitro. *Leukemia research*, 12, 897-904.
- THORNALLEY, P. J. 1985. Monosaccharide autoxidation in health and disease. *Environ Health Perspect*, 64, 297-307.
- THORNALLEY, P. J. 1988. Modification of the glyoxalase system in human red blood cells by glucose in vitro. *Biochemical Journal*, 254, 751-755.

- THORNALLEY, P. J. 1990. The glyoxalase system: new developments towards functional characterization of a metabolic pathway fundamental to biological life. *Biochemical Journal*, 269, 1.
- THORNALLEY, P. J. 1991. Population genetics of human glyoxalases. *Heredity*, 67, 139-42.
- THORNALLEY, P. J. 1993. The glyoxalase system in health and disease. *Molecular aspects of medicine*, 14, 287-371.
- THORNALLEY, P. J. 1998a. Cell activation by glycated proteins. AGE receptors, receptor recognition factors and functional classification of AGEs. *Cellular and molecular biology (Noisy-le-Grand, France)*, 44, 1013-1023.
- THORNALLEY, P. J. 1998b. Glutathione-dependent detoxification of  $\alpha$ -oxoaldehydes by the glyoxalase system: involvement in disease mechanisms and antiproliferative activity of glyoxalase I inhibitors. *Chemico-biological interactions*, 111, 137-151.
- THORNALLEY, P. J., BATTAH, S., AHMED, N., KARACHALIAS, N., AGALOU, S., BABAEI-JADIDI, R. & DAWNAY, A. 2003. Quantitative screening of advanced glycation endproducts in cellular and extracellular proteins by tandem mass spectrometry. *Biochemical Journal*, 375, 581-592.
- THORNALLEY, P. J., EDWARDS, L. G., KANG, Y., WYATT, C., DAVIES, N., LADAN, M. J. & DOUBLE, J. 1996. Antitumour activity of Sp-bromobenzylglutathione cyclopentyl diester in vitro and in vivo: inhibition of glyoxalase I and induction of apoptosis. *Biochemical pharmacology*, 51, 1365-1372.
- THORNALLEY, P. J., IRSHAD, Z., XUE, M. & RABBANI, N. Disturbance of the Glyoxalase System in Human Vascular Endothelial Cells by High Glucose In Vitro and Reversal by trans-Resveratrol. *DIABETES*, 2014. AMER DIABETES ASSOC 1701 N BEAUREGARD ST, ALEXANDRIA, VA 22311-1717 USA, A10-A10.
- THORNALLEY, P. J., LANGBORG, A. & MINHAS, H. S. 1999. Formation of glyoxal, methylglyoxal and 3-deoxyglucosone in the glycation of proteins by glucose. *Biochem J*, 344 Pt 1, 109-16.
- THORNALLEY, P. J. & RABBANI, N. 2014. Detection of oxidized and glycated proteins in clinical samples using mass spectrometry — A user's perspective. *Biochimica et Biophysica Acta (BBA) - General Subjects*, 1840, 818-829.
- THORNALLEY, P. J., WARIS, S., FLEMING, T., SANTARIUS, T., LARKIN, S. J., WINKLHOFER-ROOB, B. M., STRATTON, M. R. & RABBANI, N. 2010. Imidazopurinones are markers of physiological genomic damage linked to DNA instability and glyoxalase 1-associated tumour multidrug resistance. *Nucleic acids research*, 38, 5432-5442.

- TIMMERS, S., KONINGS, E., BILET, L., HOUTKOOPER, R. H., VAN DE WEIJER, T., GOOSSENS, G. H., HOEKS, J., VAN DER KRIEKEN, S., RYU, D. & KERSTEN, S. 2011. Calorie restriction-like effects of 30 days of resveratrol supplementation on energy metabolism and metabolic profile in obese humans. *Cell metabolism*, 14, 612-622.
- TOMÉ-CARNEIRO, J., LARROSA, M., GONZÁLEZ-SARRÍAS, A., A TOMAS-BARBERAN, F., TERESA GARCIA-CONESA, M. & CARLOS ESPIN, J. 2013. Resveratrol and clinical trials: the crossroad from in vitro studies to human evidence. *Current pharmaceutical design*, 19, 6064-6093.
- TOMÉ-CARNEIRO, J., GONZÁLVEZ, M., LARROSA, M., GARCÍA-ALMAGRO, F. J., AVILÉS-PLAZA, F., PARRA, S., YÁÑEZ-GASCÓN, M. J., RUIZ-ROS, J. A., GARCÍA-CONESA, M. T. & TOMÁS-BARBERÁN, F. A. 2012. Consumption of a grape extract supplement containing resveratrol decreases oxidized LDL and Apo B in patients undergoing primary prevention of cardiovascular disease: A triple-blind, 6-month follow-up, placebo-controlled, randomized trial. *Molecular nutrition & food research*, 56, 810-821.
- TURIÁK, L., OZOHANICS, O., MARINO, F., DRAHOS, L. & VÉKEY, K. 2011. Digestion protocol for small protein amounts for nano-HPLC-MS (MS) analysis. *Journal of proteomics*, 74, 942-947.
- TURSINAWATI, Y., HAKIM, R. F., ROHMANI, A., KARTIKADEWI, A. & SANDRA, F. 2020. CAPN10 SNP-19 is Associated with Susceptibility of Type 2 Diabetes Mellitus: A Javanese Case-control Study. *The Indonesian Biomedical Journal*, 12, 109-14.
- TUTTOLOMONDO, A., DI RAIMONDO, D., PECORARO, R., ARNAO, V., PINTO, A. & LICATA, G. 2012. Atherosclerosis as an inflammatory disease. *Current pharmaceutical design*, 18, 4266-4288.
- TYLER, M. I. & WILKINS, M. R. 2000. Identification of proteins by amino acid composition after acid hydrolysis. *Proteome Research: Two-Dimensional Gel Electrophoresis and Identification Methods*. Springer.
- UM, J.-H., PARK, S.-J., KANG, H., YANG, S., FORETZ, M., MCBURNEY, M. W., KIM, M. K., VIOLLET, B. & CHUNG, J. H. 2010. AMP-activated protein kinase-deficient mice are resistant to the metabolic effects of resveratrol. *Diabetes*, 59, 554-563.
- VADIVELOO, T., JEFFCOATE, W., DONNAN, P. T., COLHOUN, H. C., MCGURNAGHAN, S., WILD, S., MCCRIMMON, R., LEESE, G. P. & GROUP, S. D. R. N. E. 2018. Amputation-free survival in 17,353 people at high risk for foot ulceration in diabetes: a national observational study. *Diabetologia*, 61, 2590-2597.
- VALLON, V. 2011. The proximal tubule in the pathophysiology of the diabetic kidney. *American Journal of Physiology-Regulatory, Integrative and Comparative Physiology*, 300, R1009-R1022.

- VANDER JAGT, D. L. 1993. Glyoxalase II: molecular characteristics, kinetics and mechanism. *Biochemical Society transactions*, 21, 522.
- VANDER JAGT, D. L., HASSEBROOK, R. K., HUNSAKER, L. A., BROWN, W. M. & ROYER, R. E. 2001. Metabolism of the 2-oxoaldehyde methylglyoxal by aldose reductase and by glyoxalase-I: roles for glutathione in both enzymes and implications for diabetic complications. *Chemico-biological interactions*, 130, 549-562.
- VANDER JAGT, D. L. & HUNSAKER, L. A. 2003. Methylglyoxal metabolism and diabetic complications: roles of aldose reductase, glyoxalase-I, betaine aldehyde dehydrogenase and 2-oxoaldehyde dehydrogenase. *Chemico-biological interactions*, 143, 341-351.
- VERZIIL, N., DEGROOT, J., OLDEHINKEL, E., BANK, R. A., THORPE, S. R., BAYNES, J. W., BAYLISS, M. T., BIJLSMA, J. W., LAFEBER, F. P. & TEKOPPELE, J. M. 2000. Age-related accumulation of Maillard reaction products in human articular cartilage collagen. *Biochemical Journal*, 350, 381-387.
- VERZOLA, D., GANDOLFO, M. T., GAETANI, G., FERRARIS, A., MANGERINI, R., FERRARIO, F., VILLAGGIO, B., GIANIORIO, F., TOSETTI, F. & WEISS, U. 2008. Accelerated senescence in the kidneys of patients with type 2 diabetic nephropathy. *American Journal of Physiology-Renal Physiology*, 295, F1563-F1573.
- VINCE, R. & DALUGE, S. 1971. Glyoxalase inhibitors. A possible approach to anticancer agents. *Journal of medicinal chemistry*, 14, 35-37.
- VINCE, R., DALUGE, S. & WADD, W. B. 1971. Inhibition of glyoxalase I by S-substituted glutathiones. *Journal of medicinal chemistry*, 14, 402-404.
- VLISSARA, H. & URIBARRI, J. 2014. Advanced glycation end products (AGE) and diabetes: cause, effect, or both? *Current diabetes reports*, 14, 1-10.
- VOIGHT, B. F., SCOTT, L. J., STEINTHORSDDOTTIR, V., MORRIS, A. P., DINA, C., WELCH, R. P., ZEGGINI, E., HUTH, C., AULCHENKO, Y. S. & THORLEIFSSON, G. 2010. Twelve type 2 diabetes susceptibility loci identified through large-scale association analysis. *Nature genetics*, 42, 579.
- VUGUIN, P. M., HARTIL, K., KRUSE, M., KAUR, H., LIN, C.-L. V., FIALLO, A., GLENN, A. S., PATEL, A., WILLIAMS, L. & SEKI, Y. 2013. Shared effects of genetic and intrauterine and perinatal environment on the development of metabolic syndrome. *PLoS One*, 8, e63021.
- WANG, A. Y. M. 2011. Cardiovascular risk in diabetic end-stage renal disease patients. *Journal of diabetes*, 3, 119-131.
- WANG, H., NAGHAVI, M., ALLEN, C., BARBER, R. M., BHUTTA, Z. A., CARTER, A., CASEY, D. C., CHARLSON, F. J., CHEN, A. Z. & COATES, M. M. 2016. Global,

- regional, and national life expectancy, all-cause mortality, and cause-specific mortality for 249 causes of death, 1980–2015: a systematic analysis for the Global Burden of Disease Study 2015. *The lancet*, 388, 1459-1544.
- WANG, J., ZHANG, Q., LI, S., CHEN, Z., TAN, J., YAO, J. & DUAN, D. 2020a. Low molecular weight fucoidan alleviates diabetic nephropathy by binding fibronectin and inhibiting ECM-receptor interaction in human renal mesangial cells. *International journal of biological macromolecules*, 150, 304-314.
- WANG, P., GAO, J., KE, W., WANG, J., LI, D., LIU, R., JIA, Y., WANG, X., CHEN, X. & CHEN, F. 2020b. Resveratrol reduces obesity in high-fat diet-fed mice via modulating the composition and metabolic function of the gut microbiota. *Free Radical Biology and Medicine*, 156, 83-98.
- WANG, S. Y., CHEN, C.-T., SCIARAPPA, W., WANG, C. Y. & CAMP, M. J. 2008. Fruit quality, antioxidant capacity, and flavonoid content of organically and conventionally grown blueberries. *Journal of Agricultural and Food Chemistry*, 56, 5788-5794.
- WANG, S. Y., CHEN, C.-T., WANG, C. Y. & CHEN, P. 2007. Resveratrol content in strawberry fruit is affected by preharvest conditions. *Journal of Agricultural and Food Chemistry*, 55, 8269-8274.
- WANG, X.-M. 2013. Early life programming and metabolic syndrome. *World Journal of Pediatrics*, 9, 5-8.
- WANG, Y., CATANA, F., YANG, Y., RODERICK, R. & VAN BREEMEN, R. B. 2002. An LC-MS method for analyzing total resveratrol in grape juice, cranberry juice, and in wine. *Journal of agricultural and food chemistry*, 50, 431-435.
- WAUTERS, J.-P. & UEHLINGER, D. 2004. Non-medical factors influencing peritoneal dialysis utilization: the Swiss experience. *Nephrology Dialysis Transplantation*, 19, 1363-1367.
- WHITE, C. A., ALLEN, C. M., AKBARI, A., COLLIER, C. P., HOLLAND, D. C., DAY, A. G. & KNOLL, G. A. 2019. Comparison of the new and traditional CKD-EPI GFR estimation equations with urinary inulin clearance: a study of equation performance. *Clinica Chimica Acta*, 488, 189-195.
- WHITE, S., CASS, A., ATKINS, R. & CHADBAN, S. 2005. Chronic kidney disease in the general population. *Advances in chronic kidney disease*, 12, 5-13.
- WHO 2016. Global report on diabetes.
- WILCOX, T., NEWMAN, J. D., MALDONADO, T. S., ROCKMAN, C. & BERGER, J. S. 2018. Peripheral vascular disease risk in diabetic individuals without coronary heart disease. *Atherosclerosis*, 275, 419-425.

- WIŚNIEWSKI, J. R., ZOUGMAN, A., NAGARAJ, N. & MANN, M. 2009. Universal sample preparation method for proteome analysis. *Nature methods*, 6, 359-362.
- WOLF, G., SCHROEDER, R., ZAHNER, G., STAHL, R. A. & SHANKLAND, S. J. 2001. High glucose-induced hypertrophy of mesangial cells requires p27Kip1, an inhibitor of cyclin-dependent kinases. *The American journal of pathology*, 158, 1091-1100.
- WONG, D. H., VILLANUEVA, J. A., CRESS, A. B. & DULEBA, A. J. 2010. Effects of resveratrol on proliferation and apoptosis in rat ovarian theca-interstitial cells. *Molecular human reproduction*, 16, 251-259.
- WONG, S., MENG, C. & FENN, J. 1988. Multiple charging in electrospray ionization of poly (ethylene glycols). *The Journal of Physical Chemistry*, 92, 546-550.
- WOO, J.-H., LIM, J. H., KIM, Y.-H., SUH, S.-I., CHANG, J.-S., LEE, Y. H., PARK, J.-W. & KWON, T. K. 2004. Resveratrol inhibits phorbol myristate acetate-induced matrix metalloproteinase-9 expression by inhibiting JNK and PKC  $\delta$  signal transduction. *Oncogene*, 23, 1845-1853.
- XIAO, R., SHEN, S., YU, Y., PAN, Q., KUANG, R. & HUANG, H. 2019. TMSB10 promotes migration and invasion of cancer cells and is a novel prognostic marker for renal cell carcinoma. *International journal of clinical and experimental pathology*, 12, 305.
- XIE, S., SINHA, R. A., SINGH, B. K., LI, G. D., HAN, W. & YEN, P. M. 2013. Resveratrol induces insulin gene expression in mouse pancreatic  $\alpha$ -cells. *Cell & Bioscience*, 3, 47.
- XU, C.-L., CHEN, L., LI, D., CHEN, F.-T., SHA, M.-L. & SHAO, Y. 2020a. Acyl-CoA Thioesterase 8 and 11 as Novel Biomarkers for Clear Cell Renal Cell Carcinoma. *Frontiers in genetics*, 11, 1576.
- XU, J., WEI, W. B., YUAN, M. X., YUAN, S. Y., WAN, G., ZHENG, Y. Y., LI, Y. B., WANG, S., XU, L. & FU, H. J. 2012. Prevalence and risk factors for diabetic retinopathy: the Beijing Communities Diabetes Study 6. *Retina*, 32, 322-329.
- XU, Z., GENG, J., ZHANG, S., ZHANG, K., YANG, L., LI, J. & LI, J. 2020b. A Mobile-Based Intervention for Dietary Behavior and Physical Activity Change in Individuals at High Risk for Type 2 Diabetes Mellitus: Randomized Controlled Trial. *JMIR mHealth and uHealth*, 8, e19869.
- XUE, M., MOMIJI, H., RABBANI, N., BARKER, G., BRETSCHEIDER, T., SHMYGOL, A., RAND, D. A. & THORNALLEY, P. J. 2015a. Frequency modulated translocational oscillations of Nrf2 mediate the antioxidant response element cytoprotective transcriptional response. *Antioxidants & redox signaling*, 23, 613-629.
- XUE, M., MOMIJI, H., RABBANI, N., BRETSCHEIDER, T., RAND, D. A. & THORNALLEY, P. J. 2015b. Frequency modulated translocational oscillations of

- Nrf2, a transcription factor functioning like a wireless sensor. *Biochemical Society Transactions*, 43, 669-673.
- XUE, M., RABBANI, N., MOMIJI, H., IMBASI, P., ANWAR, M. M., KITTERINGHAM, N., PARK, B. K., SOUMA, T., MORIGUCHI, T. & YAMAMOTO, M. 2012. Transcriptional control of glyoxalase 1 by Nrf2 provides a stress-responsive defence against dicarbonyl glycation. *Biochemical Journal*, 443, 213-222.
- XUE, M., RABBANI, N. & THORNALLEY, P. J. Glyoxalase in ageing. *Seminars in cell & developmental biology*, 2011. Elsevier, 293-301.
- XUE, M., WEICKERT, M. O., QURESHI, S., KANDALA, N.-B., ANWAR, A., WALDRON, M., SHAFIE, A., MESSENGER, D., FOWLER, M. & JENKINS, G. 2016. Improved glycemic control and vascular function in overweight and obese subjects by glyoxalase 1 inducer formulation. *Diabetes*, 65, 2282-2294.
- YAGIHASHI, S., MIZUKAMI, H. & SUGIMOTO, K. 2011. Mechanism of diabetic neuropathy: where are we now and where to go? *Journal of Diabetes Investigation*, 2, 18-32.
- YAJNIK, C. S., DESHPANDE, S., JACKSON, A., REFSUM, H., RAO, S., FISHER, D., BHAT, D., NAIK, S., COYAJI, K. & JOGLEKAR, C. 2008. Vitamin B 12 and folate concentrations during pregnancy and insulin resistance in the offspring: the Pune Maternal Nutrition Study. *Diabetologia*, 51, 29-38.
- YAMASHITA, M. & FENN, J. B. 1984. Negative ion production with the electrospray ion source. *The Journal of Physical Chemistry*, 88, 4671-4675.
- YAMAZOYE, S. 1936. GLYOXALASE AND ITS CO-ENZYME: III. The Mechanism of the Action of Glutathione as the Co-Enzyme of Glyoxalase. *The Journal of Biochemistry*, 23, 319-334.
- YANG, Y.-M., CHEN, J.-Z., WANG, X.-X., WANG, S.-J., HU, H. & WANG, H.-Q. 2008. Resveratrol attenuates thromboxane A2 receptor agonist-induced platelet activation by reducing phospholipase C activity. *European journal of pharmacology*, 583, 148-155.
- YANO, N., SUZUKI, D., ENDOH, M., CAO, T. N., DAHDAH, J. R., TSENG, A., STABILA, J. P., MCGONNIGAL, B. G., PADBURY, J. F. & TSENG, Y.-T. 2009. High ambient glucose induces angiotensin-independent AT-1 receptor activation, leading to increases in proliferation and extracellular matrix accumulation in MES-13 mesangial cells. *Biochemical Journal*, 423, 129-143.
- YAO, D. & BROWNLEE, M. 2010. Hyperglycemia-induced reactive oxygen species increase expression of the receptor for advanced glycation end products (RAGE) and RAGE ligands. *Diabetes*, 59, 249-255.



- YATAO, X., SAEED, M., KAMBOH, A., ARAIN, M., AHMAD, F., SUHERYANI, I., ABD EL-HACK, M., ALAGAWANY, M., SHAH, Q. & CHAO, S. 2018. The potentially beneficial effects of supplementation with hesperidin in poultry diets. *World's Poultry Science Journal*, 74, 265-276.
- YEUNG, W.-C. G., RAWLINSON, W. D. & CRAIG, M. E. 2011. Enterovirus infection and type 1 diabetes mellitus: systematic review and meta-analysis of observational molecular studies. *Bmj*, 342, d35.
- YIN, Y., XU, Y., MA, H. & TIAN, X. 2017. Hesperetin ameliorates cardiac inflammation and cardiac fibrosis in streptozotocin-induced diabetic rats by inhibiting NF- $\kappa$ B signaling pathway.
- YIU, W. H., WONG, D. W., CHAN, L. Y., LEUNG, J. C., CHAN, K. W., LAN, H. Y., LAI, K. N. & TANG, S. C. 2014. Tissue kallikrein mediates pro-inflammatory pathways and activation of protease-activated receptor-4 in proximal tubular epithelial cells. *PLoS one*, 9, e88894.
- YONAMINE, C. Y., PINHEIRO-MACHADO, E., MICHALANI, M. L., ALVES-WAGNER, A. B., ESTEVES, J. V., FREITAS, H. S. & MACHADO, U. F. 2017. Resveratrol improves glycemic control in type 2 diabetic obese mice by regulating glucose transporter expression in skeletal muscle and liver. *Molecules*, 22, 1180.
- YU, W., FU, Y. C. & WANG, W. 2012. Cellular and molecular effects of resveratrol in health and disease. *Journal of cellular biochemistry*, 113, 752-759.
- YUAN, T., YANG, T., CHEN, H., FU, D., HU, Y., WANG, J., YUAN, Q., YU, H., XU, W. & XIE, X. 2019. New insights into oxidative stress and inflammation during diabetes mellitus-accelerated atherosclerosis. *Redox biology*, 20, 247-260.
- ZABALA, A., DARSALIA, V., HOLZMANN, M. J., FRANZÉN, S., SVENSSON, A. M., ELIASSON, B., PATRONE, C., NYSTRÖM, T. & JONSSON, M. 2020. Risk of first stroke in people with type 2 diabetes and its relation to glycaemic control: A nationwide observational study. *Diabetes, Obesity and Metabolism*, 22, 182-190.
- ZAFAR, M. & NAQVI, S. N.-U.-H. 2010. Effects of STZ-Induced Diabetes on the Relative Weights of Kidney, Liver and Pancreas in Albino Rats: A Comparative Study. *International Journal of Morphology*, 28.
- ZAJAC, J., SHRESTHA, A., PATEL, P. & PORETSKY, L. 2010. The main events in the history of diabetes mellitus. *Principles of diabetes mellitus*. Springer.
- ZARE JAVID, A., HORMOZNEJAD, R., YOUSEFIMANESH, H. A., ZAKERKISH, M., HAGHIGHI-ZADEH, M. H., DEGHAN, P. & RAVANBAKHS, M. 2017. The impact of resveratrol supplementation on blood glucose, insulin, insulin resistance, triglyceride, and periodontal markers in type 2 diabetic patients with chronic periodontitis. *Phytotherapy research*, 31, 108-114.

- ZHANG, X., SAADDINE, J. B., CHOU, C.-F., COTCH, M. F., CHENG, Y. J., GEISS, L. S., GREGG, E. W., ALBRIGHT, A. L., KLEIN, B. E. & KLEIN, R. 2010. Prevalence of diabetic retinopathy in the United States, 2005-2008. *Jama*, 304, 649-656.
- ZHANG, Y., LI, Y., NIEPEL, M. W., KAWANO, Y., HAN, S., LIU, S., MARSILI, A., LARSEN, P. R., LEE, C.-H. & COHEN, D. E. 2012. Targeted deletion of thioesterase superfamily member 1 promotes energy expenditure and protects against obesity and insulin resistance. *Proceedings of the National Academy of Sciences*, 109, 5417-5422.
- ZHONG, V. W., JUHAERI, J. & MAYER-DAVIS, E. J. 2018. Trends in hospital admission for diabetic ketoacidosis in adults with type 1 and type 2 diabetes in England, 1998–2013: a retrospective cohort study. *Diabetes Care*, 41, 1870-1877.
- ZHU, C., DONG, Y., LIU, H., REN, H. & CUI, Z. 2017. Hesperetin protects against H<sub>2</sub>O<sub>2</sub>-triggered oxidative damage via upregulation of the Keap1-Nrf2/HO-1 signal pathway in ARPE-19 cells. *Biomedicine & Pharmacotherapy*, 88, 124-133.
- ZISMAN, A., PERONI, O. D., ABEL, E. D., MICHAEL, M. D., MAUVAIS-JARVIS, F., LOWELL, B. B., WOJTASZEWSKI, J. F., HIRSHMAN, M. F., VIRKAMAKI, A. & GOODYEAR, L. J. 2000. Targeted disruption of the glucose transporter 4 selectively in muscle causes insulin resistance and glucose intolerance. *Nature medicine*, 6, 924-928.

## Appendix I-Table of total identified cytosolic proteins in hRPTECs

<b>Protein accession numbers</b>	<b>Protein name</b>	<b>Gene accession numbers</b>
P35237	Serpin B6	SERPINB6
Q00341	Vigilin	HDLBP
P46781	40S ribosomal protein S9	RPS9
Q07020	60S ribosomal protein L18	RPL18
O14979	Heterogeneous nuclear ribonucleoprotein D-like	HNRNPDL
P07203	Glutathione peroxidase;Glutathione peroxidase 1	GPX1
O60841	Eukaryotic translation initiation factor 5B	EIF5B
Q01082	Spectrin beta chain, non-erythrocytic 1	SPTBN1
P27635	60S ribosomal protein L10	RPL10
Q15185	Prostaglandin E synthase 3	PTGES3
O00584	Ribonuclease T2	RNASSET2
Q9Y4L1	Hypoxia up-regulated protein 1	HYOU1
P0DPI2	Glutamine amidotransferase-like class 1 domain-containing protein 3A, mitochondrial	GATD3A
Q9BUJ2-4	Heterogeneous nuclear ribonucleoprotein U-like protein 1	HNRNPUL1
P18621-3	60S ribosomal protein L17	RPL17
Q8IXQ4	GPALPP motifs-containing protein 1	GPALPP1
P06396-2	Gelsolin	GSN
P42330	Aldo-keto reductase family 1 member C3	AKR1C3
P26440	Isovaleryl-CoA dehydrogenase, mitochondrial	IVD
Q16629	Serine/arginine-rich splicing factor 7	SRSF7
P42765	3-ketoacyl-CoA thiolase, mitochondrial	ACAA2
P08865	40S ribosomal protein SA	RPSA
Q8NF91	Nesprin-1	SYNE1
P04632	Calpain small subunit 1	CAPNS1
R4GMU8	Late endosomal/lysosomal adaptor and MAPK and MTOR activator 5	LAMTOR5
E9PDF2	2-oxoglutarate dehydrogenase, mitochondrial	OGDH
Q53SF7	Cordon-bleu protein-like 1	COBL1
P0DMV9	Heat shock 70 kDa protein 1B;Heat shock 70 kDa protein 1A	HSPA1A
P49419-4	Alpha-aminoacidic semialdehyde dehydrogenase	ALDH7A1
Q9UDY2	Tight junction protein ZO-2	TJP2
Q03154	Aminoacylase-1	ACY1
C9JH19	Cathepsin D	CTSD
P06132	Uroporphyrinogen decarboxylase	UROD
Q16555	Dihydropyrimidinase-related protein 2	DPYSL2
A0A1W2PNV4	Uncharacterized protein	N/A
Q00839	Heterogeneous nuclear ribonucleoprotein U	HNRNPU
Q92841	Probable ATP-dependent RNA helicase DDX17	DDX17
A0A1W2PQS6	RPS10-NUDT3 readthrough	RPS10-NUDT3
Q14108	Lysosome membrane protein 2	SCARB2
Q5T5H1	Alpha-endosulfine	ENSA

E9PF55	Tensin-1	TNS1
P68400	Casein kinase II subunit alpha	CSNK2A1
P35241	Radixin	RDX
P46777	60S ribosomal protein L5	RPL5
P62263	40S ribosomal protein S14	RPS14
P08237	ATP-dependent 6-phosphofructokinase, muscle type	PFKM
P14735	Insulin-degrading enzyme	IDE
Q9Y2W1	Thyroid hormone receptor-associated protein 3	THRAP3
P54725	UV excision repair protein RAD23 homolog A	RAD23A
D6R9D6	RNA-binding protein 47	RBM47
A0MZ66	Shootin-1	KIAA1598
Q99798	Aconitate hydratase, mitochondrial	ACO2
P62753	40S ribosomal protein S6	RPS6
Q9UUK9	ADP-sugar pyrophosphatase	NUDT5
Q12888	Tumor suppressor p53-binding protein 1	TP53BP1
P55145	Mesencephalic astrocyte-derived neurotrophic factor	MANF
Q01844	RNA-binding protein EWS	EWSR1
P63279	SUMO-conjugating enzyme UBC9	UBE2I
Q13310	Polyadenylate-binding protein 4	PABPC4
P07910	Heterogeneous nuclear ribonucleoproteins C1/C2	HNRNPC
O60812	Heterogeneous nuclear ribonucleoprotein C-like 1	HNRNPCL1
O75390	Citrate synthase;Citrate synthase, mitochondrial	CS
P49368	T-complex protein 1 subunit gamma	CCT3
P62826	GTP-binding nuclear protein Ran	RAN
P48643	T-complex protein 1 subunit epsilon	CCT5
P63165	Small ubiquitin-related modifier 1	SUMO1
P61604	10 kDa heat shock protein, mitochondrial	HSPE1
P06454	Prothymosin alpha;Prothymosin alpha, N-terminally processed;Thymosin alpha-1	PTMA
P09110	3-ketoacyl-CoA thiolase, peroxisomal	ACAA1
P13798	Acylamino-acid-releasing enzyme	APEH
Q9Y4F1	FERM, RhoGEF and pleckstrin domain-containing protein 1	FARP1
P05166	Propionyl-CoA carboxylase beta chain, mitochondrial	PCCB
P18754	Regulator of chromosome condensation	RCC1
F8VR50	Actin-related protein 2/3 complex subunit 3	ARPC3
P50613	Cyclin-dependent kinase 7	CDK7
D6R9P3	Heterogeneous nuclear ribonucleoprotein A/B	HNRNPAB
Q9UHK6	Alpha-methylacyl-CoA racemase	AMACR
P32321	Deoxycytidylate deaminase	DCTD
D6RC52	H/ACA ribonucleoprotein complex subunit 2	NHP2
D6RGI3	Septin-11	SEPTIN11
E5RJD8	Tubulin-specific chaperone A	TBCA
P62888	60S ribosomal protein L30	RPL30
P63208	S-phase kinase-associated protein 1	SKP1
E5RK69	Annexin	ANXA6
P61916	Epididymal secretory protein E1	NPC2
Q16181	Septin-7	SEPTIN7
E7EPN9	Protein PRRC2C	PRRC2C

P15311	Ezrin	EZR
E7ESD2	WASH complex subunit FAM21A	FAM21A
E7ESL0	39S ribosomal protein L22, mitochondrial	MRPL22
E7EVA0	Microtubule-associated protein	MAP4
P23588	Eukaryotic translation initiation factor 4B	EIF4B
E9PAV3	Nascent polypeptide-associated complex subunit alpha, muscle-specific form	NACA
E9PCY7	Heterogeneous nuclear ribonucleoprotein H	HNRNPH1
P29692	Elongation factor 1-delta	EEF1D
E9PK91	Bcl-2-associated transcription factor 1	BCLAF1
E9PS38	NEDD8	NEDD8
E9PLT0	Cold shock domain-containing protein E1	CSDE1
P23528	Cofilin-1	CFL1
Q14914	Prostaglandin reductase 1	PTGR1
P78371	T-complex protein 1 subunit beta	CCT2
P34949	Mannose-6-phosphate isomerase	MPI
P08195	4F2 cell-surface antigen heavy chain	SLC3A2
P09104	Enolase;Gamma-enolase	ENO2
Q8IZ83	Aldehyde dehydrogenase family 16 member A1	ALDH16A1
P68363	Tubulin alpha-1B chain	TUBA1B
P52926	High mobility group protein HMGI-C	HMGA2
P15586	N-acetylglucosamine-6-sulfatase	GNS
Q8TAD7	Overexpressed in colon carcinoma 1 protein	OCC1
F8VR42	Dynein regulatory complex subunit 2	CCDC65
Q9UBQ0	Vacuolar protein sorting-associated protein 29	VPS29
F8W031	DUF3456 domain-containing protein	N/A
P60660	Myosin light polypeptide 6	MYL6
P09651	Heterogeneous nuclear ribonucleoprotein A1	HNRNPA1
F8W726	Ubiquitin-associated protein 2-like	UBAP2L
F8WJN3	Cleavage and polyadenylation specificity factor subunit 6	CPSF6
O60232	Sjogren syndrome/scleroderma autoantigen 1	SSSCA1
P60900	Proteasome subunit alpha type;Proteasome subunit alpha type-6	PSMA6
P27695	DNA-(apurinic or apyrimidinic site) lyase;DNA-(apurinic or apyrimidinic site) lyase, mitochondrial	APEX1
Q96EK6	Glucosamine 6-phosphate N-acetyltransferase	GNPNAT1
P07942	Laminin subunit beta-1	LAMB1
P35221	Catenin alpha-1	CTNNA1
G8JLD3	ELKS/Rab6-interacting/CAST family member 1	ERC1
H0Y360	AMP deaminase 2	AMPD2
P12268	Inosine-5-monophosphate dehydrogenase 2	IMPDH2
P0DP24	Calmodulin-2	CALM2
H0Y8X4	2-deoxynucleoside 5-phosphate N-hydrolase 1	DNPH1
P52943	Cysteine-rich protein 2	CRIP2
P40939	Trifunctional enzyme subunit alpha, mitochondrial	HADHA
P06576	ATP synthase subunit beta, mitochondrial	ATP5B
P13804	Electron transfer flavoprotein subunit alpha, mitochondrial	ETFA
P09661	U2 small nuclear ribonucleoprotein A	SNRPA1
H0YMF9	WD repeat-containing protein 61	WDR61

P39687	Acidic leucine-rich nuclear phosphoprotein 32 family member A	ANP32A
P08708	40S ribosomal protein S17	RPS17
P15559	NAD(P)H dehydrogenase [quinone] 1	NQO1
P06865	Beta-hexosaminidase subunit alpha	HEXA
Q1KMD3	Heterogeneous nuclear ribonucleoprotein U-like protein 2	HNRNPUL2
I3L397	Eukaryotic translation initiation factor 5A	EIF5A
O00233	26S proteasome non-ATPase regulatory subunit 9	PSMD9
P52565	Rho GDP-dissociation inhibitor 1	ARHGDI1
J3QQZ9	Pyridoxine-5-phosphate oxidase	PNPO
J3QRS3	Myosin regulatory light chain 12A	MYL12A
P26373	60S ribosomal protein L13	RPL13
J3QT28	Mitotic checkpoint protein BUB3	BUB3
P62841	40S ribosomal protein S15	RPS15
K7ELC7	60S ribosomal protein L27	RPL27
P14314	Glucosidase 2 subunit beta	PRKCSH
P41567	Eukaryotic translation initiation factor 1	EIF1
P62316	Small nuclear ribonucleoprotein Sm D2	SNRPD2
Q13867	Bleomycin hydrolase	BLMH
Q9NP81	Serine--tRNA ligase, mitochondrial	SARS2
P46782	40S ribosomal protein S5	RPS5
P30043	Flavin reductase (NADPH)	BLVRB
P62249	40S ribosomal protein S16	RPS16
O00116	Alkyldihydroxyacetonephosphate synthase, peroxisomal	AGPS
O00154	Cytosolic acyl coenzyme A thioester hydrolase	ACOT7
O00159-2	Unconventional myosin-Ic	MYO1C
O00273	DNA fragmentation factor subunit alpha	DFFA
O00299	Chloride intracellular channel protein 1	CLIC1
E7ETU9	Procollagen-lysine,2-oxoglutarate 5-dioxygenase 2	PLOD2
O00499	Myc box-dependent-interacting protein 1	BIN1
O00515	Ladinin-1	LAD1
O00560	Syntenin-1	SDCBP
P47813	Eukaryotic translation initiation factor 1A, X-chromosomal	EIF1AX
O14744	Protein arginine N-methyltransferase 5	PRMT5
O14745	Na(+)/H(+) exchange regulatory cofactor NHE-RF1	SLC9A3R1
O14818	Proteasome subunit alpha type-7	PSMA7
O14841	5-oxoprolinase	OPLAH
O14907	Tax1-binding protein 3	TAX1BP3
O14974-3	Protein phosphatase 1 regulatory subunit 12A	PPP1R12A
O15027	Protein transport protein Sec16A	SEC16A
O15067	Phosphoribosylformylglycinamide synthase	PFAS
O15144	Actin-related protein 2/3 complex subunit 2	ARPC2
H0Y704	Zinc finger protein 185	ZNF185
O15460	Prolyl 4-hydroxylase subunit alpha-2	P4HA2
O43290	U4/U6.U5 tri-snRNP-associated protein 1	SART1
O43390	Heterogeneous nuclear ribonucleoprotein R	HNRNP
O43399	Tumor protein D54	TPD52L2

O43447	Peptidyl-prolyl cis-trans isomerase H;Peptidyl-prolyl cis-trans isomerase	PPIH
O43583	Density-regulated protein	DENR
O43707	Alpha-actinin-4	ACTN4
O43776	Asparagine--tRNA ligase, cytoplasmic	NARS
O43847	Nardilysin	NRD1
O43852	Calumenin	CALU
O60506	Heterogeneous nuclear ribonucleoprotein Q	SYNCRIP
O60547	GDP-mannose 4,6 dehydratase	GMDS
O60664	Perilipin-3	PLIN3
O60701	UDP-glucose 6-dehydrogenase	UGDH
O75083	WD repeat-containing protein 1	WDR1
O75348	V-type proton ATPase subunit G 1	ATP6V1G1
O75368	SH3 domain-binding glutamic acid-rich-like protein	SH3BGRL
O75369	Filamin-B	FLNB
O75436	Vacuolar protein sorting-associated protein 26A	VPS26A
O75531	Barrier-to-autointegration factor;Barrier-to-autointegration factor, N-terminally processed	BANF1
O75607	Nucleoplasmin-3	NPM3
O75821	Eukaryotic translation initiation factor 3 subunit G	EIF3G
O75874	Isocitrate dehydrogenase [NADP] cytoplasmic	IDH1
O75891	Cytosolic 10-formyltetrahydrofolate dehydrogenase	ALDH1L1
O75937	DnaJ homolog subfamily C member 8	DNAJC8
O75947	ATP synthase subunit d, mitochondrial	ATP5H
O75955	Flotillin-1	FLOT1
O75976	Carboxypeptidase D	CPD
O94760	N(G),N(G)-dimethylarginine dimethylaminohydrolase 1	DDAH1
O94925	Glutaminase kidney isoform, mitochondrial	GLS
O95171-3	Sciellin	SCEL
O95239-2	Chromosome-associated kinesin KIF4A	KIF4A
O95297	Myelin protein zero-like protein 1	MPZL1
O95336	6-phosphogluconolactonase	PGLS
O95817	BAG family molecular chaperone regulator 3	BAG3
O95831	Apoptosis-inducing factor 1, mitochondrial	AIFM1
O95865	N(G),N(G)-dimethylarginine dimethylaminohydrolase 2	DDAH2
O95881	Thioredoxin domain-containing protein 12	TXNDC12
P00338	L-lactate dehydrogenase A chain	LDHA
P00352	Retinal dehydrogenase 1	ALDH1A1
P00367	Glutamate dehydrogenase 1, mitochondrial	GLUD1
P00441	Superoxide dismutase [Cu-Zn]	SOD1
P00491	Purine nucleoside phosphorylase	PNP
P00492	Hypoxanthine-guanine phosphoribosyltransferase	HPRT1
P00505	Aspartate aminotransferase, mitochondrial	GOT2
P00558	Phosphoglycerate kinase 1	PGK1
P02511	Alpha-crystallin B chain	CRYAB
P02545	Prelamin-A/C;Lamin-A/C	LMNA
P02751	Fibronectin;Anastellin;Ugl-Y1;Ugl-Y2;Ugl-Y3	FN1
P04040	Catalase	CAT
P04066	Tissue alpha-L-fucosidase	FUCA1

P04075	Fructose-bisphosphate aldolase A;Fructose-bisphosphate aldolase	ALDOA
P04083	Annexin A1	ANXA1
P04179	Superoxide dismutase [Mn], mitochondrial	SOD2
P04181	Ornithine aminotransferase, mitochondrial	OAT
P04406	Glyceraldehyde-3-phosphate dehydrogenase	GAPDH
P04424	Argininosuccinate lyase	ASL
P04792	Heat shock protein beta-1	HSPB1
P05023	Sodium/potassium-transporting ATPase subunit alpha-1	ATP1A1
P05091	Aldehyde dehydrogenase, mitochondrial	ALDH2
P05106	Integrin beta-3;Integrin beta	ITGB3
P05165	Propionyl-CoA carboxylase alpha chain, mitochondrial	PCCA
P05387	60S acidic ribosomal protein P2	RPLP2
P05455	Lupus La protein	SSB
P05556	Integrin beta-1	ITGB1
P05783	Keratin, type I cytoskeletal 18	KRT18
P05976	Myosin light chain 1/3, skeletal muscle isoform	MYL1
P06703	Protein S100;Protein S100-A6	S100A6
P06733	Alpha-enolase	ENO1
P06737	Glycogen phosphorylase, liver form	PYGL
P06744	Glucose-6-phosphate isomerase	GPI
P06748	Nucleophosmin	NPM1
P06753-2	Tropomyosin alpha-3 chain	TPM3
P06756	Integrin alpha-V	ITGAV
P07108	Acyl-CoA-binding protein	DBI
P07195	L-lactate dehydrogenase B chain	LDHB
P07237	Protein disulfide-isomerase	P4HB
P07355	Annexin A2;Annexin	ANXA2
P07602	Prosaposin;Saposin-A;Saposin-B-Val;Saposin-B;Saposin-C;Saposin-D	PSAP
P07737	Profilin-1	PFN1
P07741	Adenine phosphoribosyltransferase	APRT
P07814	Bifunctional glutamate/proline--tRNA ligase;Glutamate--tRNA ligase;Proline--tRNA ligase	EPRS
P07858	Cathepsin B;Cathepsin B light chain;Cathepsin B heavy chain	CTSB
P07900	Heat shock protein HSP 90-alpha	HSP90AA1
P07954	Fumarate hydratase, mitochondrial	FH
P08133	Annexin A6;Annexin	ANXA6
P08238	Heat shock protein HSP 90-beta	HSP90AB1
P08621	U1 small nuclear ribonucleoprotein 70 kDa	SNRNP70
P08670	Vimentin	VIM
P08758	Annexin A5;Annexin	ANXA5
P09012	U1 small nuclear ribonucleoprotein A	SNRPA
P09382	Galectin-1	LGALS1
P09417	Dihydropteridine reductase	QDPR
P09525	Annexin A4;Annexin	ANXA4
P09622	Dihydrolipoyl dehydrogenase, mitochondrial;Dihydrolipoyl dehydrogenase	DLD



P09936	Ubiquitin carboxyl-terminal hydrolase isozyme L1;Ubiquitin carboxyl-terminal hydrolase	UCHL1
P09960	Leukotriene A-4 hydrolase	LTA4H
P09972	Fructose-bisphosphate aldolase C;Fructose-bisphosphate aldolase	ALDOC
P10253	Lysosomal alpha-glucosidase;76 kDa lysosomal alpha-glucosidase;70 kDa lysosomal alpha-glucosidase	GAA
P10451	Osteopontin	SPP1
P10599	Thioredoxin	TXN
P10768	S-formylglutathione hydrolase	ESD
P10809	60 kDa heat shock protein, mitochondrial	HSPD1
P11021	78 kDa glucose-regulated protein	HSPA5
P11047	Laminin subunit gamma-1	LAMC1
P11142	Heat shock cognate 71 kDa protein	HSPA8
P11216	Glycogen phosphorylase, brain form	PYGB
P11413	Glucose-6-phosphate 1-dehydrogenase	G6PD
P11586	C-1-tetrahydrofolate synthase, cytoplasmic	MTHFD1
P11766	Alcohol dehydrogenase class-3	ADH5
P11940	Polyadenylate-binding protein 1	PABPC1
P12004	Proliferating cell nuclear antigen	PCNA
P12081	Histidine--tRNA ligase, cytoplasmic	HARS
P12270	Nucleoprotein TPR	TPR
P12429	Annexin A3;Annexin	ANXA3
P12814	Alpha-actinin-1	ACTN1
P12955	Xaa-Pro dipeptidase	PEPD
P12956	X-ray repair cross-complementing protein 6	XRCC6
P13639	Elongation factor 2	EEF2
P13667	Protein disulfide-isomerase A4	PDIA4
P13674	Prolyl 4-hydroxylase subunit alpha-1	P4HA1
P13693	Translationally-controlled tumor protein	TPT1
P14324	Farnesyl pyrophosphate synthase	FDPS
P14550	Alcohol dehydrogenase [NADP(+)]	AKR1A1
P14618	Pyruvate kinase PKM	PKM
P14625	Endoplasmic	HSP90B1
P15121	Aldose reductase	AKR1B1
P15144	Aminopeptidase N	ANPEP
P15170-2	Eukaryotic peptide chain release factor GTP-binding subunit ERF3A	GSPT1
P15531	Nucleoside diphosphate kinase A	NME1
P16152	Carbonyl reductase [NADPH] 1	CBR1
P16278	Beta-galactosidase	GLB1
P16949	Stathmin	STMN1
P16989-2	Y-box-binding protein 3	YBX3
P17096	High mobility group protein HMG-I/HMG-Y	HMGA1
P17096-2	High mobility group protein HMG-I/HMG-Y	HMGA1
P17174	Aspartate aminotransferase, cytoplasmic	GOT1
P17980	26S protease regulatory subunit 6A	PSMC3
P17987	T-complex protein 1 subunit alpha	TCP1
P18124	60S ribosomal protein L7	RPL7

P18206	Vinculin	VCL
P18669	Phosphoglycerate mutase 1	PGAM1
P18859	ATP synthase-coupling factor 6, mitochondrial	ATP5J
P19338	Nucleolin	NCL
P19367	Hexokinase-1	HK1
P20042	Eukaryotic translation initiation factor 2 subunit 2	EIF2S2
P20618	Proteasome subunit beta type-1	PSMB1
P20810	Calpastatin	CAST
P21399	Cytoplasmic aconitate hydratase	ACO1
P21980	Protein-glutamine gamma-glutamyltransferase 2	TGM2
P22307	Non-specific lipid-transfer protein	SCP2
P22314	Ubiquitin-like modifier-activating enzyme 1	UBA1
P22392	Nucleoside diphosphate kinase B	NME2
P22626	Heterogeneous nuclear ribonucleoproteins A2/B1	HNRNPA2B1
P23246	Splicing factor, proline- and glutamine-rich	SFPQ
P23284	Peptidyl-prolyl cis-trans isomerase B	PIIB
P23378	Glycine dehydrogenase (decarboxylating), mitochondrial	GLDC
P23381	Tryptophan--tRNA ligase, cytoplasmic;T1-TrpRS;T2-TrpRS	WARS
P23396	40S ribosomal protein S3	RPS3
P23526	Adenosylhomocysteinase	AHCY
P24534	Elongation factor 1-beta	EEF1B2
P24752	Acetyl-CoA acetyltransferase, mitochondrial	ACAT1
P25685	DnaJ homolog subfamily B member 1	DNAJB1
P25705	ATP synthase subunit alpha, mitochondrial	ATP5A1
P25786	Proteasome subunit alpha type-1	PSMA1
P26006	Integrin alpha-3;Integrin alpha-3 heavy chain;Integrin alpha-3 light chain	ITGA3
P26038	Moesin	MSN
P26639	Threonine--tRNA ligase, cytoplasmic	TARS
P27105	Erythrocyte band 7 integral membrane protein	STOM
P27348	14-3-3 protein theta	YWHAQ
P27797	Calreticulin	CALR
P27824	Calnexin	CANX
P28066	Proteasome subunit alpha type-5	PSMA5
P28074	Proteasome subunit beta type-5	PSMB5
P28838	Cytosol aminopeptidase	LAP3
P29034	Protein S100-A2	S100A2
P29401	Transketolase	TKT
P29966	Myristoylated alanine-rich C-kinase substrate	MARCKS
P30038	Delta-1-pyrroline-5-carboxylate dehydrogenase, mitochondrial	ALDH4A1
P30040	Endoplasmic reticulum resident protein 29	ERP29
P30041	Peroxiredoxin-6	PRDX6
P30044	Peroxiredoxin-5, mitochondrial	PRDX5
P30048	Thioredoxin-dependent peroxide reductase, mitochondrial	PRDX3
P30050	60S ribosomal protein L12	RPL12
P30084	Enoyl-CoA hydratase, mitochondrial	ECHS1
P30085	UMP-CMP kinase	CMPK1

P30086	Phosphatidylethanolamine-binding protein 1	PEBP1
P30101	Protein disulfide-isomerase A3	PDIA3
P30153	Serine/threonine-protein phosphatase 2A 65 kDa regulatory subunit A alpha isoform	PPP2R1A
P30520	Adenylosuccinate synthetase isozyme 2	ADSS
P30533	Alpha-2-macroglobulin receptor-associated protein	LRPAP1
P30622	CAP-Gly domain-containing linker protein 1	CLIP1
P31040	Succinate dehydrogenase [ubiquinone] flavoprotein subunit, mitochondrial	SDHA
P31150	Rab GDP dissociation inhibitor alpha	GDI1
P31153	S-adenosylmethionine synthase isoform type-2	MAT2A
P31937	3-hydroxyisobutyrate dehydrogenase, mitochondrial	HIBADH
P31939	Bifunctional purine biosynthesis protein ATIC	ATIC
P31942	Heterogeneous nuclear ribonucleoprotein H3	HNRNPH3
P31946	14-3-3 protein beta/alpha	YWHAB
P31948	Stress-induced-phosphoprotein 1	STIP1
P31949	Protein S100-A11;Protein S100-A11, N-terminally processed	S100A11
P34896-3	Serine hydroxymethyltransferase, cytosolic	SHMT1
P34931	Heat shock 70 kDa protein 1-like	HSPA1L
P34932	Heat shock 70 kDa protein 4	HSPA4
P35269	General transcription factor IIF subunit 1	GTF2F1
P35579	Myosin-9	MYH9
P35606	Coatomer subunit beta	COPB2
P35613	Basigin	BSG
P35998	26S protease regulatory subunit 7	PSMC2
P36551	Oxygen-dependent coproporphyrinogen-III oxidase, mitochondrial	CPOX
P36578	60S ribosomal protein L4	RPL4
P36871	Phosphoglucomutase-1	PGM1
P36957	Dihydrolipoyllysine-residue succinyltransferase component of 2-oxoglutarate dehydrogenase complex, mitochondrial	DLST
P37108	Signal recognition particle 14 kDa protein	SRP14
P37802	Transgelin-2	TAGLN2
P37837	Transaldolase	TALDO1
P38117	Electron transfer flavoprotein subunit beta	ETFB
P38159	RNA-binding motif protein, X chromosome	RBMX
P38606	V-type proton ATPase catalytic subunit A	ATP6V1A
P38646	Stress-70 protein, mitochondrial	HSPA9
P38919	Eukaryotic initiation factor 4A-III;Eukaryotic initiation factor 4A-III, N-terminally processed	EIF4A3
P39019	40S ribosomal protein S19	RPS19
P39023	60S ribosomal protein L3	RPL3
P40121	Macrophage-capping protein	CAPG
P40222	Alpha-taxilin	TXLNA
P40261	Nicotinamide N-methyltransferase	NNMT
P40855	Peroxisomal biogenesis factor 19	PEX19
P40925	Malate dehydrogenase, cytoplasmic	MDH1

P40926	Malate dehydrogenase, mitochondrial	MDH2
P41091	Eukaryotic translation initiation factor 2 subunit 3	EIF2S3
P41250	Glycine--tRNA ligase	GARS
P41252	Isoleucine--tRNA ligase, cytoplasmic	IARS
P42126	Enoyl-CoA delta isomerase 1, mitochondrial	ECI1
P42166	Lamina-associated polypeptide 2, isoform alpha;Thymopoietin;Thymopentin	TMPO
P42677	40S ribosomal protein S27	RPS27
P43034	Platelet-activating factor acetylhydrolase IB subunit alpha	PAFAH1B1
P43490	Nicotinamide phosphoribosyltransferase	NAMPT
P43686	26S protease regulatory subunit 6B	PSMC4
P46108	Adapter molecule crk	CRK
P46821	Microtubule-associated protein 1B	MAP1B
P46940	Ras GTPase-activating-like protein IQGAP1	IQGAP1
P47755	F-actin-capping protein subunit alpha-2	CAPZA2
B1AK87	F-actin-capping protein subunit beta	CAPZB
P47897	Glutamine--tRNA ligase	QARS
P48735	Isocitrate dehydrogenase [NADP], mitochondrial	IDH2
P49189	4-trimethylaminobutyraldehyde dehydrogenase	ALDH9A1
P49321	Nuclear autoantigenic sperm protein	NASP
P49411	Elongation factor Tu, mitochondrial	TUFM
P49588	Alanine--tRNA ligase, cytoplasmic	AARS
P49589	Cysteine--tRNA ligase, cytoplasmic	CARS
P49748	Very long-chain specific acyl-CoA dehydrogenase, mitochondrial	ACADVL
P49792	E3 SUMO-protein ligase RanBP2	RANBP2
P50395	Rab GDP dissociation inhibitor beta	GDI2
P50502	Hsc70-interacting protein;Putative protein FAM10A5	ST13
P50990	T-complex protein 1 subunit theta	CCT8
P51149	Ras-related protein Rab-7a	RAB7A
P51570	Galactokinase	GALK1
P51858	Hepatoma-derived growth factor	HDGF
P51991	Heterogeneous nuclear ribonucleoprotein A3	HNRNPA3
P51991-2	Heterogeneous nuclear ribonucleoprotein A3	HNRNPA3
P52209	6-phosphogluconate dehydrogenase, decarboxylating	PGD
P52272	Heterogeneous nuclear ribonucleoprotein M	HNRNPM
P52597	Heterogeneous nuclear ribonucleoprotein F	HNRNPF
P52888	Thimet oligopeptidase	THOP1
P52907	F-actin-capping protein subunit alpha-1	CAPZA1
P53396	ATP-citrate synthase	ACLY
P53634	Dipeptidyl peptidase 1	CTSC
P53985	Monocarboxylate transporter 1	SLC16A1
P53999	Activated RNA polymerase II transcriptional coactivator p15	SUB1
P54136	Arginine--tRNA ligase, cytoplasmic	RARS
P54577	Tyrosine--tRNA ligase, cytoplasmic	YARS
P55072	Transitional endoplasmic reticulum ATPase	VCP
P55084	Trifunctional enzyme subunit beta, mitochondrial	HADHB
P55263	Adenosine kinase	ADK

P55786	Puromycin-sensitive aminopeptidase	NPEPPS
P56537	Eukaryotic translation initiation factor 6	EIF6
P58546	Myotrophin	MTPN
P60174	Triosephosphate isomerase	TPI1
P60709	Actin, cytoplasmic 1;Actin, cytoplasmic 1, N-terminally processed	ACTB
P60842	Eukaryotic initiation factor 4A-I	EIF4A1
P60866	40S ribosomal protein S20	RPS20
P60903	Protein S100-A10	S100A10
P60981	Dextrin	DSTN
P61158	Actin-related protein 3	ACTR3
P61221	ATP-binding cassette sub-family E member 1	ABCE1
P61247	40S ribosomal protein S3a	RPS3A
P61956	Small ubiquitin-related modifier 2	SUMO2
P61978	Heterogeneous nuclear ribonucleoprotein K	HNRNPK
P61981	14-3-3 protein gamma;14-3-3 protein gamma, N-terminally processed	YWHAG
P62070	Ras-related protein R-Ras2	RRAS2
P62195	26S protease regulatory subunit 8	PSMC5
P62241	40S ribosomal protein S8	RPS8
P62258	14-3-3 protein epsilon	YWHAE
P62280	40S ribosomal protein S11	RPS11
P62328	Thymosin beta-4	TMSB4X
P62424	60S ribosomal protein L7a	RPL7A
P62701	40S ribosomal protein S4, X isoform	RPS4X
P62805	Histone H4	HIST1H4A
P62851	40S ribosomal protein S25	RPS25
P62877	E3 ubiquitin-protein ligase RBX1	RBX1
P62899	60S ribosomal protein L31	RPL31
P62906	60S ribosomal protein L10a	RPL10A
P62913	60S ribosomal protein L11	RPL11
P62937	Peptidyl-prolyl cis-trans isomerase A	PPIA
P62942	Peptidyl-prolyl cis-trans isomerase FKBP1A	FKBP1A
P62979	Ubiquitin-40S ribosomal protein S27a	RPS27A
P63104	14-3-3 protein zeta/delta	YWHAZ
P63172	Dynein light chain Tctex-type 1	DYNLT1
P63220	40S ribosomal protein S21	RPS21
P63244	Guanine nucleotide-binding protein subunit beta-2-like 1	GNB2L1
P63313	Thymosin beta-10	TMSB10
P67775	Serine/threonine-protein phosphatase 2A catalytic subunit alpha isoform	PPP2CA
P67809	Nuclease-sensitive element-binding protein 1	YBX1
P67936	Tropomyosin alpha-4 chain	TPM4
P68104	Elongation factor 1-alpha 1	EEF1A1
P68366	Tubulin alpha-4A chain	TUBA4A
P68371	Tubulin beta-4B chain	TUBB4B
P78417	Glutathione S-transferase omega-1	GSTO1
P80303	Nucleobindin-2	NUCB2
P80723	Brain acid soluble protein 1	BASP1

P84098	Ribosomal protein L19	RPL19
P98082	Disabled homolog 2	DAB2
Q00688	Peptidyl-prolyl cis-trans isomerase FKBP3	FKBP3
Q00796	Sorbitol dehydrogenase	SORD
Q01105	Protein SET	SET
Q01130	Serine/arginine-rich splicing factor 2	SRSF2
Q01469	Fatty acid-binding protein, epidermal	FABP5
Q01518	Adenylyl cyclase-associated protein 1	CAP1
Q01813	ATP-dependent 6-phosphofructokinase, platelet type	PFKP
Q02252	Methylmalonate-semialdehyde dehydrogenase [acylating], mitochondrial	ALDH6A1
Q02790	Peptidyl-prolyl cis-trans isomerase FKBP4	FKBP4
Q02818	Nucleobindin-1	NUCB1
Q02878	60S ribosomal protein L6	RPL6
Q02952	A-kinase anchor protein 12	AKAP12
Q03001	Dystonin	DST
Q04323	UBX domain-containing protein 1	UBXN1
<b>Q04760</b>	<b>Lactoylglutathione lyase</b>	<b>GLO1</b>
Q04917	14-3-3 protein eta	YWHAH
Q05209	Tyrosine-protein phosphatase non-receptor type 12	PTPN12
E9PGZ1	Caldesmon	CALD1
Q06203	Amidophosphoribosyltransferase	PPAT
Q06210	Glutamine--fructose-6-phosphate aminotransferase [isomerizing] 1	GFPT1
Q06830	Peroxiredoxin-1	PRDX1
Q07021	Complement component 1 Q subcomponent-binding protein, mitochondrial	C1QBP
Q07075	Glutamyl aminopeptidase	ENPEP
Q07955-3	Serine/arginine-rich splicing factor 1	SRSF1
Q08257	Quinone oxidoreductase	CRYZ
Q09028-4	Histone-binding protein RBBP4	RBBP4
Q09666	Neuroblast differentiation-associated protein AHNAK	AHNAK
Q10713	Mitochondrial-processing peptidase subunit alpha	PMPCA
Q12765	Secernin-1	SCRN1
Q12792	Twinfilin-1	TWF1
Q12904	Aminoacyl tRNA synthase complex-interacting multifunctional protein 1	AIMP1
Q12906	Interleukin enhancer-binding factor 3	ILF3
Q12913	Receptor-type tyrosine-protein phosphatase eta;Protein-tyrosine-phosphatase	PTPRJ
Q13126	S-methyl-5-thioadenosine phosphorylase	MTAP
Q13162	Peroxiredoxin-4	PRDX4
Q13185	Chromobox protein homolog 3	CBX3
Q13200	26S proteasome non-ATPase regulatory subunit 2	PSMD2
Q13228	Selenium-binding protein 1	SELENBP1
Q13242	Serine/arginine-rich splicing factor 9	SRSF9
Q13263	Transcription intermediary factor 1-beta	TRIM28
Q13347	Eukaryotic translation initiation factor 3 subunit I	EIF3I
Q13409	Cytoplasmic dynein 1 intermediate chain 2	DYNC1I2

Q13428	Treacle protein	TCOF1
Q13435	Splicing factor 3B subunit 2	SF3B2
Q13442	28 kDa heat- and acid-stable phosphoprotein	PDAP1
Q13451	Peptidyl-prolyl cis-trans isomerase FKBP5	FKBP5
Q13501	Sequestosome-1	SQSTM1
Q13561	Dynactin subunit 2	DCTN2
Q13564	NEDD8-activating enzyme E1 regulatory subunit	NAE1
Q13637	Ras-related protein Rab-32	RAB32
Q13813	Spectrin alpha chain, non-erythrocytic 1	SPTAN1
Q14019	Coactosin-like protein	COTL1
Q14103	Heterogeneous nuclear ribonucleoprotein D0	HNRNPD
Q14151	Scaffold attachment factor B2	SAFB2
Q14195	Dihydropyrimidinase-related protein 3	DPYSL3
Q14247	Src substrate cortactin	CTTN
Q14376	UDP-glucose 4-epimerase	GALE
Q14444	Caprin-1	CAPRIN1
Q14554	Protein disulfide-isomerase A5	PDIA5
Q14677	Clathrin interactor 1	CLINT1
Q14697	Neutral alpha-glucosidase AB	GANAB
Q14764	Major vault protein	MVP
Q14847	LIM and SH3 domain protein 1	LASP1
Q15056	Eukaryotic translation initiation factor 4H	EIF4H
Q15075	Early endosome antigen 1	EEA1
Q15084	Protein disulfide-isomerase A6	PDIA6
Q15147	1-phosphatidylinositol 4,5-bisphosphate phosphodiesterase beta-4	PLCB4
Q15149	Plectin	PLEC
Q15181	Inorganic pyrophosphatase	PPA1
Q15274	Nicotinate-nucleotide pyrophosphorylase [carboxylating]	QPRT
Q15293	Reticulocalbin-1	RCN1
Q15370	Transcription elongation factor B polypeptide 2	TCEB2
Q15393	Splicing factor 3B subunit 3	SF3B3
Q15417	Calponin-3	CNN3
Q15435	Protein phosphatase 1 regulatory subunit 7	PPP1R7
Q15637	Splicing factor 1	SF1
Q15691	Microtubule-associated protein RP/EB family member 1	MAPRE1
Q15717	ELAV-like protein 1	ELAVL1
Q15907	Ras-related protein Rab-11B	RAB11B
Q15942	Zyxin	ZYX
Q16186	Proteasomal ubiquitin receptor ADRM1	ADRM1
Q16270	Insulin-like growth factor-binding protein 7	IGFBP7
Q16531	DNA damage-binding protein 1	DDB1
Q16543	Hsp90 co-chaperone Cdc37	CDC37
Q16643	Drebrin	DBN1
Q16762	Thiosulfate sulfurtransferase	TST
Q16864	V-type proton ATPase subunit F	ATP6V1F
Q32MZ4	Leucine-rich repeat flightless-interacting protein 1	LRRFIP1
Q3KQU3	MAP7 domain-containing protein 1	MAP7D1
Q53FA7	Quinone oxidoreductase PIG3	TP53I3

Q53H82	Beta-lactamase-like protein 2	LACTB2
Q5JRX3	Presequence protease, mitochondrial	PITRM1
Q5JSH3	WD repeat-containing protein 44	WDR44
Q9Y6H1	Coiled-coil-helix-coiled-coil-helix domain-containing protein 2	CHCHD2
Q5T2W1	Na(+)/H(+) exchange regulatory cofactor NHE-RF3	PDZK1
P49591	Serine--tRNA ligase, cytoplasmic	SARS
Q5T6V5	UPF0553 protein C9orf64	C9orf64
Q5TEC6	Histone H3	HIST2H3PS2
Q5VZU9	Tripeptidyl-peptidase 2	TPP2
Q60FE5	Filamin-A	FLNA
Q6GMV3	Putative peptidyl-tRNA hydrolase PTRHD1	PTRHD1
Q6IBS0	Twinfilin-2	TWF2
Q6NVY1	3-hydroxyisobutyryl-CoA hydrolase, mitochondrial	HIBCH
Q6NYC8	Phostensin	PPP1R18
Q6NZI2	Polymerase I and transcript release factor	PTRF
Q6ZMZ3	Nesprin-3	SYNE3
Q6ZN40	Tropomyosin 1 (Alpha), isoform CRA_f	TPM1
Q6ZT07	TBC1 domain family member 9	TBC1D9
Q7KZF4	Staphylococcal nuclease domain-containing protein 1	SND1
Q7Z417	Nuclear fragile X mental retardation-interacting protein 2	NUFIP2
Q7Z4V5	Hepatoma-derived growth factor-related protein 2	HDGFRP2
Q86UP2	Kinectin	KTN1
Q86V81	THO complex subunit 4	ALYREF
Q86X76	Nitrilase homolog 1	NIT1
Q8IVF2-3	Protein AHNAK2	AHNAK2
Q8N1G4	Leucine-rich repeat-containing protein 47	LRRC47
Q8N1Q1	Carbonic anhydrase 13	CA13
Q8N5N7	39S ribosomal protein L50, mitochondrial	MRPL50
Q8N8N7	Prostaglandin reductase 2	PTGR2
Q8NC51	Plasminogen activator inhibitor 1 RNA-binding protein	SERBP1
Q8NFH8	RalBP1-associated Eps domain-containing protein 2	REPS2
Q8WU90	Zinc finger CCCH domain-containing protein 15	ZC3H15
Q8WW12	PEST proteolytic signal-containing nuclear protein	PCNP
Q8WWM7	Ataxin-2-like protein	ATXN2L
Q8WZ42	Titin	TTN
Q92598	Heat shock protein 105 kDa	HSPH1
Q92804	TATA-binding protein-associated factor 2N	TAF15
Q92820	Gamma-glutamyl hydrolase	GGH
Q92945	Far upstream element-binding protein 2	KHSRP
Q93052	Lipoma-preferred partner	LPP
Q93062	RNA-binding protein with multiple splicing	RBPM5
Q969H8	Myeloid-derived growth factor	MYDGF
Q96A49	Synapse-associated protein 1	SYAP1
Q96C19	EF-hand domain-containing protein D2	EFHD2
Q96C90	Protein phosphatase 1 regulatory subunit 14B	PPP1R14B
Q96DC8	Enoyl-CoA hydratase domain-containing protein 3, mitochondrial	ECHDC3
Q96DG6	Carboxymethylenebutenolidase homolog	CMBL



Q96FQ6	Protein S100-A16	S100A16
Q96G03	Phosphoglucomutase-2	PGM2
Q96GK7	Fumarylacetoacetate hydrolase domain-containing protein 2A	FAHD2A
Q96HC4	PDZ and LIM domain protein 5	PDLIM5
Q96I24	Far upstream element-binding protein 3	FUBP3
Q96I25	Splicing factor 45	RBM17
Q96IJ6	Mannose-1-phosphate guanyltransferase alpha	GMPPA
Q96IZ0	PRKC apoptosis WT1 regulator protein	PAWR
Q96KP4	Cytosolic non-specific dipeptidase	CNDP2
Q96M93	Adenosine deaminase domain-containing protein 1	ADAD1
Q96QK1	Vacuolar protein sorting-associated protein 35	VPS35
Q99497	Protein deglycase DJ-1	PARK7
Q99536	Synaptic vesicle membrane protein VAT-1 homolog	VAT1
Q99584	Protein S100-A13	S100A13
Q99873	Protein arginine N-methyltransferase 1	PRMT1
Q99961	Endophilin-A2	SH3GL1
Q9BPW8	Protein NipSnap homolog 1	NIPSNAP1
Q9BQ61	Uncharacterized protein C19orf43	C19orf43
Q9BQA1	Methylosome protein 50	WDR77
Q9BR76	Coronin-1B	CORO1B
Q9BRK5	45 kDa calcium-binding protein	SDF4
Q9BRP8	Partner of Y14 and mago	WIBG
Q9BS26	Endoplasmic reticulum resident protein 44	ERP44
Q9BTY2	Plasma alpha-L-fucosidase	FUCA2
Q9BX68	Histidine triad nucleotide-binding protein 2, mitochondrial	HINT2
Q9BXW6	Oxysterol-binding protein-related protein 1	OSBPL1A
Q9BYT8	Neurolysin, mitochondrial	NLN
Q9BZK7	F-box-like/WD repeat-containing protein TBL1XR1	TBL1XR1
Q9C0C2	182 kDa tankyrase-1-binding protein	TNKS1BP1
Q9H3P7	Golgi resident protein GCP60	ACBD3
Q9H4A4	Aminopeptidase B	RNPEP
Q9H7C9	Mth938 domain-containing protein	AAMDC
Q9H910	Hematological and neurological expressed 1-like protein	HN1L
Q9H993	Protein-glutamate O-methyltransferase	ARMT1
Q9HAU0	Pleckstrin homology domain-containing family A member 5	PLEKHA5
Q9HAV7	GrpE protein homolog 1, mitochondrial	GRPEL1
Q9HCC0	Methylcrotonoyl-CoA carboxylase beta chain, mitochondrial	MCCC2
Q9NQR4	Omega-amidase NIT2	NIT2
Q5T6H7	Xaa-Pro aminopeptidase 1	XPNPEP1
Q9NR45	Sialic acid synthase	NANS
Q9NRV9	Heme-binding protein 1	HEBP1
Q9NSE4	Isoleucine--tRNA ligase, mitochondrial	IARS2
Q9NWH9	SAFB-like transcription modulator	SLTM
Q9NX46	Poly (ADP-ribose) glycohydrolase ARH3	ADPRHL2
Q9NY33	Dipeptidyl peptidase 3	DPP3
Q9NYL9	Tropomodulin-3	TMOD3

Q9NZB2	Constitutive coactivator of PPAR-gamma-like protein 1	FAM120A
Q9NZL9	Methionine adenosyltransferase 2 subunit beta	MAT2B
Q9NZZ3	Charged multivesicular body protein 5	CHMP5
Q9P2E9	Ribosome-binding protein 1	RRBP1
Q9P2J5	Leucine--tRNA ligase, cytoplasmic	LARS
Q9UBQ7	Glyoxylate reductase/hydroxypyruvate reductase	GRHPR
Q9UBR2	Cathepsin Z	CTSZ
Q9UHD8	Septin-9	SEP-09
Q9UHG0	Doublecortin domain-containing protein 2	DCDC2
Q9UHV9	Prefoldin subunit 2	PFDN2
Q9UJ70	N-acetyl-D-glucosamine kinase	NAGK
Q9UJA5	tRNA (adenine(58)-N(1))-methyltransferase non-catalytic subunit TRM6	TRMT6
Q9UJU6	Drebrin-like protein	DBNL
Q9UKY7	Protein CDV3 homolog	CDV3
Q9ULV4	Coronin-1C;Coronin	CORO1C
Q9UMS4	Pre-mRNA-processing factor 19	PRPF19
Q9UMX0	Ubiquilin-1	UBQLN1
Q9UNZ2	NSFL1 cofactor p47	NSFL1C
Q9UPA5	Protein bassoon	BSN
Q9UQ35	Serine/arginine repetitive matrix protein 2	SRRM2
Q9UQ80	Proliferation-associated protein 2G4	PA2G4
Q9Y224	UPF0568 protein C14orf166	C14orf166
Q9Y285	Phenylalanine--tRNA ligase alpha subunit	FARSA
Q9Y2D5	A-kinase anchor protein 2	AKAP2
Q9Y2D8	Afadin- and alpha-actinin-binding protein	SSX2IP
Q9Y2H0	Disks large-associated protein 4	DLGAP4
Q9Y2T3	Guanine deaminase	GDA
Q9Y2V2	Calcium-regulated heat stable protein 1	CARHSP1
Q9Y2Z0	Suppressor of G2 allele of SKP1 homolog	SUGT1
Q9Y333	U6 snRNA-associated Sm-like protein LSm2	LSM2
Q9Y383	Putative RNA-binding protein Luc7-like 2	LUC7L2
Q9Y3C6	Peptidyl-prolyl cis-trans isomerase-like 1	PPIL1
Q9Y3F4	Serine-threonine kinase receptor-associated protein	STRAP
Q9Y3I0	tRNA-splicing ligase RtcB homolog	RTCB
Q9Y3U8	60S ribosomal protein L36	RPL36
Q9Y490	Talin-1	TLN1
Q9Y5K6	CD2-associated protein	CD2AP
Q9Y5Z4	Heme-binding protein 2	HEBP2
Q9Y608	Leucine-rich repeat flightless-interacting protein 2	LRRFIP2
Q9Y617	Phosphoserine aminotransferase	PSAT1
Q9Y6I3	Epsin-1	EPN1
Q9Y6N5	Sulfide:quinone oxidoreductase, mitochondrial	SQRDL
Q9Y6U3	Adseverin	SCIN
Q9BZE1	39S ribosomal protein L37, mitochondrial	MRPL37
S4R3H4	Apoptotic chromatin condensation inducer in the nucleus	ACIN1

## Appendix II-Table of total identified cytosolic proteins in MCs

<b>Protein accession numbers</b>	<b>Protein name</b>	<b>Gene accession numbers</b>
P07602	Prosaposin	PSAP
Q8IV08	Phospholipase D3	PLD3
Q9UBR2	Cathepsin Z	CTSZ
P22570	NADPH:adrenodoxin oxidoreductase, mitochondrial	FDXR
O95810	Serum deprivation-response protein	SDPR
P06737	Glycogen phosphorylase	PYGL
Q13011	Delta (3,5)-Delta (2,4)-dienoyl-CoA isomerase, mitochondrial	ECH1
P12277	Creatine kinase B-type	CKB
Q15274	Nicotinate-nucleotide pyrophosphorylase [carboxylating]	QPRT
Q16881	Thioredoxin reductase 1	TXNRD1
P26440	Isovaleryl-CoA dehydrogenase	IVD
P19367	Hexokinase-1	HK1
P50453	Serpin B9	SERPINB9
P0CG29	Glutathione S-transferase theta-2	GSTT2
E9PMS6	LIM domain only protein 7	LMO7
Q9Y570	Protein phosphatase methylesterase 1	PPME1
Q86V21	Acetoacetyl-CoA synthetase	AACS
Q8NCN5	Pyruvate dehydrogenase phosphatase regulatory subunit, mitochondrial	PDPR
Q96AT1	Uncharacterized protein KIAA1143	KIAA1143
P21980	Protein-glutamine gamma-glutamyltransferase 2	TGM2
P05091	Aldehyde dehydrogenase	ALDH2
P38117	Electron transfer flavoprotein subunit beta	ETFB
Q6X734	NIF3-like protein 1	NIF3L1
Q86TX2	Acyl-coenzyme A thioesterase 1	ACOT1
P21266	Glutathione S-transferase Mu 3	GSTM3
Q9UI42	Carboxypeptidase A4	CPA4
Q16822	Phosphoenolpyruvate carboxykinase [GTP], mitochondrial	PCK2
P13804	Electron transfer flavoprotein subunit alpha, mitochondrial	ETFA
P48735	Isocitrate dehydrogenase [NADP], mitochondrial	IDH2
P11177	Pyruvate dehydrogenase E1 component subunit beta, mitochondrial	PDHB
Q53FA7	Quinone oxidoreductase PIG3	TP53I3
P16278	Beta-galactosidase	GLB1
P52926	High mobility group protein HMGI-C	HMGA2
P15559	NAD(P)H dehydrogenase [quinone] 1	NQO1
O94760	N(G), N(G)-dimethylarginine dimethyl amino hydrolase 1	DDAH1
Q9Y617	Phosphoserine aminotransferase	PSAT1

P05783	Keratin, type I cytoskeletal 18	KRT18
P42574	Caspase-3	CASP3
P09936	Ubiquitin carboxyl-terminal hydrolase isozyme L1	UCHL1
P30084	Enoyl-CoA hydratase, mitochondrial	ECHS1
Q9NR45	Sialic acid synthase	NANS
P30048	Thioredoxin-dependent peroxide reductase, mitochondrial	PRDX3
P00441	Superoxide dismutase [Cu-Zn]	SOD1
P49748	Very long-chain specific acyl-CoA dehydrogenase, mitochondrial	ACADVL
P07339	Cathepsin D	CTSD
P04792	Heat shock protein beta-1	HSPB1
P30041	Peroxiredoxin-6	PRDX6
Q9UJ70	N-acetyl-D-glucosamine kinase	NAGK
P30044	Peroxiredoxin-5, mitochondrial	PRDX5
Q06210	Glutamine--fructose-6-phosphate aminotransferase [isomerizing] 1	GFPT1
P30040	Endoplasmic reticulum resident protein 29	ERP29
P32119	Peroxiredoxin-2	PRDX2
P36871	Phosphoglucomutase-1	PGM1
P00387	NADH-cytochrome b5 reductase 3	CYB5R3
P07686	Beta-hexosaminidase subunit beta	HEXB
P31949	Protein S100-A11	S100A11
Q9BRA2	Thioredoxin domain-containing protein 17	TXNDC17
Q6NZI2	Polymerase I and transcript release factor	PTRF
P19105	Myosin regulatory light chain 12A	MYL12A
P11216	Glycogen phosphorylase, brain form	PYGB
P07741	Adenine phosphoribosyltransferase	APRT
P14324	Farnesyl pyrophosphate synthase	FDPS
P46063	ATP-dependent DNA helicase Q1	RECQL
D6RA82	Annexin	ANXA3
P49189	4-trimethylaminobutyraldehyde dehydrogenase	ALDH9A1
Q9H488	GDP-fucose protein O-fucosyltransferase 1	POFUT1
P62937	Peptidyl-prolyl cis-trans isomerase A	PPIA
P08758	Annexin A5	ANXA5
P15586	N-acetylglucosamine-6-sulfatase	GNS
O75368	SH3 domain-binding glutamic acid-rich-like protein	SH3BGR1
Q9H7C9	Mth938 domain-containing protein	AAMDC
P31150	Rab GDP dissociation inhibitor alpha	GDI1
O75874	Isocitrate dehydrogenase [NADP] cytoplasmic	IDH1
P02751	Fibronectin	FN1
Q06830	Peroxiredoxin-1	PRDX1
Q13162	Peroxiredoxin-4	PRDX4
Q14019	Coactosin-like protein	COTL1
P59998	Actin-related protein 2/3 complex subunit 4	ARPC4
P49419	Alpha-aminoadipic semialdehyde dehydrogenase	ALDH7A1
P07237	Protein disulfide-isomerase	P4HB
P11021	Endoplasmic reticulum chaperone BiP	HSPA5
Q92820	Gamma-glutamyl hydrolase	GGH

P23284	Peptidyl-prolyl cis-trans isomerase B	PIIB
P14618	Pyruvate kinase PKM	PKM
P30101	Protein disulfide-isomerase A3	PDIA3
P00491	Purine nucleoside phosphorylase	PNP
P15121	Aldose reductase	AKR1B1
Q99798	Aconitate hydratase	ACO2
P04181	Ornithine aminotransferase	OAT
P41250	Glycine--tRNA ligase	GARS
P40925	Malate dehydrogenase, cytoplasmic	MDH1
O60701	UDP-glucose 6-dehydrogenase	UGDH
P12081	Histidine--tRNA ligase, cytoplasmic	HARS
P09622	Dihydrolipoyl dehydrogenase	DLD
P36957	Dihydrolipoyllysine-residue succinyltransferase component of 2-oxoglutarate dehydrogenase complex, mitochondrial	DLST
P23526	Adenosylhomocysteinase	AHCY
P40429	60S ribosomal protein L13a	RPL13A
P11940	Polyadenylate-binding protein 1	PABPC1
P26373	60S ribosomal protein L13	RPL13
Q92598	Heat shock protein 105 kDa	HSPH1
P35269	General transcription factor IIF subunit 1	GTF2F1
P46777	60S ribosomal protein L5	RPL5
Q14195	Dihydropyrimidinase-related protein 3	DPYSL3
Q9BUJ2	Heterogeneous nuclear ribonucleoprotein U-like protein 1	HNRNPUL1
P62910	60S ribosomal protein L32	RPL32
O15067	Phosphoribosylformylglycinamide synthase	PFAS
P07355	Annexin A2	ANXA2
P43034	Platelet-activating factor acetylhydrolase IB subunit alpha	PAFAH1B1
P61586	Transforming protein RhoA	RHOA
Q15075	Early endosome antigen 1	EEA1
P07910	Heterogeneous nuclear ribonucleoproteins C1/C2	HNRNPC
P48681	Nestin	NES
P62701	40S ribosomal protein S4, X isoform	RPS4X
Q99879	Histone H2B	H2BFS
Q9H910	Hematological and neurological expressed 1-like protein	HN1L
O75347	Tubulin-specific chaperone A	TBCA
P13639	Elongation factor 2	EEF2
P62424	60S ribosomal protein L7a	RPL7A
Q14444	Caprin-1	CAPRIN1
Q01844	RNA-binding protein EWS	EWSR1
P63279	SUMO-conjugating enzyme UBC9	UBE2I
O43396	Thioredoxin-like protein 1	TXNL1
P27695	DNA-(apurinic or apyrimidinic site) lyase, mitochondrial	APEX1
P52565	Rho GDP-dissociation inhibitor 1	ARHGDI1
Q16643	Drebrin	DBN1

Q9UKY7	Protein CDV3 homolog	CDV3
P08133	Annexin A6	ANXA6
P62913	60S ribosomal protein L11	RPL11
Q01105	Protein SET	SET
Q96C19	EF-hand domain-containing protein D2	EFHD2
Q9UHD9	Ubiquilin-2	UBQLN2
Q9Y383	Putative RNA-binding protein Luc7-like 2	LUC7L2
P61221	ATP-binding cassette sub-family E member 1	ABCE1
P63104	14-3-3 protein zeta/delta	YWHAZ
P61981	14-3-3 protein gamma	YWHAG
P62917	60S ribosomal protein L8	RPL8
Q02878	60S ribosomal protein L6	RPL6
Q15942	Zyxin	ZYX
Q07955	Serine/arginine-rich splicing factor 1	SRSF1
P08238	Heat shock protein HSP 90-beta	HSP90AB1
P31943	Heterogeneous nuclear ribonucleoprotein H	HNRNPH1
P06748	Nucleophosmin	NPM1
P20700	Lamin-B1	LMNB1
S4R417	40S ribosomal protein S15	RPS15
E7EQT4	Apoptotic chromatin condensation inducer in the nucleus	ACIN1
P08621	U1 small nuclear ribonucleoprotein 70 kDa	SNRNP70
P10412	Histone H1.4	HIST1H1E
P18124	60S ribosomal protein L7	RPL7
P27348	14-3-3 protein theta	YWHAQ
P40222	Alpha-taxilin	TXLNA
P42677	40S ribosomal protein S27	RPS27
Q02952	A-kinase anchor protein 12	AKAP12
Q9UK76	Hematological and neurological expressed 1 protein	HN1
Q9Y4Z0	U6 snRNA-associated Sm-like protein LSm4	LSM4
O14776	Transcription elongation regulator 1	TCERG1
P25685	DnaJ homolog subfamily B member 1	DNAJB1
P31153	S-adenosylmethionine synthase isoform type-2	MAT2A
P52597	Heterogeneous nuclear ribonucleoprotein F	HNRNPF
Q13185	Chromobox protein homolog 3	CBX3
Q13428	Treacle protein	TCOF1
O43707	Alpha-actinin-4	ACTN4
P05388	60S acidic ribosomal protein P0	RPLP0
P07900	Heat shock protein HSP 90-alpha	HSP90AA1
P11047	Laminin subunit gamma-1	LAMC1
Q04917	14-3-3 protein eta	YWHAH
O96019	Actin-like protein 6A	ACTL6A
P39023	60S ribosomal protein L3	RPL3
P42167	Lamina-associated polypeptide 2, isoforms beta/gamma	TMPO
Q5SW79	Centrosomal protein of 170 kDa	CEP170
Q9UBE0	SUMO-activating enzyme subunit 1	SAE1
Q13148	TAR DNA-binding protein 43	TARDBP
P68400	Casein kinase II subunit alpha	CSNK2A1

Q15185	Prostaglandin E synthase 3	PTGES3
P84098	Ribosomal protein L19	RPL19
P61254	60S ribosomal protein L26	RPL26
Q00839	Heterogeneous nuclear ribonucleoprotein U	HNRNPU
Q09028	Histone-binding protein RBBP4	RBBP4
Q9GZU8	Protein FAM192A	FAM192A
O14979	Heterogeneous nuclear ribonucleoprotein D-like	HNRNPDL
O43493	Trans-Golgi network integral membrane protein 2	TGOLN2
P12270	Nucleoprotein TPR	TPR
P61956	Small ubiquitin-related modifier 2	SUMO2
Q02790	Peptidyl-prolyl cis-trans isomerase FKBP4	FKBP4
Q8NC51	Plasminogen activator inhibitor 1 RNA-binding protein	SERBP1
P49321	Nuclear autoantigenic sperm protein	NASP
Q86U42	Polyadenylate-binding protein 2	PABPN1
Q8WW12	PEST proteolytic signal-containing nuclear protein	PCNP
Q9NX55	Huntingtin-interacting protein K	HYPK
P27635	60S ribosomal protein L10	RPL10
P22626	Heterogeneous nuclear ribonucleoproteins A2/B1	HNRNPA2B1
Q07020	60S ribosomal protein L18	RPL18
Q15459	Splicing factor 3A subunit 1	SF3A1
Q9P258	Protein RCC2	RCC2
Q92841	Probable ATP-dependent RNA helicase DDX17	DDX17
O43583	Density-regulated protein	DENR
P26599	Polypyrimidine tract-binding protein 1	PTBP1
O60506	Heterogeneous nuclear ribonucleoprotein Q	SYNCRIP
P18206	Vinculin	VCL
P46778	60S ribosomal protein L21	RPL21
Q13435	Splicing factor 3B subunit 2	SF3B2
Q14103	Heterogeneous nuclear ribonucleoprotein D0	HNRNPD
P23588	Eukaryotic translation initiation factor 4B	EIF4B
P38159	RNA-binding motif protein, X chromosome	RBMX
P61006	Ras-related protein Rab-8A	RAB8A
Q12904	Aminoacyl tRNA synthase complex-interacting multifunctional protein 1	AIMP1
Q92945	Far upstream element-binding protein 2	KHSRP
Q99733	Nucleosome assembly protein 1-like 4	NAP1L4
Q9Y696	Chloride intracellular channel protein 4	CLIC4
O43670	BUB3-interacting and GLEBS motif-containing protein ZNF207	ZNF207
P29966	Myristoylated alanine-rich C-kinase substrate	MARCKS
P61313	60S ribosomal protein L15	RPL15
P67809	Nuclease-sensitive element-binding protein 1	YBX1
Q96AE4	Far upstream element-binding protein 1	FUBP1
P51991	Heterogeneous nuclear ribonucleoprotein A3	HNRNPA3
P61978	Heterogeneous nuclear ribonucleoprotein K	HNRNPK
Q8N543	Prolyl 3-hydroxylase OGFOD1	OGFOD1
P07942	Laminin subunit beta-1	LAMB1
O00422	Histone deacetylase complex subunit SAP18	SAP18

P12814	Alpha-actinin-1	ACTN1
P31942	Heterogeneous nuclear ribonucleoprotein H3	HNRNPH3
Q9C0C2	182 kDa tankyrase-1-binding protein	TNKS1BP1
Q9H773	dCTP pyrophosphatase 1	DCTPP1
Q12905	Interleukin enhancer-binding factor 2	ILF2
Q99729	Heterogeneous nuclear ribonucleoprotein A/B	HNRNPAB
Q9Y2V2	Calcium-regulated heat stable protein 1	CARHSP1
Q15257	Serine/threonine-protein phosphatase 2A activator	PPP2R4
Q92882	Osteoclast-stimulating factor 1	OSTF1
P22061	Protein-L-isoaspartate O-methyltransferase	PCMT1
Q9UHR5	SAP30-binding protein	SAP30BP
P33316	Deoxyuridine 5-triphosphate nucleotidohydrolase, mitochondrial	DUT
O43390	Heterogeneous nuclear ribonucleoprotein R	HNRNPR
F8W0J6	Nucleosome assembly protein 1-like 1	NAP1L1
P09651	Heterogeneous nuclear ribonucleoprotein A1	HNRNPA1
P23246	Splicing factor, proline- and glutamine-rich	SFPQ
P38919	Eukaryotic initiation factor 4A-III	EIF4A3
Q9BYG3	MKI67 FHA domain-interacting nucleolar phosphoprotein	NIFK
Q9Y2X3	Nucleolar protein 58	NOP58
P02786	Transferrin receptor protein 1, serum form	TFRC
P57081	tRNA (guanine-N(7)-)-methyltransferase non-catalytic subunit WDR4	WDR4
P52434	DNA-directed RNA polymerases I, II, and III subunit RPABC3	POLR2H
Q9BRP8	Partner of Y14 and mago	WIBG
O43290	U4/U6.U5 tri-snRNP-associated protein 1	SART1
Q16630	Cleavage and polyadenylation specificity factor subunit 6	CPSF6
O75934	Pre-mRNA-splicing factor SPF27	BCAS2
P16989	Y-box-binding protein 3	YBX3
Q15233	Non-POU domain-containing octamer-binding protein	NONO
Q7Z4V5	Hepatoma-derived growth factor-related protein 2	HDGFRP2
Q9BWJ5	Splicing factor 3B subunit 5	SF3B5
P23193	Transcription elongation factor A protein 1	TCEA1
P82094	TATA element modulatory factor	TMF1
O43809	Cleavage and polyadenylation specificity factor subunit 5	NUDT21
Q96C90	Protein phosphatase 1 regulatory subunit 14B	PPP1R14B
Q9Y2Z0	Suppressor of G2 allele of SKP1 homolog	SUGT1
Q99829	Copine-1	CPNE1
Q15287	RNA-binding protein with serine-rich domain 1	RNPS1
Q9H6F5	Coiled-coil domain-containing protein 86	CCDC86
Q6PKG0	La-related protein 1	LARP1
O75391	Sperm-associated antigen 7	SPAG7
P09497	Clathrin light chain B	CLTB
Q92769	Histone deacetylase 2	HDAC2



O15355	Protein phosphatase 1G	PPM1G
P22087	rRNA 2-O-methyltransferase fibrillar	FBL
Q96PK6	RNA-binding protein 14	RBM14
Q08209	Serine/threonine-protein phosphatase 2B catalytic subunit alpha isoform	PPP3CA
Q6Y7W6	PERQ amino acid-rich with GYF domain-containing protein 2	GIGYF2
O00159	Unconventional myosin-Ic	MYO1C
Q08211	ATP-dependent RNA helicase A	DHX9
D6RDG3	Transcription factor BTF3	BTF3
O75940	Survival of motor neuron-related-splicing factor 30	SMNDC1
Q8WWM7	Ataxin-2-like protein	ATXN2L
P40855	Peroxisomal biogenesis factor 19	PEX19
Q93052	Lipoma-preferred partner	LPP
P41227	N-alpha-acetyltransferase 10	NAA10
P62993	Growth factor receptor-bound protein 2	GRB2
Q8NFP7	Diphosphoinositol polyphosphate phosphohydrolase 3-alpha	NUDT10
O75534	Cold shock domain-containing protein E1	CSDE1
Q9Y2W1	Thyroid hormone receptor-associated protein 3	THRAP3
E7EQ69	N-alpha-acetyltransferase 50	NAA50
O43143	Pre-mRNA-splicing factor ATP-dependent RNA helicase DHX15	DHX15
P63167	Dynein light chain 1, cytoplasmic	DYNLL1
Q8IYB3	Serine/arginine repetitive matrix protein 1	SRRM1
Q9H307	Pinin	PNN
P19784	Casein kinase II subunit alpha	CSNK2A2
Q9NZB2	Constitutive coactivator of PPAR-gamma-like protein 1	FAM120A
P09874	Poly [ADP-ribose] polymerase 1	PARP1
Q16576	Histone-binding protein RBBP7	RBBP7
Q9NX46	Poly (ADP-ribose) glycohydrolase ARH3	ADPRHL2
Q9Y266	Nuclear migration protein nudC	NUDC
P49327	Fatty acid synthase	FASN
Q9NPD3	Exosome complex component RRP41	EXOSC4
Q9Y520	Protein PRRC2C	PRRC2C
Q92522	Histone H1x	H1FX
Q5JW30	Double-stranded RNA-binding protein Staufen homolog 1	STAU1
P43243	Matrin-3	MATR3
P35520	Cystathionine beta-synthase	CBS
P14866	Heterogeneous nuclear ribonucleoprotein L	HNRNPL
P54105	Methylosome subunit pICln	CLNS1A
P83916	Chromobox protein homolog 1	CBX1
Q9Y230	RuvB-like 2	RUVBL2
Q9BQ61	Uncharacterized protein C19orf43	C19orf43
Q9BXJ9	N-alpha-acetyltransferase 15, NatA auxiliary subunit	NAA15
P33176	Kinesin-1 heavy chain	KIF5B

P33992	DNA replication licensing factor MCM5;DNA helicase	MCM5
P49750	YLP motif-containing protein 1	YLPM1
Q9UKD2	mRNA turnover protein 4 homolog	MRTO4
Q9GZL7	Ribosome biogenesis protein WDR12	WDR12
O43684	Mitotic checkpoint protein BUB3	BUB3
Q9BWU0	Kanadaplin	SLC4A1AP
Q9Y5S9	RNA-binding protein 8A	RBM8A
Q9HB07	UPF0160 protein MYG1, mitochondrial	C12orf10
Q15631	Translin	TSN
P47897	Glutamine--tRNA ligase	QARS
P60842	Eukaryotic initiation factor 4A-I	EIF4A1
Q9NR30	Nucleolar RNA helicase 2	DDX21
Q12906	Interleukin enhancer-binding factor 3	ILF3
Q13151	Heterogeneous nuclear ribonucleoprotein A0	HNRNPA0
O00193	Small acidic protein	SMAP
P83731	60S ribosomal protein L24	RPL24
Q96A72	Protein mago nashi homolog 2	MAGOHB
P17655	Calpain-2 catalytic subunit	CAPN2
Q15424	Scaffold attachment factor B1	SAFB
P35237	Serpin B6	SERPINB6
H0Y394	Vigilin	HDLBP
P46781	40S ribosomal protein S9	RPS9
P25787	Proteasome subunit alpha type 2	PSMA2
P80303	Nucleobindin-2	NUCB2
P07203	Glutathione peroxidase 1	GPX1
O60841	Eukaryotic translation initiation factor 5B	EIF5B
Q99460	26S proteasome non-ATPase regulatory subunit 1	PSMD1
Q16186	Proteasomal ubiquitin receptor ADRM1	ADRM1
P18621	60S ribosomal protein L17	RPL17
P09132	Signal recognition particle 19 kDa protein	SRP19
Q16851	UTP--glucose-1-phosphate uridylyltransferase	UGP2
M0R264	Deoxyhypusine synthase	DHPS
O43837	Isocitrate dehydrogenase [NAD] subunit, mitochondrial	IDH3B
Q9Y3A5	Ribosome maturation protein SBDS	SBDS
Q9Y6K9	NF-kappa-B essential modulator	IKBKG
Q7Z739	YTH domain-containing family protein 3	YTHDF3
O60271	C-Jun-amino-terminal kinase-interacting protein 4	SPAG9
P62333	26S protease regulatory subunit 10B	PSMC6
Q6ZSR9	Uncharacterized protein FLJ45252	N/A
Q14978	Nucleolar and coiled-body phosphoprotein 1	NOLC1
P06396	Gelsolin	GSN
Q14192	Four and a half LIM domains protein 2	FHL2
K7EQ48	Glucose-6-phosphate isomerase	GPI
P30566	Adenylosuccinate lyase	ADSL
A0A0B4J203	FIP1-like 1 protein	N/A
Q13509	Tubulin beta-3 chain	TUBB3
P08865	40S ribosomal protein SA	RPSA

P04632	Calpain small subunit 1	CAPNS1
F8WEK0	Cordon-bleu protein-like 1	COBLL1
P0DMV8	Heat shock 70 kDa protein 1A	HSPA1A
E9PQ56	60 kDa poly(U)-binding-splicing factor	PUF60
P09493	Tropomyosin alpha-1 chain	TPM1
A0A1B0GTU4	Paxillin	PXN
Q16555	Dihydropyrimidinase-related protein 2	DPYSL2
E9PF58	Actin-related protein 2/3 complex subunit 1A	ARPC1A
P23368	NAD-dependent malic enzyme, mitochondrial	ME2
O14558	Heat shock protein beta-6	HSPB6
A0A286YFD6	Ribonucleoside-diphosphate reductase subunit M2	RRM2
Q08379	Golgin subfamily A member 2	GOLGA2
A0A2R8Y422	40S ribosomal protein S27a	RPS27AP5
Q9Y3X0	Coiled-coil domain-containing protein 9	CCDC9
P35241	Radixin	RDX
O00571	ATP-dependent RNA helicase DDX3X	DDX3X
P62263	40S ribosomal protein S14	RPS14
P08237	ATP-dependent 6-phosphofructokinase, muscle type	PFKM
P62847	40S ribosomal protein S24	RPS24
P17812	CTP synthase 1	CTPS1
P14735	Insulin-degrading enzyme	IDE
Q6PI48	Aspartate--tRNA ligase, mitochondrial	DARS2
P47914	60S ribosomal protein L29	RPL29
P55769	NHP2-like protein 1	NHP2L1
O75400	Pre-mRNA-processing factor 40 homolog A	PRPF40A
A6NDG6	Phosphoglycolate phosphatase	PGP
Q9UUK9	ADP-sugar pyrophosphatase	NUDT5
P55145	Mesencephalic astrocyte-derived neurotrophic factor	MANF
P55854	Small ubiquitin-related modifier 3	SUMO3
P62308	Small nuclear ribonucleoprotein G	SNRPG
P48444	Coatomer subunit delta	ARCN1
B1AK87	F-actin-capping protein subunit beta	CAPZB
O43847	Nardilysin	NRD1
P60891	Ribose-phosphate pyrophosphokinase 1	PRPS1
Q13310	Polyadenylate-binding protein	PABPC4
Q99439	Calponin-2	CNN2
O75390	Citrate synthase, mitochondrial	CS
O95260	Arginyl-tRNA--protein transferase 1	ATE1
Q9UBX3	Mitochondrial dicarboxylate carrier	SLC25A10
Q13126	S-methyl-5-thioadenosine phosphorylase	MTAP
P62826	GTP-binding nuclear protein Ran	RAN
F8VFP3	Myosin light polypeptide 6	MYL6
Q9H6Z4	Ran-binding protein 3	RANBP3
P63165	Small ubiquitin-related modifier 1	SUMO1
B8ZZW7	Prothymosin alpha	PTMA
C9J0J7	Profilin	PFN2
P30626	Sorcin	SRI
Q16629	Serine/arginine-rich splicing factor 7	SRSF7
P78330	Phosphoserine phosphatase	PSPH

P99999	Cytochrome c	CYCS
P13798	Acylamino-acid-releasing enzyme	APEH
P18077	60S ribosomal protein L35a	RPL35A
Q9NVA2	Septin-11	Sep-11
Q6P1N9	Putative deoxyribonuclease TATDN1	TATDN1
O60925	Prefoldin subunit 1	PFDN1
Q15369	Transcription elongation factor B polypeptide 1	TCEB1
P62888	60S ribosomal protein L30	RPL30
P29218	Inositol monophosphatase 1	IMPA1
P63208	S-phase kinase-associated protein 1	SKP1
;P48643	T-complex protein 1 subunit epsilon	CCT5
Q16181	Septin-7	Sep-07
O15347	High mobility group protein B3	HMGB3
P20810	Calpastatin	CAST
Q641Q2	WASH complex subunit FAM21A	FAM21A
O00469	Procollagen-lysine,2-oxoglutarate 5-dioxygenase 2	PLOD2
E7EVA0	Microtubule-associated protein	MAP4
E7EVH7	Kinesin light chain	N/A
Q13765	Nascent polypeptide-associated complex subunit alpha	NACA
E9PB61	THO complex subunit 4	ALYREF
P22234	Multifunctional protein ADE2	PAICS
E9PGZ1	Caldesmon	CALD1
Q969G5	Protein kinase C delta-binding protein	PRKCDBP
Q04323	UBX domain-containing protein 1	UBXN1
Q99873	Protein arginine N-methyltransferase 1	PRMT1
Q9NQP4	Prefoldin subunit 4	PFDN4
E9PRY8	Elongation factor 1-delta	EEF1D
Q14914	Prostaglandin reductase 1	PTGR1
O00233	26S proteasome non-ATPase regulatory subunit 9	PSMD9
F5GXA0	Formylglycine-generating enzyme	SUMF1
Q9Y3B8	Oligoribonuclease, mitochondrial	REXO2
P08195	4F2 cell-surface antigen heavy chain	SLC3A2
Q03426	Mevalonate kinase	MVK
Q8IZ83	Aldehyde dehydrogenase family 16 member A1	ALDH16A1
P61769	Beta-2-microglobulin	B2M
Q9HC38	Glyoxalase domain-containing protein 4	GLOD4
P43487	Ran-specific GTPase-activating protein	RANBP1
P08962	CD63 antigen	CD63
F8VWP7	Calcyphosin-2	CAPS2
Q9UBQ0	Vacuolar protein sorting-associated protein 29	VPS29
F8W031	DUF3456 domain-containing protein	CNPY2
Q9BY44	Eukaryotic translation initiation factor 2A	EIF2A
Q07157	Tight junction protein ZO-1	TJP1
G3V295	Proteasome subunit alpha type	PSMA6
P12268	Inosine-5-monophosphate dehydrogenase 2	IMPDH2
Q13439	Golgin subfamily A member 4	GOLGA4
P0DP23	Calmodulin-1	CALM1
P40939	Trifunctional enzyme subunit alpha, mitochondrial	HADHA

H0YHG0	Uncharacterized protein	N/A
P50213	Isocitrate dehydrogenase [NAD] subunit alpha, mitochondrial	IDH3A
Q9UL46	Proteasome activator complex subunit 2	PSME2
Q71UM5	40S ribosomal protein S27-like	RPS27L
P39687	Acidic leucine-rich nuclear phosphoprotein 32 family member A	ANP32A
Q9GZS3	WD repeat-containing protein 61	WDR61
O43488	Aflatoxin B1 aldehyde reductase member 2	AKR7A2
P08708	40S ribosomal protein S17	RPS17
P06865	Beta-hexosaminidase subunit alpha	HEXA
P35637	RNA-binding protein FUS	FUS
Q6FI81	Anamorsin	CIAPIN1
H7BYY1	Tropomyosin 1 (Alpha), isoform CRA_m	TPM1
H7C0E5	Zinc finger protein ZPR1	ZPR1
O95819	Mitogen-activated protein kinase kinase kinase kinase 4	MAP4K4
P63241	Eukaryotic translation initiation factor 5A-1	EIF5A
P62244	40S ribosomal protein S15a	RPS15A
J3KN67	Tropomyosin alpha-3 chain	TPM3
J3QL05	Serine/arginine-rich splicing factor 2	SRSF2
O95232	Luc7-like protein 3	LUC7L3
J3KQ32	Obg-like ATPase 1	OLA1
Q8NBJ7	Sulfatase-modifying factor 2	SUMF2
P83881	60S ribosomal protein L36a	RPL36A
P17844	Probable ATP-dependent RNA helicase DDX5	DDX5
K7EK33	DAZ-associated protein 1	DAZAP1
P61353	60S ribosomal protein L27	RPL27
P14314	Glucosidase 2 subunit beta	PRKCSH
P41567	Eukaryotic translation initiation factor 1	EIF1
P35268	60S ribosomal protein L22	RPL22
K7ERQ8	PCAF_N domain-containing protein	N/A
O14579	Coatomer subunit epsilon	COPE
O95571	Persulfide dioxygenase ETHE1, mitochondrial	ETHE1
P46782	40S ribosomal protein S5	RPS5
Q02543	60S ribosomal protein L18a	RPL18A
Q9UBC2	Epidermal growth factor receptor substrate 15-like 1	EPS15L1
O00151	PDZ and LIM domain protein 1	PDLIM1
O00154	Cytosolic acyl coenzyme A thioester hydrolase	ACOT7
O00161	Synaptosomal-associated protein 23	SNAP23
O00231	26S proteasome non-ATPase regulatory subunit 11	PSMD11
O00267	Transcription elongation factor SPT5	SUPT5H
O00273	DNA fragmentation factor subunit alpha	DFFA
O00299	Chloride intracellular channel protein 1	CLIC1
O00425	Insulin-like growth factor 2 mRNA-binding protein 3	IGF2BP3
O00499	Myc box-dependent-interacting protein 1	BIN1
Q5JXT2	Nucleolar protein 56	NOP56
Q5T1S7	Serine/threonine-protein phosphatase 6 catalytic subunit	PPP6C

O00754	Lysosomal alpha-mannosidase	MAN2B1
O00764	Pyridoxal kinase	PDXK
O14737	Programmed cell death protein 5	PDCD5
O14744	Protein arginine N-methyltransferase 5	PRMT5
O14745	Na(+)/H(+) exchange regulatory cofactor NHE-RF1	SLC9A3R1
O14818	Proteasome subunit alpha type-7	PSMA7
O14907	Tax1-binding protein 3	TAX1BP3
O14964	Hepatocyte growth factor-regulated tyrosine kinase substrate	HGS
O14974	Protein phosphatase 1 regulatory subunit 12A	PPP1R12A
O15143	Actin-related protein 2/3 complex subunit 1B	ARPC1B
O15144	Actin-related protein 2/3 complex subunit 2	ARPC2
O15145	Actin-related protein 2/3 complex subunit 3	ARPC3
O15212	Prefoldin subunit 6	PFDN6
O15305	Phosphomannomutase 2	PMM2
O15371	Eukaryotic translation initiation factor 3 subunit D	EIF3D
O15460	Prolyl 4-hydroxylase subunit alpha-2	P4HA2
O43242	26S proteasome non-ATPase regulatory subunit 3	PSMD3
O43252	Bifunctional 3-phosphoadenosine 5-phosphosulfate synthase 1	PAPSS1
O43399	Tumor protein D54	TPD52L2
O43447	Peptidyl-prolyl cis-trans isomerase H	PIIH
O43765	Small glutamine-rich tetratricopeptide repeat-containing protein alpha	SGTA
O43776	Asparagine--tRNA ligase, cytoplasmic	NARS
O43815	Striatin	STRN
O43852	Calumenin	CALU
O60256	Phosphoribosyl pyrophosphate synthase-associated protein 2	PRPSAP2
O60568	Procollagen-lysine,2-oxoglutarate 5-dioxygenase 3	PLOD3
O60664	Perilipin-3	PLIN3
O60828	Polyglutamine-binding protein 1	PQBP1
O60832	H/ACA ribonucleoprotein complex subunit 4	DKC1
O60869	Endothelial differentiation-related factor 1	EDF1
O60884	DnaJ homolog subfamily A member 2	DNAJA2
O60888	Protein CutA	CUTA
O75083	WD repeat-containing protein 1	WDR1
O75223	Gamma-glutamylcyclotransferase	GGCT
O75348	V-type proton ATPase subunit G 1	ATP6V1G1
O75369	Filamin-B	FLNB
O75436	Vacuolar protein sorting-associated protein 26A	VPS26A
O75439	Mitochondrial-processing peptidase subunit beta	PMPCB
O75494	Serine/arginine-rich splicing factor 10	SRSF10
O75506	Heat shock factor-binding protein 1	HSBP1
O75531	Barrier-to-autointegration factor	BANF1
O75533	Splicing factor 3B subunit 1	SF3B1
O75607	Nucleoplasmin-3	NPM3
O75821	Eukaryotic translation initiation factor 3 subunit G	EIF3G
O75822	Eukaryotic translation initiation factor 3 subunit J	EIF3J

O75828	Carbonyl reductase [NADPH] 3	CBR3
O75937	DnaJ homolog subfamily C member 8	DNAJC8
O76021	Ribosomal L1 domain-containing protein 1	RSL1D1
O94903	Proline synthase co-transcribed bacterial homolog protein	PROSC
O95340	Bifunctional 3-phosphoadenosine 5-phosphosulfate synthase 2	PAPSS2
O95394	Phosphoacetylglucosamine mutase	PGM3
O95456	Proteasome assembly chaperone 1	PSMG1
O95479	GDH/6PGL endoplasmic bifunctional protein	H6PD
O95817	BAG family molecular chaperone regulator 3	BAG3
O95831	Apoptosis-inducing factor 1, mitochondrial	AIFM1
Q5SSV3	N(G),N(G)-dimethylarginine dimethylaminohydrolase 2	DDAH2
O95881	Thioredoxin domain-containing protein 12	TXNDC12
P00338	L-lactate dehydrogenase A chain	LDHA
P00367	Glutamate dehydrogenase 1, mitochondrial	GLUD1
P00374	Dihydrofolate reductase	DHFR
P00492	Hypoxanthine-guanine phosphoribosyltransferase	HPRT1
P00505	Aspartate aminotransferase, mitochondrial	GOT2
P00558	Phosphoglycerate kinase 1	PGK1
P00568	Adenylate kinase isoenzyme 1	AK1
P00750	Tissue-type plasminogen activator	PLAT
P02545	Prelamin-A/C;Lamin-A/C	LMNA
P04040	Catalase	CAT
P04066	Tissue alpha-L-fucosidase	FUCA1
P04075	Fructose-bisphosphate aldolase A	ALDOA
P04080	Cystatin-B	CSTB
P04083	Annexin A1	ANXA1
P04179	Superoxide dismutase [Mn], mitochondrial	SOD2
P04406	Glyceraldehyde-3-phosphate dehydrogenase	GAPDH
P04424	Argininosuccinate lyase	ASL
P04899	Guanine nucleotide-binding protein G(i) subunit alpha-2	GNAI2
P05114	Non-histone chromosomal protein HMG-14	HMGN1
P05121	Plasminogen activator inhibitor 1	SERPINE1
P05198	Eukaryotic translation initiation factor 2 subunit 1	EIF2S1
P05204	Non-histone chromosomal protein HMG-17	HMGN2
P05386	60S acidic ribosomal protein P1	RPLP1
P05387	60S acidic ribosomal protein P2	RPLP2
P05455	Lupus La protein	SSB
P05556	Integrin beta-1	ITGB1
P06132	Uroporphyrinogen decarboxylase	UROD
P06576	ATP synthase subunit beta, mitochondrial	ATP5B
P06703	Protein S100	S100A6
P06733	Alpha-enolase	ENO1
P07108	Acyl-CoA-binding protein	DBI
P07195	L-lactate dehydrogenase B chain	LDHB
P07384	Calpain-1 catalytic subunit	CAPN1

P07437	Tubulin beta chain	TUBB
P07737	Profilin-1	PFN1
P07814	Bifunctional glutamate/proline--tRNA ligase	EPRS
P07858	Cathepsin B	CTSB
P07954	Fumarate hydratase, mitochondrial	FH
P08134	Rho-related GTP-binding protein RhoC	RHOC
P08243	Asparagine synthetase [glutamine-hydrolyzing]	ASNS
P08559	Pyruvate dehydrogenase E1 component subunit alpha, somatic form, mitochondrial	PDHA1
P08579	U2 small nuclear ribonucleoprotein B	SNRPB2
P08590	Myosin light chain 3	MYL3
P08670	Vimentin	VIM
P09012	U1 small nuclear ribonucleoprotein A	SNRPA
P09110	3-ketoacyl-CoA thiolase, peroxisomal	ACAA1
P09211	Glutathione S-transferase P	GSTP1
P09382	Galectin-1	LGALS1
P09417	Dihydropteridine reductase	QDPR
P09429	High mobility group protein B1	HMGB1
P09486	SPARC	SPARC
P09488	Glutathione S-transferase Mu 1	GSTM1
P09496	Clathrin light chain A	CLTA
P09525	Annexin A4	ANXA4
P09661	U2 small nuclear ribonucleoprotein A	SNRPA1
P09960	Leukotriene A-4 hydrolase	LTA4H
P09972	Fructose-bisphosphate aldolase C;Fructose-bisphosphate aldolase	ALDOC
Q6FI13	Histone H2A	H2AC18
P20671	Histone H2A type 1-D	HIST1H2AD
P0DN76	Splicing factor U2AF 35 kDa subunit	U2AF1
P10253	Lysosomal alpha-glucosidase	GAA
P10599	Thioredoxin	TXN
P10619	Lysosomal protective protein	CTSA
P10768	S-formylglutathione hydrolase	ESD
P10809	60 kDa heat shock protein, mitochondrial	HSPD1
P11142	Heat shock cognate 71 kDa protein	HSPA8
P11233	Ras-related protein Ral-A	RALA
P11387	DNA topoisomerase 1	TOP1
P11413	Glucose-6-phosphate 1-dehydrogenase	G6PD
P11766	Alcohol dehydrogenase class-3	ADH5
P11908	Ribose-phosphate pyrophosphokinase 2	PRPS2
P12004	Proliferating cell nuclear antigen	PCNA
P12956	X-ray repair cross-complementing protein 6	XRCC6
P13010	X-ray repair cross-complementing protein 5	XRCC5
P13667	Protein disulfide-isomerase A4	PDIA4
P13674	Prolyl 4-hydroxylase subunit alpha-1	P4HA1
P13693	Translationally-controlled tumor protein	TPT1
P13797	Plastin-3	PLS3
P13861	cAMP-dependent protein kinase type II-alpha regulatory subunit	PRKAR2A



P13995	Bifunctional methylenetetrahydrofolate dehydrogenase/cyclohydrolase, mitochondrial	MTHFD2
P14174	Macrophage migration inhibitory factor	MIF
P14550	Alcohol dehydrogenase [NADP(+)]	AKR1A1
P14625	Endoplasmic	HSP90B1
P14868	Aspartate--tRNA ligase, cytoplasmic	DARS
P15170	Eukaryotic peptide chain release factor GTP-binding subunit ERF3A	GSPT1
P15311	Ezrin	EZR
P15374	Ubiquitin carboxyl-terminal hydrolase isozyme L3	UCHL3
P15880	40S ribosomal protein S2	RPS2
P16152	Carbonyl reductase [NADPH] 1	CBR1
P16401	Histone H1.5	HIST1H1B
P16403	Histone H1.2	HIST1H1C
P16930	Fumarylacetoacetase	FAH
P16949	Stathmin	STMN1
P17096	High mobility group protein HMG-I/HMG-Y	HMGA1
P17174	Aspartate aminotransferase, cytoplasmic	GOT1
P17612	cAMP-dependent protein kinase catalytic subunit alpha	PRKACA
P17858	ATP-dependent 6-phosphofructokinase, liver type	PFKL
P17987	T-complex protein 1 subunit alpha	TCP1
P18669	Phosphoglycerate mutase 1	PGAM1
P19338	Nucleolin	NCL
P19623	Spermidine synthase	SRM
P20042	Eukaryotic translation initiation factor 2 subunit 2	EIF2S2
P20290	Transcription factor BTF3	BTF3
P20618	Proteasome subunit beta type-1	PSMB1
P20839	Inosine-5-monophosphate dehydrogenase 1	IMPDH1
P20962	Parathyrosin	PTMS
P21281	V-type proton ATPase subunit B, brain isoform	ATP6V1B2
P21291	Cysteine and glycine-rich protein 1	CSRP1
P21333	Filamin-A	FLNA
P21399	Cytoplasmic aconitate hydratase	ACO1
P22307	Non-specific lipid-transfer protein	SCP2
P22314	Ubiquitin-like modifier-activating enzyme 1	UBA1
P23381	Tryptophan--tRNA ligase, cytoplasmic	WARS
P23396	40S ribosomal protein S3	RPS3
P23497	Nuclear autoantigen Sp-100	SP100
P23528	Cofilin-1	CFL1
P23919	Thymidylate kinase	DTYMK
P23921	Ribonucleoside-diphosphate reductase large subunit	RRM1
P24534	Elongation factor 1-beta	EEF1B2
P24666	Low molecular weight phosphotyrosine protein phosphatase	ACPI
P24752	Acetyl-CoA acetyltransferase, mitochondrial	ACAT1
P25205	DNA replication licensing factor MCM3	MCM3
P25325	3-mercaptopyruvate sulfurtransferase	MPST
P25398	40S ribosomal protein S12	RPS12

P25705	ATP synthase subunit alpha, mitochondrial	ATP5A1
P25786	Proteasome subunit alpha type-1	PSMA1
P25788	Proteasome subunit alpha type-3	PSMA3
P25789	Proteasome subunit alpha type-4	PSMA4
P26022	Pentraxin-related protein PTX3	PTX3
P26038	Moesin	MSN
P26368	Splicing factor U2AF 65 kDa subunit	U2AF2
P26583	High mobility group protein B2	HMGB2
P26639	Threonine--tRNA ligase, cytoplasmic	TARS
P26641	Elongation factor 1-gamma	EEF1G
P27797	Calreticulin	CALR
P28066	Proteasome subunit alpha type-5	PSMA5
P28070	Proteasome subunit beta type-4	PSMB4
P28072	Proteasome subunit beta type-6	PSMB6
P28074	Proteasome subunit beta type-5	PSMB5
P28838	Cytosol aminopeptidase	LAP3
P29144	Tripeptidyl-peptidase 2	TPP2
P29401	Transketolase	TKT
P30038	Delta-1-pyrroline-5-carboxylate dehydrogenase, mitochondrial	ALDH4A1
P30046	D-dopachrome decarboxylase	DDT
P30050	60S ribosomal protein L12	RPL12
P30085	UMP-CMP kinase	CMPK1
P30086	Phosphatidylethanolamine-binding protein 1	PEBP1
P30153	Serine/threonine-protein phosphatase 2A 65 kDa regulatory subunit A alpha isoform	PPP2R1A
P30419	Glycylpeptide N-tetradecanoyltransferase 1	NMT1
P30520	Adenylosuccinate synthetase isozyme 2	ADSS
P30533	Alpha-2-macroglobulin receptor-associated protein	LRPAP1
P30622	CAP-Gly domain-containing linker protein 1	CLIP1
P30837	Aldehyde dehydrogenase X, mitochondrial	ALDH1B1
P31040	Succinate dehydrogenase [ubiquinone] flavoprotein subunit, mitochondrial	SDHA
P31937	3-hydroxyisobutyrate dehydrogenase, mitochondrial	HIBADH
P31939	Bifunctional purine biosynthesis protein PURH	ATIC
P31946	14-3-3 protein beta/alpha	YWHAB
P31947	14-3-3 protein sigma	SFN
P31948	Stress-induced-phosphoprotein 1	STIP1
P32455	Interferon-induced guanylate-binding protein 1	GBP1
P32969	60S ribosomal protein L9	RPL9
P34897	Serine hydroxymethyltransferase, mitochondrial	SHMT2
P34932	Heat shock 70 kDa protein 4	HSPA4
P35579	Myosin-9	MYH9
P35606	Coatomer subunit beta	COPB2
P35659	Protein DEK	DEK
P35998	26S protease regulatory subunit 7	PSMC2
P36405	ADP-ribosylation factor-like protein 3	ARL3
P36542	ATP synthase subunit gamma, mitochondrial	ATP5C1

P36551	Oxygen-dependent coproporphyrinogen-III oxidase, mitochondrial	CPOX
P36578	60S ribosomal protein L4	RPL4
P36873	Serine/threonine-protein phosphatase PP1-gamma catalytic subunit	PPP1CC
P37108	Signal recognition particle 14 kDa protein	SRP14
P37802	Transgelin-2	TAGLN2
P37837	Transaldolase	TALDO1
P38606	V-type proton ATPase catalytic subunit A	ATP6V1A
P38646	Stress-70 protein, mitochondrial	HSPA9
P39019	40S ribosomal protein S19	RPS19
P40121	Macrophage-capping protein	CAPG
P40227	T-complex protein 1 subunit zeta	CCT6A
P40261	Nicotinamide N-methyltransferase	NNMT
P40926	Malate dehydrogenase, mitochondrial	MDH2
P41091	Eukaryotic translation initiation factor 2 subunit 3	EIF2S3
P41208	Centrin-2	CETN2
P41236	Protein phosphatase inhibitor 2	PPP1R2
P41252	Isoleucine--tRNA ligase, cytoplasmic	IARS
P42126	Enoyl-CoA delta isomerase 1, mitochondrial	ECI1
P42704	Leucine-rich PPR motif-containing protein, mitochondrial	LRPPRC
P42765	3-ketoacyl-CoA thiolase, mitochondrial	ACAA2
P42766	60S ribosomal protein L35	RPL35
P42785	Lysosomal Pro-X carboxypeptidase	PRCP
P43490	Nicotinamide phosphoribosyltransferase	NAMPT
P43686	26S protease regulatory subunit 6B	PSMC4
P46087	Probable 28S rRNA (cytosine(4447)-C(5))-methyltransferase	NOP2
P46108	Adapter molecule crk	CRK
P46109	Crk-like protein	CRKL
P46776	60S ribosomal protein L27a	RPL27A
P46779	60S ribosomal protein L28	RPL28
P46783	40S ribosomal protein S10	RPS10
P46821	Microtubule-associated protein 1B	MAP1B
P46937	Transcriptional coactivator YAP1	YAP1
P47755	F-actin-capping protein subunit alpha-2	CAPZA2
P47813	Eukaryotic translation initiation factor 1A, X-chromosomal	EIF1AX
P48147	Prolyl endopeptidase	PREP
P48163	NADP-dependent malic enzyme	ME1
P48634	Protein PRRC2A	PRRC2A
P49006	MARCKS-related protein	MARCKSL1
P49368	T-complex protein 1 subunit gamma	CCT3
P49411	Elongation factor Tu, mitochondrial	TUFM
P49458	Signal recognition particle 9 kDa protein	SRP9
P49588	Alanine--tRNA ligase, cytoplasmic	AARS
P49589	Cysteine--tRNA ligase, cytoplasmic	CARS
P49591	Serine--tRNA ligase, cytoplasmic	SARS

P49720	Proteasome subunit beta type-3	PSMB3
P49721	Proteasome subunit beta type-2	PSMB2
P49736	DNA replication licensing factor MCM2	MCM2
P49773	Histidine triad nucleotide-binding protein 1	HINT1
P50395	Rab GDP dissociation inhibitor beta	GDI2
P50454	Serpin H1	SERPINH1
P50479	PDZ and LIM domain protein 4	PDLIM4
P50502	Hsc70-interacting protein	ST13
P50552	Vasodilator-stimulated phosphoprotein	VASP
P50914	60S ribosomal protein L14	RPL14
P50990	T-complex protein 1 subunit theta	CCT8
P50991	T-complex protein 1 subunit delta	CCT4
P51148	Ras-related protein Rab-5C	RAB5C
P51149	Ras-related protein Rab-7a	RAB7A
P51570	Galactokinase	GALK1
P51858	Hepatoma-derived growth factor	HDGF
P52209	6-phosphogluconate dehydrogenase, decarboxylating	PGD
P52272	Heterogeneous nuclear ribonucleoprotein M	HNRNPM
P52788	Spermine synthase	SMS
P52888	Thimet oligopeptidase	THOP1
P52907	F-actin-capping protein subunit alpha-1	CAPZA1
P53004	Biliverdin reductase A	BLVRA
P53041	Serine/threonine-protein phosphatase 5	PPP5C
P53396	ATP-citrate synthase	ACLY
P53582	Methionine aminopeptidase 1	METAP1
P53597	Succinyl-CoA ligase [ADP/GDP-forming] subunit alpha, mitochondrial	SUCLG1
P53602	Diphosphomevalonate decarboxylase	MVD
P53634	Dipeptidyl peptidase 1	CTSC
P53999	Activated RNA polymerase II transcriptional coactivator p15	SUB1
P54136	Arginine--tRNA ligase, cytoplasmic	RARS
P54577	Tyrosine--tRNA ligase, cytoplasmic	YARS
P54652	Heat shock-related 70 kDa protein 2	HSPA2
P54687	Branched-chain-amino-acid aminotransferase, cytosolic	BCAT1
P54727	UV excision repair protein RAD23 homolog B	RAD23B
P55010	Eukaryotic translation initiation factor 5	EIF5
P55036	26S proteasome non-ATPase regulatory subunit 4	PSMD4
P55072	Transitional endoplasmic reticulum ATPase	VCP
P55081	Microfibrillar-associated protein 1	MFAP1
P55263	Adenosine kinase	ADK
P55735	Protein SEC13 homolog	SEC13
P55786	Puromycin-sensitive aminopeptidase	NPEPPS
P55809	Succinyl-CoA:3-ketoacid coenzyme A transferase 1, mitochondrial	OXCT1
P55884	Eukaryotic translation initiation factor 3 subunit B	EIF3B
P56192	Methionine--tRNA ligase, cytoplasmic	MARS
P56537	Eukaryotic translation initiation factor 6	EIF6

P58546	Myotrophin	MTPN
P60174	Triosephosphate isomerase	TPI1
P60510	Serine/threonine-protein phosphatase 4 catalytic subunit	PPP4C
P60709	Actin, cytoplasmic 1	ACTB
P60866	40S ribosomal protein S20	RPS20
P60903	Protein S100-A10	S100A10
P60953	Cell division control protein 42 homolog	CDC42
P60981	Dextrin	DSTN
P60983	Glia maturation factor beta	GMFB
P61019	Ras-related protein Rab-2A	RAB2A
P61020	Ras-related protein Rab-5B	RAB5B
P61106	Ras-related protein Rab-14	RAB14
P61158	Actin-related protein 3	ACTR3
P61160	Actin-related protein 2	ACTR2
P61163	Alpha-centractin	ACTR1A
P61204	ADP-ribosylation factor 3	ARF3
P61224	Ras-related protein Rap-1b	RAP1B
P61247	40S ribosomal protein S3a	RPS3A
P61457	Pterin-4-alpha-carbinolamine dehydratase	PCBD1
P61513	60S ribosomal protein L37a	RPL37A
P61604	10 kDa heat shock protein, mitochondrial	HSPE1
P61758	Prefoldin subunit 3	VBP1
P61970	Nuclear transport factor 2	NUTF2
P62081	40S ribosomal protein S7	RPS7
P62136	Serine/threonine-protein phosphatase PP1-alpha catalytic subunit	PPP1CA
P62140	Serine/threonine-protein phosphatase PP1-beta catalytic subunit	PPP1CB
P62191	26S protease regulatory subunit 4	PSMC1
P62195	26S protease regulatory subunit 8	PSMC5
P62241	40S ribosomal protein S8	RPS8
P62249	40S ribosomal protein S16	RPS16
P62258	14-3-3 protein epsilon	YWHAE
P62266	40S ribosomal protein S23	RPS23
P62269	40S ribosomal protein S18	RPS18
P62273	40S ribosomal protein S29	RPS29
P62277	40S ribosomal protein S13	RPS13
P62280	40S ribosomal protein S11	RPS11
P62310	U6 snRNA-associated Sm-like protein LSm3	LSM3
P62314	Small nuclear ribonucleoprotein Sm D1	SNRPD1
P62316	Small nuclear ribonucleoprotein Sm D2	SNRPD2
P62328	Thymosin beta-4	TMSB4X
P62714	Serine/threonine-protein phosphatase 2A catalytic subunit beta isoform	PPP2CB
P62750	60S ribosomal protein L23a	RPL23A
P62753	40S ribosomal protein S6	RPS6
P62805	Histone H4	HIST1H4A
P62820	Ras-related protein Rab-1A	RAB1A

P62829	60S ribosomal protein L23	RPL23
P62851	40S ribosomal protein S25	RPS25
P62854	40S ribosomal protein S26	RPS26
P62857	40S ribosomal protein S28	RPS28
P62873	Guanine nucleotide-binding protein G(I)/G(S)/G(T) subunit beta-1	GNB1
P62877	E3 ubiquitin-protein ligase RBX1	RBX1
P62899	60S ribosomal protein L31	RPL31
P62906	60S ribosomal protein L10a	RPL10A
P62942	Peptidyl-prolyl cis-trans isomerase	FKBP1A
P62987	Ubiquitin-60S ribosomal protein L40	UBA52
P62995	Transformer-2 protein homolog beta	TRA2B
P63000	Ras-related C3 botulinum toxin substrate 1	RAC1
P63173	60S ribosomal protein L38	RPL38
P63220	40S ribosomal protein S21	RPS21
P63244	Guanine nucleotide-binding protein subunit beta-2-like 1	GNB2L1
P63261	Actin, cytoplasmic 2;Actin, cytoplasmic 2, N-terminally processed	ACTG1
P63313	Thymosin beta-10	TMSB10
P67936	Tropomyosin alpha-4 chain	TPM4
P68032	Actin, gamma-enteric smooth muscle	ACTG2
P68036	Ubiquitin-conjugating enzyme E2 L3	UBE2L3
P68104	Elongation factor 1-alpha 1	EEF1A1
P68363	Tubulin alpha-1B chain	TUBA1B
P68371	Tubulin beta-4B chain	TUBB4B
P68402	Platelet-activating factor acetylhydrolase IB subunit beta	PAFAH1B2
P68431	Histone H3.1	H3C1
P78371	T-complex protein 1 subunit beta	CCT2
P78417	Glutathione S-transferase omega-1	GSTO1
P80723	Brain acid soluble protein 1	BASP1
P82909	28S ribosomal protein S36, mitochondrial	MRPS36
P84090	Enhancer of rudimentary homolog	ERH
P98082	Disabled homolog 2	DAB2
Q00688	Peptidyl-prolyl cis-trans isomerase FKBP3	FKBP3
Q00796	Sorbitol dehydrogenase	SORD
Q01082	Spectrin beta chain, non-erythrocytic 1	SPTBN1
Q01433	AMP deaminase 2	AMPD2
Q01469	Fatty acid-binding protein, epidermal	FABP5
Q01518	Adenylyl cyclase-associated protein 1	CAP1
Q01581	Hydroxymethylglutaryl-CoA synthase, cytoplasmic	HMGCS1
Q01813	ATP-dependent 6-phosphofructokinase, platelet type	PFKP
Q01995	Transgelin	TAGLN
Q02218	2-oxoglutarate dehydrogenase, mitochondrial	OGDH
Q02809	Procollagen-lysine,2-oxoglutarate 5-dioxygenase 1	PLOD1
Q02818	Nucleobindin-1	NUCB1
P56539	Caveolin-1	CAV1
Q04446	1,4-alpha-glucan-branching enzyme	GBE1

<b>Q04760</b>	<b>Lactoylglutathione lyase</b>	<b>GLO1</b>
Q05682	Caldesmon	CALD1
Q06203	Amidophosphoribosyltransferase	PPAT
Q06323	Proteasome activator complex subunit 1	PSME1
Q07021	Complement component 1 Q subcomponent-binding protein, mitochondrial	C1QBP
Q07065	Cytoskeleton-associated protein 4	CKAP4
Q07666	KH domain-containing, RNA-binding, signal transduction-associated protein 1	KHDRBS1
Q07954	Prolow-density lipoprotein receptor-related protein 1	LRP1
Q08257	Quinone oxidoreductase	CRYZ
Q08378	Golgin subfamily A member 3	GOLGA3
Q08752	Peptidyl-prolyl cis-trans isomerase D	PPID
Q08J23	tRNA (cytosine(34)-C(5))-methyltransferase	NSUN2
Q09666	Neuroblast differentiation-associated protein AHNAK	AHNAK
Q0ZGT2	Nexilin	NEXN
Q10713	Mitochondrial-processing peptidase subunit alpha	PMPCA
Q12765	Secernin-1	SCRN1
Q12792	Twinfilin-1	TWF1
Q12841	Follistatin-related protein 1	FSTL1
Q12874	Splicing factor 3A subunit 3	SF3A3
Q12888	Tumor suppressor p53-binding protein 1	TP53BP1
Q13155	Aminoacyl tRNA synthase complex-interacting multifunctional protein 2	AIMP2
Q13200	26S proteasome non-ATPase regulatory subunit 2	PSMD2
Q13242	Serine/arginine-rich splicing factor 9	SRSF9
Q13243	Serine/arginine-rich splicing factor 5	SRSF5
Q13247	Serine/arginine-rich splicing factor 6	SRSF6
Q13263	Transcription intermediary factor 1-beta	TRIM28
Q13283	Ras GTPase-activating protein-binding protein 1	G3BP1
Q13347	Eukaryotic translation initiation factor 3 subunit I	EIF3I
Q13405	39S ribosomal protein L49, mitochondrial	MRPL49
Q13409	Cytoplasmic dynein 1 intermediate chain 2	DYNC1I2
Q13442	28 kDa heat- and acid-stable phosphoprotein	PDAP1
Q13451	Peptidyl-prolyl cis-trans isomerase FKBP5	FKBP5
Q13501	Sequestosome-1	SQSTM1
Q13526	Peptidyl-prolyl cis-trans isomerase NIMA-interacting 1	PIN1
Q13547	Histone deacetylase 1	HDAC1
Q13561	Dynactin subunit 2	DCTN2
Q13564	NEDD8-activating enzyme E1 regulatory subunit	NAE1
Q13630	GDP-L-fucose synthase	TSTA3
Q13813	Spectrin alpha chain, non-erythrocytic 1	SPTAN1
Q13838	Spliceosome RNA helicase DDX39B	DDX39B
Q13867	Bleomycin hydrolase	BLMH
Q13885	Tubulin beta-2A chain	TUBB2A
Q13907	Isopentenyl-diphosphate Delta-isomerase 1	IDI1
Q14011	Cold-inducible RNA-binding protein	CIRBP

Q14137	Ribosome biogenesis protein BOP1	BOP1
Q14151	Scaffold attachment factor B2	SAFB2
Q14157	Ubiquitin-associated protein 2-like	UBAP2L
Q14247	Src substrate cortactin	CTTN
Q14257	Reticulocalbin-2	RCN2
Q14315	Filamin-C	FLNC
Q14376	UDP-glucose 4-epimerase	GALE
Q14558	Phosphoribosyl pyrophosphate synthase-associated protein 1	PRPSAP1
Q14696	LDLR chaperone MESD	MESDC2
Q14697	Neutral alpha-glucosidase AB	GANAB
Q14847	LIM and SH3 domain protein 1	LASP1
Q14974	Importin subunit beta-1	KPNB1
Q14980	Nuclear mitotic apparatus protein 1	NUMA1
Q15007	Pre-mRNA-splicing regulator WTAP	WTAP
Q15008	26S proteasome non-ATPase regulatory subunit 6	PSMD6
Q15019	Septin-2	SEPTIN2
Q15046	Lysine--tRNA ligase	KARS
Q15056	Eukaryotic translation initiation factor 4H	EIF4H
Q15067	Peroxisomal acyl-coenzyme A oxidase 1	ACOX1
Q15084	Protein disulfide-isomerase A6	PDIA6
Q15102	Platelet-activating factor acetylhydrolase IB subunit gamma	PAFAH1B3
Q15121	Astrocytic phosphoprotein PEA-15	PEA15
Q15149	Plectin	PLEC
Q15181	Inorganic pyrophosphatase	PPA1
Q15293	Reticulocalbin-1	RCN1
Q15365	Poly(rC)-binding protein 1	PCBP1
Q15370	Transcription elongation factor B polypeptide 2	TCEB2
Q15393	Splicing factor 3B subunit 3	SF3B3
Q15404	Ras suppressor protein 1	RSU1
Q15435	Protein phosphatase 1 regulatory subunit 7	PPP1R7
Q15637	Splicing factor 1	SF1
Q15691	Microtubule-associated protein RP/EB family member 1	MAPRE1
Q15717	ELAV-like protein 1	ELAVL1
Q15843	NEDD8	NEDD8
Q15907	Ras-related protein Rab-11B	RAB11B
Q16204	Coiled-coil domain-containing protein 6	CCDC6
Q16222	UDP-N-acetylhexosamine pyrophosphorylase	UAP1
Q16270	Insulin-like growth factor-binding protein 7	IGFBP7
Q16531	DNA damage-binding protein 1	DDB1
Q16543	Hsp90 co-chaperone Cdc37	CDC37
Q16658	Fascin	FSCN1
Q16762	Thiosulfate sulfurtransferase	TST
Q1KMD3	Heterogeneous nuclear ribonucleoprotein U-like protein 2	HNRNPUL2
Q2NL82	Pre-rRNA-processing protein TSR1 homolog	TSR1
Q32MZ4	Leucine-rich repeat flightless-interacting protein 1	LRRFIP1



Q32P28	Prolyl 3-hydroxylase 1	LEPRE1
P22392	Nucleoside diphosphate kinase B	NME2
Q3MHD2	Protein LSM12 homolog	LSM12
Q53H82	Beta-lactamase-like protein 2	LACTB2
Q5HYB6	Epididymis luminal protein 189	DKFZp686J1372
Q5JRX3	Presequence protease, mitochondrial	PITRM1
Q5JSH3	WD repeat-containing protein 44	WDR44
Q5QPL9	RNA-binding protein Raly	RALY
Q5SSJ5	Heterochromatin protein 1-binding protein 3	HP1BP3
Q5T123	SH3 domain-binding glutamic acid-rich-like protein 3	SH3BGRL3
Q5T1J5	Putative coiled-coil-helix-coiled-coil-helix domain-containing protein CHCHD2P9, mitochondrial	CHCHD2P9
Q5T6F2	Ubiquitin-associated protein 2	UBAP2
Q5T6H7	Xaa-Pro aminopeptidase 1	XPNPEP1
Q5TFE4	5-nucleotidase domain-containing protein 1	NT5DC1
Q9H4G4	Golgi-associated plant pathogenesis-related protein 1	GLIPR2
Q6GMV3	Putative peptidyl-tRNA hydrolase PTRHD1	PTRHD1
Q6IBS0	Twinfilin-2	TWF2
Q6NVY1	3-hydroxyisobutyryl-CoA hydrolase, mitochondrial	HIBCH
Q6P2Q9	Pre-mRNA-processing-splicing factor 8	PRPF8
Q6UXH1	Cysteine-rich with EGF-like domain protein 2	CRELD2
Q6YP21	Kynurenine--oxoglutarate transaminase 3	CCBL2
Q6ZN40	Tropomyosin 1 (Alpha), isoform CRA_f	TPM1
Q7KZF4	Staphylococcal nuclease domain-containing protein 1	SND1
Q7Z417	Nuclear fragile X mental retardation-interacting protein 2	NUFIP2
Q7Z422	SUZ domain-containing protein 1	SZRD1
Q7Z4H8	KDEL motif-containing protein 2	KDELC2
Q7Z5L9	Interferon regulatory factor 2-binding protein 2	IRF2BP2
Q7Z7K6	Centromere protein V	CENPV
Q86SX6	Glutaredoxin-related protein 5, mitochondrial	GLRX5
Q86TI2	Dipeptidyl peptidase 9	DPP9
Q86UP2	Kinectin	KTN1
Q8IVD9	NudC domain-containing protein 3	NUDCD3
Q8IVF2	Protein AHNAK2	AHNAK2
Q8IVL6	Prolyl 3-hydroxylase 3	LEPREL2
Q8IVM0	Coiled-coil domain-containing protein 50	CCDC50
Q8IWE2	Protein NOXP20	FAM114A1
Q8N1G4	Leucine-rich repeat-containing protein 47	LRRC47
Q8N7H5	RNA polymerase II-associated factor 1 homolog	PAF1
Q8NBJ5	Procollagen galactosyltransferase 1	COLGALT1
Q8NBS9	Thioredoxin domain-containing protein 5	TXNDC5
Q8NCW5	NAD(P)H-hydrate epimerase	APOA1BP
Q8ND56	Protein LSM14 homolog A	LSM14A
Q8NE71	ATP-binding cassette sub-family F member 1	ABCF1
Q8NFH3	Nucleoporin Nup43	NUP43
Q8NFH4	Nucleoporin Nup37	NUP37
Q8TAE8	Growth arrest and DNA damage-inducible proteins-interacting protein 1	GADD45GIP1

Q8TD16	Protein bicaudal D homolog 2	BICD2
Q8TDN6	Ribosome biogenesis protein BRX1 homolog	BRIX1
Q8TEA8	D-tyrosyl-tRNA(Tyr) deacylase 1;D-tyrosyl-tRNA(Tyr) deacylase	DTD1
Q8WU90	Zinc finger CCCH domain-containing protein 15	ZC3H15
Q8WUP2	Filamin-binding LIM protein 1	FBLIM1
Q8WX93	Palladin	PALLD
Q92686	Neurogranin;NEUG(55-78)	NRGN
Q92688	Acidic leucine-rich nuclear phosphoprotein 32 family member B	ANP32B
Q92733	Proline-rich protein PRCC	PRCC
Q92734	Protein TFG	TFG
Q92783	Signal transducing adapter molecule 1	STAM
Q92804	TATA-binding protein-associated factor 2N	TAF15
Q92890	Ubiquitin fusion degradation protein 1 homolog	UFD1L
Q92930	Ras-related protein Rab-8B	RAB8B
Q969E4	Transcription elongation factor A protein-like 3	TCEAL3
Q969H8	Myeloid-derived growth factor	MYDGF
Q96A49	Synapse-associated protein 1	SYAP1
Q96AY3	Peptidyl-prolyl cis-trans isomerase FKBP10	FKBP10
Q96B97	SH3 domain-containing kinase-binding protein 1	SH3KBP1
Q96BJ3	Axin interactor, dorsalization-associated protein	AIDA
Q96CN7	Isochorismatase domain-containing protein 1	ISOC1
Q96CT7	Coiled-coil domain-containing protein 124	CCDC124
Q96CV9	Optineurin	OPTN
Q96D15	Reticulocalbin-3	RCN3
Q96DG6	Carboxymethylenebutenolidase homolog	CMBL
Q96EK6	Glucosamine 6-phosphate N-acetyltransferase	GNPNAT1
Q96FQ6	Protein S100-A16	S100A16
Q96FX7	tRNA (adenine(58)-N(1))-methyltransferase catalytic subunit	TRMT61A
Q96G03	Phosphoglucomutase-2	PGM2
Q96GA3	Protein LTV1 homolog	LTV1
Q96GK7	Fumarylacetoacetate hydrolase domain-containing protein 2A	FAHD2A
Q96GX9	Methylthioribulose-1-phosphate dehydratase	APIP
Q96HC4	PDZ and LIM domain protein 5	PDLIM5
Q96HE7	ERO1-like protein alpha	ERO1L
Q96I99	Succinyl-CoA ligase [GDP-forming] subunit beta, mitochondrial	SUCLG2
Q96IJ6	Mannose-1-phosphate guanyltransferase alpha	GMPPA
Q96IZ0	PRKC apoptosis WT1 regulator protein	PAWR
Q96KP4	Cytosolic non-specific dipeptidase	CNDP2
Q96M27	Protein PRRC1	PRRC1
Q96QK1	Vacuolar protein sorting-associated protein 35	VPS35
Q99426	Tubulin-folding cofactor B	TBCB
Q99436	Proteasome subunit beta type-7	PSMB7
Q99447	Ethanolamine-phosphate cytidyltransferase	PCYT2
Q99471	Prefoldin subunit 5	PFDN5

Q99497	Protein deglycase DJ-1	PARK7
Q99536	Synaptic vesicle membrane protein VAT-1 homolog	VAT1
Q99543	DnaJ homolog subfamily C member 2	DNAJC2
Q99575	Ribonucleases P/MRP protein subunit POP1	POP1
Q99613	Eukaryotic translation initiation factor 3 subunit C	EIF3C
Q99614	Tetratricopeptide repeat protein 1	TTC1
Q99615	DnaJ homolog subfamily C member 7	DNAJC7
Q99622	Protein C10	C12orf57
Q99714	3-hydroxyacyl-CoA dehydrogenase type-2	HSD17B10
Q99832	T-complex protein 1 subunit eta	CCT7
Q99961	Endophilin-A2	SH3GL1
Q9BPX5	Actin-related protein 2/3 complex subunit 5-like protein	ARPC5L
Q9BQ52	Zinc phosphodiesterase ELAC protein 2	ELAC2
Q9BQA1	Methylosome protein 50	WDR77
Q9BR76	Coronin-1B	CORO1B
Q9BRF8	Serine/threonine-protein phosphatase CPPED1	CPPED1
Q9BRK5	45 kDa calcium-binding protein	SDF4
Q9BS26	Endoplasmic reticulum resident protein 44	ERP44
Q9BT78	COP9 signalosome complex subunit 4	COPS4
Q9BTT0	Acidic leucine-rich nuclear phosphoprotein 32 family member E	ANP32E
Q9BU89	Deoxyhypusine hydroxylase	DOHH
Q9BV57	1,2-dihydroxy-3-keto-5-methylthiopentene dioxygenase	ADI1
Q9BWD1	Acetyl-CoA acetyltransferase, cytosolic	ACAT2
Q9BX68	Histidine triad nucleotide-binding protein 2, mitochondrial	HINT2
Q9BXR0	Queuine tRNA-ribosyltransferase	QTRT1
Q9BY43	Charged multivesicular body protein 4a	CHMP4A
Q9BY77	Polymerase delta-interacting protein 3	POLDIP3
Q9BZE4	Nucleolar GTP-binding protein 1	GTPBP4
Q9BZK7	F-box-like/WD repeat-containing protein TBL1XR1	TBL1XR1
Q9H0D6	5-3 exoribonuclease 2	XRN2
Q9H0U4	Ras-related protein Rab-1B	RAB1B
Q9H1E3	Nuclear ubiquitous casein and cyclin-dependent kinase substrate 1	NUCKS1
Q9H2D6	TRIO and F-actin-binding protein	TRIOBP
Q9H2U2	Inorganic pyrophosphatase 2, mitochondrial	PPA2
Q9H3K6	BolA-like protein 2	BOLA2
Q9H3P7	Golgi resident protein GCP60	ACBD3
Q9H444	Charged multivesicular body protein 4b	CHMP4B
Q9H4A4	Aminopeptidase B	RNPEP
Q9H8Y8	Golgi reassembly-stacking protein 2	GORASP2
Q9H993	Protein-glutamate O-methyltransferase	ARMT1
Q9HA64	Ketosamine-3-kinase	FN3KRP
Q9HAV7	GrpE protein homolog 1, mitochondrial	GRPEL1
Q9HC35	Echinoderm microtubule-associated protein-like 4	EML4
Q9HD15	Steroid receptor RNA activator 1	SRA1

Q9NNW5	WD repeat-containing protein 6	WDR6
Q9NP61	ADP-ribosylation factor GTPase-activating protein 3	ARFGAP3
Q9NP97	Dynein light chain roadblock-type 1	DYNLRB1
Q9NQC3	Reticulon-4	RTN4
Q9NQR4	Omega-amidase NIT2	NIT2
Q9NRL3	Striatin-4	STRN4
Q9NRR5	Ubiquilin-4	UBQLN4
Q9NRV9	Heme-binding protein 1	HEBP1
Q9NRX4	14 kDa phosphohistidine phosphatase	PHPT1
Q9NSD9	Phenylalanine--tRNA ligase beta subunit	FARSB
Q9NUJ1	Mycophenolic acid acyl-glucuronide esterase, mitochondrial	ABHD10
Q9NUQ6	SPATS2-like protein	SPATS2L
Q9NWT6	Hypoxia-inducible factor 1-alpha inhibitor	HIF1AN
Q9NWW4	UPF0587 protein C1orf123	C1orf123
Q9NX58	Cell growth-regulating nucleolar protein	LYAR
Q9NXG2	THUMP domain-containing protein 1	THUMPD1
Q9NXH9	tRNA (guanine(26)-N(2))-dimethyltransferase	TRMT1
Q9NY33	Dipeptidyl peptidase 3	DPP3
Q9NYF8	Bcl-2-associated transcription factor 1	BCLAF1
Q9NYL9	Tropomodulin-3	TMOD3
Q9NZ08	Endoplasmic reticulum aminopeptidase 1	ERAP1
Q9NZL9	Methionine adenosyltransferase 2 subunit beta	MAT2B
Q9NZM1	Myoferlin	MYOF
Q9NZZ3	Charged multivesicular body protein 5	CHMP5
Q9P016	Thymocyte nuclear protein 1	THYN1
Q9P1F3	Costars family protein ABRACL	ABRACL
Q9P2E9	Ribosome-binding protein 1	RRBP1
Q9P2J5	Leucine--tRNA ligase, cytoplasmic	LARS
Q9UBQ7	Glyoxylate reductase/hydroxypyruvate reductase	GRHPR
Q9UBT2	SUMO-activating enzyme subunit 2	UBA2
Q9UDR5	Alpha-aminoadipic semialdehyde synthase, mitochondrial	AASS
Q9UDT6	CAP-Gly domain-containing linker protein 2	CLIP2
Q9UGI8	Testin	TES
Q9UHB6	LIM domain and actin-binding protein 1	LIMA1
Q9UHD8	Septin-9	SEPTIN9
Q9UHV9	Prefoldin subunit 2	PFDN2
Q9UHY7	Enolase-phosphatase E1	ENOPH1
Q9UII2	ATPase inhibitor, mitochondrial	ATPIF1
Q9UJU6	Drebrin-like protein	DBNL
Q9ULC4	Malignant T-cell-amplified sequence 1	MCTS1
Q9ULV4	Coronin-1C;Coronin	CORO1C
Q9UMS0	NFU1 iron-sulfur cluster scaffold homolog, mitochondrial	NFU1
Q9UMS4	Pre-mRNA-processing factor 19	PRPF19
Q9UMX0	Ubiquilin-1	UBQLN1
Q9UN86	Ras GTPase-activating protein-binding protein 2	G3BP2
Q9UNZ2	NSFL1 cofactor p47	NSFL1C

Q9UPT8	Zinc finger CCCH domain-containing protein 4	ZC3H4
Q9UQ35	Serine/arginine repetitive matrix protein 2	SRRM2
Q9UQ80	Proliferation-associated protein 2G4	PA2G4
Q9Y224	UPF0568 protein C14orf166	C14orf166
Q9Y265	RuvB-like 1	RUVBL1
Q9Y281	Cofilin-2	CFL2
Q9Y285	Phenylalanine--tRNA ligase alpha subunit	FARSA
Q9Y2D5	A-kinase anchor protein 2	AKAP2
Q9Y2G5	GDP-fucose protein O-fucosyltransferase 2	POFUT2
Q9Y2S6	Translation machinery-associated protein 7	TMA7
Q9Y305	Acyl-coenzyme A thioesterase 9, mitochondrial	ACOT9
Q9Y315	Deoxyribose-phosphate aldolase	DERA
Q9Y3F4	Serine-threonine kinase receptor-associated protein	STRAP
Q9Y3I0	tRNA-splicing ligase RtcB homolog	RTCB
Q9Y3U8	60S ribosomal protein L36	RPL36
Q9Y490	Talin-1	TLN1
Q9Y4L1	Hypoxia up-regulated protein 1	HYOU1
Q9Y5A9	YTH domain-containing family protein 2	YTHDF2
Q9Y5J1	U3 small nucleolar RNA-associated protein 18 homolog	UTP18
Q9Y5P6	Mannose-1-phosphate guanyltransferase beta	GMPPB
Q9Y5Z4	Heme-binding protein 2	HEBP2
Q9Y606	tRNA pseudouridine synthase A	PUS1
Q9Y680	Peptidyl-prolyl cis-trans isomerase FKBP7	FKBP7
R4GNH3	26S proteasome regulatory subunit 6A	PSMC3
Q9BZE1	39S ribosomal protein L37, mitochondrial	MRPL37
Q9Y3A3	MOB-like protein phocein	MOB4